Role of vesicular glutamate transporter 3 and optineurin in metabotropic glutamate receptor 5 signaling

Karim Ibrahim

A thesis submitted to the University of Ottawa in partial fulfillment of the requirements for the degree of

Doctor of Philosophy

in

Cellular and Molecular Medicine

Department of Cellular and Molecular Medicine
Faculty of Medicine
University of Ottawa

AUTHORIZATION

Permission to include two figures from Ibrahim, K.S., Abd-Elrahman, K.S., Mestikawy, S. El, and Ferguson, S.S.G. (2020). *Targeting Vesicular Glutamate Transporter Machinery: Implications on Metabotropic Glutamate Receptor 5 Signaling and Behavior*. Mol. Pharmacol. 98: 314–327 as part of this thesis was obtained from the American society for pharmacology and experimental therapeutics.

No permission was required to include the following articles in this thesis:

- Ibrahim, K.S., Mestikawy, S. El, Abd-Elrahman, K.S., and Ferguson, S.S.G. (2022). *VGLUT3 Ablation Differentially Modulates Glutamate Receptor Densities in Mouse Brain*. ENeuro 9: ENEURO.0041-22.2022.

  eNeuro articles are published under the Creative Commons Attribution 4.0 International (CC BY 4.0) license. Per the terms of this license, it is not necessary to obtain permission or pay a fee to reuse *eNeuro* content, provided that a full acknowledgment is made to the original publication in *eNeuro*. https://creativecommons.org/licenses/by/4.0/

- Ibrahim, K.S., McLaren, C.J., Abd-Elrahman, K.S., and Ferguson, S.S.G. (2021). *Optineurin deletion disrupts metabotropic glutamate receptor 5-mediated regulation of ERK1/2, GSK3β/ZBTB16, mTOR/ULK1 signaling in autophagy*. Biochem. Pharmacol. 185: 114427.

  The authors publishing in *Biochemical Pharmacology*, as an Elsevier journal, have the right to include the article in a thesis or dissertation whether in full or in part, subject to proper acknowledgment. No written permission from Elsevier is necessary. This right extends to the posting of the thesis to the university's repository. https://www.elsevier.com/about/policies/copyright

ABSTRACT

Metabotropic glutamate receptor 5 (mGluR5) is a key regulator of numerous brain functions including memory, cognition, and motor behavior. Dysregulation of mGluR5 signaling is evident in Huntington's disease (HD) neuropathology, an inherited, neurodegenerative disease characterized with progressive deterioration in motor, cognitive, and psychiatric functions. In this context, two cellular proteins draw particular interest for this thesis: vesicular glutamate transporter 3 (VGLUT3) and optineurin (OPTN). VGLUT3 modulates glutamate release from selected neurons that are affected by HD, while OPTN is a mGluR5-interacting protein and contributes to neuronal vulnerability in HD. However, current evidence on their involvement in mGluR5 signaling and HD pathogenesis is still lacking. Using VGLUT3 knockout (VGLUT3$^{-/-}$) mice, we showed that this transporter dynamically regulated glutamate receptor densities in different brain regions. Of note, VGLUT3 deletion upregulated mGluR5 in the cerebral cortex and the striatum, unlike the hippocampus which exhibited reduced mGluR5 cell surface densities. We then crossed VGLUT3$^{-/-}$ mice with the zQ175 knock-in mouse model of HD (zQ175:VGLUT3$^{-/-}$) to assess the impact of VGLUT3 transmission loss on HD progression. The longitudinal behavioral assessment revealed that VGLUT3 ablation rescued the deficits in motor coordination and short-term memory in both male and female zQ175 mice throughout 15 months of age. Furthermore, VGLUT3 deletion rescued striatal cell loss likely via activation of Akt and ERK1/2 cellular pathways, with no impact on total mutant huntingtin aggregation or the associated microgliosis. To delineate the role of OPTN in mGluR5 signaling, we employed a CRISPR/Cas9 OPTN-deficient cell line and global OPTN knockout mice. We demonstrated that OPTN was essential for mGluR5-mediated canonical signaling and ERK1/2 activation in both the

striatal cell line, STHdh$^{Q7/Q7}$, and acute hippocampal slices. We then showed that OPTN deletion impaired autophagic machinery via GSK3β/ZBTB16 and mTOR/ULK1 signaling pathways downstream of mGluR5. This work offers novel insights into the molecular roles of VGLUT3 transmission and OPTN in mGluR5 signaling and provides a rationale for their targeting to therapeutically mitigate pathological mGluR5 signaling in HD.

TABLE OF CONTENTS

LIST OF FIGURES

LIST OF TABLES

LIST OF ABBREVIATIONS

4E-BP1	Eukaryotic initiation factor 4E–binding protein 1
5HT	Serotonin
AC	Adenylate cyclase
ACh	Acetylcholine
AD	Alzheimer's disease
Akt	Protein kinase B
AMPAR	α-amino-3-hydroxy-5-methyl-4-isoxazole propionic acid receptor
ATG	Autophagy-related protein
Aβ	Amyloid β protein
BDNF	Brain-derived neurotrophic factor
CAIN	Calcineurin inhibitor protein
cAMP	Cyclic adenosine monophosphate
CKK	Cholecystokinin
CREB	cAMP response element-binding protein
CTEP	2-chloro-4-[2-[2,5-dimethyl-1-[4-(trifluoromethoxy)phenyl]imidazol-4-yl]ethynyl]pyridine
D1R	Dopamine receptor 1
DAG	Diacylglycerol
DHPG	3,5-Dihydroxyphenylglycine
ER	Endoplasmic reticulum
ERK1/2	Extracellular signal-regulated kinase 1/2
GABA	γ-Aminobutyric acid
GKAP	Guanylate kinase-associated protein

GPCRs	G protein-coupled receptors
GSK3β	Glycogen synthase kinase 3β
HD	Huntington’s disease
HTT	Huntingtin protein
iGluR	Ionotropic glutamate receptor
IP_3	Inositol 1,4,5-trisphosphate
LIR	LC3B-interacting region
LTD	Long-term depression
LTP	Long-term potentiation
M1 mAChR	Muscarinic M1 acetylcholine receptor
MEK	Mitogen-activated protein kinases
mGluR	Metabotropic glutamate receptor
mHTT	Mutant huntingtin protein
MPEP	2-methyl-6-(phenylethynyl)-pyridine
MSNs	Medium spiny neurons
mTOR	Mammalian target of rapamycin
NAc	Nucleus accumbens
NAM	Negative allosteric modulator
NF-kB	Nuclear factor kappa B
NEMO	NF-kB-essential molecule
NMDAR	N-methyl-D-aspartate receptor
OPTN	Optineurin protein
p70S6K	Ribosomal S6 kinase

PAM	Positive allosteric modulator
PD	Parkinson’s disease
PDK1/2	Phosphoinositide-dependent kinase 1/2
PI3K	Phosphoinositide 3-kinase
PIKE	Phosphoinositide 3 kinase enhancer
PKA	Protein kinase A
PKC	Protein kinase C
PLC	Phospholipase C
polyQ	Polyglutamine expansion
PRD	Proline-rich domain
PSD95	Post-synaptic density protein-95
Pyk2	Proline-rich tyrosine kinase 2
Rab8	Ras-related protein 8
REST/NRSF	Repressor element-1 transcription factor/neuron restrictive silencer factor
SHANK	SH3 and multiple ankyrin repeat domains
SLC17	Solute Carrier 17
TANs	Tonically active interneurons
TBK1	TANK binding kinase 1
TNF	Tumor necrosis factor
UBAN	Ubiquitin-binding domain
ULK1	Unc-51-like kinase activity
VAChT	Vesicular acetylcholine transporter
VFT	Venus Flytrap

VGLUT	Vesicular glutamate transporter
VIAAT	Vesicular inhibitory amino acid transporter
VMAT	Vesicular monoamine transporter
VPS34	Vacuolar protein sorting 34/class III phosphoinositide 3-kinase
VTA	Ventral tegmental area
ZBTB16	Zinc finger and BTB domain-containing protein 16

To My Wonderful Family

ACKNOWLEDGEMENTS

I would like to start by acknowledging and thanking my supervisor, **Dr. Stephen Ferguson**, for giving me the opportunity to join the lab. I am genuinely grateful for your invaluable guidance and heartfelt support throughout the years of my studies. Your vast knowledge and humble attitude were a strong motivation for me and continue to surprise me every day. You have supported me from day one, and no words can describe my gratitude toward you. Dr. Ferguson, please accept my HUGE thanks.

I would also like to thank the members of my thesis advisory committee: **Dr. Paul Albert**, **Dr. Mario Tiberi**, and **Dr. Ruth Slack**. They have been instrumental in the success of my research by supporting me and providing me with great feedback and advice.

Next, I would like to acknowledge the second in command in our lab, **Dr. Khaled Abdelrahman**. I don't think things would have progressed the way they did without your sincere mentorship and continuous support. I want to express my deepest gratitude to you for your support and for always being an excellent friend and amazing mentor. Your presence for students/staff in the lab helped create a healthy and productive work environment and allowed our efforts to move forward, so thank you for that.

I would like to acknowledge several people who directly contributed to this work. I thank our collaborator, **Dr. Salah El Mestikawy**, for his advice and for providing the mouse model for the VGLUT3 project. **Shaunessy Hutchinson**, for her genotyping and animal breeding efforts. **Tash-Lynn Colson**, for her cheerful, positive attitude and invaluable assistance in this work. I would also like to thank **Caitlyn McLaren** for her dedication and hard work in the OPTN project. In addition, I am very grateful to Mark

and Gail Marcogliese and Nicole Bégin-Heick Graduate fellowships for supporting part of my stipend during the doctoral program.

It is also important to acknowledge the assistance and efforts of the staff at the Animal Behavior and Physiology Core and Louise Pelletier Histology Core facilities at the University of Ottawa. A special thanks to **Mirela Barclay** for teaching me how to properly conduct my animal experiments and for providing me with continuous assistance.

I would like to thank and express my gratitude to each one in the “Ferguson Tribe”, past and present, for sharing their expertise and assisting in this work. I cannot thank you enough for the stimulating conversations and your company. A special thanks to **Dr. Maha Hammad** for her advice and sincerity in teaching me cell culture experiments. I would also like to thank our new postdoc fellow **Dr. Zoë Tasma** for her assistance in reviewing my thesis and for offering valuable suggestions.

A special thanks to my close friends who were my second family, **Mohamad Taha, Hamood AlSudais, and Husni AlNaji**. I really would not have made it that far without you! Thanks for always sticking around!

Finally, and yet importantly, I could not have completed this thesis without the prayers, love, encouragement, and unwavering support from my family. You are my life's greatest blessing! **Dad**, you inspired me to be who I am today. I truly miss you, but you have never left my heart. **Mom**, you are my superhero! No words can do justice to what you have done for me and our family. I hope I make you proud, I am forever indebted! **My brothers**, thank you for your love, support, and understanding. I love you.

Chapter 1.
General introduction

G protein-coupled receptors (GPCRs) are the largest family of cell membrane proteins, with more than 800 identified in the human proteome (Foord et al., 2005). Being involved in various physiological and pathological regulations, GPCRs are critical for eukaryotic signal transduction and regulate a wide array of signaling cascades in response to neurotransmitters, hormones, ions, photons, odorants, and other stimuli (Fredriksson et al., 2003; Hauser et al., 2017). The complexity and diversity of GPCR signaling networks make these receptors valuable drug targets for many diseases.

1.1. GPCR structure and signaling

All GPCRs are composed of an extracellular N terminus, an intracellular C terminus, and a transmembrane heptahelical bundle connected by extracellular and intracellular loops (Hilger et al., 2018). At the cellular level, GPCRs are coupled with heterotrimeric G proteins; Gα, Gβ, and Gγ. In the absence of a ligand, GDP-bound Gα together with G$\beta\gamma$ are attached to the plasma membrane (Neer, 1995; Li et al., 2002). The canonical signaling cascade requires a conformational switch of GPCRs that mediates the rearrangement of their principal effectors, the heterotrimeric G proteins, to start the transduction pathway (Hilger et al., 2018). Upon ligand binding, GPCRs are activated and act as guanine nucleotide exchange factors promoting GTP-bound Gα dissociation from the G$\beta\gamma$ complex. Gα intrinsic GTPase activity catalyzes the hydrolysis of GTP leading to the reassociation of Gα with G$\beta\gamma$ for the next round of activation (Neer, 1995; Vögler et al., 2008). In addition, G$\beta\gamma$ recruits a number of GPCR kinases and acts as a negative feedback loop to phosphorylate and inhibit receptor activation. In addition, G protein-coupled receptor kinase (GRK)-mediated phosphorylation promotes GPCRs binding to β-arrestins followed by their internalization

into vesicles (Ferguson, 2001; Magalhaes et al., 2012). Remarkably, GPCR signaling can be mediated either on the cell surface or intracellularly from within vesicles (Eichel and von Zastrow, 2018). In addition, GPCRs can signal independently of G protein mechanisms such via β-arrestin-mediated signaling via Src and mitogen-activated kinase pathways (Luttrell et al., 1999; Ferguson, 2007; Luttrell, 2008; Magalhaes et al., 2012). GPCRs can also mediate cell signaling by acting as scaffolds for the recruitment of GPCR interacting proteins, located either in the transmembrane or intracellularly, that can further modulate GPCR function and signal transduction (Bockaert et al., 2010).

All organisms encode different G proteins subtypes, and different heterotrimeric combinations of these proteins preferentially activate various downstream signaling cascades. There are four different Gα protein families: G$\alpha_{s,}$ G$\alpha_{i/o}$, G$\alpha_{q/11}$, and G$\alpha_{12/13}$ (Wettschureck and Offermanns, 2005). Gα_{s} and G$\alpha_{i/o}$ regulate adenylate cyclase (AC) activities, where Gα_{s} stimulates and G$\alpha_{i/o}$ suppresses AC activation. Gα_{s}-mediated AC activation catalyzes the conversion of ATP to cAMP and ultimately increases cAMP intracellular levels, which acts as a secondary messenger and subsequently activates its major target, protein kinase A (PKA) (Beebe, 1994; Sassone-Corsi, 2012). The third Gα protein family, G$\alpha_{q/11}$ binds and triggers phospholipase C (PLC) activation which in turn catalyzes the conversion of phosphatidylinositol 4,5-bisphosphate to inositol 1,4,5-trisphosphate (IP_3) and diacylglycerol (DAG) (Kadamur and Ross, 2013). Finally, G$\alpha_{12/13}$ targets Rho guanine-nucleotide exchange factor and regulates actin cytoskeleton organization such as neurite retraction (Katoh et al., 1998; Suzuki et al., 2009). Therefore, the GPCR-G protein system represents a complex hub with versatile multi-protein signaling mechanisms.

1.1.1. GPCR Classes

There are different classification methods for GPCRs based on their physiological and structural features (Foord et al., 2005). The most frequently used method groups GPCRs into six classes: A, B, C, D, E, and F (Attwood and Findlay, 1994; Kolakowski, 1994), and is based on amino acid sequence similarities and functional correlations between GPCRs from both vertebrates and invertebrates. A more recent classification system has been developed for mammalian GPCRs and is based on the phylogenetic tree of the identified 800 human GPCR sequences (Schiöth and Fredriksson, 2005). In this GRAFS method, GPCRs are grouped into five families: Glutamate, Rhodopsin, Adhesion, Frizzled/taste2, and Secretin. The latter two classification methods are similar with one major difference in the further division of class B GPCRs into Secretin and Adhesion receptor families.

Class C GPCRs include glutamate, γ-Aminobutyric acid (GABA), calcium (Ca^{2+})-sensing, and taste receptors. They exhibit the typical seven transmembrane helices with an extensive (~600 residues) extracellular N-terminal domain, known as a Venus Flytrap (VFT) (Kniazeff et al., 2011). The extracellular region is comprised of two lobes that undergo a conformational change upon binding of ligands such as glutamate, GABA, or Ca^{2+}, evoking rearrangements to the transmembrane domains via cysteine-rich region (Bessis et al., 2002; Kniazeff et al., 2011). This activation mechanism is applicable in all Class C GPCRs with the exception of $GABA_B$ receptor, which lacks a cysteine-rich region, implying that VFT can directly activate the transmembrane helices in this receptor (Kniazeff et al., 2011).

1.1.2. Glutamate receptors

Glutamate responses are primarily mediated via two classes of receptors, ionotropic (iGluRs) and metabotropic (mGluRs) glutamate receptors. These two receptor classes are functionally distinct based on the observation of glutamate-evoked excitatory currents (Curtis et al., 1959) and/or secondary messengers formation (Sladeczek et al., 1985). mGluRs mediate relatively slower cellular responses via G protein-dependent and -independent signaling cascades while iGluRs are ligand-gated ion channels that mediate fast excitatory ionic currents in cells (Traynelis et al., 2010; Ribeiro et al., 2011). The iGluR family comprises three receptor subtypes: α-amino-3-hydroxy-5-methyl-4-isoxazole propionic acid (AMPARs), N-methyl-D-aspartate (NMDARs), and kainate receptors (Traynelis et al., 2010). iGluRs are widely expressed across various brain regions with minor variation, and typically multiple subtypes exist on the same neuron (Hadzic et al., 2017). AMPARs and kainate receptors elicit comparable biophysical responses. Both receptors promptly open within 1 ms of glutamate binding and evoke fast excitatory currents that provide initial depolarization and typically facilitate NMDAR channel activation. However, NMDAR activation is relatively delayed as its channel are blocked by Mg^{2+} ions and neuronal depolarization mediates Ca^{2+} influx that ultimately activates selected intracellular kinases and phosphatases (Traynelis et al., 2010).

mGluRs belong to class C GPCRs that exist as constitutive dimers and promote the dissociation of the G protein Gα- and G$\beta\gamma$-subunits with subsequent change in levels of secondary messengers, regulation of ion channels, or stimulation of G protein-independent pathways (Pin et al., 2003; Gerber et al., 2007; Ribeiro et al.,

2011). mGluRs are classified into three subcategories based on sequence homology, ligand selectivity, and mode of G protein coupling (Pin et al., 2003; Katritch et al., 2013). Group I mGluR, which consists of mGluR1 and mGluR5, preferentially couples to $G\alpha_{q/11}$ proteins and mediates downstream signaling via stimulation of the PLC/protein kinase C (PKC) pathway (**Figure 1.1.**) (Abdul-Ghani et al., 1996; Dhami and Ferguson, 2006). Group II includes mGluR2 and mGluR3, while group III includes mGluR4, mGluR6, mGluR7, and mGluR8. All of group II and III mGluRs are coupled to inhibitory $G_{i/o}$ proteins that suppress cyclic adenosine monophosphate (cAMP) formation via inhibition of AC (Schoepp, 2001), with the exception of mGluR3 that can inhibit guanylate cyclase as well (Wroblewska et al., 2006).

1.1.3. Metabotropic glutamate receptor 5 (mGluR5)

All members of mGluRs are predominantly located in the perisynaptic zones of neuronal terminals. Both group II and III mGluRs exist primarily presynaptically as autoreceptors regulating glutamate release. However, in some neurons, mGluR2/3 can also be expressed at postsynaptic sites (Neki et al., 1996; Ohishi et al., 1998; Schoepp, 2001). On the other hand, Group I mGluRs are located in the vicinity of iGluRs at postsynaptic sites, where they actively regulate neuronal excitability (Shigemoto et al., 1993; Luján et al., 1996). Similarly, mGluR5 is primarily localized in the postsynaptic densities and can also be found presynaptically and in the nuclear membrane of neurons (Shigemoto et al., 1993; Takumi et al., 1999; Jong et al., 2005). In addition to neurons, mGluR5 expression is rich in glial cells such as astrocytes and microglia (Biber et al., 2001; Byrnes et al., 2009). Across the brain, mGluR5 is expressed in the hippocampus, striatum, cerebral cortex, olfactory bulb, and thalamus

(Shigemoto et al., 1993; Romano et al., 1995). Owing to its role in various signal transduction mechanisms regulating synaptic maintenance, neuronal survival, and development (**Figure 1.1.**), mGluR5 is considered an attractive pharmacological target for the treatment of different neurodegenerative and neurological diseases (Ribeiro et al., 2017; Abd-Elrahman and Ferguson, 2022; Su et al., 2022).

1.1.3.1. mGluR5 canonical signaling

mGluR5 canonical signaling primarily depends on the affinity displayed towards a particular G protein subclass. Being primarily coupled to $G\alpha_{q/11}$ proteins, mGluR5 activates the PLC/PKC/Ca^{2+} pathway (**Figure 1.1.**) (Dhami and Ferguson, 2006). PKC has been proposed to trigger the activation of other cellular pathways such as phospholipase A_2, phospholipase D, and mitogen-activated protein kinases (MEK), along with the regulation of numerous ion channels (Hermans and Challiss, 2001; Ribeiro et al., 2017). In addition to $G\alpha_{q/11}$ protein coupling, mGluR1/5 can couple to alternative G proteins ($G_{i/o}$ and/or G_s). However, this is largely influenced by the cellular context and levels of mGluR5 expression (Abe et al., 1992; Joly et al., 1995; Francesconi and Duvoisin, 1998; Balázs et al., 2002).

1.1.3.2. mGluR5-dependent regulation of NMDARs

The interaction between mGluR5 and NMDARs is crucial for proper neuronal excitation and synaptic plasticity formation (Harvey and Collingridge, 1993; Awad et al., 2000). This interaction is mediated via cellular protein scaffolds including Homer, post-synaptic density protein-95 (PSD95), and SHANK that activate Ca^{2+}-dependent signaling cascades and regulate synaptic function and transmission (**Figure 1.1.**) (Tu et al., 1998, 1999; Husi et al., 2000). Interestingly, mGluR5 activation drives the

exchange of NMDAR subunit NR2B to NR2A resulting in modification of the receptor signaling cascade and indicating that modulation by mGluR5 may be dependent on the NMDAR subtype (Matta et al., 2011). The mGluR5/NMDAR crosstalk is also dependent on biased mGluR5 signaling as treatment with mGluR5 positive allosteric modulator (PAM), VU0409551, selectively potentiates mGluR5 coupling to $G\alpha_{q/11}$ signaling but not mGluR5-mediated potentiation of NMDAR currents (Rook et al., 2015). On the other hand, NMDARs can reverse mGluR5 desensitization via dephosphorylation of PKC phosphorylation sites on mGluR5 (Alagarsamy et al., 1999). Overall, these highlight the complexity within mGluR5 signaling profiles in mediating neuronal excitability and synaptic plasticity responses.

1.1.3.3. mGluR5-dependent activation of ERK1/2 signaling

A variety of noncanonical signaling events involved in synaptic plasticity, neuronal proliferation, and survival are orchestrated via mGluR5. Extracellular signal-regulated kinase 1/2 (ERK1/2) represents a vital downstream mediator in mGluR5-dependent synaptic plasticity mechanisms encompassing; gene transcription regulation, messenger RNA (mRNA) translation, and synaptic protein synthesis (Banko et al., 2006; Stoppel et al., 2017; Ibrahim et al., 2021). Remarkably, mGluR5-mediated ERK1/2 activation can occur in PKC -dependent and -independent mechanisms (**Figure 1.1.**) (Fitzjohn et al., 2001; Hermans and Challiss, 2001). For instance, mGluR5 couples to β-arrestin2 to trigger ERK1/2 phosphorylation and mediate mGluR-dependent synaptic plasticity responses (Lefkowitz and Shenoy, 2005; Eng et al., 2016; Stoppel et al., 2017). Knocking out β-arrestin2 in mice impairs ERK1/2 signaling and synaptic protein synthesis in response to mGluR5 activation with minimal alterations in $G\alpha_{q/11}$ -

mediated cellular Ca^{2+} release (Eng et al., 2016; Stoppel et al., 2017). In addition, Homer scaffolding proteins have been shown to link mGluR5 to ERK1/2 signaling and play a role in mGluR5-mediated transcriptional regulation in neurons (Guhan and Lu, 2004; Mao et al., 2005). Disrupting Homer1/mGluR5 interactions using either Tat-fusion peptides or small interfering RNAs reduces mGluR5-stimulated ERK1/2 activation (Mao et al., 2005). In addition to its role in synaptic plasticity mechanisms, mGluR5-mediated ERK1/2 signaling can regulate activity-dependent neuronal excitability. For instance, mGluR5 activation attenuates inhibitory glycinergic currents via ERK-dependent phosphorylation of α1 subunit-containing glycine receptor (Zhang et al., 2019).

1.1.3.4. mGluR5-dependent activation of PI3K/Akt/mTOR signaling

Phosphoinositide 3 kinase (PI3K)/protein kinase B (Akt)/mammalian target of rapamycin (mTOR) pathway is one of the main signaling cascades involved in mGluR5-dependent regulation of protein synthesis, synaptic plasticity, and autophagy (Hou and Klann, 2004; Kim et al., 2011; Perluigi et al., 2015). Stimulation of group I mGluRs enhance the formation of a scaffold complex comprising mGluR, Homer, and GTPase phosphoinositide 3 kinase enhancers (PIKEs) that promote PI3K activation (Rong et al., 2003; Guhan and Lu, 2004). Activation of PI3K catalyzes the phosphorylation of phosphoinositide-dependent kinase 1/2 (PDK1/2), which subsequently phosphorylates and activates Akt, leading to the stimulation of mTOR signaling cascade (**Figure 1.1.**) (Porta et al., 2014; Dibble and Cantley, 2015). Ribosomal S6 kinase (p70S6K) and eukaryotic initiation factor 4E–binding protein 1 (4E-BP1) are activated downstream of this pathway, both molecules are vital for mGluR5-induced mRNA translation and long-term depression (LTD) (Hou and Klann, 2004; Ronesi and Huber, 2008). Disrupting the

interaction of mGluR5 with Homer and PIKE attenuates PI3K/Akt/mTOR signaling and ultimately disrupts synaptic protein synthesis (Mao et al., 2005; Ronesi and Huber, 2008).

1.1.3.5. mGluR5 regulation of autophagy

Autophagy is an essential lysosomal degradative process that contributes to cellular homeostasis via the degradation and recycling of long-lived, aggregated, and misfolded proteins, clearing damaged organelles, and extracellular pathogens (Nixon, 2013). Emerging evidence has depicted mGluR5 involvement in the regulation of autophagy via multiple convergent cellular pathways (**Figure 1.1.**). Unc-51-like kinase 1 (ULK1) is a protein kinase critical for the initiation of autophagosome formation and is directly regulated by mTOR signaling (Zachari and Ganley, 2017). ULK1 exists in an autophagosome initiation protein complex that comprises autophagy-related protein 101 and 13 (ATG101, ATG13) and focal adhesion kinase family interacting protein of 200 kDa (FIP200) (Ganley et al., 2009). Activation of ULK1 leads to the translocation of a protein complex containing beclin1 and class III phosphoinositide 3-kinase (VPS34) from the cytoskeleton to preautophagosomal structure to induce autophagosome formation (Nixon, 2013; Russell et al., 2013; Zachari and Ganley, 2017). This process is suppressed by inhibitory ULK1 phosphorylation at Ser757 mediated via mTOR complex, and this has been linked to impaired mGluR5-dependent autophagy signaling in mouse models of Alzheimer's Disease (AD) and Huntington's Disease (HD) (Abd-Elrahman et al., 2017, 2018). On the other hand, mGluR5 can regulate autophagy via the zinc finger and BTB domain containing 16 (ZBTB16)-dependent pathway (**Figure 1.1.**) (Abd-Elrahman et al., 2017, 2020b). ZBTB16 exists in multiple E3 ubiquitin-protein

ligase complexes and can be phosphorylated by glycogen synthase kinase 3β (GSK3β) at Ser184/Thr282 (Zhang et al., 2015). This leads to ZBTB16 autoubiquitination and degradation (Zhang et al., 2015). In addition, ZBTB16 phosphorylation disrupts its interaction with autophagy adaptor ATG14, a component of the VPS34 autophagic complex, reducing ATG14 degradation and thereby promoting autophagy flux (Russell et al., 2013; Zhang et al., 2015). Therefore, GSK3β/ZBTB16 provides a regulatory link between autophagy and proteasome machineries within the cell. Overactivation of mGluR5 signaling in AD and HD mouse models inhibits GSK3β activity via phosphorylation at Ser9 resulting in the accumulation of ZBTB16 and ultimately suppressing autophagic flux (Abd-Elrahman et al., 2017, 2018, 2020b). This aberrant signaling is likely regulated through the PI3K/Akt pathway which acts as a mediator for mGluR5-mediated suppression of GSK3β activation (Beaulieu et al., 2009; Beurel et al., 2015). Together, mGluR5-regulated autophagy appears to be crucial in orchestrating the balance between levels of synaptic protein synthesis as well as clearing misfolded aggregates from synapses.

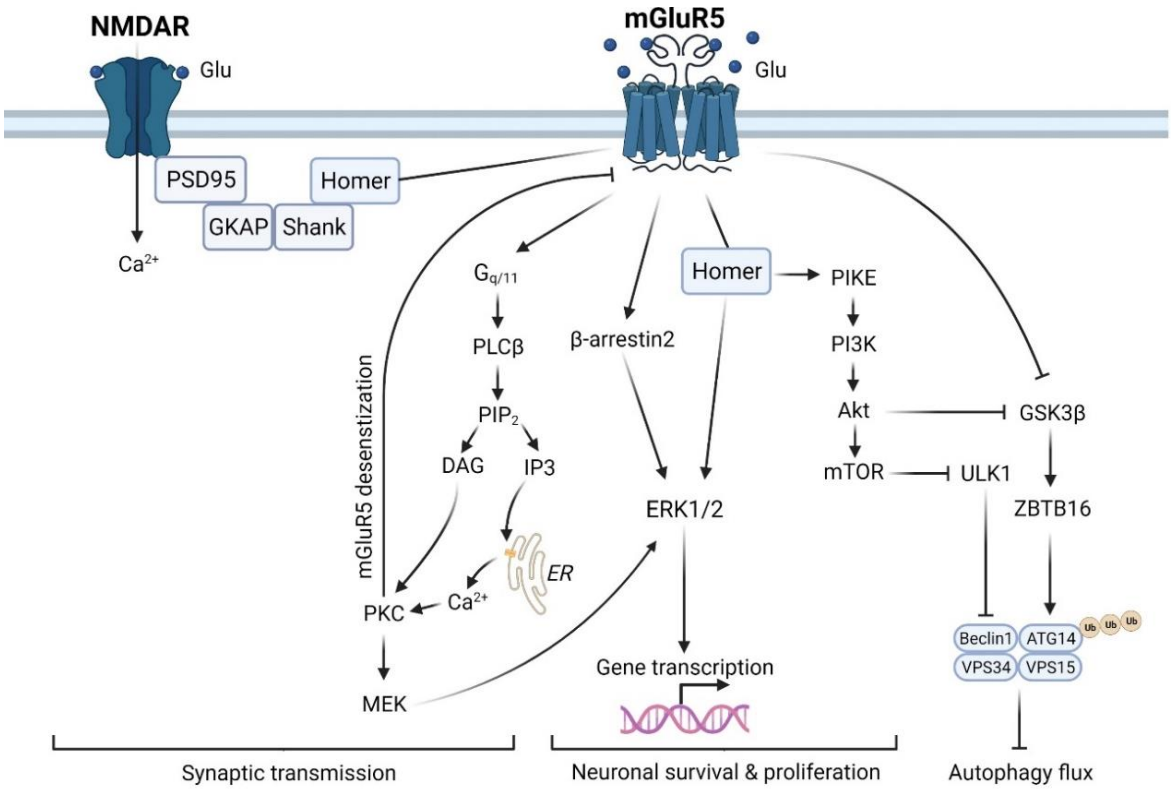

Figure 1.1. Metabotropic glutamate receptor 5 (mGluR5) canonical and noncanonical signaling. Glutamate (Glu) binds to mGluR5 and promotes the activation of $G_{\alpha q/11}$ proteins, stimulating phospholipase β (PLCβ) to catalyze the breakdown of phosphatidylinositol 4,5-bisphosphate (PIP2) and form diacylglycerol (DAG) and inositol 1,4,5-trisphosphate (IP_3), the latter promotes the release of Ca^{2+} from intracellular stores. Both DAG and Ca^{2+} activate protein kinase C (PKC), which can activate mitogen-activated protein kinase (MEK). In addition, mGluR5-mediated PKC activation leads to stimulation of N-methyl-d-aspartic acid receptors (NMDARs) by increasing channel open probability. mGluR5 physically interacts and associates with NMDARs via a complex involving Homer, SH3, and multiple ankyrin repeat domains (SHANK) protein, postsynaptic density-95 (PSD95), and guanylate kinase-associated protein (GKAP). mGluR5 can trigger ERK1/2 activation via Homer and β-arrestin2. Furthermore, Homer proteins couple mGluR5 to phosphoinositide 3 kinase enhancer (PIKE), leading to enhanced phosphoinositide 3 kinase (PI3K) activity. PI3K activates protein kinase B (Akt) that ultimately activates the mammalian target of rapamycin (mTOR) signaling complex. mGluR5-mediated ERK1/2 and Akt/mTOR signaling

promote cellular processes involved in neuronal survival and proliferation. Moreover, mTOR can phosphorylate and suppress unc-51-like kinase 1 (ULK1) catalytic activity to abolish the phosphorylation of beclin1 required for autophagy induction by class III phosphoinositide 3-kinase (VPS34) complexes. mGluR5 promotes inhibitory phosphorylation of glycogen synthase kinase 3β (GSK3β) which increases levels of zinc finger and BTB domain-containing protein 16 (ZBTB16). This leads to ubiquitination and proteasomal degradation of autophagy-related 14 (ATG14) protein which disrupts the VPS34 complex and inhibits autophagic flux. The figure is created using BioRender.

1.2. Vesicular glutamate transporters

The quantal exocytic release of neurotransmitters depends on their transport and subsequent packaging into synaptic vesicles. Such activity is mediated via transporter proteins located mainly on synaptic vesicles, as well as the plasma membrane to facilitate the vesicle recycling process (Fernández-Alfonso et al., 2006; Hua et al., 2011). Glutamate packaging into synaptic vesicles is considered a key step in escorting glutamate to the neurotransmitter pathway, away from metabolic pathways (Otis, 2001). Vesicular glutamate transporters (VGLUTs) together with v-type proton-pump ATPase cooperatively ensure sufficient concentration of glutamate into synaptic vesicles prior to its exocytotic release into the synaptic cleft. In this process, proton-pump ATPases generate an electrochemical proton gradient across vesicular membranes that is efficiently harnessed by VGLUTs in order to function properly (Fremeau et al., 2004). In addition, the vesicular membrane harbors glycolytic ATP-generating enzymes; glyceraldehyde-3-phosphate dehydrogenase/3-phosphoglycerate kinase complex and pyruvate kinase which are essential for VGLUTs' active transport function (Ikemoto et al., 2003; Fremeau et al., 2004; Ishida et al., 2009).

VGLUTs are members of the Solute Carrier 17 (SLC17) phosphate transporter family, and three isoforms (VGLUT1-3) have been identified in mammalian tissues (Fremeau et al., 2004; El Mestikawy et al., 2011). VGLUTs exhibit various regional localizations across the brain. Based on their distribution, VGLUTs perform distinct physiologic functions, with no alterations in their uptake functions (Kaneko and Fujiyama, 2002; Preobraschenski et al., 2014). In the adult brain, VGLUT1 and VGLUT2 have complementary regional distributions. VGLUT1 is predominantly expressed in the

telencephalon including the cerebral cortex, hippocampus, and amygdala, while VGLUT2 is mainly expressed in the diencephalon and lower brain stem regions (Kaneko and Fujiyama, 2002; Fremeau et al., 2004). However, in some regions within the developing and adult brains, VGLUT1 and VGLUT2 can colocalize on the same glutamatergic neuron (Fremeau et al., 2004; Herzog et al., 2006; Persson et al., 2006). Both VGLUT1 and VGLUT2 can indirectly modulate glutamate release from presynaptic nerve terminals. Some reports have shown that synaptic quantal size and magnitude of both miniature and evoked excitatory postsynaptic potentials are proportional to the numbers of VGLUT copies on synaptic vesicles (Wojcik et al., 2004; Wilson, 2005; Moechars et al., 2006). Yet, these findings are still a matter of debate.

Unlike VGLUT1/2 widespread topography in the brain, VGLUT3 is expressed by selected neurons and interneurons scattered in different brain regions (Herzog et al., 2004; Vigneault et al., 2015). In particular, VGLUT3 is expressed in neurons that co-release glutamate with non-glutamatergic neurotransmitters such as acetylcholine (ACh), serotonin (5HT), or GABA (Fremeau et al., 2002; Gras et al., 2002; Schäfer et al., 2002). In these neurons, VGLUT3 mediates and presumably influences the packaging of glutamate and co-released neurotransmitters. For instance, cholinergic interneurons in the striatum, also known as tonically active interneurons (TANs), express VGLUT3 and co-release glutamate with ACh (Gras et al., 2008). These dual currents are notably dependent on VGLUT3 expression (Gras et al., 2008; Higley et al., 2011; Nelson et al., 2014). Serotoninergic and GABAergic neurons also recruit VGLUT3-mediated signaling to regulate glutamatergic excitatory inputs onto

hippocampal pyramidal neurons (Varga et al., 2009; Amilhon et al., 2010; Zimmermann et al., 2015).

Similar to VGLUT3, recent evidence has implicated VGLUT1/2 in regulating glutamate co-transmission with other neurotransmitters such as GABA, monoamine, and ACh in different classes of neurons (reviewed in Trudeau and El Mestikawy, 2018). In these neurons, VGLUTs can modify the vesicle's capacity to accumulate these neurotransmitters, in part via glutamate-mediated changes in pH gradient (Aguilar et al., 2017). On the other hand, co-released neurotransmitters can modulate glutamate release via a regulatory feedback loop. This dynamic co-transmission has significant implications on motor and reward behaviors and is compromised in a number of psychiatric disorders (El Mestikawy et al., 2011; Trudeau and El Mestikawy, 2018). Collectively, this shows that VGLUT expression is essential in finetuning glutamatergic transmission across various types of neurons and potentially influences co-released neurotransmitters.

1.2.1. VGLUT3 neurotransmission

Unraveling the complex role of VGLUT3-mediated regulation of different brain circuits has garnered much interest due to its unique cellular and anatomical features (Ibrahim et al., 2020; Favier et al., 2021). Compared with VGLUT1/2, VGLUT3 has the particularity to be expressed in both the soma and dendritic processes of primarily "non-glutamatergic" neurons located in the raphe nuclei, striatum, hippocampus, cerebral cortex, inner hair cells, and transiently in the cerebellum (Gras et al., 2002, 2005; Ruel et al., 2008; Seal et al., 2008; Amilhon et al., 2010). This depicts the subtle, yet complex,

role of VGLUT3-dependent glutamate co-transmission and its influence on various brain functions and dysfunctions.

1.2.1.1. VGLUT3 signaling in the striatum

VGLUT3 mediates the storage and release of glutamate from two neuronal populations within the striatum; TANs and, to a lesser extent, serotonergic raphe neurons (El Mestikawy et al., 2011; Belmer et al., 2019) (**Figure 1.2.**). Although they are relatively less abundant in the striatum, TANs provide VGLUT3-dependent mono- and di-synaptic synaptic contacts to different striatal neurons (Nelson et al., 2014; Kljakic et al., 2017; Rehani et al., 2019). Deletion of VGLUT3 in TANs diminishes postsynaptic responses on both fast-spiking GABAergic interneurons and medium spiny neurons (MSNs) (Higley et al., 2011; Nelson et al., 2014). Remarkably, mGluRs regulate synaptic potentials in TANs, as the activation of mGluR group I or group II either facilitate or suppress TANs excitability within the striatum, respectively (Pisani et al., 2002; Bonsi et al., 2005). Additionally, VGLUT3-mediated neurotransmission provides proxy regulation onto dopaminergic neurons in the nucleus accumbens (NAc). Sakae et al. (2015) showed that genetic deletion of VGLUT3 disinhibited dopaminergic efflux in the NAc of mice. Intriguingly, this observation was mirrored following inhibition of striatal mGluRs in wild-type, not VGLUT3 knockout mice, suggesting that VGLUT3 signaling suppresses dopamine efflux in the NAc via mGluR-dependent mechanisms (Sakae et al., 2015). Overall, this indicates that VGLUT3 signaling axis plays a vital role in maintaining the dynamic balance of excitatory/inhibitory inputs within striatal networks.

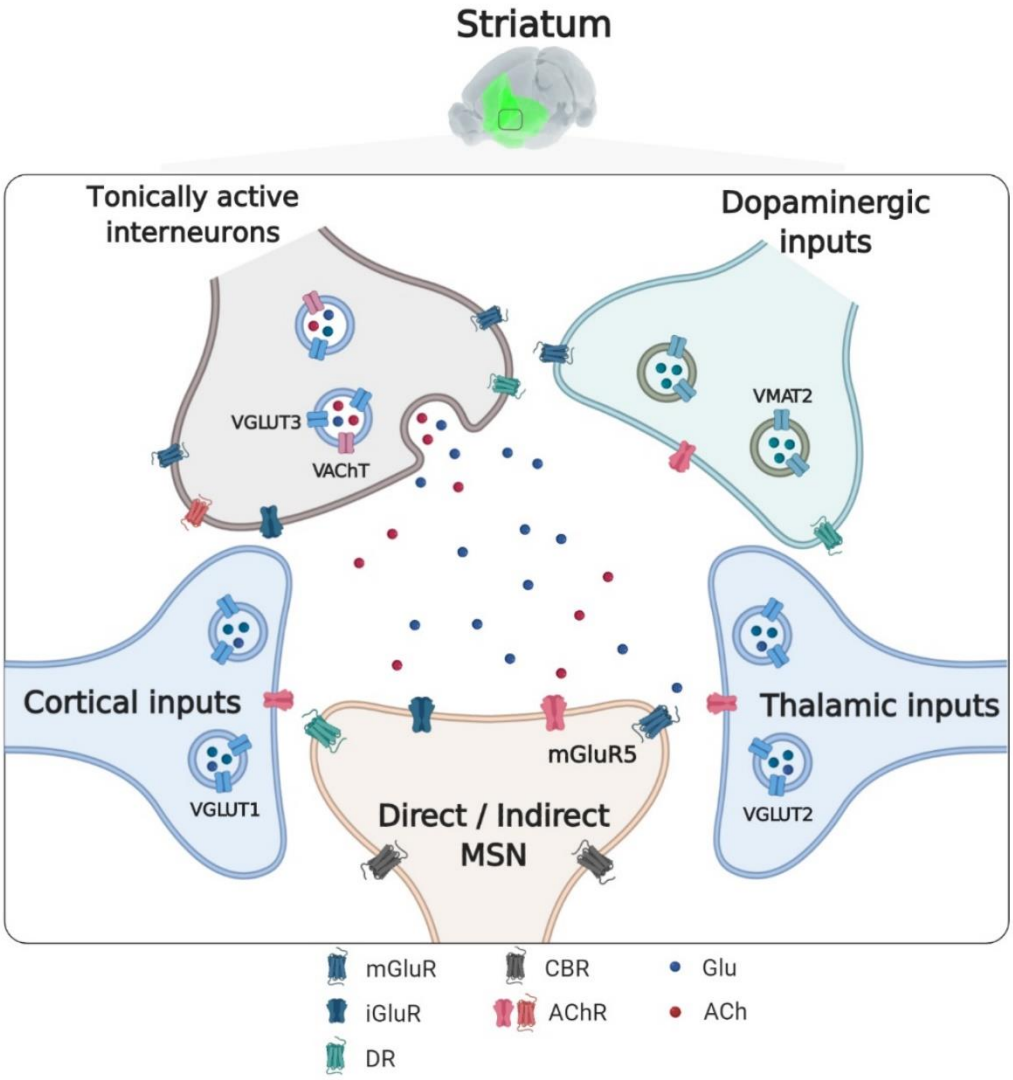

Figure 1.2. VGLUT3 signaling axis in the striatum. Striatal medium spiny neurons (MSNs) form synaptic connections with VGLUT3^{+} tonically active interneurons**.** MSNs also receive glutamatergic afferents from cortical (VGLUT1) and thalamic (VGLUT2) neurons. Dopaminergic inputs from the substantia nigra serve as a modulator for this glutamatergic axis within the striatum. DR, dopamine receptors; CBR, cannabinoid receptors; AChR, acetylcholine receptors; Glu, glutamate; ACh, acetylcholine; VMAT2, vesicular monoamine transporter 2; VAChT, vesicular acetylcholine transporter (Ibrahim et al., 2020).

1.2.1.2. VGLUT3 signaling in the hippocampus

Glutamatergic neurotransmission constitutes the majority of hippocampal circuits; regulating neuronal excitability, network synchronization, and integrating synaptic plasticity inputs from both pyramidal neurons and interneurons (reviewed in Basu and Siegelbaum, 2015). While VGLUT3 is not expressed by pyramidal neurons, VGLUT3 is found in regular-spiking GABAergic interneurons (cholecystokinin (CKK))-positive basket cells) (Somogyi et al., 2004), in addition to subsets of serotoninergic fibers projecting to the hippocampus (Somogyi et al., 2004; Amilhon et al., 2010) (**Figure 1.3.**). VGLUT3-positive basket cells form invaginating synapses with pyramidal cells expressing glutamate and GABA receptors. At these synapses, it is hypothesized that basket cell terminals co-release GABA, glutamate, and CCK, all of which glutamate modulate synaptic functions and neuronal excitability (Omiya et al., 2015; Pelkey et al., 2020). In a study investigating the impact of VGLUT3 signaling on GABAergic neurotransmission, Fasano et al. (2017) showed that glutamate released via VGLUT3 fine-tunes and dampens GABAergic currents onto CA1 pyramidal neurons through presynaptic mGluR group III autoreceptors (Fasano et al., 2017). Together, this highlights the direct involvement of VGLUT3-positive neurons in fine-tuning glutamatergic and GABAergic co-transmission in hippocampal networks.

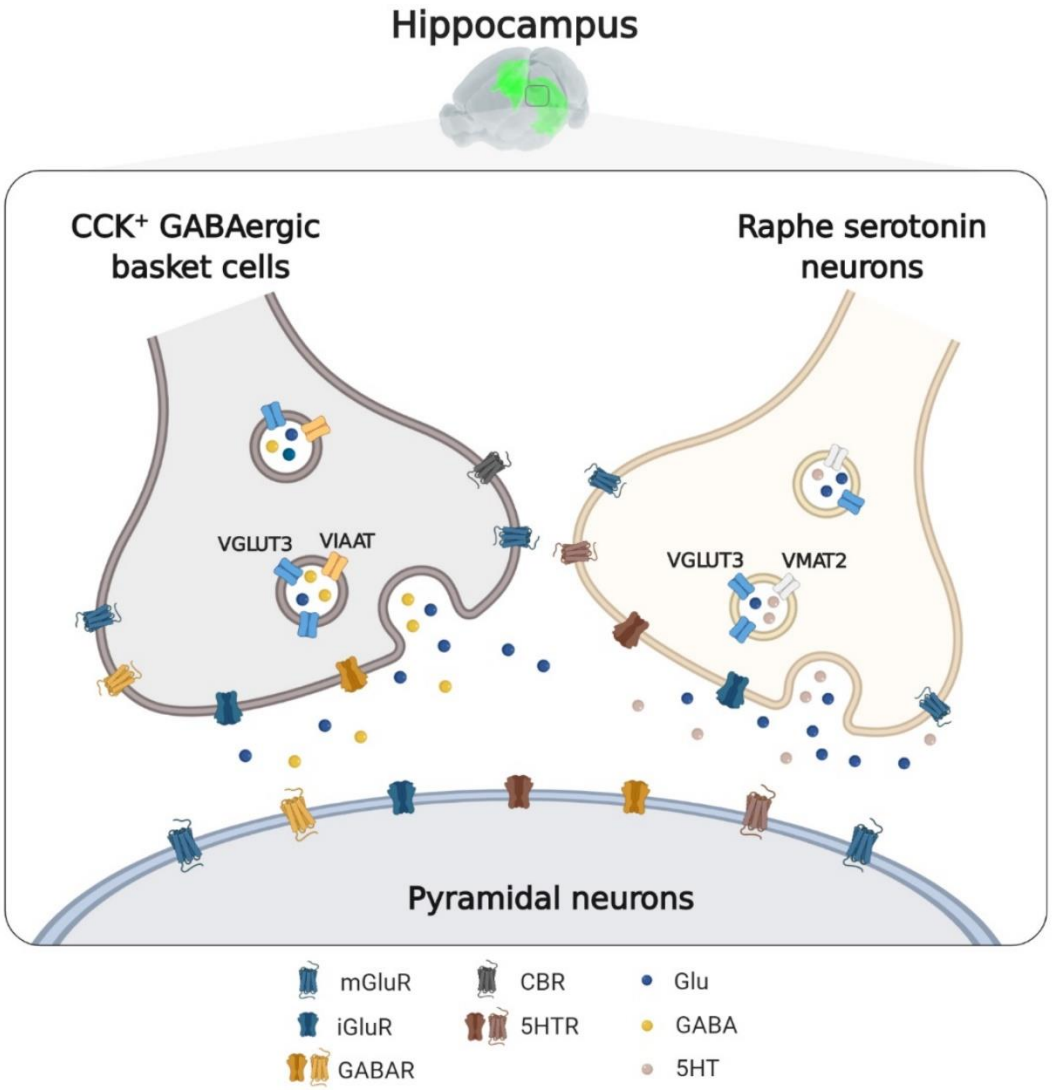

Figure 1.3. VGLUT3 signaling axis in the hippocampus. VGLUT3 is expressed in cholecystokinin (CKK)$^{+}$ GABAergic basket cells which form synaptic connections with glutamatergic pyramidal neurons of the CA1 region. Additionally, pyramidal neurons receive inputs from subpopulations of VGLUT3-expressing terminals from raphe projection neurons. GABAR, GABA receptors; CBR, cannabinoid receptors; 5HTR, serotonin receptors; Glu, glutamate; 5HT, serotonin; VIAAT, vesicular inhibitory amino acid transporter; VMAT2, vesicular monoamine transporter 2 (Ibrahim et al., 2020).

1.2.1.3. VGLUT3 signaling in the raphe network

Raphe nuclei are heterogeneous neuronal populations, with primarily serotoninergic neurons, that exhibit poorly defined cytoarchitecture, and their projections run along the brainstem rostrocaudal extension (Meessen and Olszewski, 1950; Olszewski and Baxter, 1954; Taber et al., 1960). Recent evidence has depicted the neuromodulatory role of glutamate in raphe serotoninergic neurons. Specifically, VGLUT3-mediated neurotransmission was reported in large neuronal populations comprising both dorsal and medial raphe nuclei (Fremeau et al., 2002; Amilhon et al., 2010; Hioki et al., 2010; Wang et al., 2019), that project to different regions across the forebrain including; the hippocampus, striatum, and lateral septum (Dahlström and Fuxe, 1964; Qi et al., 2014; Belmer et al., 2019). Loss of VGLUT3 attenuates $5HT_{1A}$ autoreceptor-mediated neurotransmission in raphe nuclei along with paradoxical suppression of serotoninergic neurotransmission to the projection areas such as the hippocampus and cerebral cortex (Amilhon et al., 2010). Furthermore, VGLUT3-positive serotonergic neurons form a neural pathway to the NAc via the ventral tegmental area (VTA) neurons, which ultimately regulate reward circuitry (Qi et al., 2014; Wang et al., 2019). Specifically, VGLUT3-dependent glutamate release from raphe neurons modulates VTA activity in which the excitatory VGLUT3 inputs evoke and augment VTA dopaminergic neurotransmission into the NAc, an effect that is coordinated via serotoninergic neurotransmission (Wang et al., 2019; Cunha et al., 2020). Overall, this shows that VGLUT3 can be a vital regulator of dopaminergic and serotoninergic transmission along the raphe nuclei/VTA pathway.

1.2.1.4. Role of VGLUT3 in mouse behavior and neurological disorders

In attempt to understand the functional significance of VGLUT3 transmission, VGLUT3 knockout (VGLUT3$^{-/-}$) mice have been generated (Gras et al., 2008). VGLUT3$^{-/-}$ mice exhibit similar body weights and food intake as adult wild-type littermates (Gras et al., 2008). Consistent with this, genetic silencing of VGLUT3 in mouse striatum has no impact on their eating behavior (Favier et al., 2020). In addition, VGLUT3$^{-/-}$ mice exhibit intact memory function and the ability to learn, albeit mild impairments in working memory were noted (Fazekas et al., 2019). Since VGLUT3 neurotransmission is mediated via subpopulations of interneurons scattered in multiple brain microcircuits, knocking out VGLUT3 results in nonconvulsive, intermittent cortical seizures in the electroencephalogram; however, these are not accompanied by tonic-clonic motor activity (Gras et al. 2008; Seal et al. 2008). Furthermore, VGLUT3$^{-/-}$ mice show normal exploratory behavior in their home cage and normal motor coordination, although they are hyperactive during the wake, active phase compared to wild-type littermates (Gras et al., 2008; Divito et al., 2015). VGLUT3 is also expressed in sensory centers including olfactory bulb and auditory hair cells (Ruel et al., 2008; Seal et al., 2008; Tatti et al., 2014). Therefore, VGLUT3-null mice are congenitally deaf (Seal et al., 2008), and a mutation in the *Slc17a8* gene, which encodes VGLUT3, is associated with progressive, high-frequency nonsyndromic deafness in humans (Ruel et al., 2008).

Several lines of evidence have depicted a role for VGLUT3 signaling in anxiety-related behaviors. Under physiological conditions, raphe/amygdala nuclei modulate stress response mechanisms via the hypothalamic-pituitary-adrenal (HPA) axis (Pompili et al., 2010). Loss of VGLUT3 promotes the activation of the HPA axis in mice, resulting

in an anxious phenotype in both newborn and adult mice (Amilhon et al., 2010; Horváth et al., 2018). Novelty-induced hypophagia is also evident in VGLUT3$^{-/-}$ mice compared to wild-type animals (Amilhon et al., 2010). More so, when assessed in different conflict-based paradigms, VGLUT3$^{-/-}$ mice display marked neophobic behavior, further confirming the link between VGLUT3 transmission and anxiety vulnerability (Amilhon et al., 2010; Balázsfi et al., 2018).

Given its involvement in striatal circuitry, several reports have highlighted the role of VGLUT3 in regulating motor and rewarding behaviors in rodents. In particular, VGLUT3 loss leads to evident circadian-dependent increases in dopamine synthesis and release within the striatum which accounts for the hyperlocomotor phenotype in mice (Divito et al., 2015). In addition, the locomotor deficits following dopamine depletion are also improved upon disrupting VGLUT3 signaling (Divito et al., 2015). Moreover, VGLUT3 loss attenuates levodopa (L-DOPA)-induced dyskinetic and dystonic responses in animal models (Gangarossa et al., 2016), suggesting that regulation of striatal dopamine signaling is dependent on VGLUT3 neurotransmission. On the other hand, VGLUT3 neurotransmission regulates the phenotypic deficits associated with drugs of abuse. Global VGLUT3 knock out blunts acute and chronic amphetamine-induced stereotypies in mice (Mansouri-Guilani et al., 2019). Furthermore, striatal VGLUT3 signaling regulates cocaine reward-seeking behavior in animals. Loss of VGLUT3 augments cocaine-reinforcing properties in mice, as assessed in conditioned place preference and operant self-administration paradigms (Sakae et al., 2015). Overall, this indicates that VGLUT3 transmission plays an evident role in striatal-based phenotypic behaviors.

1.3. Huntington's disease (HD)

HD is a rare but devastating disorder affecting 10-13 in 100,000 people of European descent (Evans et al., 2013; Fisher and Hayden, 2014). In Canada, 13 per 100,000 of the general population are diagnosed with HD, with 3,760 more at high risk for developing HD, whereas the occurrence is relatively low in Asian populations (Fisher and Hayden, 2014; Bates et al., 2015). HD is a progressive, autosomal dominant disease caused by trinucleotide CAG repeats expansion in exon 1 of the *Htt* gene on chromosome 4 (MacDonald et al., 1993). This mutation leads to polyglutamine expansion (polyQ) in the N-terminal region of huntingtin protein (HTT) with subsequent aggregation within neurons (MacDonald et al., 1993). Mutations in the huntingtin protein (mHTT) have been associated with a cascade of deleterious events that progressively impair motor, cognitive, and neuropsychiatric functions (MacDonald et al., 1993; Bates et al., 2015). Pathologically, HD is characterized by neurodegeneration of the basal ganglia, mainly the striatum, followed by atrophy of neocortical brain regions (MacDonald et al., 1993). The clinical presentation in patients show variations depending on the severity of the affected brain regions. Typically, subjects with more than 39 CAG repeats are prone to the development of HD symptoms (Andrew et al., 1993; Ross and Tabrizi, 2011). Nevertheless, many studies on premanifest HD patients have reported asymptomatic alterations occurring several years prior to the formal diagnosis (Andrew et al., 1993; Ross and Tabrizi, 2011). Despite the extensive preclinical and clinical research, to date, therapeutic options for HD are limited to palliative management as no disease-modifying therapies are yet available (Dash and Mestre, 2020; Tabrizi et al., 2022).

1.3.1. HD Symptoms

HD symptoms manifest in three consecutive stages. In the early stages, patients experience mood disorders, sleep disturbances, and mild dysfunctions in motor coordination and cognition (Wiegand et al., 1991; Julien et al., 2007; Solomon et al., 2007). In the second stage, patients start to develop excessive and involuntary movements (chorea) and evident deterioration in motor skills such as swallowing, speech, and gait (Bates et al., 2015). This is also associated with deficits in cognitive capacities which typically follow subcortical patterns, and manifest as impaired emotion recognition, slowness in mental processing, and disturbances in both executive and visuospatial functions (Papoutsi et al., 2014; Bates et al., 2015). Furthermore, deterioration in both short-term and long-term memories starts to develop before the onset of motor symptoms, and it progresses through the entire course of the disease (Montoya et al., 2006). In the third stage, bradykinesia and body rigidity replace chorea, ultimately leading to a general decline in health and inevitable death occurring within 15-20 years of disease onset (Li and Li, 2004; Bates et al., 2015). This hypokinetic phase shows an association with disease duration and CAG repeat length, unlike chorea (Rosenblatt et al., 2006). Furthermore, various psychiatric symptoms are evident in HD patients, and to a lesser extent at the premanifest stage, including anxiety, irritability, apathy, depression, disinhibition, obsessive-compulsive behavior, and psychosis (Craufurd et al., 2001; Walker, 2007; Bates et al., 2015). Neuroinflammation is another feature in HD patients, affecting both central and peripheral nervous systems (Rocha et al., 2016). Significant microglial activation was reported in post-mortem

specimens from the striatum, globus pallidus, and the cortex of HD patients (Myers et al., 1991).

1.3.2. Huntingtin protein (HTT)

HTT is a large protein that consists of 3144 amino acids with a size of about 350 kDa (Parsons and Raymond, 2015). HTT is mostly expressed in the cytoplasm with the ability to localize in the nucleus through specific sequences at both N- and C- termini of the protein (Xia et al., 2003; Desmond et al., 2012). Polyglutamine expansions at the N-terminus of HTT disrupt its ability to interact with nuclear pore proteins leading to nuclear accumulation (Cornett et al., 2005; Parsons and Raymond, 2015).

1.3.2.1. Functions of HTT

HTT elicits various physiological functions in both the developing and mature nervous systems. HTT is vital for early embryonic development and neurogenesis, and knocking out HTT in mice leads to embryonic lethality at E7 prior to the emergence of the nervous system (Nasir et al., 1995; Zeitlin et al., 1995). More so, mice expressing less than 50% of the normal protein, show evident malformations in their cerebral cortex and striatum (White et al., 1997). In addition, HTT acts as a scaffolding protein interacting with β-tubulin and microtubules (Hoffner et al., 2002). It also interacts with the dynein/dynactin complex and regulates the intracellular trafficking processes (Caviston et al., 2007). In the nucleus, HTT is involved in the transcriptional regulation of the brain-derived neurotrophic factor (BDNF) gene, a pro-survival that is vital for neuronal survival and growth (Zuccato et al., 2001, 2003). HTT sequesters and inhibits the cytoplasmic activity of repressor element-1 transcription factor/neuron restrictive silencer factor (REST/NRSF) that negatively regulates BDNF transcription (Zuccato et

al., 2001, 2003). Furthermore, HTT is critical for normal synaptic transmission as it is associated with presynaptic vesicles (DiFiglia et al., 1995), as well as postsynaptic PSD95 scaffolds in the nerve terminals (Sun et al., 2001). Additionally, HTT is required for the correct development of cortical and striatal excitatory synapses. Silencing the *Htt* gene in developing mouse cortex accelerates cortical and striatal excitatory synapses formation and maturation through postnatal day 21 (McKinstry et al., 2014). Overall, this underscores the variety of cellular processes that are regulated via HTT and that disruption of such physiological mechanisms potentially underlies HD pathogenesis.

1.3.3. HD mouse models

Numerous HD animal models have been generated in attempt to understand HD pathogenesis and evaluate potential therapeutics. Prior to the discovery of genetic mutation causing HD, animals with striatal lesions via neurotoxins were employed as HD animal models (McGeer and McGeer, 1976; Beal et al., 1986). The bases for these models were the observation that the striatum was the primary site of neurodegeneration in HD and that intrastriatal injections of glutamate receptor agonists led to selective loss of the GABAergic MSNs mimicking the clinical presentation of HD pathology in humans (Coyle and Schwarcz, 1976; Hantraye et al., 1990). The first models employed were injected with neurotoxins such as ibotenic acid or kainic acid. Later, these agents were replaced by quinolinic acid as it relatively spared striatal interneurons, mimicking the reported pathology in HD patients (Coyle and Schwarcz, 1976; McGeer and McGeer, 1976; Beal et al., 1991).

Since HD is a monogenic disease, emerging molecular technology has led to the development of genetic mouse models to capture the genetic component of the disease pathogenesis. Over 20 different rodent models of HD have been generated (reviewed in Pouladi et al., 2013; Chang et al., 2015). The rodent models can be grouped into three broad categories according to the approach used for their generation (Pouladi et al., 2013; Chang et al., 2015). First, N-terminal transgenic animals carry the 5' portion of the human *HTT* gene containing expanded CAG repeats. R6/1 and R6/2 mice are the most commonly used mouse models belonging to this category (Mangiarini et al., 1996). Second, full-length transgenic models carry the full-length human *HTT gene* sequence and express polyQ expanded full-length HTT protein. The most widely used models belonging to this group are YAC128 and BACHD mice (Slow et al., 2003; Gray et al., 2008). The third category is the knock-in models in which the HD mutation is reproduced by engineering CAG repeats of varying lengths into the mouse *Htt* genomic locus. The commonly used animals under this category are the *Hdh* Q111, Q140, and zQ175 mouse models (Wheeler et al., 1999; Menalled et al., 2003, 2012). Models within each category differ in size and species of origin of the *Htt* gene (mouse or human), CAG repeat numbers, promoters that drive expression of the HTT proteins, and their background strain (Pouladi et al., 2013; Chang et al., 2015). Thus, each model exhibits a fairly different characteristic phenotype.

1.3.3.1. Knock-in HD mouse models

Several different allelic series of knock-in mice have been generated by introducing CAG repeats of varying lengths directly into the mouse *Htt* gene. For instance, *Hdh* Q111, Q140, Q150, and zQ175 mouse models exhibit CAG repeat

lengths of approximately 109, 140, 150, and 188 repeats, respectively (Wheeler et al., 1999; Lin et al., 2001; Menalled et al., 2003, 2012). As homozygosity is very rare in humans, these models best mimic the genetics of HD being able to express a copy of each wild-type and mutant *Htt* gene by their heterozygous mice. The main caveat for these models, however, is that they exhibit delayed onset of HD behavioral deficits and neuropathology despite having good construct validity (Pouladi et al., 2013). For example, zQ175 mice start to develop motor function deficits between 7-9 months of age, as opposed to 2 months for transgenic models, such as BACHD, or 1 month for truncated HD models, such as R6/2 (Menalled et al., 2009, 2012). Thus, to accelerate the phenotypic progression, homozygous mice are often employed and they typically show robust behavioral abnormalities and HTT aggregate pathology (Wheeler, 2002; Hickey et al., 2008; Menalled et al., 2012; Pouladi et al., 2013). In addition, most of the knock-in lines have normal life spans except for homozygous zQ175 and *Hdh* Q150 mice which reach end-stage disease at around 23 months of age (Woodman et al., 2007; Menalled et al., 2012).

1.3.4. HD pathophysiology

HD pathophysiology is complex despite the monogenic nature of the disease. This is due to the rich HTT interactome with various proteins involved in transcription, cell cycle regulation, cell signaling, cellular organization, protein transport, and proteostasis (Shirasaki et al., 2012). Thus, mutations in HTT can lead to large-scale destabilization of cell proteome and subsequently disrupt multiple cellular processes. At the root of HD is the mutant *HTT* gene and its protein products including both full-length and short protein fragments that are generated at transcriptional and post-translational

levels. A considerable body of evidence indicates that HTT fragmentation is a critical step in HD pathogenesis (Sieradzan et al., 1999; Legleiter et al., 2010; Ast et al., 2018). HTT fragments can be detected in full-length HD mouse models and young presymptomatic mice prior to the aggregate formation (Landles et al., 2010), and similar fragments have been isolated from post-mortem brain specimens from patients (Lunkes et al., 2002). The small mHTT fragments are mostly generated via aberrant splicing of the mHTT transcript leading to the production of short HTT exon1 protein (Sathasivam et al., 2013). Other fragments can be generated via proteolytic cleavage by caspases, calpains, and other proteases (Wellington et al., 2002; Gafni et al., 2004). In addition, polyglutamine expansions alter different post-translational modifications sites on mHTT that, in turn, modify its structural properties, cleavage, and ultimately affecting its toxicity (Sathasivam et al., 2013; Hughes et al., 2014).

Aggregation of mHTT forms inclusion bodies that contain highly ordered amyloid fibers with low detergent solubility. These inclusions can sequester numerous cellular proteins leading to deleterious cellular functions and contributing to the complex loss-of-function phenotype (Soto, 2003). However, several reports have provided evidence that large inclusions are not correlated with cytotoxicity and might represent an adaption strategy in which mHTT is partitioned into a less pervasive structure (Kim et al., 1999; Arrasate et al., 2004; Miller et al., 2011). Indeed, aggregate formation is a complex multi-step process that involves mHTT monomer assembly into a range of intermediate oligomeric species prior to inclusion formation (Scherzinger et al., 1999; Thakur et al., 2009; Kar et al., 2011). The spectrum of oligomeric conformations has made it challenging to understand the pathogenic role of each mHTT species as they can co-

exist and disrupt multiple cellular pathways simultaneously (Labbadia and Morimoto, 2013; Bates et al., 2015).

Mutations in HTT evoke disruptions in neuronal activities that are coordinated by various neurotransmitters involved in synaptic activity and plasticity such as; glutamate, dopamine, GABA, ACh, endocannabinoids, and adenosine (reviewed in Smith-Dijak et al., 2019). For instance, dopamine transmission in the basal ganglia is vital for the regulation of motor functions (Haber, 2014). In HD, dopamine levels are increased at the early stages of the disease (Bird, 1980; Garrett and Soares-da-Silva, 1992), while they are evidently reduced in HD striatum at later stages (Kish et al., 1987; Ginovart, 1997; Bohnen et al., 2000). The dopaminergic alterations in the HD striatum are also associated with hypocholinergic neurotransmission in the striatum. Reduced levels of choline acetyltransferase, vesicular acetylcholine transporter (VAChT), and muscarinic acetylcholine receptors (mAChRs) are evident in the striatum of post-mortem HD brains (Robin Hiley and Bird, 1974; D'Souza and Waldvogel, 2016). Likewise, choline levels are reduced in the cerebrospinal fluid of HD patients (Manyam et al., 1990). Additionally, GABAergic inhibitory transmission is also impaired in HD. Post-mortem analyses in HD patients show a decrease in GABA receptor binding coupled with reductions in GABA concentrations in the striatum (Perry et al., 1973; Reisine et al., 1979; Faull et al., 1993). In addition to impairments in corticostriatal synapses, these neurotransmission alterations are also evident in the cortex and the hippocampus (Milnerwood et al., 2006; Estrada-Sánchez and Rebec, 2013; Veldman and Yang, 2018). Remarkably, studying glutamatergic impairments in HD has received considerable interest as striatal MSNs

receive dense glutamatergic afferents from both cortical and thalamic regions which ultimately shape their activities and functions (Raymond et al., 2011).

1.3.4.1. Glutamate neurotransmission in HD

The pathogenesis of HD involves evident disruptions of glutamatergic neurotransmission including both its release and uptake mechanisms, and its postsynaptic signaling that collectively promote the excitotoxic insults onto MSNs. In HD mice, glutamate release is increased, particularly at the early stages of the disease, and this is followed by evident loss of glutamatergic terminals in the corticostriatal pathway (reviewed in Raymond et al., 2011; Ribeiro et al., 2017). For instance, reduced levels of VGLUT1 contribute to a glutamatergic imbalance in HD mice that potentially lead to dysfunctions in corticostriatal synaptic transmissions (Giralt et al., 2011a; Berry et al., 2012). Similarly, disruptions in iGluRs and mGluRs signaling contribute to HD neurodegeneration (Zeron et al., 2002; Schiefer et al., 2004; Eidelberg et al., 2011). Activation of mGluR1/5 via 3,5-Dihydroxyphenylglycine (DHPG) augments NMDAR-dependent membrane depolarization and intracellular Ca^{2+} flux in healthy MSNs, while relatively sparing striatal interneurons, suggesting that MSN vulnerability to excitotoxicity is dependent on mGluR1/5 activation (Calabresi et al., 1999). In HD, mHTT sensitizes both mGluR1/5-dependent IP_3 receptors activation (Tang et al., 2003, 2005; Ribeiro et al., 2010) and NMDARs activation (Chen et al., 1999; Sun et al., 2001) which ultimately results in augmented intracellular Ca^{2+} mobilization, and contributes to excitotoxic striatal lesioning. Furthermore, suppressing presynaptic glutamate release via activation of group II mGluRs (mGluR2/3) has been proposed as a potential strategy to treat HD. Activation of mGluR2/3 rescues striatal neuron loss, attenuates the

pathological hyperactivity, and increases the survival time of R6/2 HD mice (Schiefer et al., 2004; Reiner et al., 2012). Similar observations were reported by our group in which administration of a mGluR2/3 agonist significantly improved neuronal survival, reduced mHTT aggregation, and reduced microglia recruitment in the striatum of zQ175 mice (Li et al., 2021). Overall, these reports highlight the evident involvement of pre- and post-synaptic domains of the glutamate transmission axis in HD pathophysiology.

1.3.4.1.1. Role of mGluR5 signaling in HD

Given its rich expression in neuronal and glial cells of the cerebral cortex, striatum, and hippocampus, recent evidence has highlighted the role of aberrant mGluR5 signaling in HD pathogenesis (Niswender and Conn, 2010; Ribeiro et al., 2017). mGluR1/5 signaling has a dual function, being able to promote either neuroprotection or neuronal death, depending on drug incubation paradigms and neuronal types (Bruno et al., 2001). Pharmacological blockade of mGluR5 using 2-methyl-6-(phenylethynyl)-pyridine (MPEP) improves mice motor performance and leads to increased survival in R6/2 HD mice, albeit it does not reduce mHTT aggregate formation (Schiefer et al., 2004). Treatment with the same antagonist attenuates glutamate-induced Ca^{2+} release and neuronal apoptosis in primary MSNs cultured from YAC128 HD mice (Tang et al., 2005). Likewise, the genetic deletion of mGluR5 in *Hdh* Q111 HD mice improves motor performance in the rotarod test and decreases the number of mHTT intranuclear inclusions (Ribeiro et al., 2014).

mGluR5 negative allosteric modulators (NAMs) play a vital role in reversing HD pathology in mice. For instance, treatment of zQ175 mice with CTEP reduces HD neuropathology via improving neuronal survival, lowering mHTT aggregate burden, and

reducing microglia recruitment in the striatum of both male and female mice (Abd-Elrahman et al., 2017; Li et al., 2022). Particularly, CTEP treatment facilitates mGluR5-mediated autophagy by reducing the expression of ZBTB16, a key component of the ZBTB16-Cullin3-Roc1 E3-ubiquitin ligase complex, and preventing the breakdown of autophagy adaptor ATG14 (Abd-Elrahman et al., 2017). mGluR5 antagonism also activates unc-51-like kinase 1 (ULK1) which is essential for autophagosome formation (Ganley et al., 2009; Abd-Elrahman et al., 2017). Such facilitation in autophagic signaling is coupled with mitigation of aberrant PI3K/Akt/mTOR signaling and facilitation of cAMP response element-binding protein (CREB)-mediated expression of BDNF (Abd-Elrahman and Ferguson, 2019). Similarly, CTEP treatment modulates the expression of REST/NRSF via the N-cadherin/β-catenin complex in zQ175 mice (de Souza et al., 2020).

On the other hand, mGluR5 PAMs have also proven effective in rescuing striatal degeneration in BACHD mice (Doria et al., 2013). mGluR5 PAMs are biased agonists that can selectively activate pro-survival signaling pathways with minimal influence from excitotoxic signaling pathways (Zhang et al., 2005; Chen et al., 2012; Doria et al., 2013). Chronic treatment with mGluR5 PAM, 3-Cyano-N-(1,3-diphenyl-1H-pyrazol-5-yl)benzamide (CDPPB), rescues HD memory deficits and neuronal cell loss along with a reduction in mHTT aggregation in BACHD mice (Doria et al., 2015). Moreover, CDPPB increases BDNF expression levels and activates ERK1/2 signaling, both vital for neuronal cell survival signaling and synaptic plasticity (Doria et al., 2013, 2015). Similar improvements in cognitive functions are also noted in BACHD mice treated with another mGluR5 PAM, VU0409551 (Doria et al., 2018). VU0409551 treatment improves

dendritic spine density and upregulates the expression of proteins vital for synaptic plasticity including c-Fos, BDNF, and PSD95 (Doria et al., 2018). Overall, these reports underscore the vital role of mGluR5 in rescuing striatal degeneration in HD.

1.3.4.1.2. Role of VGLUTs in HD

VGLUT neuronal expression and functions are markedly altered in different animal models of HD. For instance, expression levels of VGLUT1-labeled terminals are evidently diminished in the striatum of both R6/1 and R6/2 HD mice compared to wild-type littermates (Giralt et al., 2011a; Anglada-Huguet et al., 2016). In another study conducted on premanifest heterozygous Q140 HD mice, VGLUT2-labeled thalamostriatal terminals exhibit early and persistent decline followed by a significant loss of VGLUT1-labeled corticostriatal terminals at a later stage of the disease (Deng et al., 2013). Similarly, VGLUT1 and VGLUT2 levels are reduced in the dorsal striatum of zQ175 mice starting from 9 months of age (Zarate et al., 2021; Alpaugh et al., 2022), indicating a potential defect in glutamatergic innervation to the striatum. However, the involvement of VGLUT3 transmission in HD is currently unclear. It was reported that TANs, which express VGLUT3, are resistant to neurodegenerative influences of mHTT aggregates (Fremeau et al., 2002; Okita et al., 2012), despite the impaired cholinergic neurotransmission elicited by these interneurons (Smith et al., 2006). Furthermore, mHTT does not affect both the activities and the expression levels of VGLUT3 in cultured cells from BACHD mice (Lee et al., 2013), suggesting that VGLUT3 transmission is an interesting modulator of striatal cells excitability in an mHTT-independent fashion.

1.3.4.2. Dysregulation of autophagy in HD

Impairment in autophagy machinery is evident in HD mouse models and in striatal tissues collected from HD patients (Martinez-Vicente et al., 2010). Particularly, autophagosomes can form and fuse efficiently with lysosomes, however, their cytosolic cargo contents are markedly reduced in HD cells. This effect is coupled with an abnormal association between mHTT and P62, a marker for autophagosome cargo recognition (Martinez-Vicente et al., 2010). Likewise, impaired mHTT autophagic clearance is associated with elevated P62 levels along with disruptions in ULK1 activation in zQ175 HD mice (Abd-Elrahman et al., 2017). The compromised ULK1 activation disrupts the phosphorylation of ATG14 and autophagosome nucleation protein, beclin1, ultimately suppressing VPS34 kinase activity (Wold et al., 2016). Furthermore, accumulated mHTT can sequester beclin1 and impair its turnover and function (Shibata et al., 2006). Interestingly, the upregulation of casein kinase 2, an upstream P62 kinase, reduces mHTT large inclusion formation, highlighting the important link between impaired autophagy and mHTT aggregate formation (Matsumoto et al., 2011).

Wild-type HTT is also vital for maintaining proper autophagy flux. The HTT C-terminal domain exhibits structural similarities and comparable binding activities to the autophagy scaffold protein ATG11 (Ochaba et al., 2014). Depletion of HTT impairs the degradation of autophagosomes recruited for mitochondria engulfment (Zheng et al., 2010), and blocks autophagosomes' retrograde transport along neuronal axons (Wong and Holzbaur, 2014b). HTT can also bind P62 and ULK1 to facilitate autophagy flux (Rui et al., 2015). Remarkably, the degree of autophagy can also predict the age of

onset of HD. For instance, single nucleotide polymorphism in ATG7 is associated with an earlier onset of HD in patients (Metzger et al., 2010). More so, the expression levels of beclin1 decrease in an age-dependent fashion in HD brains (Shibata et al., 2006). Overall, these studies further support the crucial pathophysiological role of autophagy in HD pathogenesis.

1.4. Optineurin

Optineurin (OPTN), originally named FIP2, is a cytosolic protein first isolated in 1998 and was identified as a binding partner of the adenovirus E3-14.7K protein (Li et al., 1998). The protein later received its current name as its variants were associated with dominantly inherited adult-onset primary open-angle glaucoma (Rezaie et al., 2002). The human *OPTN* gene is located on the 10p13 chromosome, and the genomic region is approximately 37 kb. The mRNA transcript comprises 16 exons, the first 3 of which are noncoding sequences while the remaining 13 exons encode the protein (Rezaie et al., 2005; Ying and Yue, 2016). Human OPTN is a 74 kDa cytosolic protein comprised of 577 amino acids, and the mouse *Optn* gene shares 78% homology to human *OPTN* and codes for a 584 amino acid protein (67 kDa) (Rezaie and Sarfarazi, 2005).

OPTN is ubiquitously expressed in many tissues including the brain, heart, liver, skeletal muscle, and eye (Rezaie and Sarfarazi, 2005; Rezaie et al., 2005). Structure-wise, OPTN contains multiple domains including a Nuclear Factor Kappa B (NF-kB)-essential molecule (NEMO)-like domain, basic leucine zipper, multiple coiled-coil motifs, a ubiquitin-binding domain (UBAN), a LC3B-interacting region (LIR), and a carboxyl-terminal C2H2 type of zinc finger (Slowicka et al., 2016) (**Figure 1.4.**). OPTN interacts with itself to form homo-oligomers protein complexes in cells (Gao et al., 2014). In addition, OPTN has been shown to interact with a variety of cellular proteins including; HTT, Ras-related protein 8 (Rab8), mGluRs, myosin VI, transferrin receptor, transcription factor IIIA, LC3/GABARAP, TANK (TRAF-associated NF-kB activator) binding kinase 1 (TBK1), and HECT domain and ankyrin repeat-containing E3 ubiquitin

protein ligase 1 (HACE1) (Ying and Yue, 2016). These interactions underlie the diverse OPTN cellular functions such as vesicle trafficking, Golgi apparatus maintenance, regulation of the NF-kB pathway, cell division control, anti-bacterial and antiviral signaling, and autophagy (Slowicka et al., 2016). Furthermore, our group provided the first evidence that OPTN/mGluR interaction can modulate Group I mGluR signaling (Anborgh et al., 2005). Particularly, overexpression of OPTN attenuates agonist-dependent mGluR1 coupling to PLCβ and subsequently suppresses inositol phosphate formation in cells (Anborgh et al., 2005).

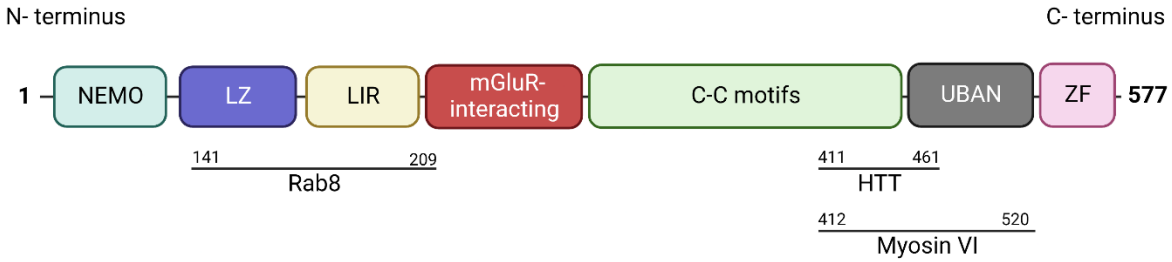

Domains	Position
NF-κB essential modulator **(NEMO)**	31-97 aa
Leucine zipper **(LZ)**	141-161 aa
LC3-interacting region **(LIR)**	169-184 aa
mGluR interacting region	202-246 aa
Multiple coiled-coil **(C-C) domains**	230-445 aa
Ubiquitin-binding domain (UBD) of ABIN proteins and NEMO **(UBAN)**	421-507 aa
Zinc finger **(ZF)**	551-576 aa

Figure 1.4. Schematic representation of the human optineurin protein domain organization. The interacting regions of optineurin with its binding partners are defined below the scheme. Optineurin interacts with group I mGluR (mGluR1/5) via its mGluR-interacting region. In addition, optineurin can act as an autophagic adaptor that is recruited to the autophagic complex via its ubiquitin-binding domain (UBAN) and its LC3-interacting region (LIR) in both selective and nonselective autophagic pathways. Optineurin also interacts with both Rab8 and myosin VI forming a functional complex that is important for Golgi complex perinuclear organization and various endocytic pathways. Similarly, huntingtin protein (HTT) interacts with optineurin and Rab8 on the Golgi complex and mediates lysosomal trafficking. The figure is created using BioRender.

1.4.1. OPTN cellular functions

1.4.1.1. Regulation of vesicular trafficking and stabilization of the Golgi apparatus

Intracellularly, OPTN is found proximal to vesicular structures such as the Golgi apparatus, endosomes, and autophagosomes (Hattula and Peränen, 2000; Sahlender et al., 2005; del Toro et al., 2009) where it regulates various steps in the endocytic, exocytic, and lysosomal trafficking networks. OPTN maintains the Golgi complex perinuclear organization via linking myosin VI to the Rab8-Golgi complex (Sahlender et al., 2005). In addition, OPTN can help mediate post-Golgi formation of secretory vesicles via complexing with myosin VI to deliver clathrin adaptor protein 1B-dependent cargos to the basolateral surface in cells (Au et al., 2007; Bond et al., 2011). Interestingly, HTT affects OPTN affinity to the Golgi complex and is potentially involved in the stabilization of the Golgi in an OPTN-dependent manner (del Toro et al., 2009). Mutations in HTT uncouple the OPTN/Rab8 complex at the Golgi and perturbs post-Golgi trafficking to lysosomal compartments (del Toro et al., 2009). Collectively, OPTN plays a key role as an adaptor protein in maintaining Golgi organization and coordination of post-Golgi trafficking.

1.4.1.2. Regulation of the NF-κB pathway

The NF-κB pathway is critical for the transcription of various genes involved in neuroinflammation, apoptosis, and LTP-dependent synaptic plasticity (Boersma et al., 2011; Mincheva-Tasheva and Soler, 2013). OPTN has been shown to suppress early stages of pro-inflammatory cytokine/chemokine-induced NF-κB signaling *in vitro* across different cell lines. This is mediated via blocking cytokine receptor signaling in response to extracellular stimuli such as tumor necrosis factor (TNF), lipopolysaccharide (LPS),

or Interleukin 1 beta (Schwamborn et al., 2000; Sudhakar et al., 2009; Nakazawa et al., 2016; Montecalvo et al., 2017). Furthermore, as a homolog of NEMO, OPTN competitively disrupts the formation of IκB kinase (IKK) complexes that are essential for NF-κB activation (Schwamborn et al., 2000; Zhu et al., 2007). On the other hand, several *in vivo* studies have reported that induction of NF-κB by TNF or LPS in immune cells may not be regulated by OPTN (Munitic et al., 2013; Markovinovic et al., 2018), suggesting that the role of OPTN in NF-κB signaling is dependent on the cellular context involved.

1.4.1.3. Autophagy and mitophagy

OPTN acts as an autophagy receptor/adaptor that is recruited to the autophagic complex via its UBAN domain and, together with its LIR region, interacts with LC3B in both selective and nonselective autophagic cascades. OPTN also promotes the transformation of inactive cytosolic LC3B form (LC3B-I) to membrane-bound LC3B-II via phosphatidylethanolamine conjugation (Bansal et al., 2018; Ryan and Tumbarello, 2018). Phosphorylation of Ser177 in the LIR via TBK1 enhances OPTN affinity to LC3B, while phosphorylation of Ser473 in the UBAN enhances the affinity to ubiquitin chains, and both promote the maturation of autophagosomes (Ying and Yue, 2016). More so, during the autophagosome-lysosome fusion process, OPTN links autophagosomes to myosin VI and adaptor protein TOM1 promoting autophagosome maturation and fusion (Tumbarello et al., 2012). Furthermore, E3 ubiquitin ligase, HACE1, catalyzes OPTN ubiquitination at Lys193 residue adjacent to LIR thereby enhancing LC3B lipidation and activation (Liu et al., 2014).

Mitophagy is the autophagic degradation of defective mitochondria following damage and stress. The process is commenced by depolarized mitochondria that stabilizes phosphatase and tensin homolog-induced kinase 1 (PINK1) on the outer membrane recruiting and activating parkin, a cytosolic E3 ubiquitin ligase (Kane et al., 2014). Once activated, parkin ubiquitinates mitochondrial outer membrane proteins that recruit and associate with OPTN via its UBAN domain (Lazarou, 2015). This is followed by OPTN-mediated recruitment of other autophagic factors such as ATG12, ULK1, and WD-repeat phosphoinositide interacting protein 1 (WIPI1) to focal spots proximal to mitochondria (Lazarou et al., 2015). Subsequently, OPTN initiates autophagosome formation to engulf damaged mitochondria via its LIR region (Wong and Holzbaur, 2014a). Depletion of OPTN attenuates LC3B recruitment to mitochondria and disrupts mitochondrial degradation (Wong and Holzbaur, 2014a). Furthermore, OPTN can phosphorylate and activate TBK1, creating a signal amplification loop via the combined recruitment of OPTN/TBK1 on ubiquitinated mitochondria (Richter et al., 2016). Overall, this depicts OPTN's direct involvement in facilitating different steps of the cellular autophagic machinery.

1.4.2. Role of OPTN in HD

Being an autophagy receptor and modulator of vesicle trafficking processes, OPTN is implicated in HD pathogenesis (Schwab et al., 2012; Ying and Yue, 2016). In the cerebral cortex of HD patients, OPTN can be found in neuronal intranuclear, neuropil, and perikaryal inclusion bodies (Schwab et al., 2012). Similarly, OPTN is colocalized with mHTT inclusion bodies in R6/2 HD mice (Shen et al., 2015). It is also

hypothesized that cell-type-specific expression of OPTN in the striatum might play a role in striatal neuron vulnerability in HD (Okita et al., 2012). In particular, OPTN is abundantly expressed in the striatal interneurons whereas lower levels of OPTN are observed in the MSNs. This expression pattern is complementary to the neuronal loss seen in the striatum of HD patients (Okita et al., 2012). More so, it has been suggested that OPTN recognizes and degrades polyQ-expanded HTT via its C-terminal, not LIR, domain which results in a reduction in mHTT-mediated cell death (Korac et al., 2013; Moharir et al., 2022). On the other hand, polyQ expansion in mHTT interferes with its interaction with OPTN thereby affecting LC3 recruitment to mitochondria, and ultimately impairing mitophagy (Franco-Iborra et al., 2021). Interestingly, overexpression of mHTT in cells augments OPTN-mediated attenuation of mGluR1/5 coupling to PLC and inositol phosphate formation (Anborgh et al., 2005), suggesting that the interplay between mHTT and OPTN contributes to pathological mGluR5 signaling in HD.

1.5. Rationale and hypothesis

Aberrant signaling via glutamate receptors, in particular mGluR5, evidently contributes to striatal neurodegeneration in HD animal models (Lewerenz and Maher, 2015; Abd-Elrahman et al., 2017; Ribeiro et al., 2017; Li et al., 2022). VGLUT3 represents a unique modulator of glutamate release from selected striatal and cortical neurons and exhibits an overlapping distribution with mGluR5 (Ibrahim et al., 2020). Despite its potential involvement, the role of VGLUT3 in HD progression remains largely unknown. **Therefore, I hypothesized that VGLUT3-mediated regulation of corticostriatal circuits is affected in HD, and that suppression of this regulation could potentially modify mGluR5 activity, excitotoxic neuronal insults, and**

subsequent behavioral deficits in HD mice. On the other hand, evidence depicts the involvement of OPTN in HD pathology as an autophagy adaptor for mHTT (Okita et al., 2012). In addition, our laboratory previously reported that OPTN can interact with mGluR5 (Anborgh et al., 2005). Yet, the molecular mechanisms by which OPTN can regulate mGluR5 downstream signaling remain largely unexplored. **Hence, I hypothesized that OPTN acts as a downstream mediator for mGluR5 signaling and that OPTN ablation disrupts mGluR5-mediated autophagy in neurons.** This OPTN/mGluR5 crosstalk could have implications on the pathophysiology of neurodegenerative disorders including HD.

The specific aims of this thesis are: (1) to investigate the role of VGLUT3 transmission in metabotropic and inotropic glutamate receptor regulation in the brain, (2) to assess the impact of VGLUT3 deletion in HD pathogenesis and progression in mice, and (3) to investigate the role of OPTN in mGluR5-dependent canonical and autophagic signaling.

Chapter 2.
VGLUT3 ablation differentially modulates glutamate receptor densities in mouse brain

VGLUT3 ablation differentially modulates glutamate receptor densities in mouse brain

Karim S. Ibrahim[1,2,3], Salah El Mestikawy[4,5], Khaled S. Abd-Elrahman[1,2,3,#], and Stephen S. G. Ferguson[1,2,#]

[1] University of Ottawa Brain and Mind Institute, [2] Department of Cellular and Molecular Medicine, University of Ottawa, 451 Smyth Road, Ottawa, Ontario, K1H 8M5, Canada.

[3] Department of Pharmacology and Toxicology, Faculty of Pharmacy, Alexandria University, Alexandria, 21521, Egypt.

[4] Neuroscience Paris Seine – Institut de Biologie Paris Seine (NPS–IBPS) INSERM, CNRS, Sorbonne Université, Paris, France.

[5] Department of Psychiatry, Douglas Hospital Research Center, McGill University, Verdun, Quebec, Canada.

[#] KSA-E and SSGF contributed equally to this work as senior authors.

Correspondence to

Stephen Ferguson, PhD
Department of Cellular and Molecular Medicine
Faculty of Medicine, University of Ottawa
451 Smyth Rd, Ottawa, ON, K1H 8M5
Tel: (613) 562-5800 Ext 8889
Email: sferguso@uottawa.ca

Article published 20 April 2022 in eNeuro, 9 (3) ENEURO.0041-22.2022; DOI: https://doi.org/10.1523/ENEURO.0041-22.2022

Authors' Contributions: KSI, KSA-E, and SSGF were responsible for the conception and design of the experiments. KSI performed experiments and data analysis and wrote the manuscript. SEM, KSA-E, and SSGF edited the manuscript and supervised the study.

2.1. Abstract

Type 3 vesicular glutamate transporter (VGLUT3) represents a unique modulator of glutamate release from both non-glutamatergic and glutamatergic varicosities within the brain. Despite its limited abundance, VGLUT3 is vital for the regulation of glutamate signaling and therefore modulates the activity of various brain microcircuits. However, little is known on how glutamate receptors are regulated by VGLUT3 across different brain regions. Here, we employed VGLUT3 constitutive knockout (VGLUT3$^{-/-}$) mice and explored how VGLUT3 deletion influences total and cell surface expression of different ionotropic and metabotropic glutamate receptors. VGLUT3 deletion upregulated the overall expression of metabotropic glutamate receptors, mGluR5 and mGluR2/3 in the cerebral cortex. In contrast, no change in levels of ionotropic NMDARs glutamate receptors was observed in the cerebral cortex of VGLUT3$^{-/-}$ mice. We noted a significant reduction in cell surface levels of mGluR5, NMDAR2A, NMDAR2B, as well as reductions in dopaminergic D1 (D1R) and muscarinic M1 receptors (M1 mAChR) in the hippocampus of VGLUT3$^{-/-}$ mice. Furthermore, mGluR2/3 total expression and mGluR5 cell surface levels were elevated in the striatum of VGLUT3$^{-/-}$ mice. Lastly, AMPAR subunit GluA1 was significantly upregulated throughout cortical, hippocampal, and striatal brain regions of VGLUT3$^{-/-}$ mice. Together, these findings complement and further support the evidence that VGLUT3 dynamically regulates glutamate receptor densities in several brain regions. These results suggest that VGLUT3 may play an intricate role in shaping glutamatergic signaling and plasticity in several brain areas.

2.2. Introduction

The atypical type 3 vesicular glutamate transporter (VGLUT3) is a unique member of the Solute Carrier 17a (SLC17a) transporter family that mediates vesicular packaging of glutamate in primarily non-glutamatergic varicosities, as well as subpopulations of glutamatergic neurons in the brain (Fremeau et al., 2004; El Mestikawy et al., 2011). VGLUT3 is expressed by discrete populations of neurons and interneurons in the cerebral cortex, raphe nuclei, hippocampus, striatum, olfactory bulb, inner hair cells, and transiently expressed in the cerebellum (Gras et al., 2002; Herzog et al., 2004; El Mestikawy et al., 2011). In addition to its well-characterized vesicular glutamate transport functions, VGLUT3 modulates acetylcholine, serotonin, and GABA transmission (Gras et al., 2002; Somogyi et al., 2004; Trudeau and El Mestikawy, 2018). Functionally, VGLUT3 plays an important role in the neuronal networks involved in motor coordination, reward processing, and cognition (Ibrahim et al., 2020).

Evidence shows that VGLUT3 can modify glutamate release and mediate tonic excitatory postsynaptic inputs via both ionotropic (iGluR) and metabotropic (mGluR) glutamate receptors (Nelson et al., 2014; Sakae et al., 2015; Fasano et al., 2017). For instance, genetic deletion of VGLUT3 diminishes excitatory currents from tonically active interneurons that are mediated via α-amino-3-hydroxy-5-methyl-4-isoxazole propionic acid receptors (AMPARs) and N-methyl-D-aspartate receptors (NMDARs) on the MSNs and GABAergic interneurons of the striatum (Higley et al., 2011; Nelson et al., 2014). Similarly, VGLUT3 regulates dopamine and GABA efflux via mGluR-dependent mechanisms in the nucleus accumbens and in the hippocampus (Sakae et al., 2015; Fasano et al., 2017). The overlapping distribution of VGLUT3 with different

members of mGluRs strongly suggests that VGLUT3/mGluR crosstalk is vital for synaptic plasticity modulation in various brain microcircuits (Fasano et al., 2017; Ibrahim et al., 2020). However, it remains unclear how glutamate receptors can be regulated by VGLUT3 neurotransmission across different brain regions. In this study, we employed VGLUT3 knockout mice (VGLUT3$^{-/-}$) to assess whether loss of VGLUT3 alters total and cell surface expression of glutamate receptors in the brain.

We report that the loss of VGLUT3 in mice upregulates the total expression of mGluR5 and mGluR2/3 while downregulating NMDAR2B and dopaminergic D1 (D1R) cell surface expression in the cerebral cortex. Furthermore, significant reductions in cell surface expression of mGluR5, NMDAR2A/B, D1R, and muscarinic M1 (M1 mAChR) receptors are observed in the hippocampus of VGLUT3$^{-/-}$ mice. In addition, mGluR2/3 total expression and mGluR5 cell surface levels are higher in the striatum of VGLUT3$^{-/-}$ mice. Finally, AMPAR subunit GluA1 total expression is upregulated throughout cortical, hippocampal, and striatal brain regions of VGLUT3$^{-/-}$ mice. Together, these results provide evidence that glutamate receptor densities are dynamically regulated by VGLUT3 in several brain areas, highlighting the key role of this atypical transporter in the regulation of glutamatergic signaling and potentially synaptic plasticity in these circuits.

2.3. Materials and methods

2.3.1. Reagents

NeutrAvidin agarose beads (29200), goat anti-rabbit (G-21234) immunoglobulin G (IgG; H + L) cross-adsorbed horseradish peroxidase (HRP) secondary antibody, and rabbit anti–β-actin (PA1-183) were from Thermo Fisher Scientific (Waltham, Massachusetts). Rabbit anti-mGluR 2/3 (ab6438), anti-dopamine receptor D1 (ab20066), and anti-vinculin (ab129002) were from Abcam (Cambridge, Massachusetts). Rabbit anti-mGluR5 (AB5675), anti-NMDAR2A (AB1555), anti-NMDAR2B (AB1557), anti-glutamate receptor-1 (AMPA1; AB1504), and anti-muscarinic acetylcholine receptor (M1 mAChR; M9808) were from Sigma Aldrich (St. Louis, Missouri). Reagents used for Western blotting were from Bio-Rad (Mississauga, Canada), and all other biochemical reagents were from Sigma-Aldrich (St. Louis, Missouri).

2.3.2. Animals

All experimental protocols were approved by the Institutional Animal Care Committee and were in compliance with the Canadian Council of Animal Care guidelines. Animals were group-housed under a constant 12-hour light/dark cycle and given food and water *ad libitum*. Heterozygous knockout VGLUT3 mice (VGLUT3$^{-/+}$) on a C57BL/6 background were used as breeding pairs to establish the mouse colony. Six-month-old wild-type (WT) and homozygous VGLUT3 knockout (VGLUT3$^{-/-}$) male littermates were used for experiments.

2.3.3. Cell surface biotinylation and immunoblotting

Cell surface biotinylation and immunoblotting experiments were performed as previously reported (Abd-Elrahman et al., 2018; Ibrahim et al., 2021). Mice were euthanized by live cervical dislocation followed by rapid decapitation and dissection of the cerebral cortex, hippocampus, and striatum. Tissues were cross-chopped with a McIlwain tissue chopper at a slice thickness of 300 µm and were recovered for 40 min at 37°C in artificial cerebrospinal (ACSF) solution (127 mM NaCl, 2 mM KCl, 1 mM $CaCl_2$, 1 mM $MgSO_4$, 10 mM glucose, 1.2 mM KH_2PO_4, 26 mM NaH_2CO_3, pH 7.4) gassed with 95% O_2/5% CO_2. Samples were transferred to tubes and incubated with 1 mg/mL sulfo-NHS-SS-biotin in ACSF for 45 min on ice, and then washed three times with ACSF. Biotinylation was then quenched with 100 mM glycine in ACSF for 70 min on ice. Following three washes in ACSF, samples were homogenized and lysed in RIPA buffer (1% Nonidet P 40 substitute, 0.5% sodium deoxycholate, 0.1% sodium dodecyl sulfate, 50 mM Tris-HCl, 150 mM NaCl, and 5 mM EDTA, pH 7.2) containing protease inhibitors (100 µM AEBSF, 80 nM aprotinin, 2 µM leupeptin, 5 µM Bestatin, 1.5 µM E-64, and 1 µM pepstatin A). Protein lysates were centrifuged at 18,000 *x* g at 4^{o}C for 10 min. The supernatant was then collected, and total protein concentrations were quantified using DC protein assay kit (Bio-Rad). Biotinylated fractions in 500 µg samples were captured with NeutrAvidin agarose beads and were eluted in β-mercaptoethanol containing 3x SDS sample buffer (187.5 mM Tris-HCl, 6% sodium dodecyl sulfate, 30% glycerol, 0.006% Bromophenol Blue). Total protein lysates were also aliquoted and diluted to 1 µg/µl in a mixture of lysis buffer and β-mercaptoethanol containing 3x SDS sample buffer and boiled for 10 min at 90 °C.

Aliquots containing a total of 30-40 µg of proteins were resolved by electrophoresis on 6% and 7.5% SDS-polyacrylamide gel electrophoresis and transferred onto nitrocellulose membranes. Blots were blocked in Tris-buffered saline (pH 7.6) containing 0.05% of Tween 20 (TBST) and 5% nonfat dry milk for 1 hr at room temperature. Blots were then incubated overnight at 4 °C with primary antibodies diluted (1:1000) in TBST containing 1% nonfat dry milk. Membranes were washed 3 times in TBST and incubated with secondary antibodies (anti-rabbit) diluted (1:5000) in TBST containing 1% nonfat dry milk for 1 h. Blots were imaged using the Bio-Rad Chemidoc Gel imaging system. Band densities were quantified using Image Lab software and normalized to the loading control.

2.3.4. Statistical analysis

Means ± SEM and sample sizes for each independent experiment are shown in the figure legends. Data were analyzed with GraphPad Prism 9 for normality and statistical significance. Two-tailed unpaired Student's t-test was used for comparisons. Significance level was set at $P < 0.05$.

2.4. Results

2.4.1. VGLUT3 deletion differentially alters glutamatergic and non-glutamatergic receptor densities in the mouse cerebral cortex

VGLUT3 is localized in cortical layers II and VI as well as in subpopulations of interneurons within the cerebral cortex (Schäfer et al., 2002; Herzog et al., 2004). Therefore, we assessed cell surface densities of mGluR5 and mGluR2/3, as both receptors actively modulate synaptic plasticity responses in cortical circuits and are potentially regulated by VGLUT3-expressing fibers (Ballester-Rosado et al., 2010; Joffe et al., 2020; Abd-Elrahman and Ferguson, 2022). We found that VGLUT3 deletion significantly elevated mGluR5 and mGluR2/3 expression levels in the cerebral cortex of VGLUT3$^{-/-}$ male mice compared to WT mice (**Figure 2.1A and 2.1B**). Both NMDARs and AMPARs mediate VGLUT3 signaling in different brain areas (Higley et al., 2011; Nelson et al., 2014; Wang et al., 2019). We, therefore, assessed the expression of NMDARs and AMPARs via probing for their essential regulatory subunits NMDAR2A/2B and GluA1, respectively (Paoletti et al., 2013; Henley and Wilkinson, 2016). We detected no change in the total expression levels of NMDAR2A/2B subunits in the cortex of VGLUT3$^{-/-}$ mice compared to WT mice (**Figure 2.1C and 2.1D**). However, cell surface expression of NMDAR2B, but not NMDAR2A, was significantly reduced in the cortex of VGLUT3$^{-/-}$ mice (**Figure 2.1C and 2.1D**). On the contrary, loss of VGLUT3 significantly upregulated cell surface and total expression levels of AMPAR subunit GluA1 (**Figure 2.1E**) (Henley and Wilkinson, 2016).

Given that VGLUT3-positive neurons actively regulate dopaminergic and cholinergic neurotransmission (Trudeau and El Mestikawy, 2018), we probed for

dopaminergic D1Rs and muscarinic M1 mAChRs that are enriched in cortical GABAergic interneurons and pyramidal neurons, respectively (Levey et al., 1991; Anagnostaras et al., 2003; Puig et al., 2014). VGLUT3 ablation did not alter the total expression of either D1R or M1 mAChR in the cortex of VGLUT3$^{-/-}$ mice (**Figure 2.1F and 2.1G**). However, cell surface D1R level but not M1 mAChR was significantly reduced in the cortex of VGLUT3$^{-/-}$ mice (**Figure 2.1F and 2.1G**).

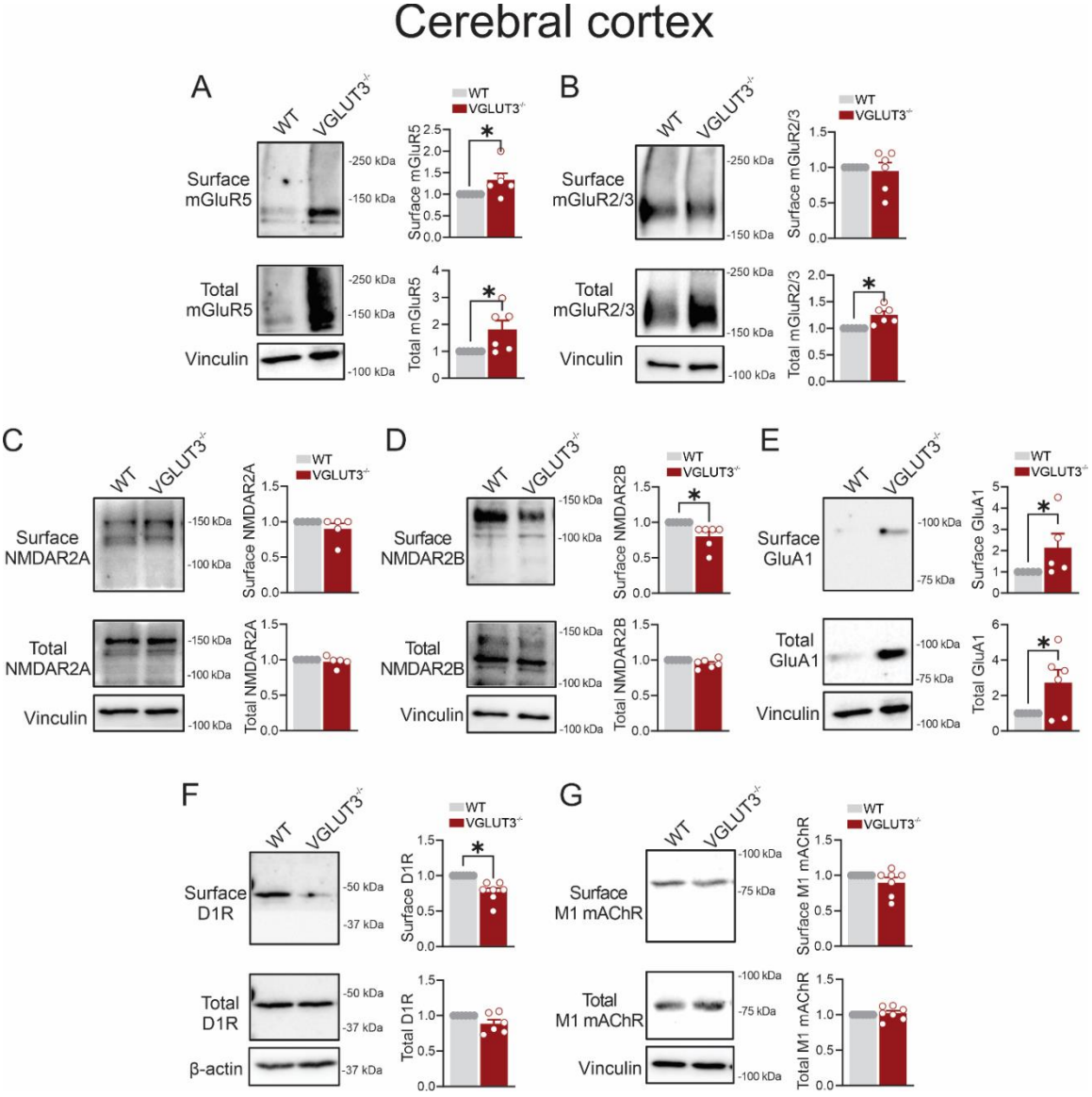

Figure 2.1. The effect of VGLUT3 deletion on glutamate and non-glutamate receptor expression in the mouse cerebral cortex. Representative immunoblots and quantification of cell surface and total levels of (A) mGluR5, (B) mGluR2/3, (C) NMDAR2A, (D) NMDAR2B, (E) GluA1, (F) D1R, and (G) M1 mAChR in cortical lysates from VGLUT3 knockout (VGLUT3$^{-/-}$) and C57Bl/6 (WT) male mice. Data are means ± SEM (n= 5-6 mice per group), normalized to the respective surface or total WT values. * $P < 0.05$ assessed by unpaired Student's t-test.

2.4.2. Deletion of VGLUT3 reduces cell surface levels of mGluR5, NMDAR, D1R, and M1 mAChR in the hippocampus

Within the hippocampus, mGluRs and iGluRs are expressed in both excitatory glutamatergic and inhibitory GABAergic interneurons, with distinct patterns for each receptor subtype (Reiner and Levitz, 2018). Hippocampal VGLUT3 is found in subpopulations of GABAergic interneurons, cholecystokinin (CCK)-positive basket cells, as well as in subsets of VGLUT3-expressing serotoninergic terminals (Somogyi et al., 2004; Amilhon et al., 2010). In the hippocampus of VGLUT3$^{-/-}$ mice, we found that cell surface mGluR5 levels were significantly reduced, with no change in their total expression levels (**Figure 2.2A**). In addition, both cell surface and total expression levels of mGluR2/3 remained unaffected by VGLUT3 deletion in mice (**Figure 2.2B**). However, cell surface fractions, but not total expression, of NMDAR2A and NMDAR2B were significantly reduced in the hippocampus of VGLUT3$^{-/-}$ mice (**Figure 2.2C and 2.2D**). Furthermore, total but not cell surface GluA1 levels were elevated in the hippocampus of VGLUT3$^{-/-}$ mice (**Figure 2.2E**). Loss of VGLUT3 reduced cell surface D1R and M1 mAChR levels without altering their total expression in the hippocampus (**Figure 2.2F and 2.2G**).

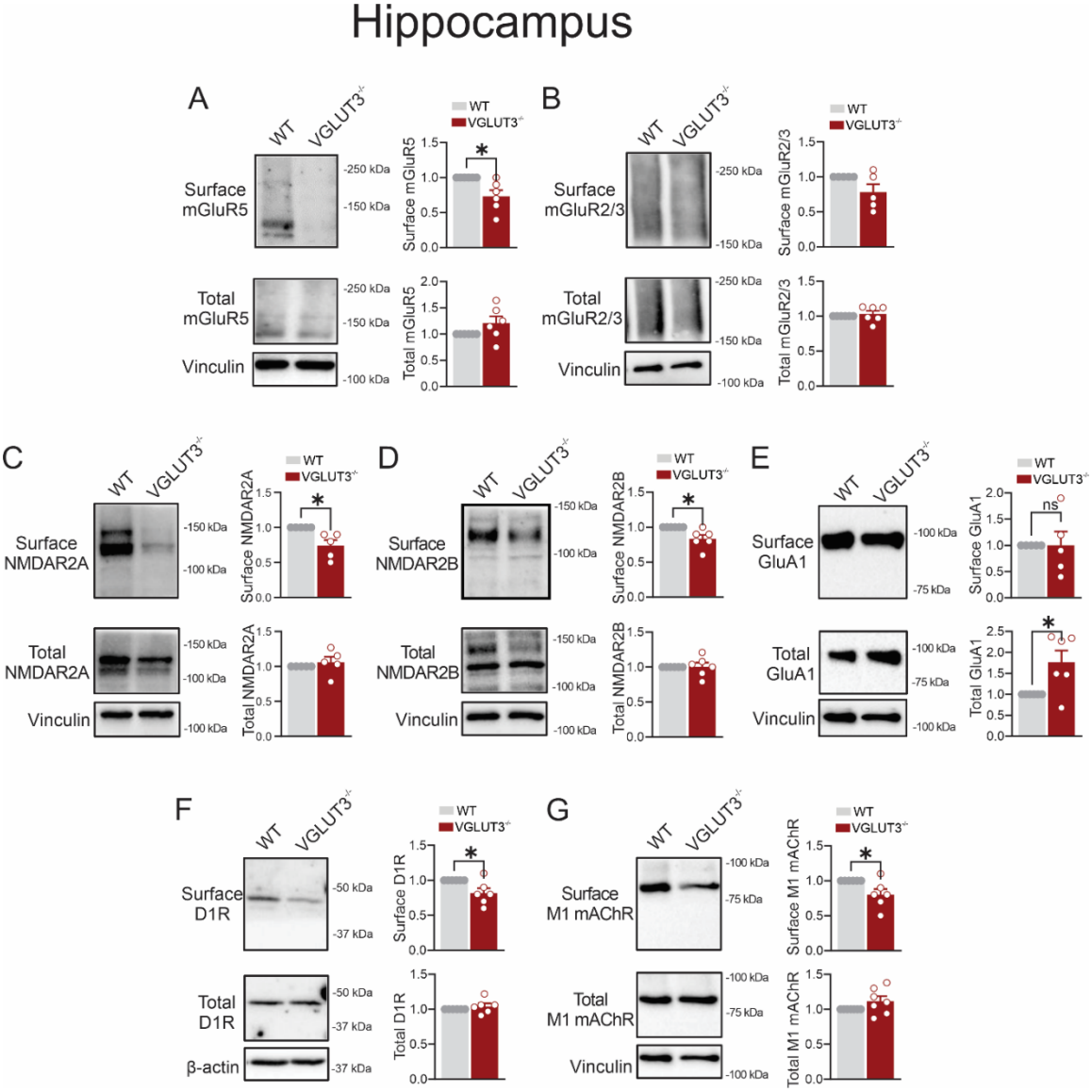

Figure 2.2. The effect of VGLUT3 deletion on glutamate and non-glutamate receptor expression in the mouse hippocampus. Representative immunoblots and quantification of cell surface and total levels of (A) mGluR5, (B) mGluR2/3, (C) NMDAR2A, (D) NMDAR2B, (E) GluA1, (F) D1R, and (G) M1 mAChR in hippocampal lysates from VGLUT3 knockout (VGLUT3$^{-/-}$) and C57Bl/6 (WT) male mice. Data are means ± SEM (n = 5-6 mice per group), normalized to the respective surface or total WT values. * $P < 0.05$ assessed by unpaired Student's t-test.

2.4.3. VGLUT3 loss increases the total expression of mGluR2/3, AMPARs, and cell surface mGluR5 levels in the striatum

Striatal VGLUT3 signaling is chiefly mediated via cholinergic interneurons (Higley et al., 2011; Gonzales and Smith, 2015). These interneurons use both acetylcholine and glutamate to fine-tune dopaminergic inputs onto the medium spiny neurons, ultimately regulating striatal network activities (Gras et al., 2008; Higley et al., 2011; Sakae et al., 2015). We found that loss of VGLUT3 increased cell surface mGluR5 levels in the striatum, with no detectable changes in cell surface mGluR2/3 levels (**Figure 2.3A and 2.3B**). However, total mGluR2/3, but not mGluR5, levels were significantly elevated in the striatum of VGLUT3$^{-/-}$ mice (**Figure 2.3A and 2.3B**). We also detected no changes in the total or cell surface expression of NMDAR2A and NMDAR2B in the striatum of VGLUT3$^{-/-}$ mice compared to WT mice (**Figure 2.3C and 2.3D**). Yet, VGLUT3 loss elevated both cell surface and total expression levels of GluA1 subunits (**Figure 2.3E**). The expression of D1R and M1 mAChR in the striatum remained unaffected by VGLUT3 deletion (**Figure 2.3F and 2.3G**).

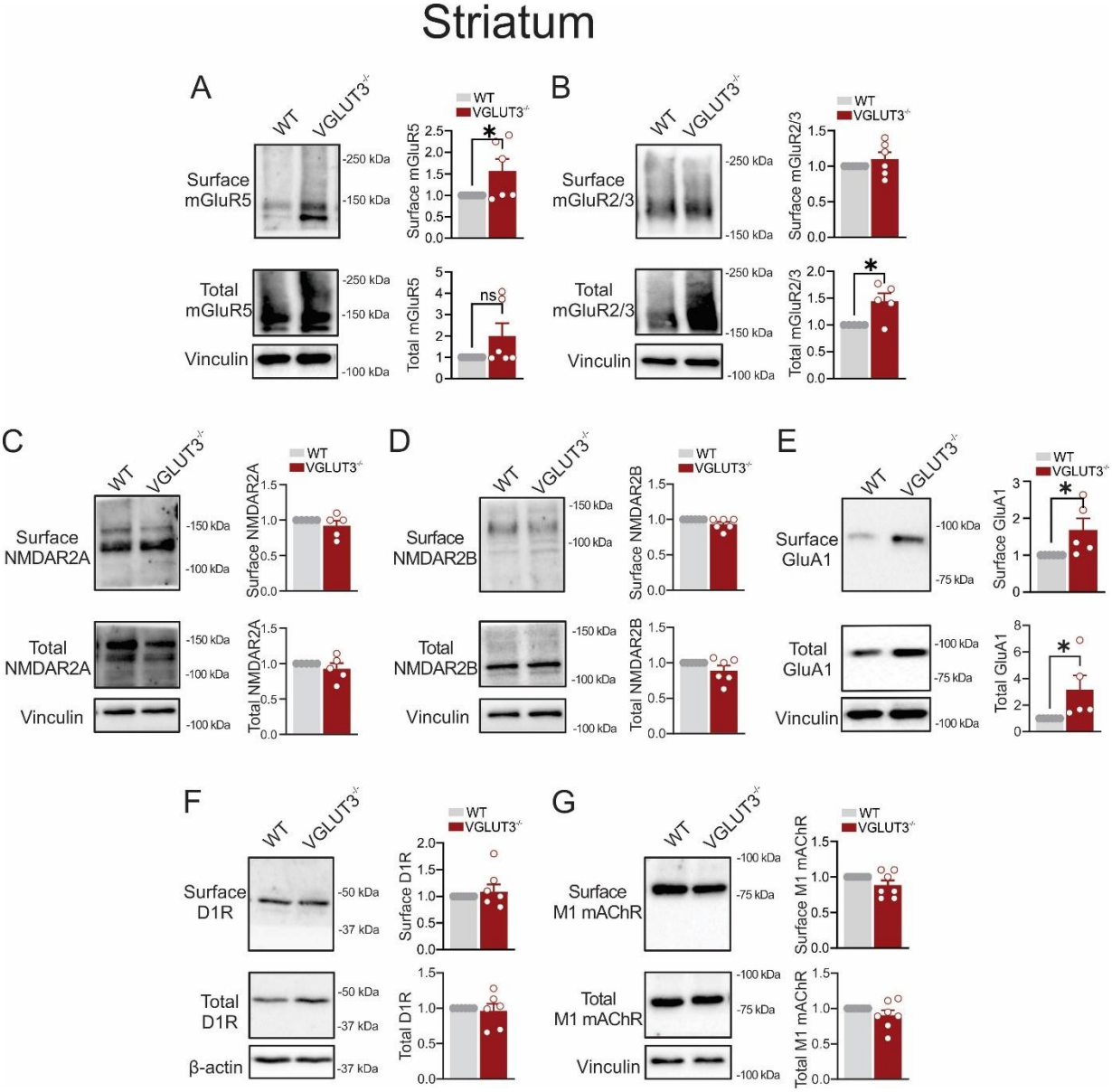

Figure 2.3. The effect of VGLUT3 deletion on glutamate and non-glutamate receptor expression in the mouse striatum. Representative immunoblots and quantification of cell surface and total levels of (A) mGluR5, (B) mGluR2/3, (C) NMDAR2A, (D) NMDAR2B, (E) GluA1, (F) D1R, and (G) M1 mAChR in striatal lysates from VGLUT3 knockout (VGLUT3$^{-/-}$) and C57Bl/6 (WT) male mice. Data are means ± SEM (n = 5-7 mice per group), normalized to the respective surface or total WT values. * *P < 0.05* assessed by unpaired Student's t-test.

2.5. Discussion

Despite the robust evidence supporting the role of VGLUT3 in regulating non-glutamatergic neurotransmission (reviewed in Trudeau and El Mestikawy, 2018; Ibrahim et al., 2020), little is known about how VGLUT3-associated networks regulate glutamatergic neurotransmission. As summarized in **Table 2.1**, we show that genetic deletion of VGLUT3 differentially alters the expression of glutamate and non-glutamate receptors in several brain areas. Specifically, VGLUT3 ablation upregulates the expression of mGluR5 and mGluR2/3 while reducing cell surface D1R levels in the cerebral cortex. In the hippocampus, VGLUT3 loss reduces cell surface levels of mGluR5, NMDAR2A/2B, as well as D1Rs and M1 mAChRs. Similarly, cell surface mGluR5 and total mGluR2/3 densities are increased in the striatum of VGLUT3$^{-/-}$ mice. Lastly, loss of VGLUT3 upregulates AMPAR subunit GluA1 in the cortex, the hippocampus, and the striatum. Together, these findings complement and provide further evidence that VGLUT3, despite its low abundance, can be a key modulator of glutamate receptor densities across the brain, highlighting its role in glutamatergic transmission, synaptic plasticity, and brain circuit homeostasis.

Evidence indicates that VGLUT3 modulates cortical and hippocampal microcircuits via CCK-positive basket cells (Herzog et al., 2004; Somogyi et al., 2004; Nguyen et al., 2020). These interneurons utilize VGLUT3-dependent glutamate to dampen GABAergic currents onto pyramidal neurons via feedback activation of presynaptic mGluR autoreceptors (Fasano et al., 2017). VGLUT3 transmission also mediates excitatory inputs onto pyramidal neurons as well as interneurons via AMPAR and NMDAR activation (Nguyen et al., 2020). Moreover, VGLUT3-expressing basket

cells form synaptic contacts with mGluR5 on pyramidal neurons in the cortical and cortex-like amygdaloid regions (Omiya et al., 2015). Consistent with these reports, we observed upregulation in both mGluR5 and AMPAR subunit GluA1 in the cortex upon deletion of VGLUT3. Yet, cell surface levels of NMDAR2B, but not NMDAR2A, were decreased in the cortex of VGLUT3$^{-/-}$ mice. This intriguing observation suggests that VGLUT3 exerts sophisticated regulation of some NMDAR subpopulations in cortical neurons. Interestingly, NMDAR2B-containing receptors exhibit slower deactivation kinetics and facilitated surface mobility compared to NMDAR2A-containing receptors (Vicini et al., 1998; Groc et al., 2006), ultimately affecting the nature of the plasticity response (Paoletti et al., 2013). Thus, the reduction in NMDAR2B cell surface levels in VGLUT3$^{-/-}$ cortex suggests that VGLUT3 may alter the induction thresholds of long-term potentiation (LTP) or depression (LTD) in the cortical neurons. This agrees with the observed decreases in cell surface D1R levels and upregulation in mGluR2/3 levels in VGLUT3$^{-/-}$ cortex, both of which actively modulate LTP and LTD induction/maintenance in the cortex (Otani et al., 1999; Huang et al., 2004; Joffe et al., 2020, 2021). Together, our findings further support the role of VGLUT3 in modulating the balance between LTP and LTD plasticity responses in cortico-hippocampal networks (Fasano et al., 2017).

The observed reductions in mGluR5 and NMDAR membrane recruitment in VGLUT3$^{-/-}$ hippocampus suggest an adaptive reduction in glutamatergic transmission strength in the hippocampal circuits. Both group I mGluRs and NMDARs represent key players in regulating synaptic metaplasticity in hippocampal neurons (Reiner and Levitz, 2018). Similarly, inputs from VGLUT3-positive interneurons are reported to modulate

metaplasticity in glutamatergic synapses within the regional circuits of the hippocampus (del Pino et al., 2017; Fasano et al., 2017). Therefore, it is possible that the reduction in mGluR5 and NMDAR cell surface levels may underlie altered metaplasticity in the ventral hippocampus of VGLUT3$^{-/-}$ mice (Fasano et al., 2017). We also noted a decrease in cell surface densities of D1R and M1 mAChR, both of which are expressed in VGLUT3-positive interneurons and regulate synaptic plasticity mechanisms and memory processing functions in the hippocampus (Cea-del Rio et al., 2010; Furini et al., 2014; Dennis et al., 2016; Puighermanal et al., 2017). Collectively, these changes in glutamatergic and non-glutamatergic receptor topographies might explain the impaired working memory and cognitive flexibility previously reported in VGLUT3$^{-/-}$ mice (Fazekas et al., 2019).

VGLUT3 signaling plays an important role in striatal microcircuits involved in reward-guided behaviors (Ibrahim et al., 2020). We show here that VGLUT3 loss triggers an increase in cell surface mGluR5, as well total mGluR2/3 levels in the striatum. Both receptors play a well-characterized role in the striatal circuits modulating drug reward and motor function (Kenny and Markou, 2004; Conn et al., 2005; Paterson and Markou, 2005; Peters and Kalivas, 2006). Thus, our findings indicate that VGLUT3, via its dynamic regulation of striatal mGluR densities, can play a critical role in the neuropathophysiology of drug addiction and movement disorders (Sakae et al., 2015; Areal et al., 2019; Ibrahim et al., 2020).

An intriguing aspect of our findings is the persistent upregulation of AMPAR subunit GluA1 across cortical, hippocampal, and striatal regions of VGLUT3$^{-/-}$ mice. This suggests that AMPAR activation may be regulated by VGLUT3 neurotransmission-

independent of NMDARs. Recent reports have shown that VGLUT3-expressing interneurons mediate excitatory inputs via AMPARs activation in the prefrontal cortex (Nguyen et al., 2020), the hippocampus (Pelkey et al., 2020), and the striatum (Nelson et al., 2014). Furthermore, synaptic scaling of AMPARs is directly implicated in central neural circuits that control spatial working memory functions (Bannerman et al., 2004; van Vugt et al., 2020) and reward behavior (Sutton et al., 2003). Thus, the observed AMPAR alterations could be potentially implicated in the impaired working memory and exacerbated cocaine hedonic effects reported in VGLUT3$^{-/-}$ mice (Divito et al., 2015; Sakae et al., 2015), and this warrants further investigation.

It is worth noting that our findings are subject to at least two limitations. First, while cell surface biotinylation is efficient in yielding highly purified plasma membrane proteins, the technique cannot provide spatial information on the precise distribution of the receptors in different synaptic domains. Second, we focused on male VGLUT3$^{-/-}$ mice as prior studies did not report major differences between male and female knockout mice, either in their phenotype or network activities (Amilhon et al., 2010; Higley et al., 2011; Divito et al., 2015; Ramet et al., 2017). Nonetheless, we can not rule out sex-dependent changes in glutamate receptor densities in VGLUT3$^{-/-}$ mice.

In summary, we provide evidence that VGLUT3, despite its low abundance, can be a key regulator of mGluR and iGluR densities in different brain regions, highlighting VGLUT3's role in synaptic function and plasticity. Moreover, because VGLUT3 regulates specialized brain circuitries involved in reward processing, emotional states, and motor coordination, this neuronal adaption of glutamate receptor densities might provide a more comprehensive understanding of VGLUT3-dependent mechanisms

underlying various neurological and neuropsychiatric disorders such as anxiety (Amilhon et al., 2010), drug addiction (Sakae et al., 2015), or motor disorders such as Parkinson's disease (Divito et al., 2015; Ribeiro et al., 2017).

Table 2.1. Summary of changes in cell surface and total receptor levels in different brain regions of VGLUT3$^{-/-}$ mice

Brain Regions	mGluR5		mGluR2/3		NMDAR2A		NMDAR2B		GluA1		D1R		M1 mAChR	
	Surface	Total	Surface	Total	Surface	Total	Surface	Total	Surface	Total	Surface	Total	Surface	Total
Cerebral cortex	↑	↑	-	↑	-	-	↓	-	↑	↑	↓	-	-	-
Hippocampus	↓	-	-	-	↓	-	↓	-	-	↑	↓	-	↓	-
Striatum	↑	-	-	↑	-	-	-	-	↑	↑	-	-	-	-

Acknowledgments: SSGF holds a Tier I Canada Research Chair in Brain and Mind. KSA-E holds clinician postdoctoral fellowships from Alberta Innovates Health Solutions and CIHR. The authors thank Shaunessy Hutchinson for breeding the mouse colony.

Competing Interests: The authors declare that they have no competing interests.

Funding: This study was supported by Canadian Institutes for Health Research (CIHR) grants (PJT-148656, PJT-165967, and PJT-178060) and funding from Krembil Foundation to SSGF.

Chapter 3.
VGLUT3 deletion rescues motor deficits and neuronal loss without affecting mutant huntingtin aggregation in zQ175 mouse model of Huntington's disease

VGLUT3 deletion rescues motor deficits and neuronal loss without affecting mutant huntingtin aggregation in zQ175 mouse model of Huntington's disease

Karim S. Ibrahim[1,2,3], Salah El Mestikawy[4,5], Khaled S. Abd-Elrahman[1,2,3,*], and Stephen S. G. Ferguson[1,2,*]

[1] University of Ottawa Brain and Mind Research Institute, [2] Department of Cellular and Molecular Medicine, University of Ottawa, 451 Smyth Road, Ottawa, Ontario, K1H 8M5, Canada.

[3] Department of Pharmacology and Toxicology, Faculty of Pharmacy, Alexandria University, Alexandria, 21521, Egypt.

[4] Neuroscience Paris Seine – Institut de Biologie Paris Seine (NPS–IBPS) INSERM, CNRS, Sorbonne Université, Paris, France.

[5] Department of Psychiatry, Douglas Hospital Research Center, McGill University, Verdun, Quebec, Canada.

* KSA-E and SSGF contributed equally to this work as senior authors.

Correspondence to

Stephen S. G. Ferguson, PhD
Department of Cellular and Molecular Medicine
Faculty of Medicine, University of Ottawa
451 Smyth Rd, Ottawa, ON, K1H 8M5
Tel: (613) 562-5800 Ext 8889
Email: sferguso@uottawa.ca

or

Khaled S. Abd-Elrahman, BPharm, PhD
Department of Cellular and Molecular Medicine
Faculty of Medicine, University of Ottawa
451 Smyth Rd, Ottawa, ON, K1H 8M5

Author contributions: KSI, KSA-E, and SSGF were responsible for the conception and design of the experiments. KSI performed experiments, data analysis and wrote the initial draft. SEM, KSA-E, and SSGF edited the manuscript and supervised the study.

3.1. Abstract

Huntington's disease (HD) is an autosomal-dominant neurodegenerative disease characterized by progressive motor and cognitive impairments, with no disease-modifying therapies yet available. HD pathophysiology involves evident impairment in glutamatergic neurotransmission leading to severe striatal neurodegeneration. The vesicular glutamate transporter 3 (VGLUT3) mediates glutamate release from selected glutamatergic and non-glutamatergic neuronal populations that are affected by HD. Nevertheless, current evidence on the role of VGLUT3 in HD pathophysiology is lacking. Here, we crossed mice lacking the *Slc17a8* gene (VGLUT3$^{-/-}$) with a heterozygous zQ175 knock-in mouse model of HD (zQ175:VGLUT3$^{-/-}$). Longitudinal assessment of motor and cognitive functions from 6-15 months of age reveals that VGLUT3 deletion rescues motor coordination and short-term memory deficits in both male and female zQ175 mice. VGLUT3 deletion also rescues neuronal loss likely via the activation of Akt and ERK1/2 in the striatum of zQ175 mice of both sexes. Consistent with the growing consensus that mutant huntingtin (mHTT) aggregates are not linked to HD progression, the motor deficits rescue in zQ175:VGLUT3$^{-/-}$ mice are not associated with a significant change in mHTT aggregation. Collectively, these findings provide novel evidence that VGLUT3, despite its limited expression, can be a vital contributor to HD pathophysiology and a viable target for HD therapeutics.

3.2. Introduction

Huntington's disease (HD) is an inherited, autosomal-dominant neurodegenerative disease caused by an expansion in the polyglutamine repeat region at the N-terminal domain of huntingtin protein (HTT) that leads to its aggregation in neurons (MacDonald et al., 1993). HD phenotype includes involuntary body movements, such as chorea and dystonia, loss of cognitive abilities, psychiatric disturbances, and inevitable death within 15-20 years of disease onset (Li and Li, 2004). HD pathology is characterized by progressive degeneration of medium spiny neurons (MSNs) in the striatum, as well as some neocortical regions (MacDonald et al., 1993). To date, no disease-modifying therapies are available for HD and therapeutic options are limited to palliative management (Dash and Mestre, 2020).

Impairment in glutamate neurotransmission is considered a hallmark of HD, primarily contributing to disease phenotype (Eidelberg et al., 2011; Lewerenz and Maher, 2015; Ribeiro et al., 2017). Expression of mutant HTT (mHTT) protein is associated with selective degeneration in the MSNs via sensitization of glutamate receptor-mediated intracellular Ca^{2+} release leading to neuronal excitotoxicity (Sun et al., 2001; Fan and Raymond, 2007). Specifically, metabotropic glutamate receptors 1/5 (mGluR1/5) together with N-methyl-D-aspartate receptors (NMDARs) augment membrane depolarization and intracellular Ca^{2+} flux in MSNs while sparing other striatal interneurons in HD animal models (Calabresi et al., 1999; Tang et al., 2003; Ribeiro et al., 2017). Additionally, inhibiting glutamate release via the chronic activation of mGluR2/3 improves motor deficits and reduces mHTT aggregate pathology in zQ175 HD mice (Li et al., 2021).

Vesicular glutamate transporter subtype 3 (VGLUT3) is a member of the SLC17a family that transports glutamate into synaptic vesicles within selected neuronal populations in the brain (Ueda, 1986; Bellocchio et al., 2000; Ibrahim et al., 2020). In particular, VGLUT3 is expressed in neuronal terminals co-releasing glutamate with other neurotransmitters, such as acetylcholine (ACh), γ-Amino butyric acid (GABA), and serotonin (Fremeau et al., 2002; Gras et al., 2002; Schäfer et al., 2002). Within the striatum, VGLUT3 mediates the release of glutamate primarily from tonically active interneurons (TANs) that provides monosynaptic and disynaptic inputs on various striatal neurons (Nelson et al., 2014; Rehani et al., 2019). Interestingly, genetic silencing of VGLUT3 signaling diminishes TAN postsynaptic responses on striatal MSNs and fast-spiking interneurons, an effect that is considered to be mediated via ionotropic glutamate receptors (Higley et al., 2011; Nelson et al., 2014). VGLUT3 ablation also alters the expression of mGluR5 and mGluR2/3 within the striatum supporting the role of VGLUT3 in fine-tuning general striatal glutamatergic signaling (Ibrahim et al., 2022). Furthermore, co-transmission via VGLUT3-mediated glutamate and ACh exert a complex dual control upon dopamine signaling which is a major regulator of striatal output and locomotor activity (Trudeau and El Mestikawy, 2018). For example, VGLUT3 ablation elicits strong protective effects against L-DOPA-induced dyskinesia in a mouse model of Parkinsonism (Gangarossa et al., 2016). Overall, these data support the notion that VGLUT3 could play a pivotal role in HD. Despite this intricate role in regulating striatal circuits, the contribution of VGLUT3 to HD pathophysiology remains largely unknown.

Here, we investigated the potential contribution of VGLUT3 in HD pathogenesis using VGLUT3-null (VGLUT3$^{-/-}$) mice crossed with a heterozygous knock-in zQ175 mouse model of HD (zQ175:VGLUT3$^{-/-}$). We report that VGLUT3 deletion rescues motor coordination and short-term memory deficits in both male and female zQ175 mice. Furthermore, VGLUT3 deletion activates ERK1/2 and Akt cellular pro-survival pathways and rescues neuronal loss in the striatum of zQ175 mice of both sexes. However, loss of VGLUT3 does not alter mHTT aggregation or microgliosis in zQ175 mice striatum. Taken together, these findings provide evidence that VGLUT3, despite its inability to alter mHTT pathology, can be a vital target for the treatment of HD symptoms.

3.3. Materials and methods

3.3.1. Reagents

Horseradish peroxidase (HRP)-conjugated anti-rabbit (G-21234) and anti-mouse (G-21040) (H+L) cross-adsorbed IgG secondary antibodies were purchased from ThermoFisher Scientific (Waltham, Massachusetts). Rabbit anti-ERK1/2 (94484) and -Iba1 (178847) antibodies were from Abcam (Cambridge, Massachusetts). Rabbit anti-ERK1/2-pT202/Y204 (9101S), -Akt (9272S), and -Akt-pS473 (9271S) antibodies were from Cell Signaling Technology (Danvers, Massachusetts). Rabbit anti-NeuN (ABN78), and mouse anti-Huntingtin clone EM48 (MAB5374) antibodies were from Sigma-Aldrich (St. Louis, Missouri). Western blot reagents were purchased from Bio-Rad Laboratories (Mississauga, Ontario), and all other biochemical reagents were purchased from Sigma-Aldrich (St. Louis, Missouri).

3.3.2. Animals

Experimental protocols were approved by the Institutional Animal Care Committee at the University of Ottawa and were in compliance with the Canadian Council of Animal Care guidelines. Animals were group-housed under a constant 12-hour light/dark cycle and given food and water *ad libitum*. Heterozygous VGLUT3 knockout mice (Gras et al., 2008) (VGLUT3$^{-/+}$) and heterozygous knock-in zQ175 mice (Jackson Laboratory stock #370476) were bred to establish littermate-control male and female mice of the following genotypes; wild-type (VGLUT3$^{+/+}$), VGLUT3$^{-/-}$, zQ175, zQ175:VGLUT3$^{-/-}$ mice. zQ175 mice carry humanized exon-1 of the *Htt* gene with ~ 186 ± 15 CAG repeat expansions on one of the alleles (Menalled et al., 2012).

Experiments were designed to assess both motor and cognitive functions of the mice starting from 6 months of age, as HD phenotype typically manifests at 8-10 months of age (Menalled et al., 2012)**.** Upon the conclusion of the behavioral assessment, 15-month-old mice were euthanized by live cervical dislocation followed by rapid decapitation, brain dissection, and randomization for immunostaining and immunoblotting experiments.

3.3.3. Behavioral analysis

Mice were habituated in the testing room for at least 30 min before the experiment, and all behavioral assessment procedures were performed blindly during the animal's dark cycle. Behavioral studies were carried out with first the open field test, followed by the novel object recognition test, rotarod test, horizontal ladder test, and forelimb grip strength test.

3.3.3.1. Novel object recognition

Mice were placed in a white box (45 cm × 45 cm × 45 cm) and their activities were tracked using an overhead-mounted camera fed to a computer in a separate room and analyzed using the Noldus EthoVision 11 software (EthoVision XT). First, mice were allowed to explore an empty box for 5 min, and 5 min later, two identical objects were placed in the box 5 cm apart. Mice were then allowed to explore the maze for 10 min and were considered to be exploring an object if their nose was within 1 cm of the object. The following day, one object was replaced with a novel object and the experiment was repeated. Time spent by each mouse exploring the objects was recorded. The percentage recognition index was computed using this formula ((Exploration time for either familiar or novel object / Total time spent exploring both objects) x 100) (Abd-

Elrahman et al., 2017, 2020a). Mice were excluded from the analysis if the exploration time for similar objects on day one of the experiment was less than 10 s.

3.3.3.2. Open field

Spontaneous locomotor activity was assessed in an open field box (45 cm × 45 cm × 45 cm). Mice were placed in the corner of an opaque white box illuminated at 250 to 300 lux. Ten minutes were given to the mice to explore the box and the activity was monitored by an overhead-mounted camera fed to a computer in a separate room. Analysis was done using the Noldus EthoVision 11 software to calculate the percentage time mobile and frequency of entries to the center (25 cm × 25 cm) during the 10-min test period (Abd-Elrahman et al., 2017).

3.3.3.3. Rotarod

Mice motor coordination was assessed using an accelerating rotarod (IITC Life Science). On the first day, mice were habituated on a still rotarod for 3 min followed by four-trial training sessions on accelerating protocol (from 4 to 45 rpm in 300 s) with a 10 min interval between each trial. The following day, mice were tested using the same training paradigm, and the times required for the mice to fall were recorded. Average latency to fall values from the four trials of the second day were used for analysis (Li et al., 2021, 2022).

3.3.3.4. Horizontal ladder

A horizontal ladder was used to assess forelimb and hindlimb coordination. The ladder is composed of two clear Plexiglass walls (69.5 cm × 15 cm) containing 121 irregularly spaced metal rungs (0.15 cm in diameter). Mice were trained for two trials by placing them at the start of the ladder and guiding them toward the end if necessary.

Mouse nests were placed at end of the ladder to serve as an incentive to cross the ladder. Mice were tested for three trials that were video-recorded and the numbers of successful/missed steps were then quantified. Percent error represents the percentage of missed steps of the total number of steps required to cross the ladder (Abd-Elrahman et al., 2017; Li et al., 2021).

3.3.3.5. Forelimb grip strength

Mice were allowed to firmly grip on a rectangular grid bar of the Chatillon DFE II Grip Strength Meter (Columbus Instruments). Each mouse was then slowly pulled away at a speed of ~2.5 cm/s horizontally from the bar till released. The value of maximal strength value was recorded. Each mouse underwent seven trials, with a 5-10 s interval in between each trial (Abd-Elrahman et al., 2017; Li et al., 2021).

3.3.4. Immunohistochemistry

Fifteen-month-old mice brains were immunostained using a peroxidase-based protocol. Formalin-fixed, paraffin-embedded brain tissues were coronally sectioned through the striatum and the cortex. Immunostaining was performed on 5-µm sections using the Leica Bond™ system using standard IHC protocol (protocol F) (Abd-Elrahman et al., 2022; Li et al., 2022). A modification of protocol F was used for rabbit antibodies, which eliminates the antibody post-primary step when used on mouse tissue. Sections stained with rabbit antibodies were pre-treated using heat-mediated antigen retrieval with either EDTA buffer (pH 9.0, epitope retrieval solution 2; AR9640) or sodium citrate buffer (pH 6.0, epitope retrieval solution 1; AR9961) for 20 min. The sections were then incubated with the neuronal nuclei (NeuN) antibody at 1:1500, or lba-1 antibody at 1:8000 for 30 min at room temperature and detected using an HRP conjugated compact

polymer system (Leica Biosystems Cat# DS9800). For huntingtin immunostaining, brain sections were blocked with Rodent Block M (Biocare Medical, California, USA) for 60 min and were incubated with mouse anti-huntingtin antibody at 1:100. Slides were then stained using DAB as the chromogen, counterstained with Hematoxylin, mounted and coverslipped. Sections were visualized with a Zeiss Axio Scan Z1 Slide Scanner with a 20× lens (Oberkochen, Germany).

Six coronal sections per mouse spanning different regions of the striatum were analyzed. For each section, two 300x300 μm^2 ROIs in the striatum were used to quantify the number of mHTT puncta, Iba-1 and NeuN labeled cells using ImageJ Cell Counter tool (National Institutes of Health, Maryland, USA) (Schneider et al., 2012; Abd-Elrahman et al., 2017; Li et al., 2021, 2022).

3.3.5. Immunoblotting

Striata were dissected from mice brains and lysed in ice-cold lysis buffer (1% Triton-X, 25 mM HEPES, 300 mM NaCl, 1.5 mM $MgCl_2$, 0.2 mM EDTA) containing protease inhibitors cocktail (100 µM AEBSF [4-(2-aminoethyl)benzenesulfonyl fluoride hydrochloride], 80 nM aprotinin, 2 µM leupeptin, 5 µM Bestatin, 1.5 µM E-64, and 1 µM pepstatin A) and phosphatase inhibitors (500 µM Na_3VO_4 and 10 mM NaF). Tissue debris was pelleted and removed by centrifugation twice at 14,500 *x* rpm at 4°C for 10 min. Supernatants were then collected, and protein concentrations were measured using DC protein assay kit (Bio-Rad, Mississauga, Ontario). Homogenates were diluted to a protein concentration of 1 µg/µL in a mix of lysis buffer and β-mercaptoethanol-containing 3X loading buffer (187.5 mM Tris-HCl, 30% glycerol, 6% sodium dodecyl

sulfate, 0.006% Bromophenol Blue), and then boiled for 10 min at 90°C. Aliquots containing 40 µg of total protein were resolved by electrophoresis on 7.5%, 10%, or 12.5% SDS-polyacrylamide gels and transferred onto nitrocellulose membranes. Blots were blocked for 1 h at room temperature in Tris-buffered saline (pH 7.6) containing 0.05% Tween 20 (TBST) and 5% nonfat dry milk at room temperature. Blots were incubated overnight at 4°C with primary antibodies diluted (1:1000) in TBST containing 1% non-fat dry milk. The next day, blots were then washed 3 times with TBST and incubated with anti-rabbit/mouse secondary antibodies (1:5000) diluted in TBST containing 1% non-fat dry milk for 1 h at room temperature. Blots were washed again in TBST and bands were visualized by incubation with 1:1 Clarity Western Peroxide and Luminol/Enhancer solutions. Imaging of the blots was done using the Bio-Rad Chemidoc Gel imaging system. Band densities were quantified using Image Lab software and normalized to the loading control or total protein for the protein/phosphoprotein of interest as indicated in each figure legend.

3.3.6. Statistical Analysis

Mean ± SEM for each independent experiment is shown in the relevant figure legends. GraphPad Prism software version 9 was used to analyze data for normality and statistical significance. Data analysis was done using either unpaired Student's t-test or two-way ANOVA followed by Tukey’s or Dunnett’s post-hoc tests to determine the source of significant interactions. Details of statistical tests are indicated in the figure legends. *P* value less than 0.05 was considered statistically significant. Data analysis for behavioral experiments was conducted in groups comprising at least 10 mice per group, and immunohistochemical and immunoblotting analyses were conducted in

groups of 5–6 mice per group. Sample sizes were determined based on previous studies (Hamilton et al., 2016; Abd-Elrahman et al., 2020a, 2022).

3.4. Results

3.4.1. VGLUT3 deletion improved memory deficits in zQ175 mice

HD is associated with cognitive impairments and dementia which accompany chorea symptoms in patients (Paulsen, 2011). Similarly, zQ175 HD mice exhibit a marked decline in memory functions when assessed using different testing paradigms (Carty et al., 2015; Abd-Elrahman et al., 2017; Piiponniemi et al., 2018). Therefore, we investigated the impact of VGLUT3 deletion on short-term memory functions using the novel object recognition test. At 6 and 9 months of age, male and female zQ175, VGLUT3$^{-/-}$, and zQ175:VGLUT3$^{-/-}$ mice exhibited intact memory functions as depicted by their ability to discriminate between novel and familiar objects that were comparable to age- and sex-matched wild-type mice (**Figure 3.1A and 3.1B**). At 12 and 15 months of age, the cognitive functions of both male and female wild-type and VGLUT3$^{-/-}$ mice remained intact but zQ175 mice of both sexes were not able to discriminate between novel and familiar objects (**Figure 3.1C and 3.1D**). In contrast, zQ175:VGLUT3$^{-/-}$ mice of both sexes showed improved recognition indices for the novel objects at 12 and 15 months of age (**Figure 3.1C and 3.1D**). Together, this suggests that the deletion of VGLUT3 can prevent short-term memory deficits in HD mice.

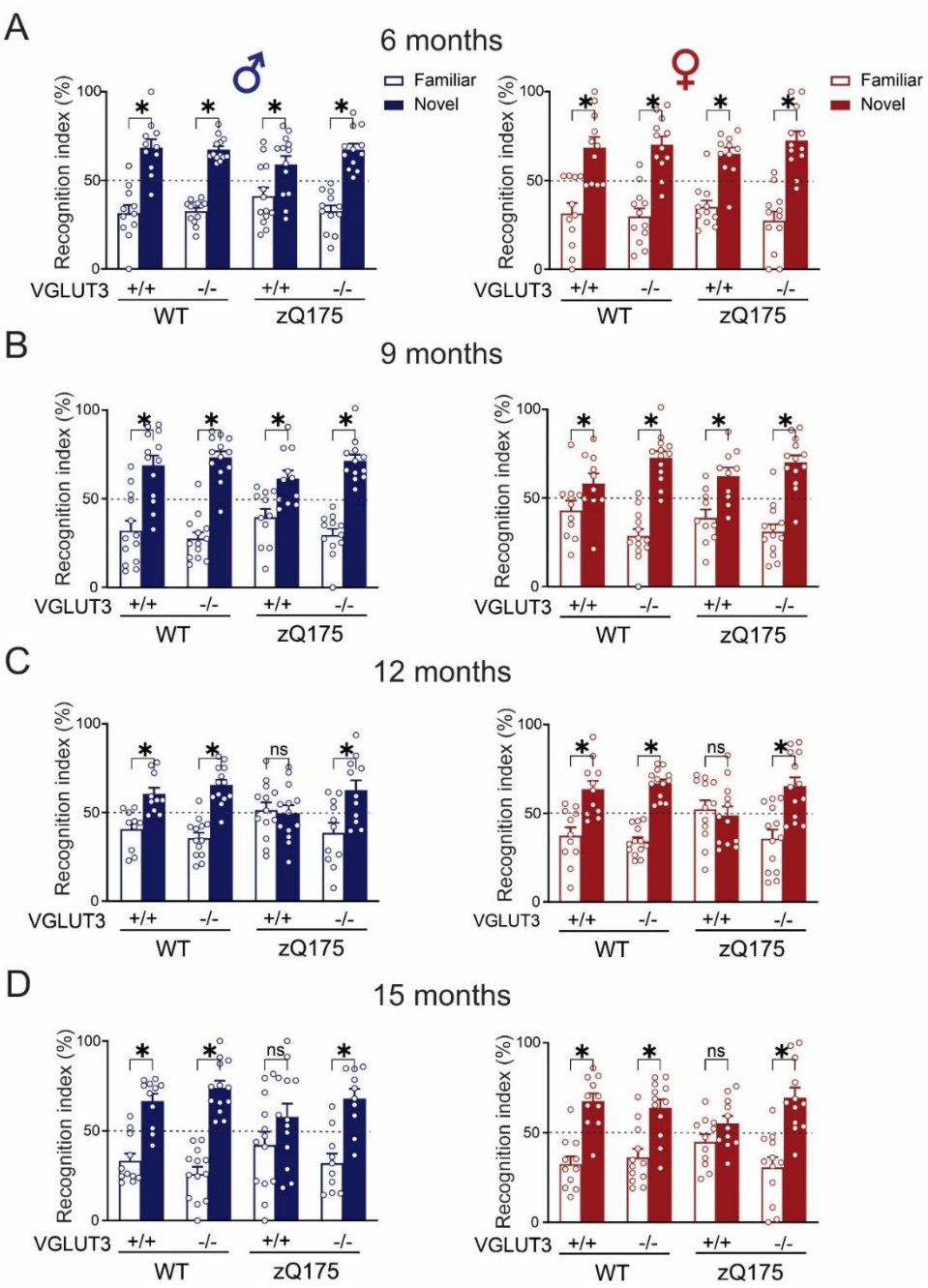

Figure 3.1. VGLUT3 loss improved short-term memory impairments in zQ175 Huntington disease mice. Means ± SEM of the recognition index for exploring a novel object versus a familiar object in novel object recognition test at (A) 6, (B) 9, (C) 12, and (D) 15 months of age in male and female wild-type (WT) and heterozygous zQ175 HD mice in the presence or absence of VGLUT3 expression (n = 10-13 mice per group). *$P < 0.05$ by two-way ANOVA followed by Tukey's post-hoc test for multiple comparisons.

3.4.2. VGLUT3 deletion mitigated impairments in motor coordination and grip strength in zQ175 mice

Reports from our laboratory and others demonstrated that zQ175 mice exhibited notable deficits in limb coordination, grip strength, and locomotor activity starting from 8-9 months of age (Menalled et al., 2012; Abd-Elrahman et al., 2017; Deng et al., 2021; Li et al., 2021). Here, we assessed limb coordination using rotarod and horizontal ladder tests, and forelimb grip force using the grip strength test. In the rotarod test, from 6 to 15 months of age, both male and female VGLUT3$^{-/-}$ exhibited similar latencies to fall when compared to age- and sex-matched wild-type mice (**Figure 3.2A**). However, we detected an age-dependent deterioration in the rotarod performance for both male and female zQ175 mice. For male mice, there was a significant difference in latency to fall at 12 and 15 months of age when compared to wild-type male mice, whereas for female zQ175 mice, significant differences in latency to fall values were observed at 6, 9, 12, and 15 months of age when compared to wild-type female mice (**Figure 3.2A**). Double mutant mice (zQ175:VGLUT3$^{-/-}$) demonstrated improved rotarod performance in both male and female mice at all ages to levels that were indistinguishable from age- and sex-matched wild-types (**Figure 3.2A**)**.** We then employed the horizontal ladder test to assess limb coordination by counting the number of missed steps while crossing a horizontal ladder with irregularly spaced steps. VGLUT3$^{-/-}$ mice of both sexes exhibited comparable percentages of missed steps at all ages when compared to age- and sex-matched wild-type mice (**Figure 3.2B**). In contrast, male and female zQ175 mice exhibited an age-dependent increase in the percentage of missed steps that was significantly different at 9, 12, and 15 months of age when compared to age- and sex-

matched wild-type mice (**Figure 3.2B**). Deletion of VGLUT3 on a zQ175 background restored limb coordination of males and females in the horizontal ladder task to values that were not significantly different from age- and sex-matched wild-type mice (**Figure 3.2B**). Grip strength was not affected by VGLUT3 deletion in both sexes and the values of forelimb grip force were comparable at all ages between VGLUT3$^{-/-}$ and age- and sex-matched wild-type mice (**Figure 3.2C**). Starting from 9 months of age, both male and female zQ175 mice exhibited significantly weakened grip strength, which was notably improved at all ages by VGLUT3 deletion to values that were indistinguishable from age- and sex-matched wild-type mice (**Figure 3.2C**). Collectively, our data indicate that VGLUT3 deletion does not impair motor functions in healthy mice but evidently rescues deficits in limb coordination and grip force in zQ175 HD mice.

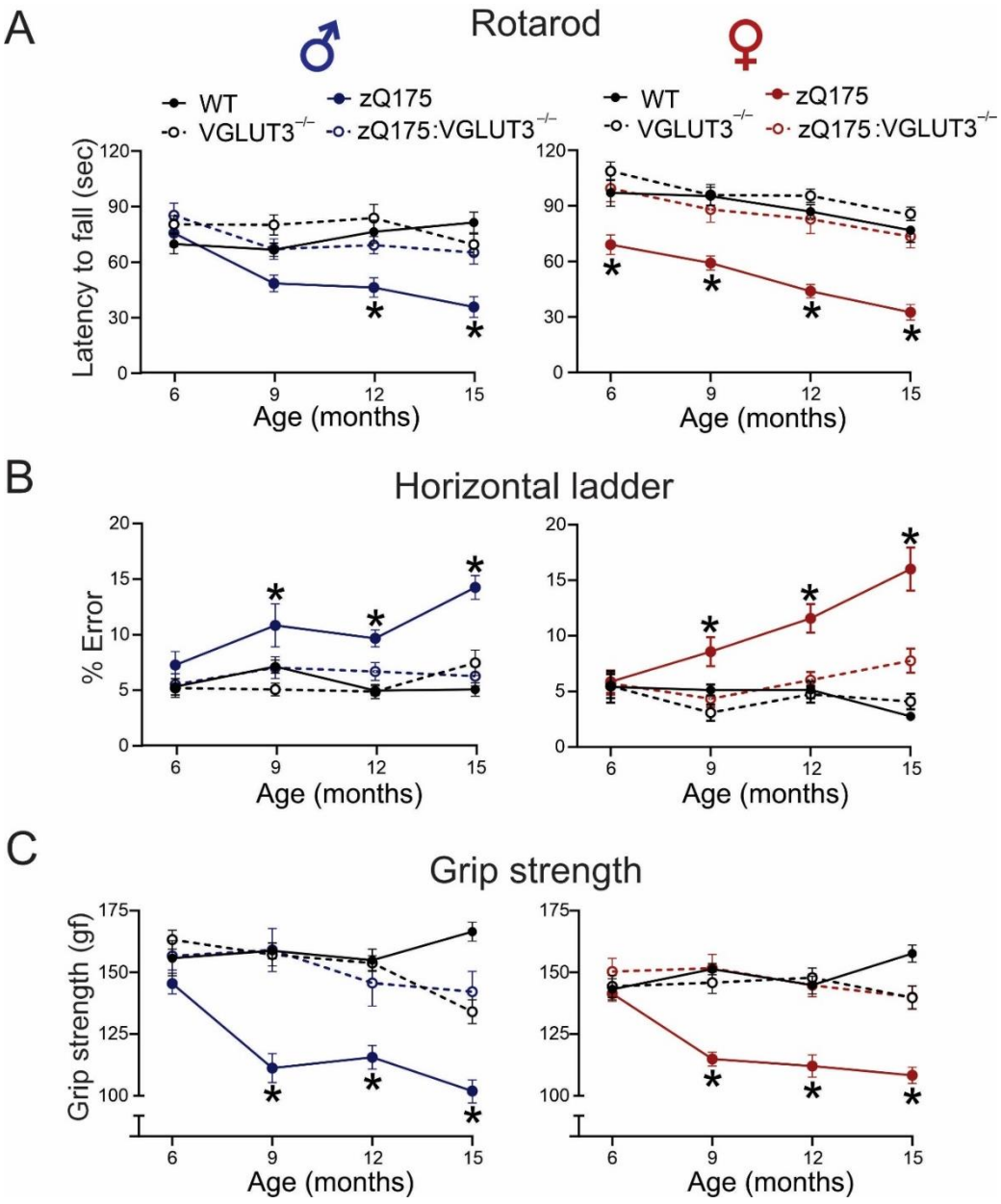

Figure 3.2. Loss of VGLUT3 rescued motor coordination deficits in zQ175 mice. (A) Latency to fall from accelerating rotarod, (B) percentage of errors made on the horizontal ladder, and (C) forepaw grip strength (gram-force (gf)) of male and female wild-type (WT) and heterozygous zQ175 HD mice in the presence or absence of VGLUT3 tested at 6, 9, 12, and 15 months of age (n = 10-13 mice per group). Data represent the means ± SEM. *$P < 0.05$ indicates significant differences compared with WT mice by two-way ANOVA followed by Dunnett's test for multiple comparisons.

3.4.3. VGLUT3 deletion did not improve anxiogenic locomotor behavior in zQ175 mice

Hypokinesia and anxiety are among the characteristic behavioral abnormalities observed in zQ175 HD mice (Menalled et al., 2012; Abd-Elrahman et al., 2017). Thus, we assessed the impact of VGLUT3 loss on anxiogenic locomotor behaviors in both male and female wild-type and zQ175 mice in the open field test. Both the male and female groups of zQ175, VGLUT3$^{-/-}$, and zQ175:VGLUT3$^{-/-}$ exhibited a progressive decline in the percent time mobile from 6-15 months of age when compared to age- and sex-matched wild-type mice (**Figure 3.3A**). However, female wild-type mice only exhibited a statistically significant difference in mobility from each of the other mouse groups at 15 months of age (**Figure 3.3A**). VGLUT3 deletion in both sexes of zQ175 mice did not reverse this decline in the percent time mobile in any of the age groups tested (**Figure 3.3A**). Interestingly, male VGLUT3$^{-/-}$, zQ175, and zQ175:VGLUT3$^{-/-}$ mice displayed a persistent decrease in the frequency to enter the center of the open field from 9-15 months. On the other hand, in female mice, the frequency of entries to the center was only impaired at 15 months of age when compared to age-matched wild-type mice (**Figure 3.3B**). Our findings indicate that VGLUT3 ablation results in anxiety-like behavior in healthy mice and therefore it is not capable of rescuing the anxiogenic behavior of HD mice.

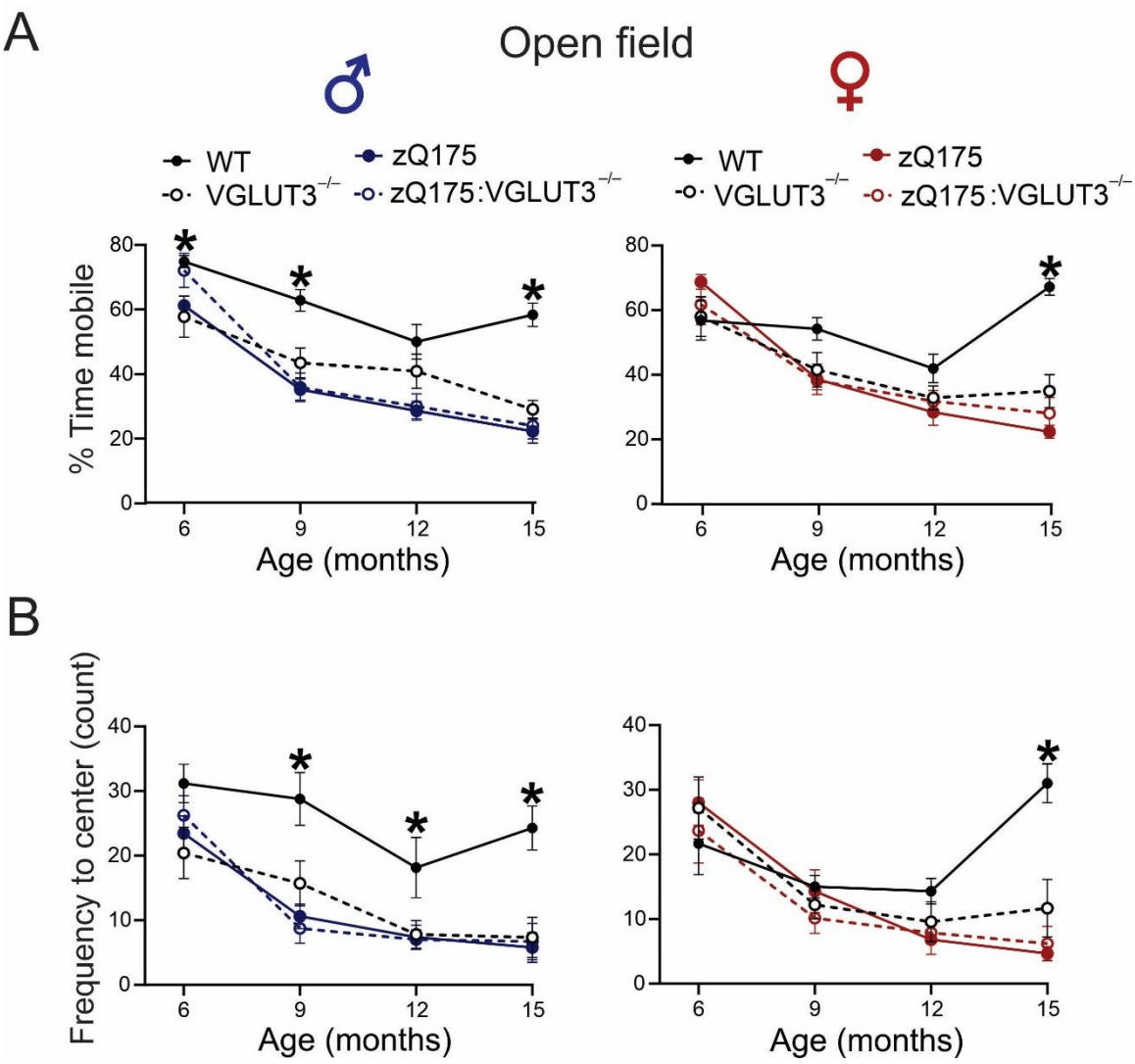

Figure 3.3. VGLUT3 loss in mice impaired anxiety-mediated locomotor performance in the open field test. (A) percent time mobile, (B) frequency of entries to the center of open field box in male and female wild-type (WT) and heterozygous zQ175 HD mice in the presence or absence of VGLUT3 tested at 6, 9, 12, and 15 months of age (n = 10-13 mice per group). Data represent the means ± SEM. **P* < 0.05 indicates significant differences as compared with zQ175 or VGLUT3$^{-/-}$ mice by two-way ANOVA followed by Dunnett's test for multiple comparisons.

3.4.4. VGLUT3 deletion rescued striatal neuronal loss and activated ERK1/2 and Akt signaling in zQ175 mice

zQ175 HD mice were previously shown to exhibit atrophic changes in both striatal and cortical regions, that correlated with HD phenotypic deficits (Heikkinen et al., 2012; Southwell et al., 2016). Here, we investigated the extent of neuronal loss in our mice by immunostaining for the neuronal nuclei marker, NeuN (Mullen et al., 1992). As previously described (Li et al., 2021, 2022), a significant decrease in the number of NeuN-labeled neurons was noted in the striatum of 15-month-old male and female zQ175 mice compared to age- and sex-matched wild-types (**Figure 3.4A and 3.4B**). Interestingly, VGLUT3 deletion in zQ175 mice prevented the loss of NeuN-labeled neurons in the striatum when compared to age- and sex-matched zQ175 mice (**Figure 3.4A and 3.4B**). Mutant HTT was previously reported to disrupt extracellular signal-regulated protein kinases (ERK1/2) and protein kinase B (Akt) signaling pathways, both are thought to be vital for neural cell development and survival (Apostol et al., 2006; Abd-Elrahman and Ferguson, 2019; Rai et al., 2019). Therefore, we assessed whether ERK1/2 and Akt phosphorylation were altered by VGLUT3 deletion in the striatum of 15-month-old wild-type and zQ175 mice. We found that genetic VGLUT3 deletion in wild-type mice increased the levels of pERK1/2 and pAkt in male but not female striatum (**Figure 3.5A and 3.5B**). In addition, pERK1/2 was increased in female, but not male zQ175 mouse striatum when compared to sex-matched wild-type controls (**Figure 3.5A and 3.5B**)**.** On the other hand, pAkt levels were increased in the striata of both male and female zQ175 mice when compared to sex-matched wild-type controls (**Figure 3.5A and 3.5B**). The genetic deletion of VGLUT3 in *zQ175* mice resulted in further

increases in pERK1/2 and pAkt levels when compared to sex-matched zQ175 and wild-type mice (**Figure 3.5A and 3.5B**). Together, the further activation in ERK1/2 and Akt pathways might underlie the prevention of neuronal loss in zQ175:VGLUT3$^{-/-}$ mice.

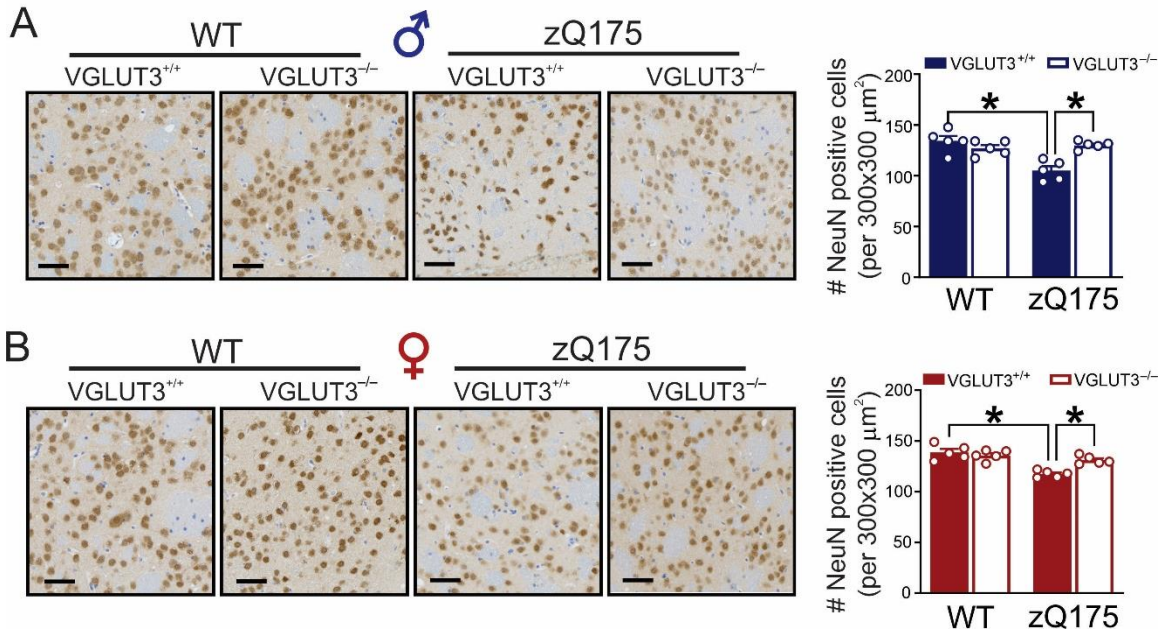

Figure 3.4. Loss of VGLUT3 mitigated striatal neuronal loss in zQ175 mice. Representative images and quantification of neuronal nuclei (NeuN) immunostaining in the striatal regions of (A) male and (B) female wild-type (WT) and heterozygous zQ175 HD mice in the presence or absence of VGLUT3. Quantification of NeuN-labeled cells is presented as the mean ± SEM of 2 striatal (300 µm x300 µm) regions from six brain slices per mouse (n= 5 for each group). Scale bar, 50 µm. *$P < 0.05$ by two-way ANOVA followed by Tukey's post-hoc test for multiple comparisons.

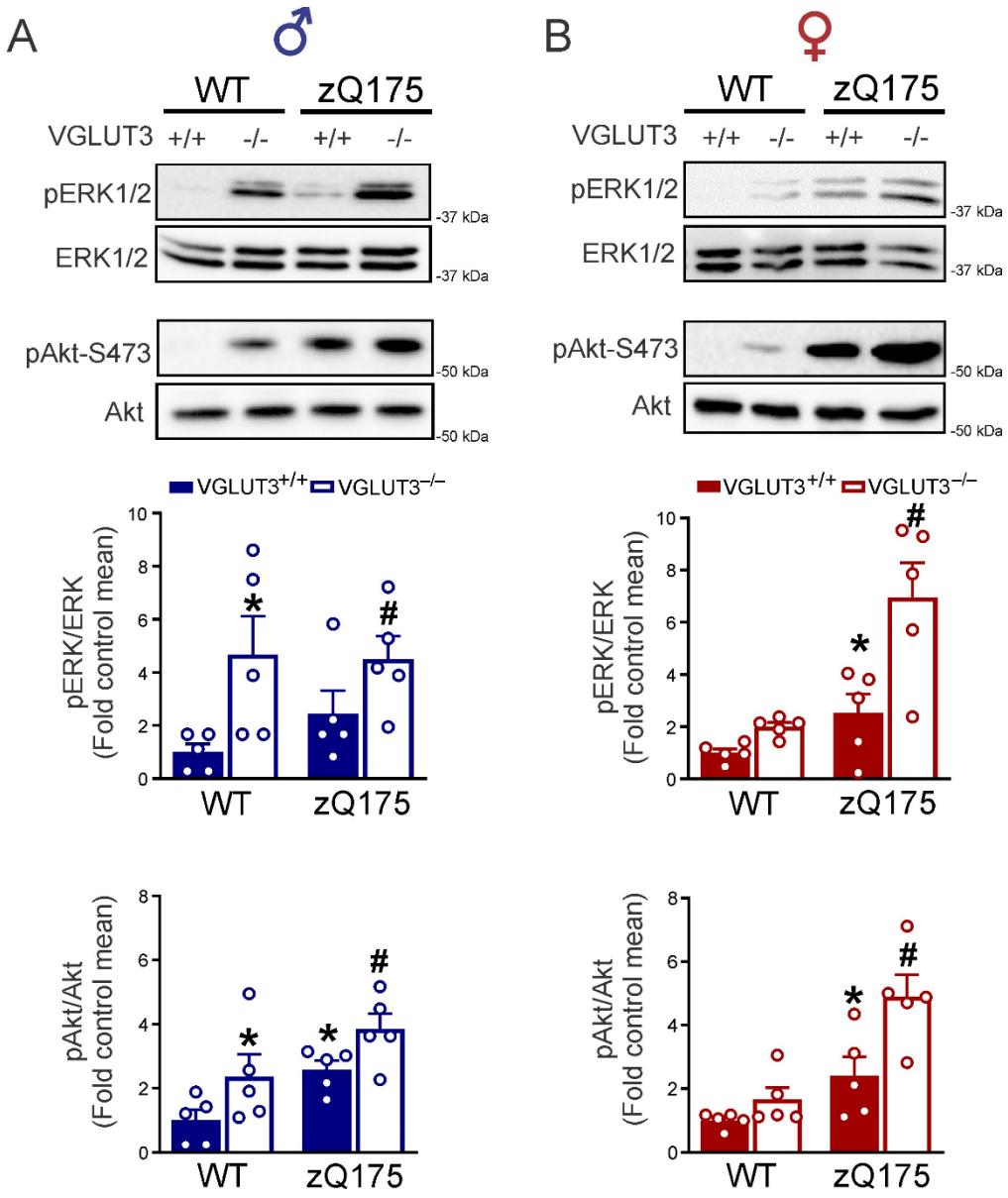

Figure 3.5. Loss of VGLUT3 activated ERK1/2 and Akt signaling in zQ175 mouse striatum. Representative western blots and quantification of ERK1/2-pT202/Y204 and Akt-pS473 levels with the corresponding total protein in the striatum of (A) male and (B) female wild-type (WT) and heterozygous zQ175 HD mice in presence or absence of VGLUT3. ERK1/2-pT202/Y204 was normalized to total ERK1/2 and Akt-pS473 was normalized to total Akt (n= 5 for each group). Values are expressed as a fraction of mean VGLUT3$^{+/+}$ WT values. Significance was assessed by two-way ANOVA followed by Tukey's post-hoc test. *Significantly different ($P < 0.05$) from WT VGLUT3$^{+/+}$ values. #Significantly different ($P < 0.05$) from zQ175:VGLUT3$^{+/+}$ values.

3.4.5. VGLUT3 deletion did not improve mHTT aggregation or microgliosis in zQ175 mice

zQ175 HD mice were previously shown to exhibit age-dependent increases in mHTT aggregate size and densities in both striatal and cortical regions starting from 6 months of age (Smith et al., 2014; Abd-Elrahman et al., 2017). In addition, mHTT aggregation evokes inflammatory responses in the basal ganglia that could further exacerbate HD pathology (Wilton and Stevens, 2020). For instance, microgliosis was previously shown to be evident in both HD patients and animal models of HD (Pavese et al., 2006; Savage et al., 2020). Here, we assessed whether the improvements in motor deficits and neuronal survival following VGLUT3 deletion were associated with a reduction in mHTT aggregation or microglia activation in 15-month-old male and female zQ175 mice. As we have previously described (Li et al., 2021, 2022), both male and female zQ175 mice exhibited evident accumulation of mHTT aggregates in the dorsal striatum (**Figure 3.6A and 3.6B**). However, the number of mHTT aggregates were unaffected by VGLUT3 deletion in either male or female zQ175 mice (**Figure 3.6A and 3.6B**). We then immunostained for ionized Ca^{2+}-binding adaptor molecule-1 (Iba1), a pan marker for microglial cells, to assess microgliosis (Imai et al., 1996; Li et al., 2021). As we previously described (Li et al., 2021, 2022), significant elevations in the numbers of Iba1-positive cells were detected in the striata of both male and female zQ175 mice compared to age- and sex-matched wild-types (**Figure 3.6C and 3.6D**). Similar to that observed for mHTT aggregates, the number of Iba1-positive cells was not affected by VGLUT3 deletion in the striata of either male or female zQ175 mice (**Figure 3.6C and 3.6D**). Our findings suggest that the neuronal rescue in zQ175:VGLUT3$^{-/-}$ mouse striatum is independent of mHTT aggregation and associated microgliosis.

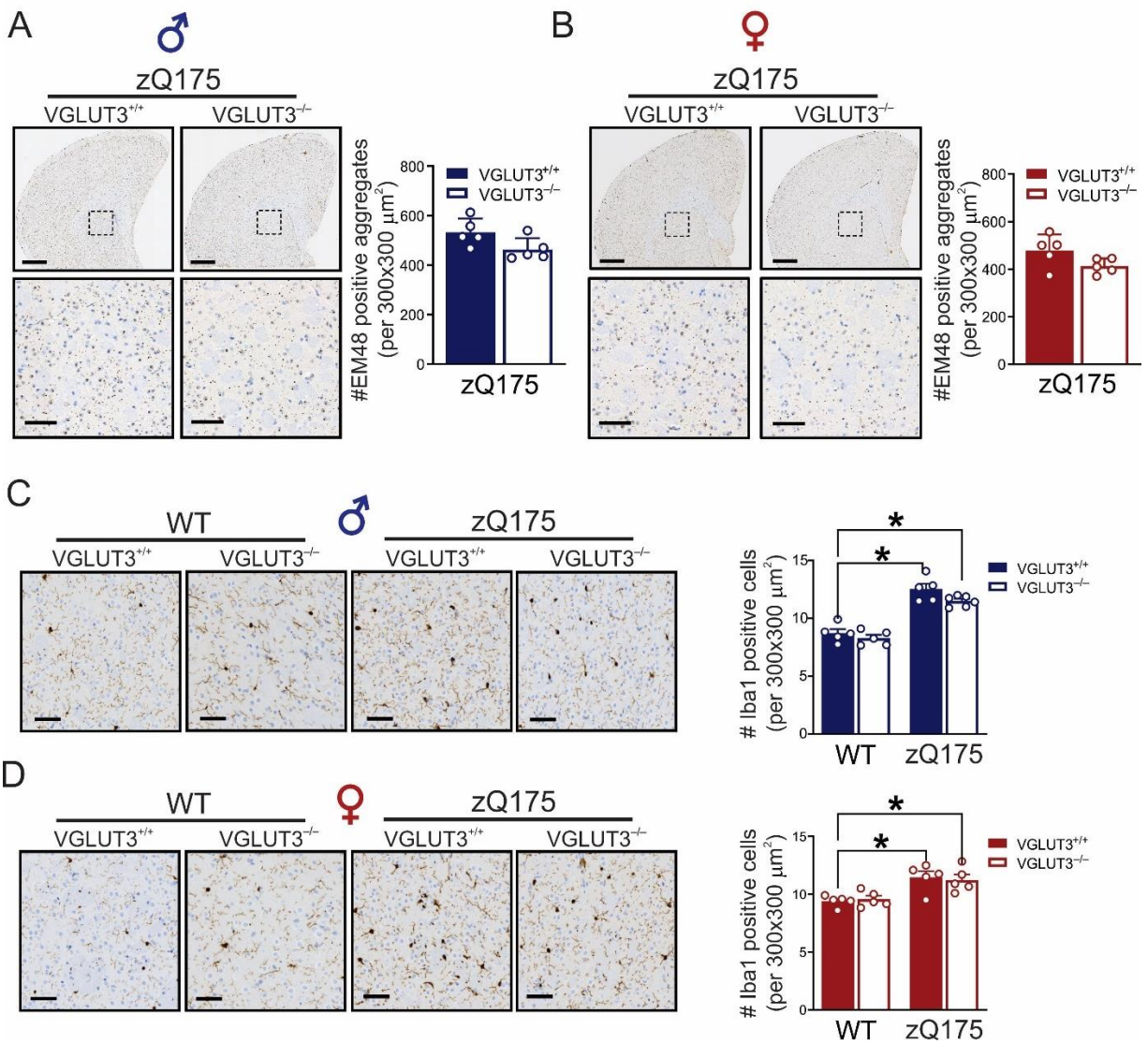

Figure 3.6. mHTT accumulation and microgliosis were unaffected by VGLUT3 deletion in zQ175 mouse striatum. Representative images of mutant huntingtin (mHTT) staining using the EM48 antibody in coronal whole-brain slice and magnified area of the striatum from (A) male and (B) female zQ175 and zQ175:VGLUT3$^{-/-}$ mice. mHTT aggregate quantification is presented as the mean ± SEM of 2 striatal regions (300 µm x300 µm) from six brain slices per mouse (n= 5 for each group). Scale bars, 500 µm for the whole slice and 50 µm for the magnified area of the striatum. Statistical significance was assessed by unpaired Student's t-test. Representative images of microglial ionized Ca^{2+} binding adaptor-1 (Iba1) immunostaining in striatal regions of (C) male and (D) female wild-type (WT) and heterozygous zQ175 HD mice in the presence

or absence of VGLUT3. Iba1-positive cell quantification is presented as the mean ± SEM of 2 striatal regions (300 µm x300 µm) from six brain slices per mouse (n= 5 for each group). Scale bar, 50 µm. *$P < 0.05$ by two-way ANOVA followed by Tukey's post-hoc test for multiple comparisons.

3.5. Discussion

VGLUT3 and glutamate/ACh contribute to anxiety (Amilhon et al., 2010), drug addiction (Sakae et al., 2015), eating disorders (Favier et al., 2020), and motor dyskinesia in Parkinson's disease (Divito et al., 2015). Here, we provide the first evidence for the involvement of VGLUT3 in modifying HD progression in mice. We show that VGLUT3 deletion rescues the progressive decline in short-term memory and motor coordination in both male and female heterozygous zQ175 HD mice. Furthermore, VGLUT3 loss activates striatal proliferative/pro-survival neuronal signaling and rescues striatal neuronal loss in heterozygous zQ175 mice of both sexes. However, mHTT aggregation and the associated microgliosis are not significantly mitigated by VGLUT3 deletion in zQ175 mice. Together, this provides evidence that VGLUT3 signaling is a key modulator of HD phenotype in mice independent of mHTT pathology and could be a promising target for the treatment of HD.

Although HD is commonly identified on the basis of motor dysfunctions, memory impairments are also evident in HD patients and animal models (Paulsen, 2011; Giralt et al., 2012; Piiponniemi et al., 2018; Li et al., 2022). In line with this evidence, we show that both male and female zQ175 HD mice exhibit cognitive impairments starting at 12 months of age. However, little evidence exists supporting the role of VGLUT3 in cognitive behaviors despite its reported involvement in hippocampal circuitries (del Pino et al., 2017; Fasano et al., 2017). Our findings suggest that VGLUT3 loss itself has no impact on novel object recognition memory in both male and female mice but, remarkably, VGLUT3 deletion rescues the memory impairments found in zQ175 HD mice of both sexes, suggesting that VGLUT3 is an important modulator of memory

circuits in HD mice. While the underlying mechanisms are yet to be elucidated, we recently reported that knocking out VGLUT3 modifies the strength of glutamatergic neurotransmission in the hippocampus (Ibrahim et al., 2022). Specifically, reductions in cell-surface levels of NMDARs and mGluR5 were detected in VGLUT3$^{-/-}$ hippocampus (Ibrahim et al., 2022). Since dysregulated signaling via both receptors is implicated in memory dysfunction (Wang and Reddy, 2017; Abd-Elrahman and Ferguson, 2022), these cell-surface reductions in NMDARs and mGluR5 may potentially delay the disruptions in synaptic plasticity responses in hippocampal neurons of HD mice (Parsons and Raymond, 2014). Indeed, much remains to be investigated regarding the mechanisms underlying these findings.

VGLUT3-positive neurons are strategically organized within glutamatergic and non-glutamatergic brain networks regulating different motor functions (Vigneault et al., 2015; Sakae et al., 2019; Ibrahim et al., 2020). Here, we find that deletion of VGLUT3 in the brain rescues the progressive decline of motor functions in both male and female heterozygous zQ175 HD mice. This corroborates current evidence showing that deletion of VGLUT3 significantly improves locomotor deficits in Parkinson's disease (Divito et al., 2015), and L-DOPA-induced dyskinesia mouse models (Gangarossa et al., 2016). Interestingly, deficits in dopaminergic and cholinergic neurotransmission are characteristic pathogenic features of HD that potentially underlie dyskinetic movements and cognitive decline in both HD patients and zQ175 HD mice (Bird, 1980; Richfield et al., 1991; Rothe et al., 2015; D'Souza and Waldvogel, 2016). Therefore, the improvement of motor functions in HD mice may be explained by the fact that VGLUT3 loss alters the dopaminergic/cholinergic balance within the striatum leading to an overall

enhancement of ambulatory activity (Gras et al., 2008; Divito et al., 2015). This shift in dopaminergic/cholinergic balance is evidenced by the ability of VGLUT3 to alter dopamine D1 receptor densities in the ventral striatum and the cortex (Sakae et al., 2015; Ibrahim et al., 2022). We also show that, similar to zQ175 mice, VGLUT3$^{-/-}$ mice and zQ175:VGLUT3$^{-/-}$ mice have reduced overall locomotor activity and anxiety-like behavior in the open field test. This may be attributed to enhanced neophobic responses displayed by VGLUT3$^{-/-}$ mice when placed in a new environment (Amilhon et al., 2010). This also reflects on the hypolocomotive behavior in VGLUT3$^{-/-}$ mice when measured during shorter periods of assessment (5-10 mins), as opposed to relative hyperactivity when assessed over longer periods (>15 mins) (Gras et al., 2008; Balázsfi et al., 2018). Taken together, our current observations provide novel evidence that VGLUT3 inhibition represents a promising therapeutic approach to slow and/or prevent HD motor phenotype in a sex-independent manner.

Aberrant ERK1/2 activation can disrupt striatal neuron survival and promote pro-apoptotic cellular signaling in zQ175 mice (Lu and Xu, 2006; Abd-Elrahman et al., 2017). However, we suspect that the augmented ERK1/2 activation in zQ175:VGLUT3$^{-/-}$ striatum preferentially engages neuroprotective mechanisms as evidenced by the rescue in neuronal loss coupled with activation in the Akt pathway, which further promotes ERK1/2-mediated pro-survival signaling (Mirza et al., 2004; Mendoza et al., 2011). This is also evident in VGLUT3$^{-/-}$ mice which elicit increased ERK1/2 activation with no reduction in the number of striatal neurons. In addition, the proper processing of motor functions via the striatum relies on intact Akt/mTOR signaling. Suppressing mTOR activity in the dorsal striatum can significantly compromise motor learning skills

in mice (Bergeron et al., 2014). In HD, unilateral injection of a constitutively active Akt downstream target, Ras homolog expressed in the brain (Rheb), can reverse striatal atrophy and improve mHTT-associated metabolic phenotypes (Lee et al., 2015). Thus, the rescue in striatal neuronal loss and HD motor deficits may be mediated, at least partially, via ERK1/2 and Akt signaling in zQ175:VGLUT3$^{-/-}$ mice.

Despite the rescue of striatal neuronal loss, cognitive function, and motor activity, we find that deletion of VGLUT3 does not modify mHTT aggregate levels in both male and female zQ175 HD mice. mHTT can evoke striatal neuronal damage via excessive activation of mGluR1/5 and NMDARs resulting in excitotoxicity (Fan and Raymond, 2007; Ribeiro et al., 2017). Interestingly, VGLUT3 mediates tonic excitatory currents via both mGluR1/5 and NMDARs onto MSNs (Higley et al., 2011; Sakae et al., 2015). Because MSNs of zQ175 mice exhibit progressive intrinsic hyperexcitability, it is possible that the lack of VGLUT3 might have lowered glutamatergic inputs further reducing excitotoxic insults in zQ175:VGLUT3$^{-/-}$ striatum (Heikkinen et al., 2012; Goodliffe et al., 2018). However, this warrants further investigations. Similar to mHTT accumulation, microgliosis in the striatum of HD mice was not modified by VGLUT3 loss. This is consistent with the lack of VGLUT3 expression in microglia and astrocytes. Thus, their recruitment and activation are likely unaltered by VGLUT3 deletion (Schäfer et al., 2002; Li et al., 2013). Taken together, our findings suggest that rescued neuronal loss in zQ175 mice by VGLUT3 deletion is independent of mHTT aggregation or their influence on microglia recruitment.

In summary, we provide evidence that loss of VGLUT3 transmission rescues long-term motor and recognition memory deficits in both male and female zQ175 mice

without altering mHTT pathology. Moreover, we report an evident rescue in striatal neuronal loss in VGLUT3-null HD mice. To date, toolkits for pharmacologic suppression of VGLUT3 are still awaited. Our findings clearly highlight the importance of exploiting this pathway for HD therapeutic management.

Acknowledgments: SSGF holds a Tier I Canada Research Chair in Brain and Mind. KSA-E holds clinician postdoctoral fellowships from the Alberta Innovates Health Solutions and Canadian Institutes for Health Research (CIHR). We thank Tash-Lynn Colson and Shaunessy Hutchinson for breeding the animals and providing technical assistance. We also thank the Behavior and Physiology Core at the University of Ottawa for their assistance. This study was supported by CIHR grants (PJT-148656, PJT-165967, and PJT-178060) and Funding from Krembil Foundation to SSGF.

Conflict of interest: The authors declare that they have no competing interests.

Preamble to Chapter 4.

In chapters 2 and 3, we showed that ablation of VGLUT3 dynamically regulates glutamate receptor densities in several regional brain networks which potentially account for the rescue in HD motor deficits and striatal neuron loss in VGLUT3-null HD mice. The data also suggest that mGluR5 can be one of the key mediators of this motor rescue since pathological mGluR5 activation impairs motor control and accelerates disease progression in HD mice (Ribeiro et al., 2017). Our group recently established evidence that mGluR5 regulates autophagic signaling in both HD and AD mouse models (Abd-Elrahman et al., 2017, 2018; Li et al., 2022). Given that OPTN is vital for autophagy regulation in addition to its reported interaction with mGluR5 (Anborgh et al., 2005; Slowicka et al., 2016), I opted in chapter 4 to investigate the role of OPTN in mGluR5 canonical and autophagic signaling to assess the potential of this pathway in modifying HD progression in animal models.

Chapter 4.
Optineurin deletion disrupts metabotropic glutamate receptor 5-mediated regulation of ERK1/2, GSK3β/ZBTB16, mTOR/ULK1 signaling in autophagy

Optineurin deletion disrupts metabotropic glutamate receptor 5-mediated regulation of ERK1/2, GSK3β/ZBTB16, mTOR/ULK1 signaling in autophagy

Karim S. Ibrahim [1,2,3,#], Caitlyn J. McLaren [1,2,#], Khaled S. Abd-Elrahman [1,2,3], Stephen S. G. Ferguson[1,2,*]

[1] University of Ottawa Brain and Mind Research Institute, [2] Department of Cellular and Molecular Medicine, University of Ottawa, 451 Smyth Road, Ottawa, Ontario, K1H 8M5, Canada.

[3] Department of Pharmacology and Toxicology, Faculty of Pharmacy, Alexandria University, Alexandria, 21521, Egypt.

[#] Contributed equally to this work

* **Correspondence to**

Stephen Ferguson, PhD
Department of Cellular and Molecular Medicine
Faculty of Medicine, University of Ottawa
451 Smyth Rd, Ottawa, ON, K1H 8M5
Tel: (613) 562-5800 Ext 8889
Email: sferguso@uottawa.ca

Article published March 2021 in Biochemical Pharmacology, 185 (3) 114427; DOI https://doi.org/10.1016/j.bcp.2021.114427

Authors Contributions: K.S.I, C.M, K.S.A and S.S.G.F were responsible for the conception and design of all experiments. K.S.I conducted the experiments and analyses in the following Figures: Figures 1, 2, 6, and 7. C.M and K.S.I performed the experiments shown in Figures: Figure 3B, 5A-C, and 8C. K.S.I and C.M performed data analysis. K.S.I and K.S.A wrote the manuscript and S.S.G.F edited the manuscript and supervised the study.

4.1. Abstract

Optineurin (OPTN) is a multifunctional protein that mediates a network of cellular processes regulating membrane trafficking, inflammatory responses, and autophagy. The OPTN-rich interactome includes group I metabotropic glutamate receptors (mGluR1 and 5), members of the $G\alpha_{q/11}$ protein receptor family. Recent evidence has shown that mGluR5, in addition to its canonical $G\alpha_{q/11}$ protein-coupled signaling, regulates autophagic machinery via mTOR/ULK1 and GSK3β/ZBTB16 pathways in both Alzheimer's and Huntington's disease mouse models. Despite its potential involvement, the role of OPTN in mediating mGluR5 downstream signaling cascades remains largely unknown. Here, we employed a CRISPR/Cas9 OPTN-deficient $STHdh^{Q7/Q7}$ striatal cell line and global OPTN knockout mice to investigate whether *Optn* gene deletion alters both mGluR5 canonical and noncanonical signaling**.** We find that OPTN is required for mGluR5-activated Ca^{2+} flux and ERK1/2 signaling following receptor activation in $STHdh^{Q7/Q7}$ cells and acute hippocampal slices. Deletion of OPTN impairs both GSK3β/ZBTB16 and mTOR/ULK1 autophagic signaling in $STHdh^{Q7/Q7}$ cells. Furthermore, mGluR5-dependent regulation of GSK3β/ZBTB16 and mTOR/ULK-1 autophagic signaling is impaired in hippocampal slices of OPTN knockout mice. Overall, we show that the crosstalk between OPTN and mGluR5 can have major implications on receptor signaling and therefore potentially contribute to the pathophysiology of neurodegenerative diseases.

4.2. Introduction

Metabotropic glutamate receptor 5 (mGluR5) is a member of the group I family of mGluRs that preferentially activate $G\alpha_{q/11}$-dependent signaling (Abe et al., 1992; Niswender and Conn, 2010). mGluR5-mediated activation of $G\alpha_{q/11}$ signaling is associated with the activation of phospholipase Cβ (PLCβ) and the generation of inositol trisphosphate (IP_3) and diacylglycerol (DAG). Both IP_3 and DAG are essential for mGluR5-dependent neuronal excitability as IP_3 mobilizes Ca^{2+} from intracellular stores, and both Ca^{2+} and DAG activate protein kinase C (PKC)-dependent signaling (Abdul-Ghani et al., 1996; Dhami and Ferguson, 2006). G protein-independent signaling of mGluR5 is also essential for supporting synaptic protein synthesis required for long-term plasticity changes. Particularly, mGluR5 activates extracellular signal-regulated kinase (ERK1/2) to phosphorylate proteins regulating mRNA translation and rapid synaptic protein synthesis (Gallagher, 2004; Mao et al., 2005; Jong et al., 2009; Nicodemo et al., 2010). Moreover, agonist-dependent activation of mGluR5 regulates protein translation via activation of protein kinase B/mammalian target of rapamycin (Akt/mTOR) pathway (Rong et al., 2003; Hou and Klann, 2004). Therefore, mGluR5 signaling via G protein-dependent and -independent mechanisms ensures dynamic regulation of neuronal excitability and synaptic plasticity required for memory formation and consolidation (Rong et al., 2003; Gallagher, 2004; Hou and Klann, 2004; Sethna et al., 2016).

Recently, mGluR5 emerged as a promising target for regulating the catabolic processing of misfolded proteins through autophagy. Neurodegenerative aggregopathies such as Alzheimer's (AD), Parkinson's (PD), and Huntington's (HD)

disease exhibit evident disruption in cellular autophagy mechanisms (Guo et al., 2018). Specifically, pathological mGluR5 activation promotes inhibitory phosphorylation of glycogen synthase kinase 3β (GSK3β) that increases the levels of Zinc finger and BTB domain-containing protein 16 (ZBTB16), a member of ZBTB16-Cullin3-Roc1 E3-ubiquitin ligase complex, leading to ubiquitination and proteasomal degradation of the autophagy-related 14 (ATG14) protein and inhibition of autophagy (Zhang et al., 2015; Abd-Elrahman et al., 2017). As well, mGluR5 activation inhibits Unc-51-like kinase activity (ULK1) and autophagy-related 13 (ATG13) protein via mTOR complex thereby disrupting autophagosome formation (Page et al., 2006; Kim et al., 2011; Abd-Elrahman and Ferguson, 2019). Pharmacological ablation of mGluR5 with the mGluR5-selective negative allosteric modulator (NAM), 2-chloro-4-[(2,5-dimethyl-1-(4-(trifluoromethoxy)phenyl)-1H-imidazol-4-yl)ethynyl] pyridine (CTEP), improved neuronal autophagic flux by reactivating two mutually non-exclusive pathways, GSK3β/ZBTB16/ATG14 and mTOR/ULK1/ATG13 in mouse models of AD and HD (Abd-Elrahman et al., 2017, 2018). Thus, regulation of autophagy by mGluR5 represents a novel receptor-dependent signaling mechanism that modulates proteotoxic aggregate accumulation and has the potential to represent a key role in neurodegeneration.

Optineurin (OPTN) is a multifunctional cytosolic protein that is involved in a network of cellular processes regulating membrane trafficking, inflammatory responses, and autophagy (Harjes and Wanker, 2003; Rezaie and Sarfarazi, 2005). OPTN, originally named FIP2, was first identified as a positive regulator of tumor necrosis factor-α (TNFα)-mediated apoptosis and as mutant huntingtin (mHTT) interacting

protein by yeast two-hybrid screen, and OPTN mutations were associated with open-angle glaucoma for which it obtained its current name (Faber, 1998; Li et al., 1998; Rezaie et al., 2002). Interestingly, OPTN was found to be ubiquitously expressed in the mammalian brain including; the cerebral cortex, striatum, hippocampus, and cerebellum (Rezaie and Sarfarazi, 2005; Okita et al., 2012). OPTN via its ubiquitin-binding domain serves as an autophagy receptor to escort ubiquitinated cellular cargos to autophagosomes (Wild et al., 2011; Slowicka et al., 2016) and therefore, it may contribute to the clearance of proteotoxic aggregates in neurodegenerative diseases. In particular, ubiquitin-positive neurofibrillary tangles and dystrophic neurites of AD patients were colocalized with OPTN (Osawa et al., 2011). OPTN was also sequestered in intranuclear and perikaryal mHTT inclusions of cortical and striatal specimens from HD patients and animal models (Harjes and Wanker, 2003; Schwab et al., 2012; Shen et al., 2015).

We have previously shown that OPTN interacts with and modulates group I mGluR signaling (Anborgh et al., 2005). Specifically, OPTN co-immunoprecipitates with both mGluR1 and mGluR5 and attenuates agonist-stimulated mGluR1 coupling to PLCβ that subsequently suppresses IP_3 formation (Anborgh et al., 2005). However, it remains less clear whether this interaction of OPTN with mGluR5 is essential for mGluR5-dependent autophagy and synaptic protein synthesis (Anborgh et al., 2005; De Marco et al., 2006; Bansal et al., 2018)**.** In the current study, we knocked out the *Optn* gene in STHdh$^{Q7/Q7}$ striatal cell line and utilized *Optn*-null mice to assess how OPTN deletion impacts mGluR5-dependent canonical and autophagic signaling. We show here that genetic deletion of OPTN enhances agonist-stimulated Ca^{2+} flux in STHdh$^{Q7/Q7}$ striatal

cells and impairs mGluR5-mediated ERK1/2 phosphorylation in both STHdh$^{Q7/Q7}$ striatal cells and acute hippocampal slices. Furthermore, our data indicate that OPTN plays a key role in regulating mGluR5 autophagic signaling via GSK3β/ZBTB16 and mTOR/ULK1 pathways in both striatal cell line and acute hippocampal slices. Taken together, these findings suggest that crosstalk between mGluR5 and OPTN is essential for mGluR5 signaling and therefore potentially implicated in the pathophysiology of neurodegenerative diseases.

4.3. Materials and Methods

4.3.1. Reagents

(S)-3,5-DHPG (0805/10) was purchased from Bio-Techne (Toronto, Ontario). CTEP was purchased from Axon Medchem (Reston, Virginia). Horseradish peroxidase (HRP)-conjugated anti-rabbit (G-21234) and anti-mouse (G-21040) IgG secondary antibodies were purchased from Thermo Fisher Scientific (Waltham, Massachusetts). Rabbit anti-vinculin (129002), -ERK1/2 (94484), -ZBTB16 (39354), -VPS34 (124905), and mouse anti-SQSTM1/P62 (56416) antibodies were purchased from Abcam (Cambridge, Massachusetts). Rabbit anti- ERK1/2-pT202/Y204 (9101S), -GSK3β-pS9 (9323S), -ULK1-pS757 (14202S), -mTOR-pS2448 (109268), -mTOR (2972), and mouse anti-GSK3β (9832S) antibodies from Cell Signaling Technology (Danvers, Massachusetts). Rabbit anti-β-Tubulin (T2200) and anti-mGluR5 (AB5675) were purchased from Millipore Sigma (St. Louis, Missouri). Rabbit anti- LC3B (NB100-2220) was from Novus Biologicals. Western blot reagents were purchased from Bio-Rad Laboratories (Mississauga, Ontario) and all other biochemical reagents were purchased from Sigma-Aldrich (St. Louis, Missouri).

4.3.2. Generation of OPTN knockout cell lines

The STHdh$^{Q7/Q7}$ cell line was provided by Dr. Ray Truant (McMaster University) and was formerly purchased from Coriell Institute for Medical Research (CH00097). STHdh$^{Q7/Q7}$ cells were derived from striatal neurons of a knock-in transgenic mouse, containing the homozygous Huntingtin (*Htt*) loci with a humanized Exon 1 comprising 7 polyglutamine repeats (Trettel, 2000).

CRISPR/Cas9 guides were designed using the Optimized CRISPR Design Tool from the Zhang Lab (http://crispr.mit.edu/) to target the first and second exon of the *Optn* gene in *Mus musculus,* as the first exon was present in isoform 1 and the second exon was common to isoform 1 and 2 of the *Optn* gene. The nucleotide region between 9408-9573 bp was used to search for guides in the first exon and the region between 18016-18126 bp was used to search for guides in the second exon. Two guides were selected based on the minimal overlap, off-target sites, and high-quality score and their sequence were as follow: OPTN guide 1 RNA sequences (5'-CACCGCTGGGGTGAACCATATTGG-3' and 3'-CGACCCCACTTGGTATAACCCAAA-5') and OPTN guide 2 RNA sequences (5'-CACCGGTCATCCTGATCTCAACGA-3' and 3'-CCAGTAGGACTAGAGTTGCTCAAA-5'). To anneal the top and bottom strands, top and bottom oligos (10 µM) per guide were ligated with nuclease-free water and T4 DNA ligase buffer (1X) by heating together on a dry heat block at 95 ºC for 3 min. The mixture was then allowed to cool down until it reached 50 ºC. Each annealing product (1:20 dilution) was then added separately to a mixture of pSpCas9(BB)-2A-Puro (PX459) V2.0 plasmid (20 ng/µl), NEBuffer 2.1 (1X), Rapid T4 DNA ligase (1:40 dilution), adenosine triphosphate (0.5 mM), BbsI restriction enzyme (1:20 dilution), and nuclease-free water. Each reaction was placed in a thermocycler with the following parameters: 12 cycles (37 ºC for 5 min, 21 ºC 5 min) and finishing with a 21 ºC hold. D5H-α competent *E. coli* cells were transformed with the ligation product of each guide and plated on a pre-warmed ampicillin-containing agar plate overnight at 37 ºC. Polymerase chain reaction (PCR) was performed to screen colonies for successful uptake of the plasmid. Three colonies were selected per guide and resuspended separately in 10 µl

of nuclease-free water. One microlitre of this diluted colony was added to a mixture of 2X phire green hot start II PCR master mix, forward primer 68 (TAAAATGGACTATCATATGC) (0.5µl/20µl), and the bottom strand of each guide (0.5 µl/20 µl). The thermocycler parameters for PCR colony screening were: 1 cycle of (98 ºC for 5 min), 27 cycles of (98 ºC for 10 s, 53 ºC for 15 s, and 72 ºC for 30 s), 1 cycle of (72 ºC for 5 min), and finishing with a 4 ºC hold. Agarose gel electrophoresis was then used to screen the PCR products compared to the negative control with no DNA per guide.

Colonies that screened positive for the plasmid and guides were grown up in Lysogeny broth (LB media). DNA from the colonies were collected, purified, and sequenced. STHdh$^{Q7/Q7}$ cells were transfected with the guide plasmids along with a GFP plasmid using polyethyleneimine. After 24 hours, fluorescence-activated cell sorting was performed to seed a single GFP-expressing cell into each well of a 96-well plate containing media. The plates were placed in an incubator at 37ºC to grow for approximately 3 weeks. Once a colony reached 90-100% confluency, colonies were expanded into 6-well plates and were then lysed with RIPA buffer (50 mM Tris-HCl, 150 mM NaCl, 5 mM EDTA, and 1% Nonidet P 40 substitute, 0.5% sodium deoxycholate, 0.1% sodium dodecyl sulfate, pH 7.2) containing protease inhibitors (100 µM AEBSF, 2 µM leupeptin, 80 nM aprotinin, 5 µM Bestatin, 1.5 µM E-64, and 1 µM pepstatin A) and phosphatase inhibitors (10mM NaF and 500µM Na_3VO_4). Western blotting was performed to screen for OPTN knockout colonies. Successful knockouts were then sent for DNA sequencing to further confirm that a successful knockout was generated.

4.3.3. Generation of OPTN knockout in mice

Animal care and experimental protocols were in accordance with the University of Ottawa Institutional Animal Care Committee and the Canadian Council of Animal Care guidelines. Animals were housed in an animal care facility on a 12-hour light/12-hour dark cycle with food and water provided *ad libitum*. Male $OPTN^{flox/wt}$ mice on a C57BL/6 background were obtained from Dr. Henry Tseng (Duke University) (Wong et al., 2020). CMV-Cre (gift of Dr. Mona Nemer, University of Ottawa) and $OPTN^{flox/wt}$ mice were used as breeding pairs to generate the current colony. Male control mice (CMV-Cre (-); $OPTN^{flox/flox}$) and global OPTN knockout (CMV-Cre (+); $OPTN^{flox/flox}$) mice are referred to as wild-type and $OPTN^{-/-}$, respectively**.**

4.3.4. Signaling experiments in $STHdh^{Q7/Q7}$ cells

$STHdh^{Q7/Q7}$ cells were maintained in Dulbecco's Modified Eagle's medium supplemented with 10% fetal bovine serum. The cells were then seeded on 6-well plates at 70–80% density 24 h prior to drug treatment. Wild-type and $OPTN^{-/-}$; $STHdh^{Q7/Q7}$ cells were starved in Hank's Balanced Salt Solution (HBSS) for 1 h and then treated with 10 µM of DHPG (mGluR1/5 agonist) for either 5 or 15 min to examine the effects of mGluR5 activation on autophagy signaling pathways. Cells were then washed twice with ice-cold HBSS and lysed for immunoblotting.

4.3.5. Signaling experiments in acute hippocampal slices

Six-month-old wild-type and $OPTN^{-/-}$ mice were euthanized by live cervical dislocation followed by rapid decapitation and the brains were dissected out. The hippocampi were coronally sliced into 300 µm slices with a McIlwain tissue chopper

(Ted Pella, Redding, California), and were recovered in ACSF solution (127 mM NaCl, 2 mM KCl, 10 mM glucose, 1.2 mM KH_2PO_4, 26 mM NaH_2CO_3, 1 mM $MgSO_4$, 1 mM $CaCl_2$, pH 7.4). Samples were gassed with 95% O_2/5% CO_2 and incubated for 90 min at 37 °C. The samples were then transferred to tubes, gassed again, and incubated for another 30 min at 37 °C. After the incubation period, all samples were treated with either 50 µM DHPG for 15 min or 10 µM CTEP (mGluR5 negative allosteric modulator) for 30 min followed by 50 µM DHPG for 15 min. Slices were then snap-frozen in liquid nitrogen and lysed for immunoblotting.

4.3.6. Immunoblotting

STHdh$^{Q7/Q7}$ cells and acute hippocampal slices were lysed in ice-cold RIPA buffer containing protease inhibitors (100 µM AEBSF, 2 µM leupeptin, 80 nM aprotinin, 5 µM Bestatin, 1.5 µM E-64, and 1 µM pepstatin A) and phosphatase inhibitors (10 mM NaF and 500 µM Na_3VO_4). Protein lysates were centrifuged at 15,000 *x* rpm (at 4ºC for 10 min) once for cell samples and twice for acute hippocampal slices. The supernatant was then collected, and total protein levels were quantified using the Bradford Protein Assay (Bio-Rad, Mississauga, Ontario). Lysates were diluted to 1 µg/µl in a mix of lysis buffer and β-mercaptoethanol containing 3x loading buffer (187.5 mM Tris-HCl, 30% glycerol, 6% sodium dodecyl sulfate, 0.006% bromophenol blue) and boiled for 10 min at 90°C. Aliquots containing a total of 35-40 µg of proteins were resolved by electrophoresis on 7.5%, 10%, or 14% SDS-polyacrylamide gel electrophoresis and transferred onto nitrocellulose membranes. Blots were blocked in Tris-buffered saline (pH 7.6) containing 0.05% of Tween 20 (TBST) and 5% nonfat dry milk for 1 hour at room temperature. Blots were then incubated overnight at 4°C with primary antibodies diluted

(1:1000) in TBST containing 1% nonfat dry milk. Membranes were washed 3 times in TBST and incubated with secondary antibodies (anti-rabbit/mouse) diluted (1:5000) in TBST containing 1% nonfat dry milk for 1 hour. Membranes were then washed 3 more times in TBST, and bands were visualized by incubation with 1:1 Clarity Western Peroxide and Luminol/Enhancer solutions (Bio-Rad, Mississauga, Ontario) for 5 min. Blots were imaged using the Bio-Rad Chemidoc Gel imaging system. Band densities were quantified using Image Lab software and normalized to the loading control or total protein for the protein/phosphoprotein of interest as indicated in each figure legend.

4.3.7. Ca^{2+} mobilization Assay

Intracellular Ca^{2+} flux assays were done using the FLUOFORTE® Ca^{2+} Assay Kit according to the manufacturer's procedure (ENZ-51017, Enzo Life Sciences, Farmingdale, New York). Briefly, wild-type and $OPTN^{-/-}$; $STHdh^{Q7/Q7}$ cells were plated on 96-well plates (6.5×10^4 cells/well). On the day of the experiment, the media were removed and replaced with 100 µl FLUOFORTE® Dye-loading solution. After a 45 min incubation at 33 ºC and 15 min at room temperature, cells were either treated with DHPG (25 and 50 µM) or 10 µM CTEP for 30 min followed by DHPG (25 and 50 µM). The fluorescence was measured (excitation = 490 nm/emission = 530 nm) for 30 s using a Synergy Neo2 Hybrid Multi-Mode Reader (BioTek, Winooski, Vermont). Folds increase in relative fluorescence units (RFU) were calculated using the following formula: fold increase in RFU = Δ maximum RFU of drug-treated wells/ basal RFU of the respective vehicle-treated well.

4.3.8. Statistical Analysis

Means ± SEM for each independent experiment were shown in the various figure legends. GraphPad Prism software was used to analyze the data for statistical significance. The statistical test used to analyze the data was a one-way or two-way ANOVA followed by Fisher's LSD comparisons or Tukey post-hoc test. A *P* value less than 0.05 was considered statistically significant.

4.4. Results

4.4.1. OPTN deletion enhanced mGluR5-activated Ca^{2+} release in $STHdh^{Q7/Q7}$ cell line

We previously demonstrated that overexpressing OPTN in HEK293 cells attenuated mGluR1-mediated IP_3 formation in response to agonist stimulation (Anborgh et al., 2005). Here, we employed CRISPR/Cas9 to knock out OPTN in $STHdh^{Q7/Q7}$ cells using two different guide RNAs to generate two OPTN knockout clones that lacked OPTN expression (OPTN KO1 and OPTN KO2; **Figure 4.1A and 4.1B**). $STHdh^{Q7/Q7}$ cells were derived from striatal neurons that endogenously express mGluR5 with no detectable mGluR1 expression (**Figure 4.1C**) (Anborgh et al., 2005). Knocking out OPTN did not alter mGluR5 expression levels in $STHdh^{Q7/Q7}$ cells (**Figure 4.1C**). We then investigated whether OPTN regulates mGluR5 canonical signaling by measuring cytosolic Ca^{2+} flux using the Ca^{2+}-specific fluorescent dye FluoForte. We found that OPTN deletion facilitated Ca^{2+} mobilization after stimulation with the mGluR1/5 agonist DHPG (25 µM and 50 µM) of both clones (**Figure 4.2A and 4.2B**). The selective mGluR5 NAM, CTEP, blocked DHPG-activated Ca^{2+} mobilization in both $OPTN^{-/-}$;$STHdh^{Q7/Q7}$ clones further confirming that Ca^{2+} release in response to DHPG was mGluR5-mediated (**Figure 4.2B**). Together, this indicated that OPTN could be a key regulator of mGluR5 canonical signaling.

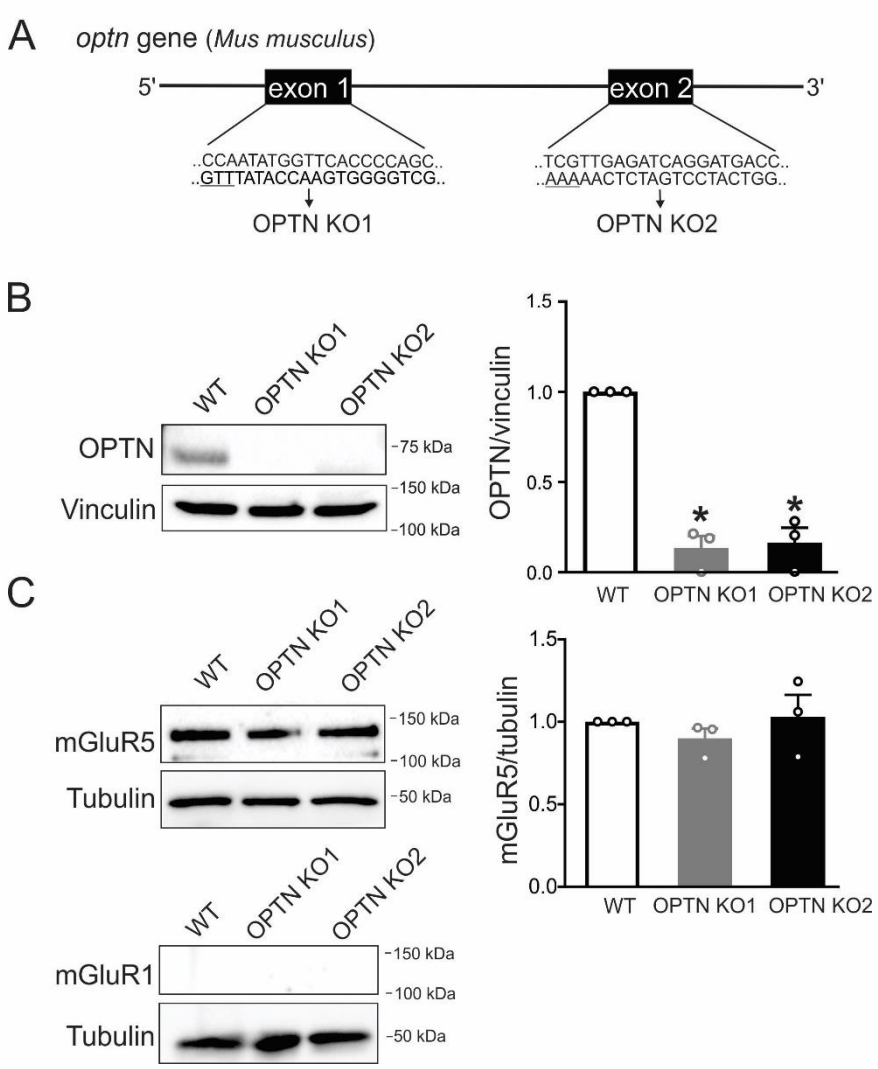

Figure 4.1. OPTN knockout in STHdh$^{Q7/Q7}$ cells does not alter mGluR5 expression. (A) Schematic representation of the sequence in *Optn* gene exon 1 and exon 2 that were targeted with guide 1 and guide 2 RNA sets, respectively. Underlined is the mutated region in sequence to create the two OPTN$^{-/-}$;STHdh$^{Q7/Q7}$ cells (OPTN KO1 and OPTN KO2). Representative immunoblots and quantification expressed as fold change in (B) OPTN, (C) mGluR5, and mGluR1 expression levels with the corresponding loading controls in wild-type (WT), OPTN KO1 and OPTN KO2 cells. OPTN was normalized to vinculin and mGluR5 was normalized to tubulin and expressed as a fraction of WT values (n=3 for each group). *denotes $P < 0.05$ versus WT cells. Statistical significance was assessed by one-way ANOVA and Tukey post-hoc test.

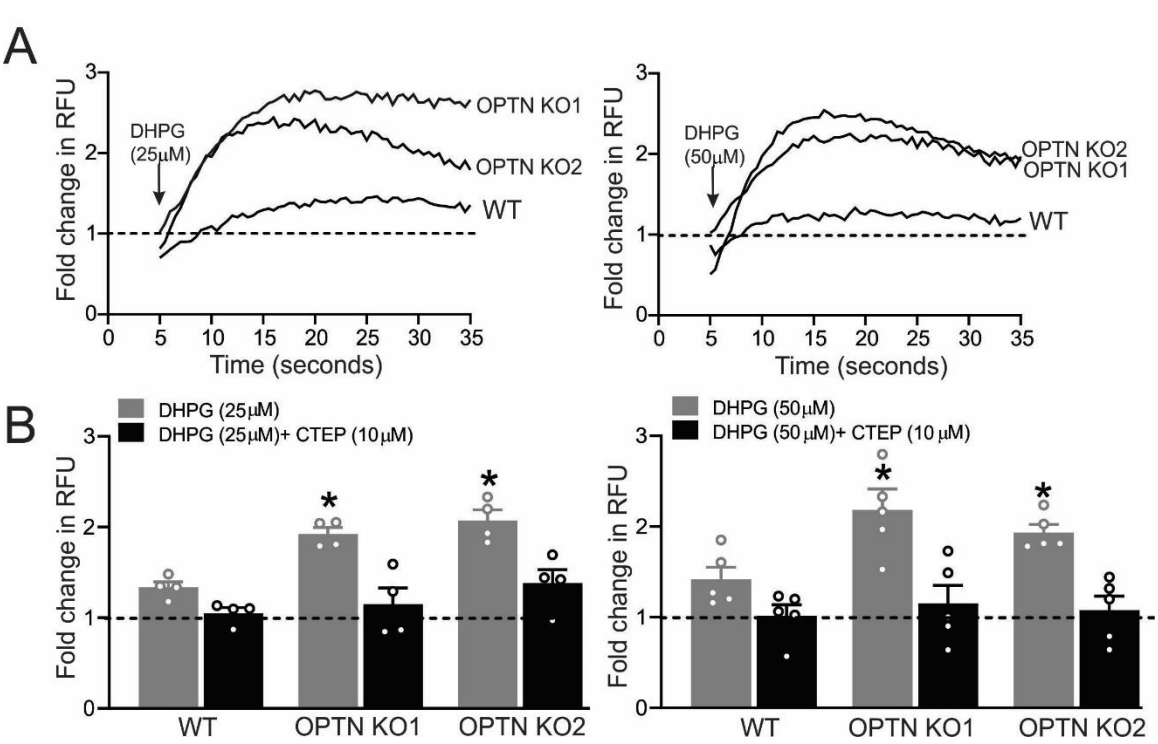

Figure 4.2. OPTN deletion impairs mGluR5-mediated Ca^{2+} flux in STHdh$^{Q7/Q7}$ cells. (A) Sample traces expressed as fold change in relative fluorescence units (RFU) of the Ca^{2+} indicator FluoForte in wild-type (WT) and OPTN$^{-/-}$;STHdh$^{Q7/Q7}$ cells (OPTN KO1 and OPTN KO2) treated with two different concentrations of mGluR group I agonist DHPG (25 μM and 50 μM). (B) Folds change in RFU of the Ca^{2+} indicator FluoForte in WT, OPTN KO1, and OPTN KO2 cells treated with DHPG (25 μM and 50 μM) in the presence and absence of 10 μM of mGluR5-selective NAM, CTEP (n=4-5 for each group). *denotes $P < 0.05$ versus DHPG-treated WT cells. Statistical significance was assessed by two-way ANOVA and Fisher's LSD comparisons.

4.4.2. Impairment of mGluR5-activated ERK1/2 phosphorylation in OPTN$^{-/-}$;STHdh$^{Q7/Q7}$ cell lines and OPTN$^{-/-}$ mouse hippocampus

Activation of mGluR5 triggers ERK1/2 phosphorylation, which was previously shown to be a key regulator of mGluR5-dependent protein synthesis and synaptic plasticity (Gallagher, 2004; Mao et al., 2005; Banko et al., 2006; Abd-Elrahman et al., 2017). We found that ERK1/2 phosphorylation was significantly enhanced following transient (5 min) exposure to DHPG in wild-type STHdh$^{Q7/Q7}$ cells, whereas DHPG-activated ERK1/2 phosphorylation was completely abolished in both OPTN$^{-/-}$;STHdh$^{Q7/Q7}$ cell clones (**Figure 4.3A**). To validate our findings in the immortalized cell lines, we investigated the impact of OPTN deletion on mGluR5 signaling in the hippocampus, an OPTN-rich brain region where many of the synaptic plasticity changes were mGluR5-mediated (Shigemoto et al., 1993; Fotuhi et al., 1994; Okita et al., 2012). We knocked out OPTN globally in C57BL/6 mice and examined the effect of acutely treating hippocampal slices for 15 min with DHPG (50 µM) in the absence or presence of CTEP (10 µM) to specifically probe for mGluR5-dependent signaling. As expected, DHPG significantly increased ERK1/2 phosphorylation in wild-type hippocampal slices, an effect that was antagonized by CTEP pre-treatment (**Figure 4.3B**). However, similar to what was observed in OPTN$^{-/-}$;STHdh$^{Q7/Q7}$ cell clones, DHPG-activated ERK1/2 phosphorylation was abolished in OPTN$^{-/-}$ hippocampal slices (**Figure 4.3B**). Taken together, these findings indicated that mGluR5-dependent activation of ERK1/2 signaling was dependent on OPTN.

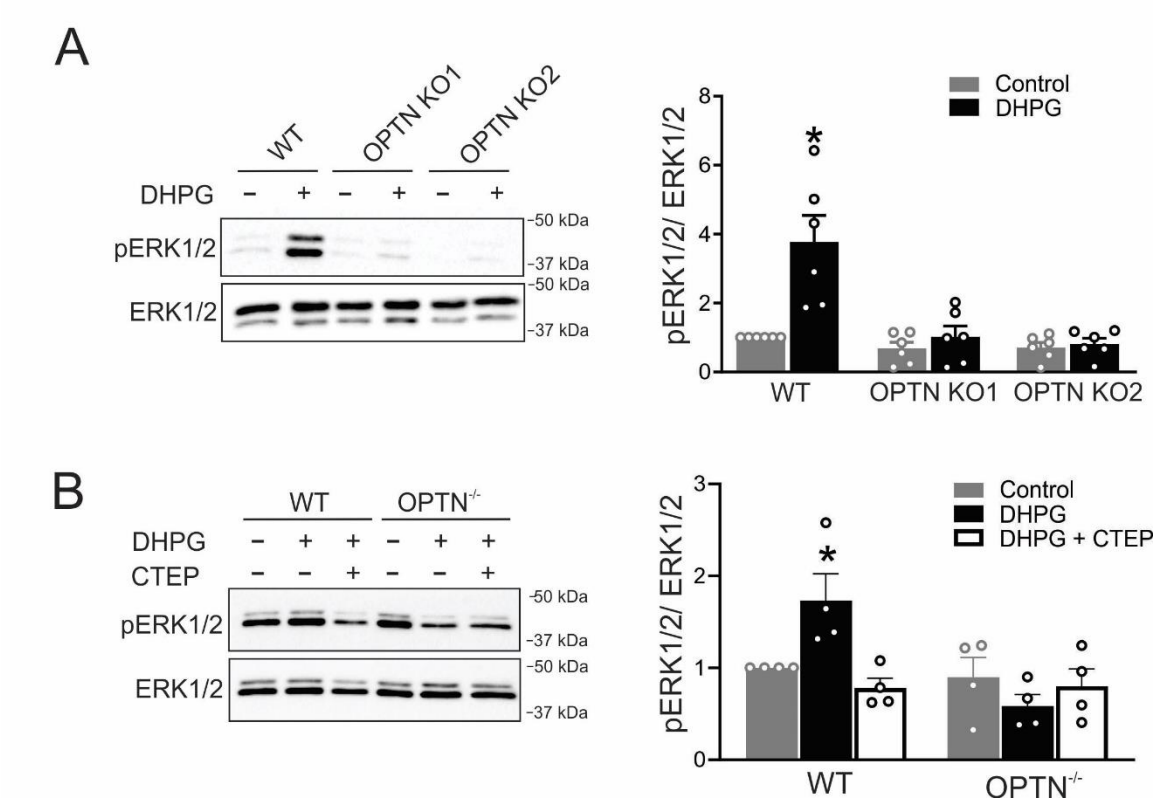

Figure 4.3. mGluR5-activated ERK1/2 phosphorylation is impaired in OPTN$^{-/-}$;STHdh$^{Q7/Q7}$ cells and OPTN$^{-/-}$ mouse hippocampus. (A) Representative immunoblots and quantification expressed as fold change in ERK1/2-pT202/Y204 as a percent of ERK1/2 in wild-type (WT) and OPTN$^{-/-}$;STHdh$^{Q7/Q7}$ cells (OPTN KO1 and OPTN KO2) treated with the mGluR group I agonist DHPG (10 µM; n=6 for each group). (B) Representative immunoblots and quantification as fold change in ERK1/2-pT202/Y204 as a percent of ERK1/2 in wild-type (WT) or OPTN$^{-/-}$ acute hippocampal slices treated with DHPG (50 µM) in the presence and absence of the mGluR5-selective NAM, CTEP (10 µM; n= 4 for each group). Values are expressed as a fraction of control WT values. *denotes $P < 0.05$ versus control WT cells. Statistical significance was assessed by two-way ANOVA and Fisher's LSD test.

4.4.3. OPTN deletion impaired GSK3β/ZBTB16 signaling in OPTN$^{-/-}$;STHdh$^{Q7/Q7}$ cell lines and OPTN$^{-/-}$ mouse hippocampus

We previously demonstrated that pathological mGluR5 signaling contributed to the accumulation of mHTT and β-amyloid (Aβ) aggregates in HD and AD, respectively (Abd-Elrahman et al., 2017, 2018, 2020b, 2020a). Specifically, mGluR5 suppressed autophagy by triggering the inhibitory phosphorylation of GSK3β at Ser9, thereby inactivating the ZBTB16-dependent autophagy pathway. Here, we investigated whether GSK3β/ZBTB16/ATG14 signaling was regulated in an OPTN-dependent manner. Treatment of either wild-type or OPTN$^{-/-}$;STHdh$^{Q7/Q7}$ clones with DHPG did not alter either GSK3β phosphorylation or the expression level of ZBTB16. Similarly, DHPG treatment did not affect vacuolar protein sorting 34 (VPS34) expression, a class III phosphatidylinositol 3-kinase that forms a complex with ATG14, Beclin-1, and p150 to initiate autophagosomes (**Figure 4.4A-C**). However, GSK3β-pS9 and ZBTB16 levels were significantly attenuated in both OPTN$^{-/-}$;STHdh$^{Q7/Q7}$ cell clones independent of DHPG treatment (**Figure 4.4A and 4.4B**). In addition, VPS34 protein expression was increased in both OPTN$^{-/-}$;STHdh$^{Q7/Q7}$ clones when compared to control cells (**Figure 4.4C**).

We then examined whether OPTN contributed to mGluR5-dependent regulation of GSK3β/ZBTB16 signaling in mouse hippocampus. Unlike what was observed in wild-type STHdh$^{Q7/Q7}$ cells, DHPG significantly increased both GSK3β phosphorylation and ZBTB16 protein expression in wild-type hippocampal slices, an effect that was attenuated by the pre-treatment of slices with 10 μM CTEP (**Figure 4.5A and 4.5B**). However, in the absence of OPTN expression, DHPG did not elicit any changes in either

GSK3β phosphorylation or ZBTB16 protein expression levels in hippocampal slices (**Figure 4.5A and 4.5B**). VPS34 expression was not changed by DHPG treatment in either wild-type or OPTN$^{-/-}$ hippocampal slices (**Figure 4.5C**). Together, these findings indicated that OPTN played a potential role in regulating GSK3β/ZBTB16-dependent autophagic signaling downstream of mGluR5.

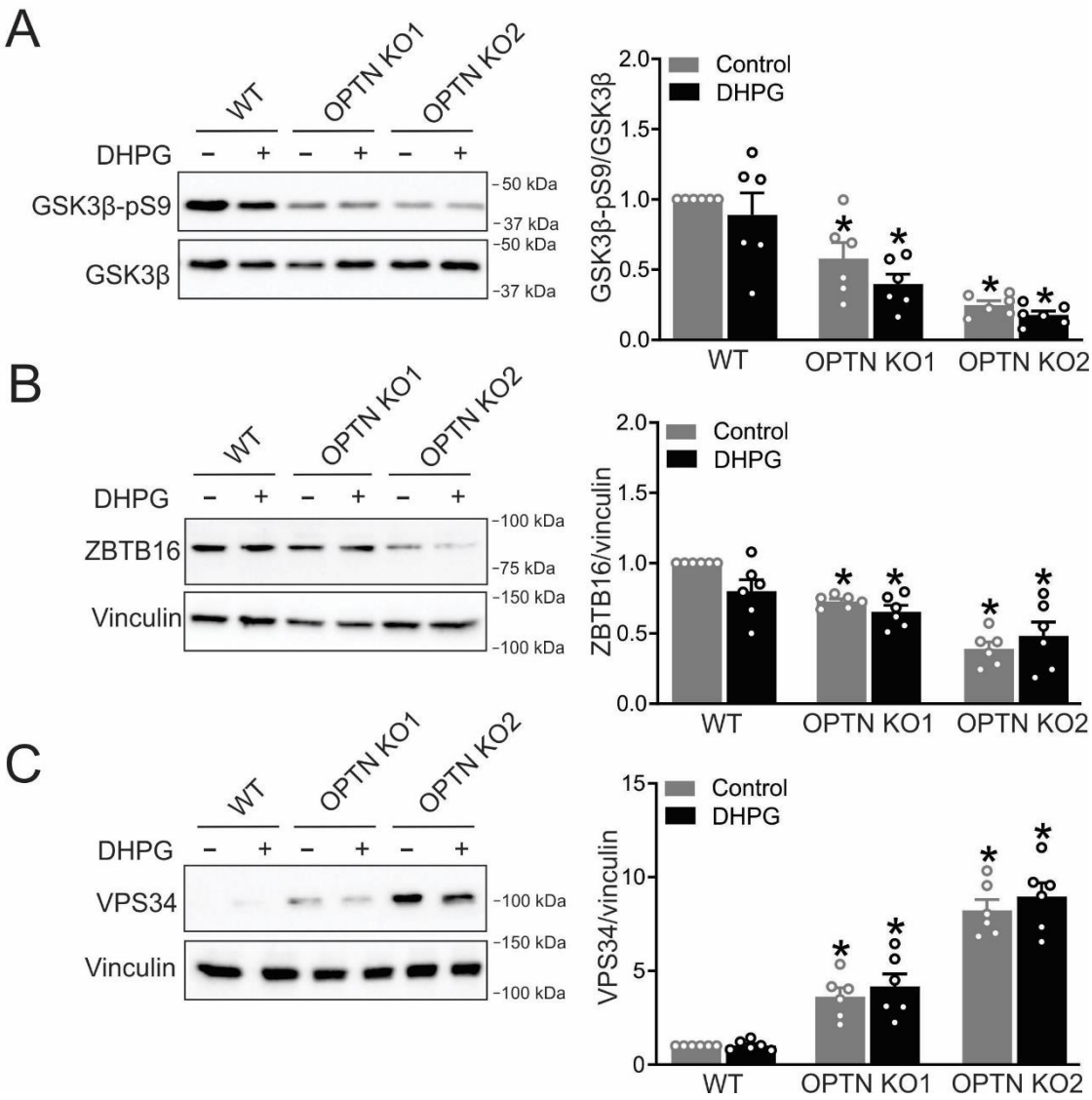

Figure 4.4. Effect of OPTN deletion on GSK3β/ZBTB16 and VPS34 signaling pathways in STHdh$^{Q7/Q7}$ cells. Representative immunoblots and quantification as fold change in (A) GSK3β-pS9, (B) ZBTB16, and (C) VPS34 protein expression with the corresponding loading controls in wild-type (WT) and OPTN$^{-/-}$;STHdh$^{Q7/Q7}$ cells (OPTN KO1 and OPTN KO2) treated with mGluR group I agonist DHPG (10 μM). GSK3β-pS9 was normalized to total GSK3β, and both ZBTB16 and VPS34 were normalized to vinculin (n= 6 for each group). Values are expressed as a fraction of control WT cells. *denotes $P < 0.05$ versus control WT cells. Statistical significance was assessed by two-way ANOVA and Fisher's LSD test.

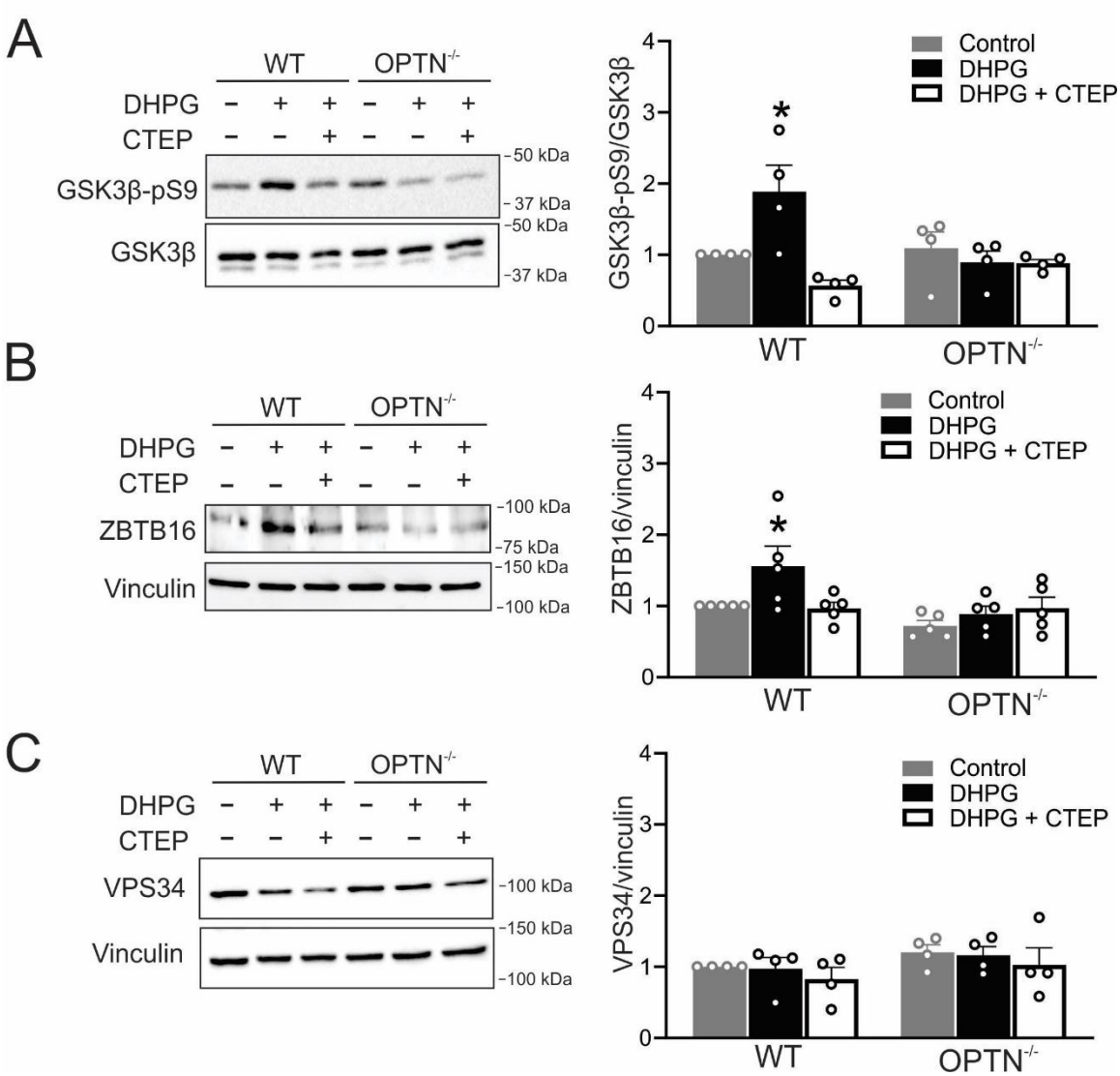

Figure 4.5. Effect OPTN deletion on GSK3β/ZBTB16 and VPS34 signaling in wild-type and OPTN$^{-/-}$ mouse hippocampus. Representative immunoblots and quantification as fold change in (A) GSK3β-pS9, (B) ZBTB16, and (C) VPS34 protein expression with the corresponding loading controls in wild-type (WT) or OPTN$^{-/-}$ acute hippocampal slices treated with mGluR group I agonist DHPG (50 μM) in the presence and absence of mGluR5-selective NAM, CTEP (10 μM). GSK3β-pS9 was normalized to total GSK3β, and both ZBTB16 and VPS34 were normalized to vinculin (n= 4-5 for each group). Values are expressed as a fraction of control WT values. *denotes $P < 0.05$ versus control WT values. Statistical significance was assessed by two-way ANOVA and Fisher's LSD comparisons.

4.4.4. OPTN deletion impaired mTOR/ULK1 signaling in OPTN$^{-/-}$;STHdh$^{Q7/Q7}$ cell lines and OPTN$^{-/-}$ mouse hippocampus

Activation of phosphoinositide 3-kinase (PI3K) by mGluR5 has been demonstrated to trigger mTOR phosphorylation at its Ser2448, the latter phosphorylates ULK1 at S757 and inhibits its catalytic activity thereby stalling autophagosome formation (Kim et al., 2011; Perluigi et al., 2015; Abd-Elrahman et al., 2018; Abd-Elrahman and Ferguson, 2019). Here, we investigated whether mTOR/ULK1 signaling was also regulated in an OPTN-dependent manner. DHPG-treated wild-type cells showed a trend toward increased mTOR-pS2448 and ULK1-pS757, yet it was not significant (**Figure 4.6A and 4.6B**). In contrast, mTOR-pS2448 and ULK1-pS757 levels were elevated in OPTN$^{-/-}$;STHdh$^{Q7/Q7}$ cells when compared to wild-type cells in a manner that was independent of agonist treatment (**Figure 4.6A and 4.6B**).

We then examined whether mGluR5 also activated mTOR/ULK1 signaling in an OPTN-dependent manner in mouse hippocampus. Exposure of hippocampal slices to 50 µM DHPG for 15 min did not elicit significant changes in the levels of mTOR-pS2448 and ULK1-pS757 in wild-type hippocampal slices. However, mTOR-pS2448 and ULK1-pS757 were significantly elevated in OPTN$^{-/-}$ hippocampal slices when compared to wild-type hippocampal slices (**Figure 4.7A and 4.7B**). Treatment of OPTN$^{-/-}$ hippocampal slices with CTEP reduced mTOR-pS2448 phosphorylation levels when compared with either untreated or DHPG-treated slices, suggesting that the basal activity of this pathway was regulated by mGluR5 (**Figure 4.7A**). Similarly, ULK1-pS757 levels in CTEP-treated OPTN$^{-/-}$ hippocampal slices were not significantly different from that observed in untreated wild-type hippocampal slices (**Figure 4.7B**). Together, our

findings in mouse hippocampus further validated the critical role of OPTN in the regulation of mTOR/ULK1 activity downstream of mGluR5.

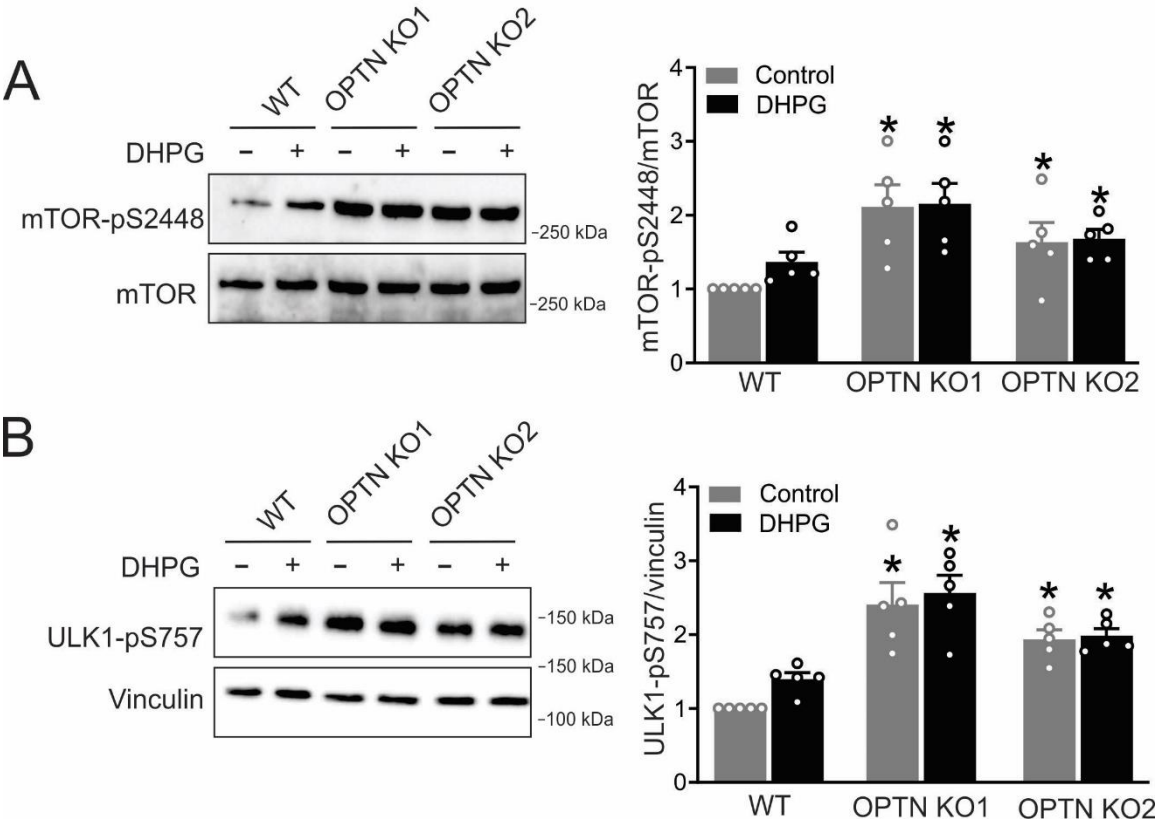

Figure 4.6. Effect of OPTN deletion on mTOR/ULK1 phosphorylation in STHdh$^{Q7/Q7}$ cell lines. Representative immunoblots and quantification as fold change in (A) mTOR-pS2448 and (B) ULK1-pS757 with the corresponding loading controls in wild-type (WT) and OPTN$^{-/-}$;STHdh$^{Q7/Q7}$ cells (OPTN KO1 and OPTN KO2) treated with mGluR group I agonist DHPG (10 μM). mTOR-pS2448 was normalized to total mTOR and ULK1-pS757 was normalized to vinculin (n= 5 for each group). Values are expressed as a fraction of control WT cells. *denotes $P < 0.05$ versus control WT cells. Statistical significance was assessed by two-way ANOVA and Fisher's LSD comparisons.

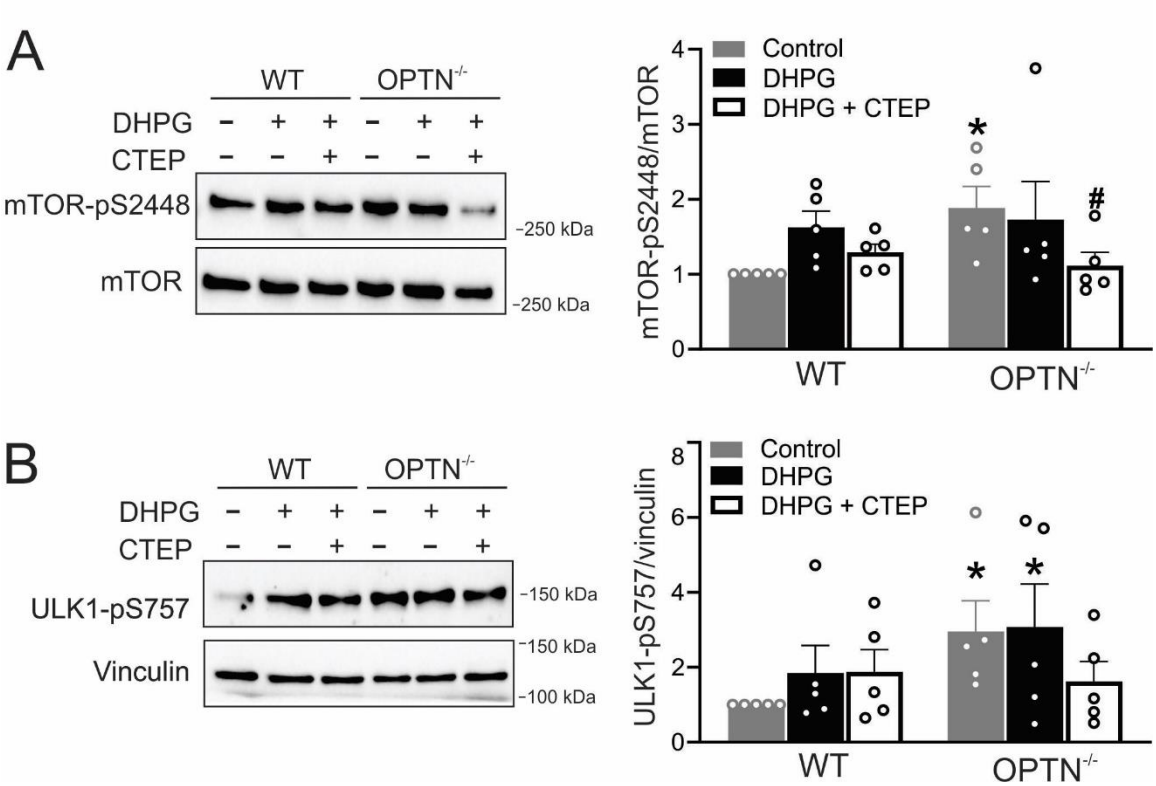

Figure 4.7. Effect of OPTN deletion on mTOR/ULK1 phosphorylation in mouse hippocampus. Representative immunoblots and quantification as fold change in (A) mTOR-pS2448 and (B) ULK1-pS757 phosphorylation with the corresponding loading controls in wild-type (WT) or OPTN$^{-/-}$ acute hippocampal slices treated with mGluR group I agonist DHPG (50 µM) in presence and absence of mGluR5-selective NAM, CTEP (10 µM). mTOR-pS2448 was normalized to total mTOR, and ULK1-pS757 was normalized to vinculin (n= 5 for each group). Values are expressed as a fraction of control WT values. $^{*}P < 0.05$ versus control WT slices and $^{\#}P < 0.05$ versus control OPTN$^{-/-}$ slices. Statistical significance was assessed by two-way ANOVA and Fisher's LSD comparisons.

4.4.5. OPTN deletion inhibited autophagy in OPTN$^{-/-}$;STHdh$^{Q7/Q7}$ cell lines and OPTN$^{-/-}$ mouse hippocampus

The ability of OPTN to regulate GSK3β/ZBTB16 and mTOR/ULK1 signaling was ultimately expected to result in altered autophagy flux (Kim et al., 2011; Zhang et al., 2015; Abd-Elrahman and Ferguson, 2019). Therefore, we tested whether the changes in ZBTB16 and ULK1 signaling in OPTN$^{-/-}$;STHdh$^{Q7/Q7}$ cell lines and OPTN$^{-/-}$ hippocampus were associated with changes in the autophagy markers P62 and LC3B. P62 was investigated because it represented a well-characterized autophagy receptor for ubiquitinated cargos bound to LC3B-labeled autophagosomes to ultimately facilitate their degradation (Nixon, 2013). DHPG treatment did not elicit changes in the expression of P62 or LC3B markers (**Figure 4.8A and 4.8B**). However, the basal protein expression levels of both P62 and LC3B were increased in both OPTN$^{-/-}$;STHdh$^{Q7/Q7}$ cell clones and were not regulated by mGluR5 agonist, when compared to P62 and LC3B protein levels in wild-type STHdh$^{Q7/Q7}$ cells (**Figure 4.8A and 4.8B**). Likewise, P62 expression level was elevated in OPTN$^{-/-}$ hippocampal slices compared to wild-type controls. However, CTEP pre-treatment significantly reduced elevated P62 levels in OPTN$^{-/-}$ hippocampal slices (**Figure 4.8C**). These findings suggested that OPTN played a key role in modulating autophagic signaling mechanisms downstream of mGluR5.

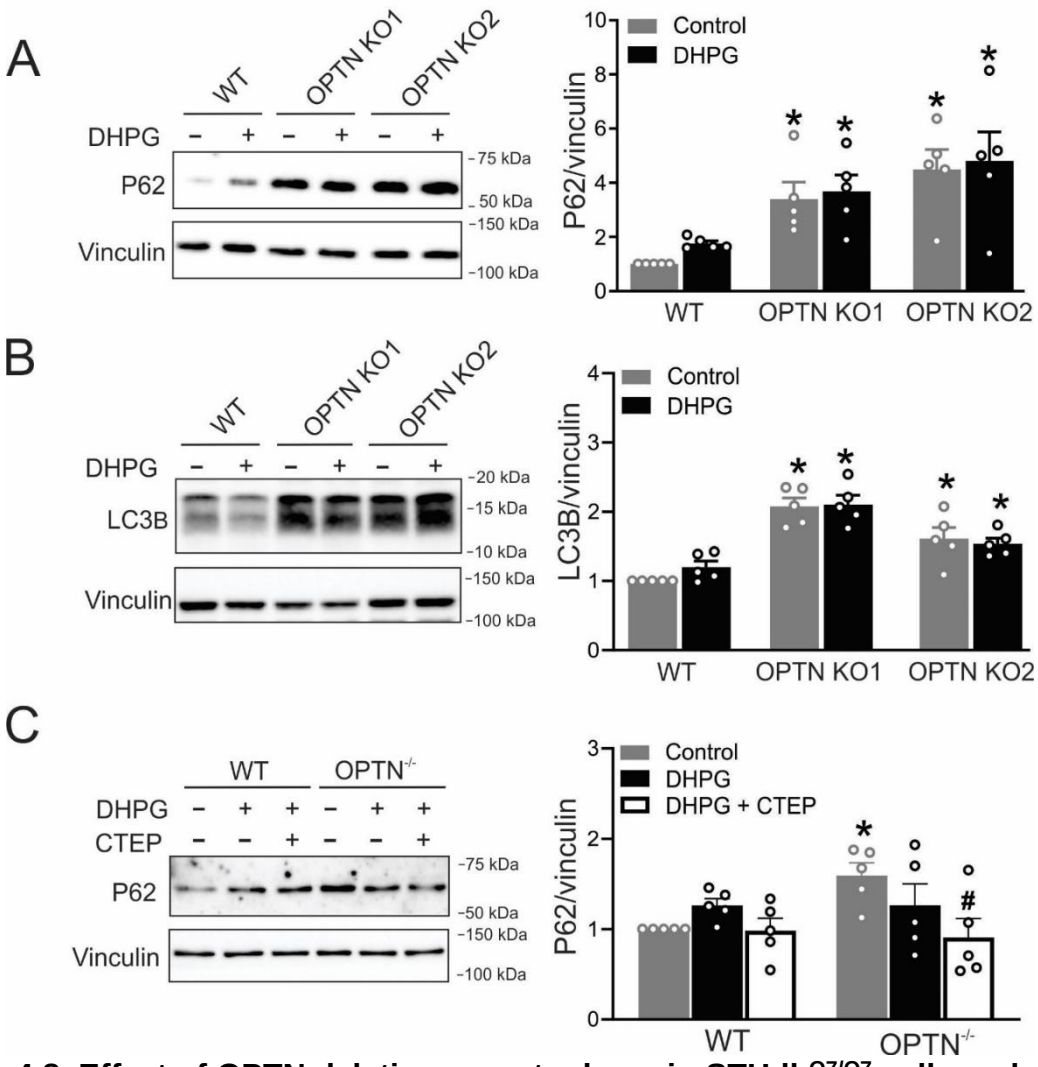

Figure 4.8. Effect of OPTN deletion on autophagy in STHdh$^{Q7/Q7}$ cells and mouse hippocampus. Representative immunoblots and quantification as fold change in (A) P62 and (B) LC3B protein expression with the corresponding loading controls in wild-type (WT) and OPTN$^{-/-}$;STHdh$^{Q7/Q7}$ cells (OPTN KO1 and OPTN KO2) treated with mGluR group I agonist DHPG (10 µM). P62 and LC3B were normalized to vinculin (n= 5 for each group). Values are expressed as a fraction of control WT cells. *denotes *P* < 0.05 versus control WT cells. Statistical significance was assessed by two-way ANOVA and Fisher's LSD comparisons. (C) Representative immunoblots and quantification as fold change in P62 protein expression with the corresponding loading controls in WT or OPTN$^{-/-}$ acute hippocampal slices treated with DHPG (50 µM) in the presence and absence of mGluR5-selective NAM, CTEP (10 µM). P62 was normalized to vinculin (n= 5 for each group). Values are expressed as a fraction of control WT

values. $^{*}P < 0.05$ versus control WT slices and $^{\#}P < 0.05$ versus control OPTN$^{-/-}$ slices. Statistical significance was assessed by two-way ANOVA and Fisher's LSD comparisons.

4.5. Discussion

OPTN represents an important modifier of the autophagic machinery in neurodegenerative aggregopathies such as AD, HD, and PD (Osawa et al., 2011; Schwab et al., 2012; Korac et al., 2013). Evidence indicates that impairment in autophagic signaling in AD and HD animal models is regulated in a mGluR5-dependent manner (Abd-Elrahman et al., 2017, 2018). Here, we have explored this functional link between OPTN and mGluR5 signaling in neurons, based on previous evidence on the molecular interaction between mGluR1/5 and OPTN in HEK-293 cells (Anborgh et al., 2005). We report that **i)** OPTN regulates mGluR5 canonical signaling by curbing DHPG-evoked Ca^{2+} flux in a $STHdh^{Q7/Q7}$ striatal cell line, **ii)** the loss of OPTN expression attenuates mGluR5-stimulated ERK1/2 signaling in $STHdh^{Q7/Q7}$ cells and acute hippocampal slices, **iii)** OPTN facilitates basal autophagic machinery via GSK3β/ZBTB16 in $STHdh^{Q7/Q7}$ cells, and mediates mGluR5 agonist-stimulated inactivation of the GSK3β/ZBTB16 pathway in acute hippocampal slices, and **iv)** OPTN knockout increases agonist-independent basal mTOR/ULK1 phosphorylation in $STHdh^{Q7/Q7}$ cells and mouse hippocampal slices, an effect that can be reversed by mGluR5 antagonism in $OPTN^{-/-}$ hippocampal slices. Since mGluR5 is highly implicated in neurodegeneration, the current findings may provide insights into the potential contribution of OPTN to the pathological signaling of mGluR5 in neurodegenerative diseases.

Group I mGluRs are primarily coupled to heterotrimeric $G\alpha_{q/11}$ signaling to promote IP_3 formation and Ca^{2+} release from the endoplasmic reticulum (ER) (Dhami and Ferguson, 2006). OPTN hinders mGluR1 coupling to PLCβ signaling via binding to the

regulatory C-tail domain of mGluR1/5 (Anborgh et al., 2005). In the present study, OPTN knockout in STHdh$^{Q7/Q7}$ cells enhances DHPG-mediated Ca^{2+} flux which is abolished by pre-treatment of cells with the highly selective mGluR5 NAM, CTEP, indicating that mGluR5-mediated canonical signaling is dependent upon OPTN. OPTN is also an important component of vesicle-trafficking protein complexes that are essential for ER functional dynamics (Sahlender et al., 2005; Slowicka et al., 2016). In particular, OPTN deficiency evokes ER stress responses which may serve to sensitize intracellular Ca^{2+} responses (Ali et al., 2019). However, we did not observe any impairment in baseline Ca^{2+} responses prior to DHPG treatment suggesting that OPTN loss selectively modifies mGluR5-regulated Ca^{2+} release. Therefore, we complement and further corroborate the current evidence on the direct involvement of OPTN in mGluR5 coupling to $G\alpha_{q/11}$/PLCβ signaling.

We find that the loss of OPTN expression completely abolishes the ability of mGluR5 to stimulate ERK1/2 activation in response to agonist treatment in both OPTN$^{-/-}$;STHdh$^{Q7/Q7}$ cells and acute hippocampal slices of OPTN$^{-/-}$ mice. Since OPTN is a binding partner of mGluR5 (Anborgh et al., 2005), this suggests that OPTN is a component of a mGluR5 signaling complex that is required for ERK1/2 activation. Specifically, mGluR5 can trigger ERK1/2 signaling via its interactions with β-arrestin2, proline-rich tyrosine kinase 2 (Pyk2), and Homer proteins in addition to the activation of Ca^{2+} and PLCβ signaling (Luttrell and Lefkowitz, 2002; Dhami and Ferguson, 2006; DeWire et al., 2007; Nicodemo et al., 2010; Stoppel et al., 2017). Thus, it is possible that OPTN, via its regulatory binding to the mGluR5 C-tail domain, is required for β-arrestin recruitment to mGluR5 and subsequent ERK1/2 activation (Anborgh et al.,

2005; Dhami and Ferguson, 2006; Stoppel et al., 2017). Moreover, impaired mGluR5-activated ERK1/2 signaling may be explained by enhanced calcineurin activity after OPTN deletion. Specifically, under basal conditions, calcineurin phosphatase activity is inhibited by calcineurin inhibitor protein (CAIN), a regulatory protein that also interacts with mGluR1/5 intracellular C-tail domain (Dale et al., 2001; Ferreira et al., 2009). Loss of OPTN may disrupt the mGluR5/calcineurin/CAIN scaffold complex ultimately leading to calcineurin activation thereby facilitating the dephosphorylation of downstream kinases including ERK1/2 (Dougherty et al., 2009; Ferreira et al., 2009). However, further studies are required to delineate the specific mechanisms underlying such observations.

OPTN induces autophagy via LC3B activation (Shen et al., 2011; Wild et al., 2011; Slowicka et al., 2016) and facilitates the recruitment of autophagy-related proteins, ATG12-5-16L1, to phagophores (Bansal et al., 2018). We did not detect a significant change following exposure to DHPG, but OPTN deletion impaired autophagy via enhancing mTOR activity and inhibiting ULK1 catalytic activity in both the cell lines and hippocampal slices. Elevated mTOR-pS448, ULK1-pS757 and P62 protein expression levels are reduced upon pre-treatment of hippocampal slices with CTEP suggesting that altered mTOR/ULK1 autophagic signaling in $OPTN^{-/-}$ mice is likely mGluR5-regulated. Indeed, mGluR5 plays a key role in shaping synaptic plasticity via the regulation of protein translation mechanisms, such as ERK1/2 and mTOR (Rong et al., 2003; Gallagher, 2004; Banko et al., 2006), that reciprocally regulate neuronal autophagic machinery (Jung et al., 2010; Settembre et al., 2011; Heras-Sandoval et al., 2014). mGluR5 can activate the PI3K/mTOR signaling cascade resulting in ULK1

phosphorylation and impairment in autophagy initiation (Rong et al., 2003; Hou and Klann, 2004; Abd-Elrahman and Ferguson, 2019). Here, we provide evidence that OPTN plays a key role in mGluR5-activated mTOR signaling that ultimately modulate ULK1-dependent autophagy further supporting the pivotal role of OPTN as an autophagy receptor.

Interestingly, we detected enhanced GSK3β activity and increased breakdown of the ubiquitin-protein ligase component, ZBTB16, along with stabilization of VPS34 levels in OPTN$^{-/-}$;STHdh$^{Q7/Q7}$ cell lines. These findings suggest that OPTN is important in maintaining a basal level of GSK3β activity that can ultimately stabilize ZBTB16 levels and autophagic flux. The loss of OPTN appears to release the brake on GSK3β activity, leading to ZBTB16 degradation and impairment in autophagosome induction and maturation. This may trigger a compensatory stabilization of the VPS34-linked autophagosome complex in an attempt to restore autophagy. It is worth mentioning that GSK3β is also a target of ERK1/2 and it is possible that impaired ERK1/2 in OPTN$^{-/-}$;STHdh$^{Q7/Q7}$ cells contributed to the reduction in the inhibitory phosphorylation of GSK3β leading to subsequent impairment in autophagosome maturation (Stambolic and Woodgett, 1994; Hetman et al., 2002; Ding et al., 2005).

Remarkably, we observe no change in the activation of the GSK3β/ZBTB16 pathway upon DHPG treatment of wild-type or OPTN$^{-/-}$;STHdh$^{Q7/Q7}$ cell lines. However, mGluR5 agonist activation suppresses GSK3β activity by facilitating the phosphorylation of GSK3β at Ser9 and the subsequent accumulation of ZBTB16 levels in wild-type hippocampal slices, an effect that is abolished in OPTN$^{-/-}$ hippocampus. This suggests that mGluR5 inversely regulates hippocampal autophagic flux via the

GSK3β/ZBTB16 pathway in an OPTN-dependent manner. This idea is supported by recent studies showing that mGluR1 regulates basal autophagy in the brain (Donoso et al., 2020), and that DHPG triggers the accumulation of LC3B-labeled autophagic vesicles in hippocampal neurons (Kallergi et al., 2022). Importantly, the current observations also uncover a novel role for OPTN in hippocampal mGluR5 signaling and provide evidence that the interaction between OPTN and mGluR5 modulate the hippocampal autophagic machinery via GSK3β/ZBTB16 and mTOR/ULK1 signaling cascade. It is possible that the discrepancy in DHPG-evoked GSK3β signaling between striatal cells and hippocampal slices is attributable to the oscillatory pattern of GSK3β phosphorylation in different brain regions (Krishnankutty et al., 2017). For instance, a recent report has shown that GSK3β-pSer9 levels are elevated in the dorsal striatum following 30 min of mGluR5 activation (Johnson and Conn, 2019), whereas a rapid activation of the Akt/GSK3β pathway is evident 5 min after mGluR5 stimulation in the hippocampus (Hou and Klann, 2004; Liu et al., 2005). Additionally, we cannot rule out the possibility that differences in mGluR5 expression levels between striatal cell lines and hippocampus tissue slices might account for differences in receptor-dependent signaling.

In summary, we provide the first mechanistic evidence that OPTN plays a pivotal role in both mGluR5 canonical and autophagic signaling. We report that OPTN facilitates both ERK1/2 signaling and autophagic signaling via GSK3β/ZBTB16 and mTOR/ULK1 pathways downstream of mGuR5 in mouse striatal cells and hippocampus. This functional interaction can be of particular importance for hippocampal plasticity responses and proteotoxic aggregate accumulation that

represent a pathological hallmark of neurodegenerative diseases such as AD and HD (Deng et al., 2017; Ribeiro et al., 2017). Thus, it further emphasizes the promising therapeutic potential of mGluR5 in mitigating synaptic toxicity induced by Aβ and mHTT.

Acknowledgments: K.S.I is a recipient of Mark and Gail Marcogliese Graduate Fellowship from the University of Ottawa Brain and Mind Research Institute. S.S.G.F holds a Tier I Canada Research Chair in Brain and Mind. K.S.A holds clinician postdoctoral fellowships from the Alberta Innovates Health Solutions and CIHR and is a Lecturer at the Department of Pharmacology & Toxicology, Faculty of Pharmacy, University of Alexandria, Egypt. We thank Dr. Ryan Russell for his guidance with CRISPR/Cas9 and Vanessa Kissner for her technical assistance in the current study. Graphical abstract was created with BioRender.com.

Ethics approval and consent to participate: All animal experiments and protocols were approved by the University of Ottawa animal care committee in accordance with the Canadian Council of Animal Care guidelines (CMM 2519). Human ethics approval is not applicable.

Competing Interests: The authors declare that they have no competing interests.

Funding: This study was supported by the Huntington's Society of Canada, the Krembil Foundation and Canadian Institutes for Health Research (CIHR) grants PJT-148656, PJT-153317, and PJT-165967 to S.S.G.F.

Chapter 5.
General discussion

The overall aim of this thesis was to delineate the contribution of VGLUT3 transmission and OPTN to mGluR5 signaling and the potential influence of this regulation on HD progression. The goal of this thesis was to address three main questions:

1. **How does VGLUT3 transmission regulate mGluR5 and other glutamate receptors in different brain regions?**
2. **What is the impact of VGLUT3 ablation on HD pathophysiology in mice?**
3. **What is the role of OPTN in mGluR5 canonical and autophagic signaling?**

The data presented in Chapters 2, 3, and 4 of this thesis summarized my research aimed at addressing these three questions**. In Chapter 2**, we showed that VGLUT3 dynamically regulated iGluRs and mGluRs densities in brain regions typically affected in HD (Ibrahim et al., 2022). Particularly, the genetic deletion of VGLUT3 elevated mGluR5 cell surface densities in the striatum. Furthermore, VGLUT3 loss upregulated the overall expression of mGluR5 in the cerebral cortex, while it significantly reduced mGluR5 cell surface expression in the hippocampus (Ibrahim et al., 2022). **In Chapter 3**, we provided evidence that VGLUT3 transmission is implicated in HD pathophysiology. Deletion of VGLUT3 rescued motor and short-term memory deficits in both male and female zQ175 HD mice throughout 15 months of age, with no impact on mHTT aggregation. More so, VGLUT3 loss rescued striatal neuronal loss in HD striatum potentially via activation of ERK1/2 and Akt signaling, both important for neuronal pro-survival pathways. **In Chapter 4**, we revealed a cellular mechanism by which the HTT-interacting protein, OPTN, regulates mGluR5 canonical and noncanonical signaling. Specifically, we demonstrated that deletion of OPTN enhanced mGluR5-mediated Ca^{2+}

flux in STHdh$^{Q7/Q7}$ striatal cell line while disrupting ERK1/2 activation in both STHdh$^{Q7/Q7}$ cells and acute hippocampal slices. We then showed that OPTN expression is important for the facilitation of autophagic machinery via GSK3β/ZBTB16 and mTOR/ULK1 signaling downstream of mGuR5. Collectively, this work provided molecular insights into the functional interaction between VGLUT3 transmission and OPTN with mGluR5, and depicted their promising potential in alleviating aberrant mGluR5 signaling in HD.

5.1. VGLUT3/mGluR5 crosstalk in corticostriatal motor circuits

Prior to the work in this thesis, most evidence depicted the overlapping expression pattern of VGLUT3-positive terminals and mGluR5 within the striatum and some cortical brain regions. VGLUT3-expressing TANs and serotonergic raphe neurons form synaptic contacts onto mGluR5-rich striatal MSNs (Romano et al., 1995; Gras et al., 2002; El Mestikawy et al., 2011). More so, VGLUT3-positive terminals innervate pyramidal neurons of the motor cortex which express mGluR5 and project to the striatum (Guimaraes et al., 2015; Omiya et al., 2015; Hintiryan et al., 2016; Sun et al., 2016). Our results suggest that VGLUT3 transmission can modulate mGluR5 activity, depicted by an upregulation in mGluR5 cell surface levels in VGLUT3$^{-/-}$ striatum and mGluR5 total expression in VGLUT3$^{-/-}$ cortex (Ibrahim et al., 2022). While the underlying mechanisms are yet to be determined, this VGLUT3-dependent mGluR5 regulation is of particular importance to striatal dopaminergic signaling. Previous evidence showed that activation of mGluR5 negatively regulates dopamine release in the NAc (Homayoun et al., 2004; Liu et al., 2008; Gupta and Young, 2018). On the other hand, cocaine-mediated augmentation in dopamine flux downregulates mGluR5 levels in the NAc (Frantz et al., 2007; Hao et al., 2010). More so, mGluR-mediated regulation

of dopamine release is evidently disrupted in the NAc of VGLUT3$^{-/-}$ mice (Sakae et al., 2015), suggesting that dopamine signaling is evidently regulated via striatal VGLUT3/mGluR5 crosstalk. In fact, mGluR5 and dopaminergic D1R converge in signal transduction and together regulate neuronal plasticity within the striatum (Paolillo et al., 1998; Voulalas, 2005; Schotanus and Chergui, 2008). Despite the elevations in mGluR5 surface densities, VGLUT3 loss elicited no change in both total and cell surface densities of D1R in the striatum (Ibrahim et al., 2022). This is in line with previous reports showing that D1R binding densities were elevated specifically in the NAc, not the entire striatum, of VGLUT3$^{-/-}$ mice (Gras et al., 2008; Divito et al., 2015; Sakae et al., 2015). We also speculate that D1R changes are dynamic and transient in nature since dopamine release is augmented in both the dorsal striatum and the NAc of VGLUT3$^{-/-}$ mice (Divito et al., 2015; Favier et al., 2020). In addition, the number of D1R-positive MSNs is not affected by VGLUT3 loss in both regions of the striatum (Divito et al., 2015; Sakae et al., 2015). Overall, this suggests that the VGLUT3-mGluR5 signaling axis plays a vital role in balancing glutamatergic and dopaminergic transmission within striatal networks.

Corticostriatal circuitry is heavily involved in motor learning and coordination in mice (Metz and Whishaw, 2002; Costa et al., 2004). Since VGLUT3 transmission coordinates corticostriatal network activity (Gras et al., 2008; Nelson et al., 2014; Deffains and Bergman, 2015), it is expected that motor functions may be modified by global VGLUT3 loss in mice. VGLUT3$^{-/-}$ mice elicit increased locomotor activities (Gras et al., 2008; Divito et al., 2015), however, limbs' coordination is intact in young male VGLUT3$^{-/-}$ mice (Gangarossa et al., 2016). In support, our findings complemented

current evidence by showing that VGLUT3$^{-/-}$ mice of both sexes exhibited intact motor coordination functions and grip strength throughout 15 months of age. Interestingly, previous reports showed that suppression of mGluR5 in mice leads to a comparable motor phenotype to VGLUT3$^{-/-}$ mice. Genetic deletion of mGluR5 in mice increased their locomotor activities with no impact on their motor coordination as assessed in the rotarod test (Gray et al., 2009; Ribeiro et al., 2014). Similar observations were noted in mice treated with selective mGluR5 blockers, 3-[(2-methyl-4-thiazolyl) ethynyl] pyridine (MTEP) or CTEP (Ribeiro et al., 2014; Abd-Elrahman et al., 2017), suggesting that VGLUT3 and mGluR5 regulate common regional circuits involved in motor coordination along the corticostriatal pathway.

5.2. Contribution of VGLUT3/mGluR5 crosstalk to HD motor rescue

Disruption of glutamatergic and non-glutamatergic signaling in the striatum evidently contribute to the motor deficits in HD patients (Graybiel et al., 1994; Cepeda et al., 2014; Hsu et al., 2018). For instance, increasing dopamine release induces chorea while reducing dopamine levels leads to akinesia in HD patients (Bird, 1980). In zQ175 HD mice, basal and evoked dopamine levels are reduced in the striatum starting from 12 months of age (Smith et al., 2014; Rothe et al., 2015). Whether these impairments are regulated via the VGLUT3-mGluR5 signaling axis is not yet clear. Remarkably, we found that VGLUT3 loss significantly improved motor coordination deficits in zQ175 mice throughout 15 months of age. A previous study from our laboratory also showed that genetic deletion of mGluR5 in *Hdh* Q111 mice improved motor coordination deficits throughout 24 months of age (Ribeiro et al., 2014). Interestingly, these mGluR5-mediated locomotor effects are dopamine-dependent

(Ribeiro et al., 2014). Therefore, it is possible that loss of VGLUT3 transmission potentially reduced mGluR5-mediated inhibition of dopaminergic neurons further increasing dopamine levels in zQ175 striatum.

We can not rule out the involvement of other neurotransmission systems in the motor rescue in VGLUT3-null HD mice. For instance, VGLUT3-expressing GABAergic interneurons provide inputs onto mGluR5-expressing pyramidal neurons of the motor cortex which project to the striatum (Romano et al., 1995; Hioki et al., 2004; Somogyi et al., 2004; Omiya et al., 2015). These interneurons can signal via both GABA and glutamate to influence cortical neuronal activity as previously reported in the hippocampus (Omiya et al., 2015; Fasano et al., 2017). Previous evidence depicted increased cortical excitability and impaired GABA-mediated inhibition of cortical neurons at early stages of HD in patients (Schippling et al., 2009; Philpott et al., 2016). Similar observations were reported in HD mice in which the frequency of Ca^{2+} transients was increased at presymptomatic and symptomatic stages, indicative of a higher firing rate in cortical pyramidal neurons (Burgold et al., 2019; Donzis et al., 2020). Therefore, it can be hypothesized that VGLUT3 ablation augmented GABAergic inhibitory currents onto cortical pyramidal neurons which, in turn, reduced striatal neuronal overactivation (Heimer et al., 2008; Fasano et al., 2017). Indeed, this warrants further investigation. Together, these findings suggest that the adaptions in corticostriatal circuitries in VGLUT3$^{-/-}$ mice observed in our experiments potentially underlie the motor improvements in HD.

Despite the rescue in motor coordination and grip strength, zQ175:VGLUT3$^{-/-}$ mice displayed decreased mobility in the open field arena. While impaired anxiogenic

locomotion in zQ175 mice is well-documented (Heikkinen et al., 2012; Abd-Elrahman et al., 2017; Li et al., 2021), it is not clear how VGLUT3/mGluR5 crosstalk is involved in this phenotype. In wild-type mice, current evidence suggests that signaling via VGLUT3 or mGluR5 differentially regulates anxiogenic locomotor behavior. While genetic ablation of mGluR5 leads to an anxiolytic-like phenotype and hyperlocomotive behavior in open field tests (Brodkin et al., 2002; Ribeiro et al., 2014), VGLUT3$^{-/-}$ mice elicit anxiety-associated behaviors including neophobia (Amilhon et al., 2010; Sakae et al., 2019). Multiple brain regions are assumed to mediate this anxiety phenotype in open field test including the cerebral cortex, raphe nuclei, and basolateral amygdala complex (Duncan et al., 1996; Abrams et al., 2005; Hale et al., 2008). In the basolateral amygdala, activation of mGluR5 elicits anxious behaviors in animals (Rahman et al., 2017). The basal amygdala receives inputs from VGLUT3-expressing serotoninergic terminals projecting from the dorsal raphe (Fremeau et al., 2002; Sengupta and Holmes, 2019). These terminals exert their fear-potentiating effects predominantly via 5HT$_{1A/2A}$ receptors with little input from glutamatergic signaling (Sengupta and Holmes, 2019), suggesting that VGLUT3-mediated glutamate does not directly activate mGluR5 in the basal amygdala. In the cortex, however, conditional knockout of mGluR5 increases mice locomotive performance in the open field (Jew et al., 2013). Given that VGLUT3$^{-/-}$ mice exhibit marked elevation in mGluR5 expression in the cerebral cortex (Ibrahim et al., 2022), this upregulation may contribute to the anxiogenic locomotor behavior in the open field test. Overall, this suggests that activation of mGluR5 signaling in selected brain regions potentially mediates the anxiogenic locomotor phenotype in VGLUT3$^{-/-}$ mice.

5.3. Hippocampal VGLUT3/mGluR5 crosstalk and its role in HD memory rescue

mGluR5 activation is essential for synaptic plasticity induction at CA1 hippocampal neuron synapses (Manahan-Vaughan, 1997; Lüscher and Huber, 2010). These neurons are innervated by VGLUT3-positive terminals from cholecystokinin $(CKK)^{+}$ GABAergic interneurons and serotoninergic fibers within the hippocampus (Somogyi et al., 2004; Amilhon et al., 2010). Here, we found that VGLUT3 loss downregulated mGluR5 cell surface levels with no impact on mGluR2/3 expression in the hippocampus of $VGLUT3^{-/-}$ mice (Ibrahim et al., 2022), suggesting that mGluR5 signaling is likely modified by VGLUT3 transmission loss. Yet, the regulation of hippocampal VGLUT3/mGluR5 crosstalk remains poorly understood. Fasano et al. (2017) reported that glutamate release via VGLUT3 can fine-tune and dampen GABAergic transmission onto CA1 hippocampal neurons. The changes in GABAergic currents are primarily mediated via presynaptic group III mGluRs, with little or no input from mGluR5 signaling (Fasano et al., 2017). On the other hand, VGLUT3 can modify serotoninergic transmission in the hippocampus which indirectly influences mGluR5 activation (Amilhon et al., 2010). The metaplastic responses triggered by VGLUT3-positive serotoninergic terminals involve the activation of selected serotonin receptors such as $5HT_{1A}$ and $5HT_{7}$, both of which have been reported to modify mGluR5-dependent LTD responses at hippocampal neuron synapses (Normann and Clark, 2005; Zhong et al., 2008; Amilhon et al., 2010; Costa et al., 2012). Overall, this suggests that the VGLUT3-mGluR5 signaling axis operates through a more complex system in regulating hippocampal circuitry.

Dysregulated mGluR5 signaling is heavily implicated in memory dysfunction mechanisms (Abd-Elrahman and Ferguson, 2022). Suppression of mGluR5 in wild-type mice disrupts certain hippocampal-dependent functions, such as working memory (Homayoun et al., 2004; de Souza et al., 2022) with no impact on memory consolidation, retrieval, and novelty memory functions (Barker et al., 2006; Hamilton et al., 2016; Abd-Elrahman et al., 2017; Li et al., 2022). Therefore, we hypothesized that alterations in mGluR5 densities mediated by VGLUT3 loss could potentially affect cognitive processes in VGLUT3$^{-/-}$ mice (Ibrahim et al., 2022). Our experiments clearly depicted intact short-term memory functions in both male and female VGLUT3$^{-/-}$ mice throughout 15 months of age. Remarkably, recent evidence also suggests that VGLUT3$^{-/-}$ mice display intact spatial learning skills and enhanced memory retention (Marcus-Sells, 2016). However, similar to mGluR5 knockout mice, VGLUT3 loss may impair working memory and cognitive flexibility in mice (Fazekas et al., 2019). This suggests that VGLUT3 and mGluR5 signaling likely converge in the regulation of selected domains relevant to memory functions, however, more robust evidence for the physiologic role of VGLUT3 in cognitive functions is warranted.

One intriguing observation is the persistent memory rescue in both male and female VGLUT3-null HD mice. Indeed, impaired hippocampal synaptic plasticity evidently contributes to the cognitive and memory deficits in both HD patients and animal models (Spargo et al., 1993; Murphy et al., 2000; Simmons et al., 2009; Paulsen, 2011; Kolodziejczyk et al., 2014). In Q175FDN mice, basal excitability at hippocampal CA1 synapses is enhanced, an effect that is coupled with impaired plasticity in both asymptomatic and symptomatic mice (Ravalia et al., 2021). These impairments can be

driven by disrupted signaling via iGluRs and mGluRs in HD. For instance, hyperexcitability of AMPARs and NMDARs are linked to abnormal plasticity responses in the hippocampus of HD mice (Hodgson et al., 1999; Ravalia et al., 2021). Likewise, pathological activation of mGluR5 significantly contributes to cognitive deficits in HD mice (Abd-Elrahman et al., 2017; Li et al., 2022). Thus, it is possible that loss of VGLUT3 reduced synaptic strength via the reduction of NMDARs and mGluR5 cell surface densities which may have improved memory deficits in HD mice (Ibrahim et al., 2022). Furthermore, given that GABAergic inhibitory currents are reduced in the pyramidal neurons of symptomatic HD mouse models (Cummings et al., 2009; Dargaei et al., 2019), it is possible that the augmented GABAergic transmission evoked by VGLUT3 ablation may play a protective role against hippocampal circuitry deficits in zQ175 mice (Fasano et al., 2017).

5.4. Sex-dependency of VGLUT3 transmission in HD

Sex differences are often not highlighted in HD, likely because of its nature of autosomal inheritance which is equally penetrant in both males and females (Smith and Dahodwala, 2014). However, it has been suggested that sex might influence disease progression and phenotype in patients. Female HD patients exhibit a faster rate of disease progression and slightly more severe phenotype, particularly in the motor and functional domains (Zielonka et al., 2013; Hentosh et al., 2021). On the other hand, a study by the Huntington Study Group, which followed HD patients prospectively for 18 months, reported that sex did not affect the functional decline in motor and cognitive behaviors in patients (Jacobs et al., 2016). Similarly, preclinical evidence suggests that the extent of motor decline in zQ175 mice is independent of sex (Menalled et al., 2012;

Rothe et al., 2015; Goodliffe et al., 2018; Li et al., 2022). Our study further extends those findings by showing that both male and female zQ175 mice exhibit comparable motor and cognitive deficits up to 15 months of age. In addition, we showed that loss of VGLUT3 in zQ175 mice equally improved HD deficits regardless of sex. Prior studies depicted no major differences between male and female animals in displaying VGLUT3$^{-/-}$ phenotype (Amilhon et al., 2010; Divito et al., 2015; Ramet et al., 2017). However, a recent report has depicted an upregulation in VGLUT3 expression in the NAc of female mice relative to male mice (López et al., 2021). While this suggests a potential sex difference in VGLUT3 signaling, an intriguing observation was reported by Ramet et al. (2017) showing that VGLUT3 uptake functions can be efficiently carried out with roughly 30% expression of the transporter in cells. Overall, our results strongly suggest that sex is not a key regulator of phenotypic rescue in VGLUT3-null HD mice.

5.5. Potential role of OPTN in pathological mGluR5 signaling in HD striatum

Mounting evidence suggests an important role for OPTN in HD pathogenesis, being an autophagy adaptor that is sequestered in mHTT inclusion bodies in the brains of HD patients and mouse models (Schwab et al., 2012; Shen et al., 2015; Ying and Yue, 2016). Additionally, mGluR5 signaling is one of the cellular processes that is evidently dysregulated in HD. For instance, mHTT augments cytosolic Ca^{2+} flux and promotes striatal excitotoxicity via sensitization of IP_3 receptors and NMDARs in a mGluR5-dependent manner (Calabresi et al., 1999; Sun et al., 2001; Tang et al., 2003; Ribeiro et al., 2010). In zQ175 mouse brains, compromised activation of mTOR/ULK1/ATG14 and GSK3β/ZBTB16/ATG14 signaling pathways lead to evident impairments in autophagic machinery (Wold et al., 2016; Abd-Elrahman et al., 2017).

Here, our findings suggest that OPTN expression is potentially protective against impaired cellular signaling in HD. First, we showed that OPTN can functionally interact with mGluR5 canonical signaling as depicted by augmented mGluR5-activated Ca^{2+} mobilization in an OPTN-null striatal cell line (Ibrahim et al., 2021). Second, we provided evidence that OPTN loss resulted in impaired autophagic machinery in both striatal cells and the hippocampus via disrupted GSK3β/ZBTB16 and mTOR/ULK1 signaling pathways downstream of mGluR5 (Ibrahim et al., 2021). Therefore, these suggest that alterations in OPTN homeostasis contribute to neuronal degeneration and excitotoxic cell death in HD. In line with this hypothesis, it was reported that OPTN is highly expressed by striatal interneurons, unlike MSNs that express significantly lower levels of OPTN (Okita et al., 2012). This OPTN cell-specific expression is complementary to the neuronal loss pattern typically observed in the striatum of HD patients (Ferrante et al., 1987; G. Vonsattel and DiFiglia, 1998; Fu et al., 2018). In addition, mGluR1/5-mediated excitotoxic Ca^{2+} responses is evident in MSNs, but not striatal interneurons (Calabresi et al., 1999; Ribeiro et al., 2017), suggesting the OPTN/mGluR5 interaction may dictate neuronal survival in the striatum. Furthermore, inefficient autophagic degradation capacity or expression of Ca^{2+}-buffering proteins have been linked to cell-specific vulnerabilities in HD striatum (Fu et al., 2018). Collectively, the current evidence highlights the potential role of OPTN in controlling impaired mGluR5 signaling and HD autophagic defects in striatal neurons.

5.6. Potential role of OPTN in mGluR5-mediated synaptic plasticity in HD

Induction and maintenance of synaptic plasticity in the hippocampus rely on the coordinated activation of various cellular signaling events including; PI3K/mTOR,

ERK1/2, and autophagy pathways (Hoeffer and Klann, 2010; Shehata et al., 2012; Rai et al., 2019). Disruption of these signaling pathways may contribute to impaired synaptic maintenance in HD (Giralt et al., 2012; Grosso Jasutkar and Yamamoto, 2021). Particularly, autophagy is vital for the homeostasis of synaptic proteins required to support plasticity changes and memory consolidation (Shehata et al., 2012; Nixon, 2013; Abd-Elrahman and Ferguson, 2022). Fasting in rats suppresses hippocampal autophagy signaling, an effect that is coupled with increased BDNF, an important regulator of hippocampal synaptic plasticity (Nikoletopoulou et al., 2017). Degradation of postsynaptic scaffolding/signaling proteins such as PSD95, SHANK3, and Arc is also regulated via autophagy (Han et al., 2010; Nikoletopoulou et al., 2017). Remarkably, mGluR5 activation in the hippocampus downregulates autophagy through activation of PI3K/mTOR and ERK1/2 signaling, both mediate rapid protein synthesis vital for synaptic plasticity (Hou and Klann, 2004; Banko et al., 2006; Heras-Sandoval et al., 2014; Abd-Elrahman and Ferguson, 2022). Our results in hippocampal slices suggest that the regulation of such synaptic processes is dependent on OPTN expression, as deletion of OPTN abolishes mGluR5-mediated ERK1/2 activation and increases basal mTOR phosphorylation that subsequently impairs ULK1 activation (Ibrahim et al., 2021). In addition, since mHTT aggregates sequester OPTN (Schwab et al., 2012; Shen et al., 2015), we suspect that reduced cytosolic availability of OPTN may contribute to the disrupted mGluR5 signaling in the hippocampus and respective HD cognitive deficits (Benn et al., 2007). While this hypothesis has yet to be verified, it has been reported that impaired hippocampal synaptic plasticity correlates with reduced ERK1/2 activation in R6/1 HD mice, an effect that is dependent on mGluR5 activation

(Milnerwood et al., 2006; Giralt et al., 2011b; Senter et al., 2016). Furthermore, we believe that impaired OPTN/mGluR5 crosstalk in HD may involve disruptions in the NF-κB pathway, an important regulator of synaptic plasticity (Khoshnan, 2004; Mincheva-Tasheva and Soler, 2013; Träger et al., 2014). OPTN can act as a negative regulator of NF-κB activity (Kachaner et al., 2012), whereas mGluR5 activation enhances NF-κB nuclear accumulation and activation in hippocampal neurons (O'Riordan et al., 2006; Sitcheran et al., 2008). Given that ERK activity is necessary for mGluR5-induced NF-κB activation (O'Riordan et al., 2006), it is possible disruption in NF-κB homeostasis in $OPTN^{-/-}$ hippocampus can be another contributing factor to impaired mGluR5-mediated plasticity in HD. Together, our results suggest that OPTN/mGluR5 crosstalk can play an important role in hippocampal-dependent memory functions.

5.7. Contribution of mGluR5/VGLUT3/OPTN crosstalk to TANs functions in HD

Within the striatum, TANs virtually target all striatal neurons and influence striatal functioning and, hence, basal ganglia outflow (Lim et al., 2014; Deffains and Bergman, 2015). In HD, TANs are resistant to mHTT-mediated neurodegeneration albeit they display structural and functional alterations that are presumed to contribute to disease pathogenesis (Graveland et al., 1985; Smith et al., 2006; Okita et al., 2012; Deng and Reiner, 2016). Our current findings depicting the contribution of both VGLUT3 and OPTN to mGluR5 signaling further support the notion that TANs are a promising target for mitigating striatal circuitry deficits in HD. This is exemplified by mGluR5 expression on TANs that directly regulate their excitability and presumably influence VGLUT3 transmission by these cells (Tallaksen-Greene et al., 1998; Pisani et al., 2001). On the other hand, as discussed in **Section 5.5**, OPTN cell-specific expression within the

striatum is highly likely to contribute to TANs' resistance to mGluR5 excitotoxic signaling (Calabresi et al., 1999; Anborgh et al., 2005; Okita et al., 2012). Therefore, interrogating the functional interplay between mGluR5, VGLUT3, and OPTN can be an interesting approach to understand their influence on TANs excitability and the subsequent impact on striatal network regulation in HD.

5.8. Future directions

The novel findings presented in this thesis have generated a number of interesting questions that could be pursued in the future. First, **what are the molecular mechanisms underlying the motor rescue in VGLUT3-null HD mice?** This would be of particular interest since the levels of mHTT aggregates were not altered in the striatum of VGLUT3-null HD mice. Indeed, large mHTT aggregates were previously presumed to be pathogenic (Ross, 1997), however, inclusions can occur without neuronal death, and vice versa (Saudou et al., 1998; Arrasate et al., 2004). More recent evidence suggests that polyQ-expanded N-terminal oligomers of HTT are the toxic species (Nagai et al., 2007; Miller et al., 2011; Nucifora et al., 2012; Sahl et al., 2012), and that the subsequent formation of inclusions might be a neuronal coping response to more toxic forms of mHTT (Arrasate et al., 2004; Nucifora et al., 2012). Therefore, it would be interesting to explore the mechanisms by which VGLUT3 ablation improves the resilience of striatal neurons to mHTT aggregation and whether the reduction in excitotoxic insults is linked to neuronal rescue seen in zQ175 mice. On the other hand, **how does mHTT accumulation potentially impact VGLUT3 transmission in HD brain?** In HD patients, TANs are typically spared (Graveland et al., 1985), albeit their functions are altered as the disease progresses. For instance, the

dendritic branching, but not neuronal numbers, of TANs is often reduced in HD mice (Deng and Reiner, 2016; Deng et al., 2021). This is coupled with a reduction in the thalamic input onto TANs and impaired cholinergic signaling in the striatum (Deng and Reiner, 2016; Lim and Surmeier, 2021). Given that TANs maintain a fine balance between VGLUT3-mediated glutamate and ACh co-transmission, investigating the impact of mHTT on VGLUT3 signaling in the striatum and other brain regions is warranted.

Another important question would be **whether there are sex differences in VGLUT3-mGluR5 cellular signaling.** Accumulated evidence, including our findings, have shown that VGLUT3 modulation results in comparable changes in brain microcircuits and phenotype of both male and female wild-type mice (Amilhon et al., 2010; Higley et al., 2011; Divito et al., 2015; Ramet et al., 2017; Kljakic et al., 2022). However, we can not rule out sex differences in VGLUT3-mGluR5 cellular signaling. Particularly, recent evidence from our group has depicted sex-dependency of mGluR5 signaling profiles in AD mice due to differences in the pathological scaffold composition formed between mGluR5 and amyloid β (Abd-Elrahman et al., 2020a; Abd-Elrahman and Ferguson, 2022). In HD, treatment with a mGluR5 blocker displayed varied efficacy between male and female zQ175 mice, suggesting a potential sex-specific difference in the signaling pathways downstream of mGluR5 (Li et al., 2022). Therefore, studying the potential contribution of biological sex in VGLUT3/mGluR5 crosstalk will provide better insights into the cellular mechanisms underlying the phenotypic rescue in VGLUT3-null HD mice.

As for OPTN, our studies provided the first indication that OPTN/mGluR5 interaction could play an integral role in mGluR5-dependent ERK1/2 phosphorylation (Ibrahim et al., 2021). This is an intriguing finding since ERK1/2 is at the crossroads of signaling involved in neuroprotection and neuronal death, and abnormal activation contributes to HD progression (Lu and Xu, 2006; Sun and Nan, 2017). Therefore, future experiments should address the following questions: **what are the molecular mechanisms involved in mGluR5-mediated ERK1/2 regulation in OPTN$^{-/-}$ cells, and how do these processes influence HD progression in mice?** Particularly, HD triggers evident impairments in PLCβ/Ca^{2+}/PKC dynamics which ultimately impacts ERK1/2 activation in striatal cells (Ribeiro et al., 2017). Furthermore, investigating the role of OPTN in HD memory deficits in mice would be the next logical step since recent evidence suggests that mutations in OPTN are linked to memory and cognitive impairments in frontotemporal dementia patients (Pottier et al., 2015; Feng et al., 2019; Dominguez et al., 2021). This will broaden our understanding of how OPTN contributes to impaired cellular signaling in HD, beyond its autophagic role, and how this influences disease phenotype in animals.

5.9. Conclusion

The pathology of HD is well-described, and despite the extensive preclinical and clinical research efforts, no disease-modifying drugs are yet available. This thesis provides novel evidence that VGLUT3, despite its limited abundance, plays an important role in HD pathophysiology via regulation of mGluR5 as well as other glutamate receptors across the brain. In addition, we uncovered a molecular mechanism by which OPTN mediates mGluR5 canonical and ERK1/2 signaling as well

as facilitation of autophagic machinery downstream of mGluR5. Given that modulation of mGluR5 evidently modifies HD progression, our findings support a rationale for targeting VGLUT3 and OPTN to therapeutically mitigate or, at least, control pathological mGluR5 signaling in HD.

References

Abd-Elrahman, K.S., Albaker, A., Souza, J.M. de, Ribeiro, F.M., Schlossmacher, M.G., Tiberi, M., et al. (2020a). Aβ oligomers induce pathophysiological mGluR5 signaling in Alzheimer's disease model mice in a sex-selective manner. Sci. Signal. *13*: eabd2494.

Abd-Elrahman, K.S., and Ferguson, S.S.G. (2019). Modulation of mTOR and CREB pathways following mGluR5 blockade contribute to improved Huntington's pathology in zQ175 mice. Mol. Brain *12*: 35.

Abd-Elrahman, K.S., and Ferguson, S.S.G. (2022). Noncanonical Metabotropic Glutamate Receptor 5 Signaling in Alzheimer's Disease. Annu. Rev. Pharmacol. Toxicol. *62*: 235–254.

Abd-Elrahman, K.S., Hamilton, A., Albaker, A., and Ferguson, S.S.G. (2020b). mGluR5 Contribution to Neuropathology in Alzheimer Mice Is Disease Stage-Dependent. ACS Pharmacol. Transl. Sci. *3*: 334–344.

Abd-Elrahman, K.S., Hamilton, A., Hutchinson, S.R., Liu, F., Russell, R.C., and Ferguson, S.S.G. (2017). mGluR5 antagonism increases autophagy and prevents disease progression in the zQ175 mouse model of Huntington's disease. Sci. Signal. *10*: eaan6387.

Abd-Elrahman, K.S., Hamilton, A., Vasefi, M., and Ferguson, S.S.G. (2018). Autophagy is increased following either pharmacological or genetic silencing of mGluR5 signaling in Alzheimer's disease mouse models. Mol. Brain *11*: 19.

Abd-Elrahman, K.S., Sarasija, S., Colson, T.-L.L., and Ferguson, S.S.G. (2022). A positive allosteric modulator for the muscarinic receptor (M1 mAChR) improves pathology and cognitive deficits in female APPswe/PSEN1ΔE9 mice. Br. J. Pharmacol. *179*: 1769–1783.

Abdul-Ghani, M.A., Valiante, T.A., Carlen, P.L., and Pennefather, P.S. (1996). Metabotropic glutamate receptors coupled to IP3 production mediate inhibition of IAHP in rat dentate granule neurons. J. Neurophysiol. *76*: 2691–2700.

Abe, T., Sugihara, H., Nawa, H., Shigemoto, R., Mizuno, N., and Nakanishi, S. (1992). Molecular characterization of a novel metabotropic glutamate receptor mGluR5 coupled to inositol phosphate/Ca2+ signal transduction. J. Biol. Chem. *267*: 13361–13368.

Abrams, J.K., Johnson, P.L., Hay-Schmidt, A., Mikkelsen, J.D., Shekhar, A., and Lowry, C.A. (2005). Serotonergic systems associated with arousal and vigilance behaviors following administration of anxiogenic drugs. Neuroscience *133*: 983–997.

Aguilar, J.I., Dunn, M., Mingote, S., Karam, C.S., Farino, Z.J., Sonders, M.S., et al. (2017). Neuronal Depolarization Drives Increased Dopamine Synaptic Vesicle Loading via VGLUT. Neuron *95*: 1074-1088.e7.

Alagarsamy, S., Marino, M.J., Rouse, S.T., Gereau IV, R.W., Heinemann, S.F., and Conn, P.J. (1999). Activation of NMDA receptors reverses desensitization of mGluR5 in native and recombinant systems. Nat. Neurosci. *2*: 234–240.

Ali, D.M., Ansari, S.S., Zepp, M., Knapp-Mohammady, M., and Berger, M.R. (2019). Optineurin downregulation induces endoplasmic reticulum stress, chaperone-mediated autophagy, and apoptosis in pancreatic cancer cells. Cell Death Discov. *5*: 128.

Alpaugh, M., Masnata, M., Rus Jacquet, A. de, Lepinay, E., Denis, H.L., Saint-Pierre, M., et al. (2022). Passive immunization against phosphorylated tau improves features of Huntington's disease pathology. Mol. Ther. *30*: 1500–1522.

Amilhon, B., Lepicard, E., Renoir, T., Mongeau, R., Popa, D., Poirel, O., et al. (2010). VGLUT3 (Vesicular Glutamate Transporter Type 3) Contribution to the Regulation of Serotonergic Transmission and Anxiety. J. Neurosci. *30*: 2198–2210.

Anagnostaras, S.G., Murphy, G.G., Hamilton, S.E., Mitchell, S.L., Rahnama, N.P., Nathanson, N.M., et al. (2003). Selective cognitive dysfunction in acetylcholine M1 muscarinic receptor mutant mice. Nat. Neurosci. *6*: 51–58.

Anborgh, P.H., Godin, C., Pampillo, M., Dhami, G.K., Dale, L.B., Cregan, S.P., et al. (2005). Inhibition of metabotropic glutamate receptor signaling by the huntingtin-binding protein optineurin. J. Biol. Chem. *280*: 34840–34848.

Andrew, S.E., Paul Goldberg, Y., Kremer, B., Telenius, H., Theilmann, J., Adam, S., et al. (1993). The relationship between trinucleotide (CAG) repeat length and clinical features of Huntington's disease. Nat. Genet. *4*: 398–403.

Anglada-Huguet, M., Giralt, A., Rué, L., Alberch, J., and Xifró, X. (2016). Loss of striatal 90-kDa ribosomal S6 kinase (Rsk) is a key factor for motor, synaptic and transcription dysfunction in Huntington's disease. Biochim. Biophys. Acta - Mol. Basis Dis. *1862*: 1255–1266.

Apostol, B.L., Illes, K., Pallos, J., Bodai, L., Wu, J., Strand, A., et al. (2006). Mutant huntingtin alters MAPK signaling pathways in PC12 and striatal cells: ERK1/2 protects against mutant huntingtin-associated toxicity. Hum. Mol. Genet. *15*: 273–285.

Areal, L.B., Hamilton, A., Martins-Silva, C., Pires, R.G.W., and Ferguson, S.S.G. (2019). Neuronal scaffolding protein spinophilin is integral for cocaine-induced behavioral sensitization and ERK1/2 activation. Mol. Brain *12*: 15.

Arrasate, M., Mitra, S., Schweitzer, E.S., Segal, M.R., and Finkbeiner, S. (2004). Inclusion body formation reduces levels of mutant huntingtin and the risk of neuronal death. Nature *431*: 805–810.

Ast, A., Buntru, A., Schindler, F., Hasenkopf, R., Schulz, A., Brusendorf, L., et al. (2018). mHTT Seeding Activity: A Marker of Disease Progression and Neurotoxicity in Models of Huntington's Disease. Mol. Cell *71*: 675-688.e6.

Attwood, T.K., and Findlay, J.B.C. (1994). Fingerprinting G-protein-coupled receptors. Protein Eng. Des. Sel. *7*: 195–203.

Au, J.S.-Y., Puri, C., Ihrke, G., Kendrick-Jones, J., and Buss, F. (2007). Myosin VI is required for sorting of AP-1B–dependent cargo to the basolateral domain in polarized MDCK cells. J. Cell Biol. *177*: 103–114.

Awad, H., Hubert, G.W., Smith, Y., Levey, A.I., and Conn, P.J. (2000). Activation of Metabotropic Glutamate Receptor 5 Has Direct Excitatory Effects and Potentiates NMDA Receptor Currents in Neurons of the Subthalamic Nucleus. J. Neurosci. *20*: 7871–7879.

Balázs, R., Miller, S., Romano, C., Vries, A. De, Chun, Y., and Cotman, C.W. (2002). Metabotropic Glutamate Receptor mGluR5 in Astrocytes: Pharmacological Properties and Agonist Regulation. J. Neurochem. *69*: 151–163.

Balázsfi, D., Fodor, A., Török, B., Ferenczi, S., Kovács, K.J., Haller, J., et al. (2018). Enhanced innate fear and altered stress axis regulation in VGluT3 knockout mice. Stress *21*: 151–161.

Ballester-Rosado, C.J., Albright, M.J., Wu, C.-S., Liao, C.-C., Zhu, J., Xu, J., et al. (2010). mGluR5 in cortical excitatory neurons exerts both cell-autonomous and -nonautonomous influences on cortical somatosensory circuit formation. J. Neurosci. *30*: 16896–909.

Banko, J.L., Hou, L., Poulin, F., Sonenberg, N., and Klann, E. (2006). Regulation of eukaryotic initiation factor 4E by converging signaling pathways during metabotropic glutamate receptor-dependent long-term depression. J. Neurosci. *26*: 2167–73.

Bannerman, D.M., Deacon, R.M.J., Brady, S., Bruce, A., Sprengel, R., Seeburg, P.H., et al. (2004). A Comparison of GluR-A-Deficient and Wild-Type Mice on a Test Battery Assessing Sensorimotor, Affective, and Cognitive Behaviors. Behav. Neurosci. *118*: 643–647.

Bansal, M., Moharir, S.C., Sailasree, S.P., Sirohi, K., Sudhakar, C., Sarathi, D.P., et al. (2018). Optineurin promotes autophagosome formation by recruiting the autophagy-related Atg12-5-16L1 complex to phagophores containing the Wipi2 protein. J. Biol. Chem. *293*: 132–147.

Barker, G.R.I., Bashir, Z.I., Brown, M.W., and Warburton, E.C. (2006). A temporally distinct role for group I and group II metabotropic glutamate receptors in object recognition memory. Learn. Mem. *13*: 178–186.

Basu, J., and Siegelbaum, S.A. (2015). The Corticohippocampal Circuit, Synaptic Plasticity, and Memory. Cold Spring Harb. Perspect. Biol. *7*: a021733.

Bates, G.P., Dorsey, R., Gusella, J.F., Hayden, M.R., Kay, C., Leavitt, B.R., et al. (2015). Huntington disease. Nat. Rev. Dis. Prim. *1*: 15005.

Beal, M., Ferrante, R., Swartz, K., and Kowall, N. (1991). Chronic quinolinic acid lesions in rats closely resemble Huntington's disease. J. Neurosci. *11*: 1649–1659.

Beal, M.F., Kowall, N.W., Ellison, D.W., Mazurek, M.F., Swartz, K.J., and Martin, J.B. (1986). Replication of the neurochemical characteristics of Huntington's disease by quinolinic acid. Nature *321*: 168–171.

Beaulieu, J.-M., Gainetdinov, R.R., and Caron, M.G. (2009). Akt/GSK3 Signaling in the Action of Psychotropic Drugs. Annu. Rev. Pharmacol. Toxicol. *49*: 327–347.

Beebe, S.J. (1994). The cAMP-dependent protein kinases and cAMP signal transduction. Semin. Cancer Biol. *5*: 285–94.

Bellocchio, E.E., Reimer, R.J., Fremeau, R.T., and Edwards, R.H. (2000). Uptake of glutamate into synaptic vesicles by an inorganic phosphate transporter. Science *289*: 957–60.

Belmer, A., Beecher, K., Jacques, A., Patkar, O.L., Sicherre, F., and Bartlett, S.E. (2019). Axonal Non-segregation of the Vesicular Glutamate Transporter VGLUT3 Within Serotonergic Projections in the Mouse Forebrain. Front. Cell. Neurosci. *13*:.

Benn, C.L., Slow, E.J., Farrell, L.A., Graham, R., Deng, Y., Hayden, M.R., et al. (2007). Glutamate receptor abnormalities in the YAC128 transgenic mouse model of Huntington's disease. Neuroscience *147*: 354–372.

Bergeron, Y., Chagniel, L., Bureau, G., Massicotte, G., and Cyr, M. (2014). mTOR signaling contributes to motor skill learning in mice. Front. Mol. Neurosci. *7*:.

Berry, C.T., Sceniak, M.P., Zhou, L., and Sabo, S.L. (2012). Developmental Up-Regulation of Vesicular Glutamate Transporter-1 Promotes Neocortical Presynaptic Terminal Development. PLoS One *7*: e50911.

Bessis, A.-S., Rondard, P., Gaven, F., Brabet, I., Triballeau, N., Prézeau, L., et al. (2002). Closure of the Venus flytrap module of mGlu8 receptor and the activation process: Insights from mutations converting antagonists into agonists. Proc. Natl. Acad. Sci. *99*: 11097–11102.

Beurel, E., Grieco, S.F., and Jope, R.S. (2015). Glycogen synthase kinase-3 (GSK3): Regulation, actions, and diseases. Pharmacol. Ther. *148*: 114–131.

Biber, K., Laurie, D.J., Berthele, A., Sommer, B., Tölle, T.R., Gebicke-Härter, P.-J., et al. (2001). Expression and Signaling of Group I Metabotropic Glutamate Receptors in Astrocytes and Microglia. J. Neurochem. *72*: 1671–1680.

Bird, E.D. (1980). Chemical pathology of Huntington's disease. Annu. Rev. Pharmacol. Toxicol. *20*: 533–51.

Bockaert, J., Perroy, J., Bécamel, C., Marin, P., and Fagni, L. (2010). GPCR Interacting Proteins (GIPs) in the Nervous System: Roles in Physiology and Pathologies. Annu. Rev. Pharmacol. Toxicol. *50*: 89–109.

Boersma, M.C.H., Dresselhaus, E.C., Biase, L.M. de, Mihalas, A.B., Bergles, D.E., and Meffert, M.K. (2011). A requirement for nuclear factor-κB in developmental and plasticity-associated synaptogenesis. J. Neurosci. *31*: 5414–5425.

Bohnen, N.I., Koeppe, R.A., Meyer, P., Ficaro, E., Wernette, K., Kilbourn, M.R., et al. (2000). Decreased striatal monoaminergic terminals in Huntington disease. Neurology *54*: 1753–1759.

Bond, L.M., Peden, A.A., Kendrick-Jones, J., Sellers, J.R., and Buss, F. (2011). Myosin VI and its binding partner optineurin are involved in secretory vesicle fusion at the plasma membrane. Mol. Biol. Cell *22*: 54–65.

Bonsi, P., Cuomo, D., Persis, C. De, Centonze, D., Bernardi, G., Calabresi, P., et al. (2005). Modulatory action of metabotropic glutamate receptor (mGluR) 5 on mGluR1 function in striatal cholinergic interneurons. Neuropharmacology *49*: 104–113.

Brodkin, J., Bradbury, M., Busse, C., Warren, N., Bristow, L.J., and Varney, M.A. (2002). Reduced stress-induced hyperthermia in mGluR5 knockout mice. Eur. J. Neurosci. *16*: 2241–2244.

Bruno, V., Battaglia, G., Copani, A., Cespédes, V.M., Galindo, M.F., Ceña, V., et al. (2001). An activity-dependent switch from facilitation to inhibition in the control of excitotoxicity by group I metabotropic glutamate receptors. Eur. J. Neurosci. *13*: 1469–78.

Burgold, J., Schulz-Trieglaff, E.K., Voelkl, K., Gutiérrez-Ángel, S., Bader, J.M., Hosp, F., et al. (2019). Cortical circuit alterations precede motor impairments in Huntington's disease mice. Sci. Rep. *9*: 6634.

Byrnes, K.R., Stoica, B., Loane, D.J., Riccio, A., Davis, M.I., and Faden, A.I. (2009). Metabotropic glutamate receptor 5 activation inhibits microglial associated inflammation and neurotoxicity. Glia *57*: 550–560.

Calabresi, P., Centonze, D., Pisani, A., and Bernardi, G. (1999). Metabotropic glutamate receptors and cell-type-specific vulnerability in the striatum: Implication for ischemia and Huntington's disease. Exp. Neurol. *158*: 97–108.

Carty, N., Berson, N., Tillack, K., Thiede, C., Scholz, D., Kottig, K., et al. (2015). Characterization of HTT Inclusion Size, Location, and Timing in the zQ175 Mouse Model of Huntington´s Disease: An In Vivo High-Content Imaging Study. PLoS One *10*: e0123527.

Caviston, J.P., Ross, J.L., Antony, S.M., Tokito, M., and Holzbaur, E.L.F. (2007). Huntingtin facilitates dynein/dynactin-mediated vesicle transport. Proc. Natl. Acad. Sci. *104*: 10045–10050.

Cea-del Rio, C.A., Lawrence, J.J., Tricoire, L., Erdelyi, F., Szabo, G., and McBain, C.J. (2010). M3 Muscarinic Acetylcholine Receptor Expression Confers Differential Cholinergic Modulation to Neurochemically Distinct Hippocampal Basket Cell Subtypes. J. Neurosci. *30*: 6011–6024.

Cepeda, C., Murphy, K.P.S., Parent, M., and Levine, M.S. (2014). The role of dopamine in huntington's disease. In Progress in Brain Research, (NIH Public Access), pp 235–254.

Chang, R., Liu, X., Li, S., and Li, X.-J. (2015). Transgenic animal models for study of the pathogenesis of Huntington's disease and therapy. Drug Des. Devel. Ther. *9*: 2179–88.

Chen, N., Luo, T., Wellington, C., Metzler, M., McCutcheon, K., Hayden, M.R., et al. (1999). Subtype-specific enhancement of NMDA receptor currents by mutant huntingtin. J. Neurochem. *72*: 1890–1898.

Chen, T., Cao, L., Dong, W., Luo, P., Liu, W., Qu, Y., et al. (2012). Protective effects of

mGluR5 positive modulators against traumatic neuronal injury through PKC-dependent activation of MEK/ERK pathway. Neurochem. Res. *37*: 983–990.

Conn, P.J., Battaglia, G., Marino, M.J., and Nicoletti, F. (2005). Metabotropic glutamate receptors in the basal ganglia motor circuit. Nat. Rev. Neurosci. *6*: 787–798.

Cornett, J., Cao, F., Wang, C.-E., Ross, C.A., Bates, G.P., Li, S.-H., et al. (2005). Polyglutamine expansion of huntingtin impairs its nuclear export. Nat. Genet. *37*: 198–204.

Costa, L., Spatuzza, M., D'Antoni, S., Bonaccorso, C.M., Trovato, C., Musumeci, S.A., et al. (2012). Activation of 5-HT7 Serotonin Receptors Reverses Metabotropic Glutamate Receptor-Mediated Synaptic Plasticity in Wild-Type and Fmr1 Knockout Mice, a Model of Fragile X Syndrome. Biol. Psychiatry *72*: 924–933.

Costa, R.M., Cohen, D., and Nicolelis, M.A.L. (2004). Differential Corticostriatal Plasticity during Fast and Slow Motor Skill Learning in Mice. Curr. Biol. *14*: 1124–1134.

Coyle, J.T., and Schwarcz, R. (1976). Lesion of striatal neurons with kainic acid provides a model for Huntington's chorea. Nature *263*: 244–246.

Craufurd, D., Thompson, J.C., and Snowden, J.S. (2001). Behavioral changes in Huntington Disease. Neuropsychiatry. Neuropsychol. Behav. Neurol. *14*: 219–26.

Cummings, D.M., Andre, V.M., Uzgil, B.O., Gee, S.M., Fisher, Y.E., Cepeda, C., et al. (2009). Alterations in Cortical Excitation and Inhibition in Genetic Mouse Models of Huntington's Disease. J. Neurosci. *29*: 10371–10386.

Cunha, C., Smiley, J.F., Chuhma, N., Shah, R., Bleiwas, C., Menezes, E.C., et al. (2020). Perinatal interference with the serotonergic system affects VTA function in the adult via glutamate co-transmission. Mol. Psychiatry 1–18.

Curtis, D.R., Phillis, J.W., and Watkins, J.C. (1959). Chemical Excitation of Spinal Neurones. Nature *183*: 611–612.

D'Souza, G.X., and Waldvogel, H.J. (2016). Targeting the Cholinergic System to Develop a Novel Therapy for Huntington's Disease. J. Huntingtons. Dis. *5*: 333–342.

Dahlström, A., and Fuxe, K. (1964). Localization of monoamines in the lower brain stem. Experientia *20*: 398–399.

Dale, L.B., Babwah, A. V., Bhattacharya, M., Kelvin, D.J., and Ferguson, S.S.G. (2001). Spatial-Temporal Patterning of Metabotropic Glutamate Receptor-mediated Inositol 1,4,5-Triphosphate, Calcium, and Protein Kinase C Oscillations. J. Biol. Chem. *276*: 35900–35908.

Dargaei, Z., Liang, X., Serranilla, M., Santos, J., and Woodin, M.A. (2019). Alterations in Hippocampal Inhibitory Synaptic Transmission in the R6/2 Mouse Model of Huntington's Disease. Neuroscience *404*: 130–140.

Dash, D., and Mestre, T.A. (2020). Therapeutic Update on Huntington's Disease: Symptomatic Treatments and Emerging Disease-Modifying Therapies.

Neurotherapeutics *17*: 1645–1659.

Deffains, M., and Bergman, H. (2015). Striatal cholinergic interneurons and cortico-striatal synaptic plasticity in health and disease. Mov. Disord. *30*: 1014–1025.

Deng, Y.-P., and Reiner, A. (2016). Cholinergic interneurons in the Q140 knockin mouse model of Huntington's disease: Reductions in dendritic branching and thalamostriatal input. J. Comp. Neurol. *524*: 3518–3529.

Deng, Y., Wang, H., Joni, M., Sekhri, R., and Reiner, A. (2021). Progression of basal ganglia pathology in heterozygous Q175 knock-in Huntington's disease mice. J. Comp. Neurol. *529*: 1327–1371.

Deng, Y.P., Wong, T., Bricker-Anthony, C., Deng, B., and Reiner, A. (2013). Loss of corticostriatal and thalamostriatal synaptic terminals precedes striatal projection neuron pathology in heterozygous Q140 Huntington's disease mice. Neurobiol. Dis. *60*: 89–107.

Deng, Z., Purtell, K., Lachance, V., Wold, M.S., Chen, S., and Yue, Z. (2017). Autophagy Receptors and Neurodegenerative Diseases. Trends Cell Biol. *27*: 491–504.

Dennis, S.H., Pasqui, F., Colvin, E.M., Sanger, H., Mogg, A.J., Felder, C.C., et al. (2016). Activation of Muscarinic M1 Acetylcholine Receptors Induces Long-Term Potentiation in the Hippocampus. Cereb. Cortex *26*: 414–426.

Desmond, C.R., Atwal, R.S., Xia, J., and Truant, R. (2012). Identification of a karyopherin β1/β2 proline-tyrosine nuclear localization signal in huntingtin protein. J. Biol. Chem. *287*: 39626–33.

DeWire, S.M., Ahn, S., Lefkowitz, R.J., and Shenoy, S.K. (2007). β-Arrestins and Cell Signaling. Annu. Rev. Physiol. *69*: 483–510.

Dhami, G.K., and Ferguson, S.S.G. (2006). Regulation of metabotropic glutamate receptor signaling, desensitization and endocytosis. Pharmacol. Ther. *111*: 260–271.

Dibble, C.C., and Cantley, L.C. (2015). Regulation of mTORC1 by PI3K signaling. Trends Cell Biol. *25*: 545–555.

DiFiglia, M., Sapp, E., Chase, K., Schwarz, C., Meloni, A., Young, C., et al. (1995). Huntingtin is a cytoplasmic protein associated with vesicles in human and rat brain neurons. Neuron *14*: 1075–1081.

Ding, Q., Xia, W., Liu, J.C., Yang, J.Y., Lee, D.F., Xia, J., et al. (2005). Erk associates with and primes GSK-3β for its inactivation resulting in upregulation of β-catenin. Mol. Cell *19*: 159–170.

Divito, C.B., Steece-Collier, K., Case, D.T., Williams, S.-P.G., Stancati, J.A., Zhi, L., et al. (2015). Loss of VGLUT3 Produces Circadian-Dependent Hyperdopaminergia and Ameliorates Motor Dysfunction and L-Dopa-Mediated Dyskinesias in a Model of Parkinson's Disease. J. Neurosci. *35*: 14983–14999.

Dominguez, J., Yu, J.T., Tan, Y.J., Ng, A., Guzman, M.F. De, Natividad, B., et al. (2021).

Novel Optineurin Frameshift Insertion in a Family With Frontotemporal Dementia and Parkinsonism Without Amyotrophic Lateral Sclerosis. Front. Neurol. *12*: 645913.

Donoso, M., Speranza, L., Kalinowska, M., Castillo, C., Sanctis, C. De, and Francesconi, A. (2020). The G protein-Coupled Metabotropic Glutamate Receptor 1 controls neuronal macroautophagy. BioRxiv Neurosci. 2020.11.02.365783.

Donzis, E.J., Estrada-Sánchez, A.M., Indersmitten, T., Oikonomou, K., Tran, C.H., Wang, C., et al. (2020). Cortical Network Dynamics Is Altered in Mouse Models of Huntington's Disease. Cereb. Cortex *30*: 2372–2388.

Doria, J., Silva, F., Souza, J. de, Vieira, L., Carvalho, T., Reis, H., et al. (2013). Metabotropic glutamate receptor 5 positive allosteric modulators are neuroprotective in a mouse model of Huntington's disease. Br. J. Pharmacol. *169*: 909–921.

Doria, J.G., Souza, J.M. de, Andrade, J.N., Rodrigues, H.A., Guimaraes, I.M., Carvalho, T.G., et al. (2015). The mGluR5 positive allosteric modulator, CDPPB, ameliorates pathology and phenotypic signs of a mouse model of Huntington's disease. Neurobiol. Dis. *73*: 163–173.

Doria, J.G., Souza, J.M. de, Silva, F.R., Olmo, I.G., Carvalho, T.G., Alves-Silva, J., et al. (2018). The mGluR5 positive allosteric modulator VU0409551 improves synaptic plasticity and memory of a mouse model of Huntington's disease. J. Neurochem. *147*: 222–239.

Dougherty, M.K., Ritt, D.A., Zhou, M., Specht, S.I., Monson, D.M., Veenstra, T.D., et al. (2009). KSR2 Is a Calcineurin Substrate that Promotes ERK Cascade Activation in Response to Calcium Signals. Mol. Cell *34*: 652–662.

Duncan, G.E., Knapp, D.J., and Breese, G.R. (1996). Neuroanatomical characterization of Fos induction in rat behavioral models of anxiety. Brain Res. *713*: 79–91.

Eichel, K., and Zastrow, M. von (2018). Subcellular Organization of GPCR Signaling. Trends Pharmacol. Sci. *39*: 200–208.

Eidelberg, D., Surmeier, D.J., and Surmeier, J. (2011). Brain networks in Huntington disease. J Clin. Investig. *121*: 484–492.

Eng, A.G., Kelver, D.A., Hedrick, T.P., and Swanson, G.T. (2016). Transduction of group I mGluR-mediated synaptic plasticity by β-arrestin2 signalling. Nat. Commun. *7*: 13571.

Estrada-Sánchez, A.M., and Rebec, G. V. (2013). Role of cerebral cortex in the neuropathology of Huntington's disease. Front. Neural Circuits *7*:.

Evans, S.J.W., Douglas, I., Rawlins, M.D., Wexler, N.S., Tabrizi, S.J., and Smeeth, L. (2013). Prevalence of adult Huntington's disease in the UK based on diagnoses recorded in general practice records. J. Neurol. Neurosurg. Psychiatry *84*: 1156–1160.

Faber, P. (1998). Huntingtin interacts with a family of WW domain proteins. Hum. Mol. Genet. *7*: 1463–1474.

Fan, M.M.Y., and Raymond, L.A. (2007). N-methyl-D-aspartate (NMDA) receptor function and excitotoxicity in Huntington's disease. Prog. Neurobiol. *81*: 272–93.

Fasano, C., Rocchetti, J., Pietrajtis, K., Zander, J.-F., Manseau, F., Sakae, D.Y., et al. (2017). Regulation of the Hippocampal Network by VGLUT3-Positive CCK- GABAergic Basket Cells. Front. Cell. Neurosci. *11*:.

Faull, R.L.M., Waldvogel, H.J., Nicholson, L.F.B., and Synek, B.J.L. (1993). Chapter 7 The distribution of GABAA-benzodiazepine receptors in the basal ganglia in Huntington's disease and in the quinolinic acid-lesioned rat. In Progress in Brain Research, pp 105–123.

Favier, M., Janickova, H., Justo, D., Kljakic, O., Runtz, L., Natsheh, J.Y., et al. (2020). Cholinergic dysfunction in the dorsal striatum promotes habit formation and maladaptive eating. J. Clin. Invest. *130*: 6616–6630.

Favier, M., Pietrancosta, N., Mestikawy, S. El, and Gangarossa, G. (2021). Leveraging VGLUT3 Functions to Untangle Brain Dysfunctions. Trends Pharmacol. Sci. *42*: 475–490.

Fazekas, C.L., Balázsfi, D., Horváth, H.R., Balogh, Z., Aliczki, M., Puhova, A., et al. (2019). Consequences of VGluT3 deficiency on learning and memory in mice. Physiol. Behav. *212*: 112688.

Feng, S., Che, C., Feng, S., Liu, C., Li, L., Li, Y., et al. (2019). Novel mutation in optineurin causing aggressive ALS+/−frontotemporal dementia. Ann. Clin. Transl. Neurol. *6*: 2377–2383.

Ferguson, S.S.G. (2001). Evolving concepts in G protein-coupled receptor endocytosis: the role in receptor desensitization and signaling. Pharmacol. Rev. *53*: 1–24.

Ferguson, S.S.G. (2007). Phosphorylation-independent attenuation of GPCR signalling. Trends Pharmacol. Sci. *28*: 173–179.

Fernández-Alfonso, T., Kwan, R., and Ryan, T.A. (2006). Synaptic Vesicles Interchange Their Membrane Proteins with a Large Surface Reservoir during Recycling. Neuron *51*: 179–186.

Ferrante, R.J., Kowall, N.W., Beal, M.F., Martin, J.B., Bird, E.D., and Richardson, E.P. (1987). Morphologic and Histochemical Characteristics of a Spared Subset of Striatal Neurons in Huntington's Disease. J. Neuropathol. Exp. Neurol. *46*: 12–27.

Ferreira, L.T., Dale, L.B., Ribeiro, F.M., Babwah, A. V., Pampillo, M., and Ferguson, S.S.G. (2009). Calcineurin Inhibitor Protein (CAIN) Attenuates Group I Metabotropic Glutamate Receptor Endocytosis and Signaling. J. Biol. Chem. *284*: 28986–28994.

Fisher, E.R., and Hayden, M.R. (2014). Multisource ascertainment of Huntington disease in Canada: Prevalence and population at risk. Mov. Disord. *29*: 105–114.

Fitzjohn, S.M., Palmer, M.J., May, J.E.R., Neeson, A., Morris, S.A.C., and Collingridge, G.L. (2001). A characterisation of long-term depression induced by metabotropic glutamate receptor activation in the rat hippocampus in vitro. J. Physiol. *537*: 421–430.

Foord, S.M., Bonner, T.I., Neubig, R.R., Rosser, E.M., Pin, J.-P., Davenport, A.P., et al. (2005). International Union of Pharmacology. XLVI. G Protein-Coupled Receptor List. Pharmacol. Rev. *57*: 279–288.

Fotuhi, M., Standaert, D.G., Testa, C.M., Penney, J.B., and Young, A.B. (1994). Differential expression of metabotropic glutamate receptors in the hippocampus and entorhinal cortex of the rat. Mol. Brain Res. *21*: 283–292.

Francesconi, A., and Duvoisin, R.M. (1998). Role of the Second and Third Intracellular Loops of Metabotropic Glutamate Receptors in Mediating Dual Signal Transduction Activation. J. Biol. Chem. *273*: 5615–5624.

Franco-Iborra, S., Plaza-Zabala, A., Montpeyo, M., Sebastian, D., Vila, M., and Martinez-Vicente, M. (2021). Mutant HTT (huntingtin) impairs mitophagy in a cellular model of Huntington disease. Autophagy *17*: 672–689.

Frantz, K.J., O'Dell, L.E., and Parsons, L.H. (2007). Behavioral and Neurochemical Responses to Cocaine in Periadolescent and Adult Rats. Neuropsychopharmacology *32*: 625–637.

Fredriksson, R., Lagerström, M.C., Lundin, L.-G., and Schiöth, H.B. (2003). The G-Protein-Coupled Receptors in the Human Genome Form Five Main Families. Phylogenetic Analysis, Paralogon Groups, and Fingerprints. Mol. Pharmacol. *63*: 1256–1272.

Fremeau, R.T., Burman, J., Qureshi, T., Tran, C.H., Proctor, J., Johnson, J., et al. (2002). The identification of vesicular glutamate transporter 3 suggests novel modes of signaling by glutamate. Proc. Natl. Acad. Sci. *99*: 14488–14493.

Fremeau, R.T., Voglmaier, S., Seal, R.P., and Edwards, R.H. (2004). VGLUTs define subsets of excitatory neurons and suggest novel roles for glutamate. Trends Neurosci. *27*: 98–103.

Fu, H., Hardy, J., and Duff, K.E. (2018). Selective vulnerability in neurodegenerative diseases. Nat. Neurosci. *21*: 1350–1358.

Furini, C.R.G., Myskiw, J.C., Schmidt, B.E., Marcondes, L.A., and Izquierdo, I. (2014). D1 and D5 dopamine receptors participate on the consolidation of two different memories. Behav. Brain Res. *271*: 212–217.

G. Vonsattel, J.P., and DiFiglia, M. (1998). Huntington Disease. J. Neuropathol. Exp. Neurol. *57*: 369–384.

Gafni, J., Hermel, E., Young, J.E., Wellington, C.L., Hayden, M.R., and Ellerby, L.M. (2004). Inhibition of Calpain Cleavage of Huntingtin Reduces Toxicity. J. Biol. Chem. *279*: 20211–20220.

Gallagher, S.M. (2004). Extracellular Signal-Regulated Protein Kinase Activation Is Required for Metabotropic Glutamate Receptor-Dependent Long-Term Depression in Hippocampal Area CA1. J. Neurosci. *24*: 4859–4864.

Gangarossa, G., Guzman, M., Prado, V.F., Prado, M.A.M., Daumas, S., Mestikawy, S.

El, et al. (2016). Role of the atypical vesicular glutamate transporter VGLUT3 in l-DOPA-induced dyskinesia. Neurobiol. Dis. *87*: 69–79.

Ganley, I.G., Lam, D.H., Wang, J., Ding, X., Chen, S., and Jiang, X. (2009). ULK1·ATG13·FIP200 Complex Mediates mTOR Signaling and Is Essential for Autophagy. J. Biol. Chem. *284*: 12297–12305.

Gao, J., Ohtsubo, M., Hotta, Y., and Minoshima, S. (2014). Oligomerization of optineurin and its oxidative stress- or E50K mutation-driven covalent cross-linking: possible relationship with glaucoma pathology. PLoS One *9*: e101206.

Garrett, M.C., and Soares-da-Silva, P. (1992). Increased Cerebrospinal Fluid Dopamine and 3,4-Dihydroxyphenylacetic Acid Levels in Huntington's Disease: Evidence for an Overactive Dopaminergic Brain Transmission. J. Neurochem. *58*: 101–106.

Gerber, U., Gee, C., and Benquet, P. (2007). Metabotropic glutamate receptors: intracellular signaling pathways. Curr. Opin. Pharmacol. *7*: 56–61.

Ginovart, N. (1997). PET study of the pre- and post-synaptic dopaminergic markers for the neurodegenerative process in Huntington's disease. Brain *120*: 503–514.

Giralt, A., Carretón, O., Lao-Peregrin, C., Martín, E.D., and Alberch, J. (2011a). Conditional BDNF release under pathological conditions improves Huntington's disease pathology by delaying neuronal dysfunction. Mol. Neurodegener. *6*: 71.

Giralt, A., Saavedra, A., Alberch, J., and Pérez-Navarro, E. (2012). Cognitive Dysfunction in Huntington's Disease: Humans, Mouse Models and Molecular Mechanisms. J. Huntingtons. Dis. *1*: 155–173.

Giralt, A., Saavedra, A., Carretón, O., Xifró, X., Alberch, J., and Pérez-Navarro, E. (2011b). Increased PKA signaling disrupts recognition memory and spatial memory: role in Huntington's disease. Hum. Mol. Genet. *20*: 4232–4247.

Gonzales, K.K., and Smith, Y. (2015). Cholinergic interneurons in the dorsal and ventral striatum: Anatomical and functional considerations in normal and diseased conditions. Ann. N. Y. Acad. Sci. *1349*: 1–45.

Goodliffe, J.W., Song, H., Rubakovic, A., Chang, W., Medalla, M., Weaver, C.M., et al. (2018). Differential changes to D1 and D2 medium spiny neurons in the 12-month-old Q175+/- mouse model of Huntington's Disease. PLoS One *13*: e0200626.

Gras, C., Amilhon, B., Lepicard, È.M., Poirel, O., Vinatier, J., Herbin, M., et al. (2008). The vesicular glutamate transporter VGLUT3 synergizes striatal acetylcholine tone. Nat. Neurosci. *11*: 292–300.

Gras, C., Herzog, E., Bellenchi, G.C., Bernard, V.R.V., Ravassard, P., Pohl, M., et al. (2002). A third vesicular glutamate transporter expressed by cholinergic and serotoninergic neurons. J. Neurosci. *22*: 5442–51.

Gras, C., Vinatier, J., Amilhon, B., Guerci, A., Christov, C., Ravassard, P., et al. (2005). Developmentally regulated expression of VGLUT3 during early post-natal life. Neuropharmacology *49*: 901–911.

Graveland, G.A., Williams, R.S., and Difiglia, M. (1985). Evidence for degenerative and regenerative changes in neostriatal spiny neurons in Huntington's disease. Science *227*: 770–773.

Gray, L., Buuse, M. Van Den, Scarr, E., Dean, B., and Hannan, A.J. (2009). Clozapine reverses schizophrenia-related behaviours in the metabotropic glutamate receptor 5 knockout mouse: Association with N-methyl-d-aspartic acid receptor up-regulation. Int. J. Neuropsychopharmacol. *12*: 45–60.

Gray, M., Shirasaki, D.I., Cepeda, C., Andre, V.M., Wilburn, B., Lu, X.-H., et al. (2008). Full-Length Human Mutant Huntingtin with a Stable Polyglutamine Repeat Can Elicit Progressive and Selective Neuropathogenesis in BACHD Mice. J. Neurosci. *28*: 6182–6195.

Graybiel, A.M., Aosaki, T., Flaherty, A.W., and Kimura, M. (1994). The Basal Ganglia and Adaptive Motor Control. Science *265*: 1826–1831.

Groc, L., Heine, M., Cousins, S.L., Stephenson, F.A., Lounis, B., Cognet, L., et al. (2006). NMDA receptor surface mobility depends on NR2A-2B subunits. Proc. Natl. Acad. Sci. *103*: 18769–18774.

Grosso Jasutkar, H., and Yamamoto, A. (2021). Do Changes in Synaptic Autophagy Underlie the Cognitive Impairments in Huntington's Disease? J. Huntingtons. Dis. *10*: 227–238.

Guhan, N., and Lu, B. (2004). Homer–PIKE complex: a novel link between mGluRI and PI 3-kinase. Trends Neurosci. *27*: 645–648.

Guimaraes, I.M., Carvalho, T.G., Ferguson, S.S., Pereira, G.S., and Ribeiro, F.M. (2015). The metabotropic glutamate receptor 5 role on motor behavior involves specific neural substrates. Mol. Brain *8*: 24.

Guo, F., Liu, X., Cai, H., and Le, W. (2018). Autophagy in neurodegenerative diseases: pathogenesis and therapy. Brain Pathol. *28*: 3–13.

Gupta, I., and Young, A.M.J. (2018). Metabotropic glutamate receptor modulation of dopamine release in the nucleus accumbens shell is unaffected by phencyclidine pretreatment: In vitro assessment using fast-scan cyclic voltammetry rat brain slices. Brain Res. *1687*: 155–161.

Haber, S.N. (2014). The place of dopamine in the cortico-basal ganglia circuit. Neuroscience *282*: 248–257.

Hadzic, M., Jack, A., and Wahle, P. (2017). Ionotropic glutamate receptors: Which ones, when, and where in the mammalian neocortex. J. Comp. Neurol. *525*: 976–1033.

Hale, M.W., Hay-Schmidt, A., Mikkelsen, J.D., Poulsen, B., Shekhar, A., and Lowry, C.A. (2008). Exposure to an open-field arena increases c-Fos expression in a distributed anxiety-related system projecting to the basolateral amygdaloid complex. Neuroscience *155*: 659–672.

Hamilton, A., Vasefi, M., Tuin, C. Vander, McQuaid, R.J., Anisman, H., and Ferguson,

S.S.G. (2016). Chronic Pharmacological mGluR5 Inhibition Prevents Cognitive Impairment and Reduces Pathogenesis in an Alzheimer Disease Mouse Model. Cell Rep. *15*: 1859–1865.

Han, I., You, Y., Kordower, J.H., Brady, S.T., and Morfini, G.A. (2010). Differential vulnerability of neurons in Huntington's disease: the role of cell type-specific features. J. Neurochem. *113*: 1073–91.

Hantraye, P., Riche, D., Maziere, M., and Isacson, O. (1990). A primate model of Huntington's disease: behavioral and anatomical studies of unilateral excitotoxic lesions of the caudate-putamen in the baboon. Exp. Neurol. *108*: 91–104.

Hao, Y., Martin-Fardon, R., and Weiss, F. (2010). Behavioral and Functional Evidence of Metabotropic Glutamate Receptor 2/3 and Metabotropic Glutamate Receptor 5 Dysregulation in Cocaine-Escalated Rats: Factor in the Transition to Dependence. Biol. Psychiatry *68*: 240–248.

Harjes, P., and Wanker, E.E. (2003). The hunt for huntingtin function: Interaction partners tell many different stories. Trends Biochem. Sci. *28*: 425–433.

Harvey, J., and Collingridge, G.L. (1993). Signal transduction pathways involved in the acute potentiation of NMDA responses by 1S,3R-ACPD in rat hippocampal slices. Br. J. Pharmacol. *109*: 1085.

Hattula, K., and Peränen, J. (2000). FIP-2, a coiled-coil protein, links Huntingtin to Rab8 and modulates, cellular morphogenesis. Curr. Biol. *10*: 1603–1606.

Hauser, A.S., Attwood, M.M., Rask-Andersen, M., Schiöth, H.B., and Gloriam, D.E. (2017). Trends in GPCR drug discovery: new agents, targets and indications. Nat. Rev. Drug Discov. *16*: 829–842.

Heikkinen, T., Lehtimäki, K., Vartiainen, N., Puoliväli, J., Hendricks, S.J., Glaser, J.R., et al. (2012). Characterization of Neurophysiological and Behavioral Changes, MRI Brain Volumetry and 1H MRS in zQ175 Knock-In Mouse Model of Huntington's Disease. PLoS One *7*: e50717.

Heimer, L., Hoesen, G.W. Van, Trimble, M., and Zahm, D.S. (2008). THE ANATOMY OF THE BASAL FOREBRAIN. In Anatomy of Neuropsychiatry, (Elsevier), pp 27–67.

Henley, J.M., and Wilkinson, K.A. (2016). Synaptic AMPA receptor composition in development, plasticity and disease. Nat. Rev. Neurosci. *17*: 337–350.

Hentosh, S., Zhu, L., Patino, J., Furr, J.W., Rocha, N.P., and Furr Stimming, E. (2021). Sex Differences in Huntington's Disease: Evaluating the <scp>Enroll-HD</scp> Database. Mov. Disord. Clin. Pract. *8*: 420–426.

Heras-Sandoval, D., Pérez-Rojas, J.M., Hernández-Damián, J., and Pedraza-Chaverri, J. (2014). The role of PI3K/AKT/mTOR pathway in the modulation of autophagy and the clearance of protein aggregates in neurodegeneration. Cell. Signal. *26*: 2694–2701.

Hermans, E., and Challiss, R.A.A.J. (2001). Structural, signalling and regulatory properties of the group I metabotropic glutamate receptors: prototypic family C G-

protein-coupled receptors. Biochem. J. *359*: 465.

Herzog, E., Gilchrist, J., Gras, C., Muzerelle, A., Ravassard, P., Giros, B., et al. (2004). Localization of VGLUT3, the vesicular glutamate transporter type 3, in the rat brain. Neuroscience *123*: 983–1002.

Herzog, E., Takamori, S., Jahn, R., Brose, N., and Wojcik, S.M. (2006). Synaptic and vesicular co-localization of the glutamate transporters VGLUT1 and VGLUT2 in the mouse hippocampus. J. Neurochem. *99*: 1011–1018.

Hetman, M., Hsuan, S.-L., Habas, A., Higgins, M.J., and Xia, Z. (2002). ERK1/2 Antagonizes Glycogen Synthase Kinase-3β-induced Apoptosis in Cortical Neurons. J. Biol. Chem. *277*: 49577–49584.

Hickey, M.A., Kosmalska, A., Enayati, J., Cohen, R., Zeitlin, S., Levine, M.S., et al. (2008). Extensive early motor and non-motor behavioral deficits are followed by striatal neuronal loss in knock-in Huntington's disease mice. Neuroscience *157*: 280–95.

Higley, M.J., Gittis, A.H., Oldenburg, I.A., Balthasar, N., Seal, R.P., Edwards, R.H., et al. (2011). Cholinergic Interneurons Mediate Fast VGluT3-Dependent Glutamatergic Transmission in the Striatum. PLoS One *6*: e19155.

Hilger, D., Masureel, M., and Kobilka, B.K. (2018). Structure and dynamics of GPCR signaling complexes. Nat. Struct. Mol. Biol.

Hintiryan, H., Foster, N.N., Bowman, I., Bay, M., Song, M.Y., Gou, L., et al. (2016). The mouse cortico-striatal projectome. Nat. Neurosci. *19*: 1100–1114.

Hioki, H., Fujiyama, F., Nakamura, K., Wu, S.X., Matsuda, W., and Kaneko, T. (2004). Chemically specific circuit composed of vesicular glutamate transporter 3- and preprotachykinin B-producing interneurons in the rat neocortex. Cereb. Cortex *14*: 1266–1275.

Hioki, H., Nakamura, H., Ma, Y.-F., Konno, M., Hayakawa, T., Nakamura, K.C., et al. (2010). Vesicular glutamate transporter 3-expressing nonserotonergic projection neurons constitute a subregion in the rat midbrain raphe nuclei. J. Comp. Neurol. *518*: 668–686.

Hodgson, J.G., Agopyan, N., Gutekunst, C.-A., Leavitt, B.R., LePiane, F., Singaraja, R., et al. (1999). A YAC Mouse Model for Huntington's Disease with Full-Length Mutant Huntingtin, Cytoplasmic Toxicity, and Selective Striatal Neurodegeneration. Neuron *23*: 181–192.

Hoeffer, C.A., and Klann, E. (2010). mTOR signaling: at the crossroads of plasticity, memory and disease. Trends Neurosci. *33*: 67–75.

Hoffner, G., Kahlem, P., and Djian, P. (2002). Perinuclear localization of huntingtin as a consequence of its binding to microtubules through an interaction with β-tubulin: relevance to Huntington's disease. J. Cell Sci. *115*: 941–948.

Homayoun, H., Stefani, M.R., Adams, B.W., Tamagan, G.D., and Moghaddam, B. (2004). Functional Interaction Between NMDA and mGlu5 Receptors: Effects on

Working Memory, Instrumental Learning, Motor Behaviors, and Dopamine Release. Neuropsychopharmacology *29*: 1259–1269.

Horváth, H.R., Fazekas, C.L., Balázsfi, D., Jain, S.K., Haller, J., and Zelena, D. (2018). Contribution of Vesicular Glutamate Transporters to Stress Response and Related Psychopathologies: Studies in VGluT3 Knockout Mice. Cell. Mol. Neurobiol. *38*: 37–52.

Hou, L., and Klann, E. (2004). Activation of the phosphoinositide 3-kinase-Akt-mammalian target of rapamycin signaling pathway is required for metabotropic glutamate receptor-dependent long-term depression. J. Neurosci. *24*: 6352–6361.

Hsu, Y.-T., Chang, Y.-G., and Chern, Y. (2018). Insights into GABA A ergic system alteration in Huntington's disease. Open Biol. *8*: 180165.

Hua, Y., Sinha, R., Thiel, C.S., Schmidt, R., Hüve, J., Martens, H., et al. (2011). A readily retrievable pool of synaptic vesicles. Nat. Neurosci. *14*: 833–839.

Huang, Y.-Y., Simpson, E., Kellendonk, C., and Kandel, E.R. (2004). Genetic evidence for the bidirectional modulation of synaptic plasticity in the prefrontal cortex by D1 receptors. Proc. Natl. Acad. Sci. *101*: 3236–3241.

Hughes, A.C., Mort, M., Elliston, L., Thomas, R.M., Brooks, S.P., Dunnett, S.B., et al. (2014). Identification of novel alternative splicing events in the huntingtin gene and assessment of the functional consequences using structural protein homology modelling. J. Mol. Biol. *426*: 1428–38.

Husi, H., Ward, M.A., Choudhary, J.S., Blackstock, W.P., and Grant, S.G.N. (2000). Proteomic analysis of NMDA receptor–adhesion protein signaling complexes. Nat. Neurosci. *3*: 661–669.

Ibrahim, K.S., Abd-Elrahman, K.S., Mestikawy, S. El, and Ferguson, S.S.G. (2020). Targeting Vesicular Glutamate Transporter Machinery: Implications on Metabotropic Glutamate Receptor 5 Signaling and Behavior. Mol. Pharmacol. *98*: 314–327.

Ibrahim, K.S., McLaren, C.J., Abd-Elrahman, K.S., and Ferguson, S.S.G. (2021). Optineurin deletion disrupts metabotropic glutamate receptor 5-mediated regulation of ERK1/2, GSK3β/ZBTB16, mTOR/ULK1 signaling in autophagy. Biochem. Pharmacol. *185*: 114427.

Ibrahim, K.S., Mestikawy, S. El, Abd-Elrahman, K.S., and Ferguson, S.S.G. (2022). VGLUT3 Ablation Differentially Modulates Glutamate Receptor Densities in Mouse Brain. ENeuro *9*: ENEURO.0041-22.2022.

Ikemoto, A., Bole, D.G., and Ueda, T. (2003). Glycolysis and glutamate accumulation into synaptic vesicles. Role of glyceraldehyde phosphate dehydrogenase and 3-phosphoglycerate kinase. J. Biol. Chem. *278*: 5929–5940.

Imai, Y., Ibata, I., Ito, D., Ohsawa, K., and Kohsaka, S. (1996). A Novel Geneiba1in the Major Histocompatibility Complex Class III Region Encoding an EF Hand Protein Expressed in a Monocytic Lineage. Biochem. Biophys. Res. Commun. *224*: 855–862.

Ishida, A., Noda, Y., and Ueda, T. (2009). Synaptic Vesicle-bound Pyruvate Kinase can

Support Vesicular Glutamate Uptake. Neurochem. Res. *34*: 807–818.

Jacobs, M., Hart, E.P., Zwet, E.W. van, Bentivoglio, A.R., Burgunder, J.M., Craufurd, D., et al. (2016). Progression of motor subtypes in Huntington's disease: a 6-year follow-up study. J. Neurol. *263*: 2080–5.

Jew, C.P., Wu, C.-S., Sun, H., Zhu, J., Huang, J.-Y., Yu, D., et al. (2013). mGluR5 Ablation in Cortical Glutamatergic Neurons Increases Novelty-Induced Locomotion. PLoS One *8*: e70415.

Joffe, M.E., Santiago, C.I., Oliver, K.H., Maksymetz, J., Harris, N.A., Engers, J.L., et al. (2020). mGlu2 and mGlu3 Negative Allosteric Modulators Divergently Enhance Thalamocortical Transmission and Exert Rapid Antidepressant-like Effects. Neuron *105*: 46-59.e3.

Joffe, M.E., Santiago, C.I., Vermudez, S.A.D., Fisher, N.M., Dogra, S., Niswender, C.M., et al. (2021). Frontal cortex genetic ablation of metabotropic glutamate receptor subtype 3 (mGlu3) impairs postsynaptic plasticity and modulates affective behaviors. Neuropsychopharmacology *46*: 2148–2157.

Johnson, K.A., and Conn, P.J. (2019). Positive allosteric modulation of metabotropic glutamate receptor 5 modulates Akt and GSK3β signaling in vivo. BioRxiv.

Joly, C., Gomeza, J., Brabet, I., Curry, K., Bockaert, J., and Pin, J. (1995). Molecular, functional, and pharmacological characterization of the metabotropic glutamate receptor type 5 splice variants: comparison with mGluR1. J. Neurosci. *15*: 3970–3981.

Jong, Y.J.I., Kumar, V., Kingston, A.E., Romano, C., and O'Malley, K.L. (2005). Functional Metabotropic Glutamate Receptors on Nuclei from Brain and Primary Cultured Striatal Neurons: ROLE OF TRANSPORTERS IN DELIVERING LIGAND. J. Biol. Chem. *280*: 30469–30480.

Jong, Y.J.I., Kumar, V., and O'Malley, K.L. (2009). Intracellular metabotropic glutamate receptor 5 (mGluR5) activates signaling cascades distinct from cell surface counterparts. J. Biol. Chem. *284*: 35827–35838.

Julien, C.L., Thompson, J.C., Wild, S., Yardumian, P., Snowden, J.S., Turner, G., et al. (2007). Psychiatric disorders in preclinical Huntington's disease. J. Neurol. Neurosurg. Psychiatry *78*: 939–943.

Jung, C.H., Ro, S.-H., Cao, J., Otto, N.M., and Kim, D.-H. (2010). mTOR regulation of autophagy. FEBS Lett. *584*: 1287–1295.

Kachaner, D., Génin, P., Laplantine, E., and Weil, R. (2012). Toward an integrative view of Optineurin functions. Cell Cycle *11*: 2808–2818.

Kadamur, G., and Ross, E.M. (2013). Mammalian Phospholipase C. Annu. Rev. Physiol. *75*: 127–154.

Kallergi, E., Daskalaki, A.-D., Kolaxi, A., Camus, C., Ioannou, E., Mercaldo, V., et al. (2022). Dendritic autophagy degrades postsynaptic proteins and is required for long-term synaptic depression in mice. Nat. Commun. *13*: 680.

Kane, L.A., Lazarou, M., Fogel, A.I., Li, Y., Yamano, K., Sarraf, S.A., et al. (2014). PINK1 phosphorylates ubiquitin to activate Parkin E3 ubiquitin ligase activity. J. Cell Biol. *205*: 143–53.

Kaneko, T., and Fujiyama, F. (2002). Complementary distribution of vesicular glutamate transporters in the central nervous system. Neurosci. Res. *42*: 243–250.

Kar, K., Jayaraman, M., Sahoo, B., Kodali, R., and Wetzel, R. (2011). Critical nucleus size for disease-related polyglutamine aggregation is repeat-length dependent. Nat. Struct. Mol. Biol. 2011 183 *18*: 328–336.

Katoh, H., Aoki, J., Yamaguchi, Y., Kitano, Y., Ichikawa, A., and Negishi, M. (1998). Constitutively Active Gα12, Gα13, and Gαq Induce Rho-dependent Neurite Retraction through Different Signaling Pathways. J. Biol. Chem. *273*: 28700–28707.

Katritch, V., Cherezov, V., and Stevens, R.C. (2013). Structure-Function of the G Protein–Coupled Receptor Superfamily. Annu. Rev. Pharmacol. Toxicol. *53*: 531–556.

Kenny, P.J., and Markou, A. (2004). The ups and downs of addiction: role of metabotropic glutamate receptors. Trends Pharmacol. Sci. *25*: 265–272.

Khoshnan, A. (2004). Activation of the I B Kinase Complex and Nuclear Factor- B Contributes to Mutant Huntingtin Neurotoxicity. J. Neurosci. *24*: 7999–8008.

Kim, J., Kundu, M., Viollet, B., and Guan, K.-L. (2011). AMPK and mTOR regulate autophagy through direct phosphorylation of Ulk1. Nat. Cell Biol. *13*: 132–141.

Kim, M., Lee, H.-S., LaForet, G., McIntyre, C., Martin, E.J., Chang, P., et al. (1999). Mutant Huntingtin Expression in Clonal Striatal Cells: Dissociation of Inclusion Formation and Neuronal Survival by Caspase Inhibition. J. Neurosci. *19*: 964–973.

Kish, S.J., Shannak, K., and Hornykiewicz, O. (1987). Elevated serotonin and reduced dopamine in subregionally divided Huntington's disease striatum. Ann. Neurol. *22*: 386–389.

Kljakic, O., Hogan-Cann, A.E., Yang, H., Dover, B., Al-Onaizi, M., Prado, M.A.M., et al. (2022). Chemogenetic activation of VGLUT3-expressing neurons decreases movement. Eur. J. Pharmacol. 175298.

Kljakic, O., Janickova, H., Prado, V.F., and Prado, M.A.M. (2017). Cholinergic/glutamatergic co-transmission in striatal cholinergic interneurons: new mechanisms regulating striatal computation. J. Neurochem. *142*: 90–102.

Kniazeff, J., Prézeau, L., Rondard, P., Pin, J.-P., and Goudet, C. (2011). Dimers and beyond: The functional puzzles of class C GPCRs. Pharmacol. Ther. *130*: 9–25.

Kolakowski, L.F. (1994). GCRDb: a G-protein-coupled receptor database. Receptors Channels *2*: 1–7.

Kolodziejczyk, K., Parsons, M.P., Southwell, A.L., Hayden, M.R., and Raymond, L.A. (2014). Striatal Synaptic Dysfunction and Hippocampal Plasticity Deficits in the Hu97/18 Mouse Model of Huntington Disease. PLoS One *9*: e94562.

Korac, J., Schaeffer, V., Kovacevic, I., Clement, A.M., Jungblut, B., Behl, C., et al. (2013). Ubiquitin-independent function of optineurin in autophagic clearance of protein aggregates. J. Cell Sci. *126*: 580–592.

Krishnankutty, A., Kimura, T., Saito, T., Aoyagi, K., Asada, A., Takahashi, S.-I., et al. (2017). In vivo regulation of glycogen synthase kinase 3β activity in neurons and brains. Sci. Rep. *7*: 8602.

Labbadia, J., and Morimoto, R.I. (2013). Huntington's disease: underlying molecular mechanisms and emerging concepts. Trends Biochem. Sci. *38*: 378–85.

Landles, C., Sathasivam, K., Weiss, A., Woodman, B., Moffitt, H., Finkbeiner, S., et al. (2010). Proteolysis of Mutant Huntingtin Produces an Exon 1 Fragment That Accumulates as an Aggregated Protein in Neuronal Nuclei in Huntington Disease*. J. Biol. Chem. *285*: 8808–8823.

Lazarou, M. (2015). Keeping the immune system in check: a role for mitophagy. Immunol. Cell Biol. *93*: 3–10.

Lazarou, M., Sliter, D.A., Kane, L.A., Sarraf, S.A., Wang, C., Burman, J.L., et al. (2015). The ubiquitin kinase PINK1 recruits autophagy receptors to induce mitophagy. Nature *524*: 309–314.

Lee, J.H., Tecedor, L., Chen, Y.H., Monteys, A.M., Sowada, M.J., Thompson, L.M., et al. (2015). Reinstating Aberrant mTORC1 Activity in Huntington's Disease Mice Improves Disease Phenotypes. Neuron *85*: 303–315.

Lee, W., Reyes, R.C., Gottipati, M.K., Lewis, K., Lesort, M., Parpura, V., et al. (2013). Enhanced Ca2+-dependent glutamate release from astrocytes of the BACHD Huntington's disease mouse model. Neurobiol. Dis. *58*: 192–199.

Lefkowitz, R.J., and Shenoy, S.K. (2005). Transduction of Receptor Signals by ß-Arrestins. Science *308*: 512–517.

Legleiter, J., Mitchell, E., Lotz, G.P., Sapp, E., Ng, C., DiFiglia, M., et al. (2010). Mutant huntingtin fragments form oligomers in a polyglutamine length-dependent manner in Vitro and in Vivo. J. Biol. Chem. *285*: 14777–14790.

Levey, A.I., Kitt, C.A., Simonds, W.F., Price, D.L., and Brann, M.R. (1991). Identification and localization of muscarinic acetylcholine receptor proteins in brain with subtype-specific antibodies. J. Neurosci. *11*: 3218–26.

Lewerenz, J., and Maher, P. (2015). Chronic glutamate toxicity in neurodegenerative diseases-What is the evidence? Front. Neurosci. *9*: 469.

Li, D., Hérault, K., Silm, K., Evrard, A., Wojcik, S., Oheim, M., et al. (2013). Lack of evidence for vesicular glutamate transporter expression in mouse astrocytes. J. Neurosci. *33*: 4434–4455.

Li, J., Ning, Y., Hedley, W., Saunders, B., Chen, Y., Tindill, N., et al. (2002). The molecule pages database. Nature.

Li, S.-H., and Li, X.-J. (2004). Huntingtin–protein interactions and the pathogenesis of Huntington's disease. Trends Genet. *20*: 146–154.

Li, S.H., Colson, T.-L.L., Abd-Elrahman, K.S., and Ferguson, S.S.G. (2021). Metabotropic Glutamate Receptor 2/3 Activation Improves Motor Performance and Reduces Pathology in Heterozygous zQ175 Huntington Disease Mice. J. Pharmacol. Exp. Ther. *379*: 74–84.

Li, S.H., Colson, T.-L.L., Abd-Elrahman, K.S., and Ferguson, S.S.G. (2022). Metabotropic Glutamate Receptor 5 Antagonism Reduces Pathology and Differentially Improves Symptoms in Male and Female Heterozygous zQ175 Huntington's Mice. Front. Mol. Neurosci. *15*:.

Li, Y., Kang, J., and Horwitz, M.S. (1998). Interaction of an Adenovirus E3 14.7-Kilodalton Protein with a Novel Tumor Necrosis Factor Alpha-Inducible Cellular Protein Containing Leucine Zipper Domains. Mol. Cell. Biol. *18*: 1601–1610.

Lim, S.A.O., Kang, U.J., and McGehee, D.S. (2014). Striatal cholinergic interneuron regulation and circuit effects. Front. Synaptic Neurosci. *6*: 1–23.

Lim, S.A.O., and Surmeier, D.J. (2021). Enhanced GABAergic Inhibition of Cholinergic Interneurons in the zQ175+/− Mouse Model of Huntington's Disease. Front. Syst. Neurosci. *14*:.

Lin, C.H., Tallaksen-Greene, S., Chien, W.M., Cearley, J.A., Jackson, W.S., Crouse, A.B., et al. (2001). Neurological abnormalities in a knock-in mouse model of Huntington's disease. Hum. Mol. Genet. *10*: 137–44.

Liu, F., Gong, X., Zhang, G., Marquis, K., Reinhart, P., and Andree, T.H. (2005). The inhibition of glycogen synthase kinase 3β by a metabotropic glutamate receptor 5 mediated pathway confers neuroprotection to Aβ peptides. J. Neurochem. *95*: 1363–1372.

Liu, F., Grauer, S., Kelley, C., Navarra, R., Graf, R., Zhang, G., et al. (2008). ADX47273 [S -(4-Fluoro-phenyl)-{3-[3-(4-fluoro-phenyl)-[1,2,4]-oxadiazol-5-yl]-piperidin-1-yl}-methanone]: A Novel Metabotropic Glutamate Receptor 5-Selective Positive Allosteric Modulator with Preclinical Antipsychotic-Like and Procognitive Activities. J. Pharmacol. Exp. Ther. *327*: 827–839.

Liu, Z., Chen, P., Gao, H., Gu, Y., Yang, J., Peng, H., et al. (2014). Ubiquitylation of Autophagy Receptor Optineurin by HACE1 Activates Selective Autophagy for Tumor Suppression. Cancer Cell *26*: 106–120.

López, A.J., Johnson, A.R., Euston, T.J., Wilson, R., Nolan, S.O., Brady, L.J., et al. (2021). Cocaine self-administration induces sex-dependent protein expression in the nucleus accumbens. Commun. Biol. *4*: 883.

Lu, Z., and Xu, S. (2006). ERK1/2 MAP kinases in cell survival and apoptosis. IUBMB Life (International Union Biochem. Mol. Biol. Life) *58*: 621–631.

Luján, R., Nusser, Z., Roberts, J.D.B., Shigemoto, R., and Somogyi, P. (1996). Perisynaptic location of metabotropic glutamate receptors mGluR1 and mGluR5 on

dendrites and dendritic spines in the rat hippocampus. Eur. J. Neurosci. *8*: 1488–1500.

Lunkes, A., Lindenberg, K.S., Ben-Haïem, L., Weber, C., Devys, D., Landwehrmeyer, G.B., et al. (2002). Proteases Acting on Mutant Huntingtin Generate Cleaved Products that Differentially Build Up Cytoplasmic and Nuclear Inclusions. Mol. Cell *10*: 259–269.

Lüscher, C., and Huber, K.M. (2010). Group 1 mGluR-Dependent Synaptic Long-Term Depression: Mechanisms and Implications for Circuitry and Disease. Neuron *65*: 445–459.

Luttrell, L.M. (2008). Reviews in Molecular Biology and Biotechnology: Transmembrane Signaling by G Protein-Coupled Receptors. Mol. Biotechnol. *39*: 239–264.

Luttrell, L.M., Ferguson, S.S.G., Daaka, Y., Miller, W.E., Maudsley, S., Rocca, G.J. Della, et al. (1999). β-Arrestin-Dependent Formation of β 2 Adrenergic Receptor-Src Protein Kinase Complexes. Science *283*: 655–661.

Luttrell, L.M., and Lefkowitz, R.J. (2002). The role of beta-arrestins in the termination and transduction of G-protein-coupled receptor signals. J. Cell Sci. *115*: 455–465.

MacDonald, M.E., Ambrose, C.M., Duyao, M.P., Myers, R.H., Lin, C., Srinidhi, L., et al. (1993). A novel gene containing a trinucleotide repeat that is expanded and unstable on Huntington's disease chromosomes. Cell *72*: 971–983.

Magalhaes, A.C., Dunn, H., and Ferguson, S.S.G. (2012). Regulation of GPCR activity, trafficking and localization by GPCR-interacting proteins. Br. J. Pharmacol. *165*: 1717–1736.

Manahan-Vaughan, D. (1997). Group 1 and 2 metabotropic glutamate receptors play differential roles in hippocampal long-term depression and long-term potentiation in freely moving rats. J. Neurosci. *17*: 3303–3311.

Mangiarini, L., Sathasivam, K., Seller, M., Cozens, B., Harper, A., Hetherington, C., et al. (1996). Exon 1 of the HD Gene with an Expanded CAG Repeat Is Sufficient to Cause a Progressive Neurological Phenotype in Transgenic Mice. Cell *87*: 493–506.

Mansouri-Guilani, N., Bernard, V., Vigneault, E., Vialou, V., Daumas, S., Mestikawy, S. El, et al. (2019). VGLUT3 gates psychomotor effects induced by amphetamine. J. Neurochem. *148*: 779–795.

Manyam, B. V., Giacobini, E., and Colliver, J.A. (1990). Cerebrospinal fluid acetylcholinesterase and choline measurements in Huntington's disease. J. Neurol. *237*: 281–284.

Mao, L., Yang, L., Tang, Q., Samdani, S., Zhang, G., and Wang, J.Q. (2005). The Scaffold Protein Homer1b/c Links Metabotropic Glutamate Receptor 5 to Extracellular Signal-Regulated Protein Kinase Cascades in Neurons. J. Neurosci. *25*: 2741–2752.

Marco, N. De, Buono, M., Troise, F., and Diez-Roux, G. (2006). Optineurin Increases Cell Survival and Translocates to the Nucleus in a Rab8-dependent Manner upon an Apoptotic Stimulus. J. Biol. Chem. *281*: 16147–16156.

Marcus-Sells, M. (2016). Role of VGLUT3 in synaptic plasticity and memory along the septotemporal axis of the hippocampus. McGill University.

Markovinovic, A., Ljutic, T., Béland, L.-C., and Munitic, I. (2018). Optineurin Insufficiency Disbalances Proinflammatory and Anti-inflammatory Factors by Reducing Microglial IFN-β Responses. Neuroscience *388*: 139–151.

Martinez-Vicente, M., Talloczy, Z., Wong, E., Tang, G., Koga, H., Kaushik, S., et al. (2010). Cargo recognition failure is responsible for inefficient autophagy in Huntington's disease. Nat. Neurosci. *13*: 567–576.

Matsumoto, G., Wada, K., Okuno, M., Kurosawa, M., and Nukina, N. (2011). Serine 403 phosphorylation of p62/SQSTM1 regulates selective autophagic clearance of ubiquitinated proteins. Mol. Cell *44*: 279–289.

Matta, J.A., Ashby, M.C., Sanz-Clemente, A., Roche, K.W., and Isaac, J.T.R. (2011). mGluR5 and NMDA Receptors Drive the Experience- and Activity-Dependent NMDA Receptor NR2B to NR2A Subunit Switch. Neuron *70*: 339–351.

McGeer, E.G., and McGeer, P.L. (1976). Duplication of biochemical changes of Huntington's chorea by intrastriatal injections of glutamic and kainic acids. Nature *263*: 517–9.

McKinstry, S.U., Karadeniz, Y.B., Worthington, A.K., Hayrapetyan, V.Y., Ozlu, M.I., Serafin-Molina, K., et al. (2014). Huntingtin Is Required for Normal Excitatory Synapse Development in Cortical and Striatal Circuits. J. Neurosci. *34*: 9455–9472.

Meessen, H., and Olszewski, J. (1950). A cytoarchitectonic atlas of the rhombencephalon of the rabbit. Brain *73*: 544–544.

Menalled, L., El-Khodor, B.F., Patry, M., Suárez-Fariñas, M., Orenstein, S.J., Zahasky, B., et al. (2009). Systematic behavioral evaluation of Huntington's disease transgenic and knock-in mouse models. Neurobiol. Dis. *35*: 319–336.

Menalled, L.B., Kudwa, A.E., Miller, S., Fitzpatrick, J., Watson-Johnson, J., Keating, N., et al. (2012). Comprehensive Behavioral and Molecular Characterization of a New Knock-In Mouse Model of Huntington's Disease: ZQ175. PLoS One *7*: e49838.

Menalled, L.B., Sison, J.D., Dragatsis, I., Zeitlin, S., and Chesselet, M.-F. (2003). Time course of early motor and neuropathological anomalies in a knock-in mouse model of Huntington's disease with 140 CAG repeats. J. Comp. Neurol. *465*: 11–26.

Mendoza, M.C., Er, E.E., and Blenis, J. (2011). The Ras-ERK and PI3K-mTOR Pathways: Cross-talk and Compensation. Trends Biochem. Sci. *36*: 320.

Mestikawy, S. El, Wallén-Mackenzie, Å., Fortin, G.M., Descarries, L., and Trudeau, L.-E. (2011). From glutamate co-release to vesicular synergy: vesicular glutamate transporters. Nat. Rev. Neurosci. *12*: 204–216.

Metz, G.A., and Whishaw, I.Q. (2002). Cortical and subcortical lesions impair skilled walking in the ladder rung walking test: a new task to evaluate fore- and hindlimb stepping, placing, and co-ordination. J. Neurosci. Methods *115*: 169–179.

Metzger, S., Saukko, M., Che, H. Van, Tong, L., Puder, Y., Riess, O., et al. (2010). Age at onset in Huntington's disease is modified by the autophagy pathway: implication of the V471A polymorphism in Atg7. Hum. Genet. *128*: 453–459.

Miller, J., Arrasate, M., Brooks, E., Libeu, C.P., Legleiter, J., Hatters, D., et al. (2011). Identifying polyglutamine protein species in situ that best predict neurodegeneration. Nat. Chem. Biol. *7*: 925–934.

Milnerwood, A.J., Cummings, D.M., Dallérac, G.M., Brown, J.Y., Vatsavayai, S.C., Hirst, M.C., et al. (2006). Early development of aberrant synaptic plasticity in a mouse model of Huntington's disease. Hum. Mol. Genet. *15*: 1690–1703.

Mincheva-Tasheva, S., and Soler, R.M. (2013). NF-κB signaling pathways: Role in nervous system physiology and pathology. Neuroscientist *19*: 175–194.

Mirza, A.M., Gysin, S., Malek, N., Nakayama, K., Roberts, J.M., and McMahon, M. (2004). Cooperative Regulation of the Cell Division Cycle by the Protein Kinases RAF and AKT. Mol. Cell. Biol. *24*: 10868–10881.

Moechars, D., Weston, M.C., Leo, S., Callaerts-Vegh, Z., Goris, I., Daneels, G., et al. (2006). Vesicular Glutamate Transporter VGLUT2 Expression Levels Control Quantal Size and Neuropathic Pain. J. Neurosci. *26*: 12055–12066.

Moharir, S.C., Raghawan, A.K., Ramaswamy, R., and Swarup, G. (2022). Autophagy-independent cytoprotection by optineurin from toxicity of aggregates formed by mutant huntingtin and mutant ataxin-3. J. Biochem. *171*: 555–565.

Montecalvo, A., Watkins, S.C., Orange, J., and Kane, L.P. (2017). Inducible turnover of optineurin regulates T cell activation. Mol. Immunol. *85*: 9–17.

Montoya, A., Price, B.H., Menear, M., and Lepage, M. (2006). Brain imaging and cognitive dysfunctions in Huntington's disease. J. Psychiatry Neurosci. *31*: 21–9.

Mullen, R.J., Buck, C.R., and Smith, A.M. (1992). NeuN, a neuronal specific nuclear protein in vertebrates. Development *116*: 201–11.

Munitic, I., Giardino Torchia, M.L., Meena, N.P., Zhu, G., Li, C.C., and Ashwell, J.D. (2013). Optineurin Insufficiency Impairs IRF3 but Not NF-κB Activation in Immune Cells. J. Immunol. *191*: 6231–6240.

Murphy, K.P.S.J., Carter, R.J., Lione, L.A., Mangiarini, L., Mahal, A., Bates, G.P., et al. (2000). Abnormal Synaptic Plasticity and Impaired Spatial Cognition in Mice Transgenic for Exon 1 of the Human Huntington's Disease Mutation. J. Neurosci. *20*: 5115–5123.

Myers, R.H., Vonsattel, J.P., Paskevich, P.A., Kiely, D.K., Stevens, T.J., Cupples, L.A., et al. (1991). Decreased Neuronal and Increased Oligodendroglial Densities in Huntington's Disease Caudate Nucleus. J. Neuropathol. Exp. Neurol. *50*: 729–742.

Nagai, Y., Inui, T., Popiel, H.A., Fujikake, N., Hasegawa, K., Urade, Y., et al. (2007). A toxic monomeric conformer of the polyglutamine protein. Nat. Struct. Mol. Biol. *14*: 332–340.

Nakazawa, S., Oikawa, D., Ishii, R., Ayaki, T., Takahashi, H., Takeda, H., et al. (2016). Linear ubiquitination is involved in the pathogenesis of optineurin-associated amyotrophic lateral sclerosis. Nat. Commun. *7*: 12547.

Nasir, J., Floresco, S.B., O'Kusky, J.R., Diewert, V.M., Richman, J.M., Zeisler, J., et al. (1995). Targeted disruption of the Huntington's disease gene results in embryonic lethality and behavioral and morphological changes in heterozygotes. Cell *81*: 811–823.

Neer, E.J. (1995). Heterotrimeric G proteins: organizers of transmembrane signals. Cell *80*: 249–57.

Neki, A., Ohishi, H., Kaneko, T., Shigemoto, R., Nakanishi, S., and Mizuno, N. (1996). Pre- and postsynaptic localization of a metabotropic glutamate receptor, mGluR2, in the rat brain: an immunohistochemical study with a monoclonal antibody. Neurosci. Lett. *202*: 197–200.

Nelson, A.B., Bussert, T.G., Kreitzer, A.C., and Seal, R.P. (2014). Striatal Cholinergic Neurotransmission Requires VGLUT3. J. Neurosci. *34*: 8772–8777.

Nguyen, R., Venkatesan, S., Binko, M., Bang, J.Y., Cajanding, J.D., Briggs, C., et al. (2020). Cholecystokinin-Expressing Interneurons of the Medial Prefrontal Cortex Mediate Working Memory Retrieval. J. Neurosci. *40*: 2314–2331.

Nicodemo, A.A., Pampillo, M., Ferreira, L.T., Dale, L.B., Cregan, T., Ribeiro, F.M., et al. (2010). Pyk2 uncouples metabotropic glutamate receptor G protein signaling but facilitates ERK1/2 activation. Mol. Brain *3*: 4.

Nikoletopoulou, V., Sidiropoulou, K., Kallergi, E., Dalezios, Y., and Tavernarakis, N. (2017). Modulation of Autophagy by BDNF Underlies Synaptic Plasticity. Cell Metab. *26*: 230-242.e5.

Niswender, C.M., and Conn, P.J. (2010). Metabotropic Glutamate Receptors: Physiology, Pharmacology, and Disease. Annu. Rev. Pharmacol. Toxicol. *50*: 295–322.

Nixon, R.A. (2013). The role of autophagy in neurodegenerative disease. Nat. Med. *19*: 983–997.

Normann, C., and Clark, K. (2005). Selective modulation of Ca2+ influx pathways by 5-HT regulates synaptic long-term plasticity in the hippocampus. Brain Res. *1037*: 187–193.

Nucifora, L.G., Burke, K.A., Feng, X., Arbez, N., Zhu, S., Miller, J., et al. (2012). Identification of novel potentially toxic oligomers formed in vitro from mammalian-derived expanded huntingtin exon-1 protein. J. Biol. Chem. *287*: 16017–16028.

O'Riordan, K.J., Huang, I.-C., Pizzi, M., Spano, P., Boroni, F., Egli, R., et al. (2006). Regulation of nuclear factor kappaB in the hippocampus by group I metabotropic glutamate receptors. J. Neurosci. *26*: 4870–9.

Ochaba, J., Lukacsovich, T., Csikos, G., Zheng, S., Margulis, J., Salazar, L., et al. (2014). Potential function for the Huntingtin protein as a scaffold for selective autophagy. Proc. Natl. Acad. Sci. *111*: 16889–16894.

Ohishi, H., Neki, A., and Mizuno, N. (1998). Distribution of a metabotropic glutamate receptor, mGluR2, in the central nervous system of the rat and mouse: an immunohistochemical study with a monoclonal antibody. Neurosci. Res. *30*: 65–82.

Okita, S., Morigaki, R., Koizumi, H., Kaji, R., Nagahiro, S., and Goto, S. (2012). Cell type-specific localization of optineurin in the striatal neurons of mice: implications for neuronal vulnerability in Huntington's disease. Neuroscience *202*: 363–370.

Olszewski, J., and Baxter, D. (1954). Cytoarchitecture of the Human Brain Stem (Basle & New York: S. Karger).

Omiya, Y., Uchigashima, M., Konno, K., Yamasaki, M., Miyazaki, T., Yoshida, T., et al. (2015). VGluT3-Expressing CCK-Positive Basket Cells Construct Invaginating Synapses Enriched with Endocannabinoid Signaling Proteins in Particular Cortical and Cortex-Like Amygdaloid Regions of Mouse Brains. J. Neurosci. *35*: 4215–4228.

Osawa, T., Mizuno, Y., Fujita, Y., Takatama, M., Nakazato, Y., and Okamoto, K. (2011). Optineurin in neurodegenerative diseases. Neuropathology *31*: 569–574.

Otani, S., Auclair, N., Desce, J.-M., Roisin, M.-P., and Crépel, F. (1999). Dopamine Receptors and Groups I and II mGluRs Cooperate for Long-Term Depression Induction in Rat Prefrontal Cortex through Converging Postsynaptic Activation of MAP Kinases. J. Neurosci. *19*: 9788–9802.

Otis, T.S. (2001). Vesicular glutamate transporters in cognito. Neuron *29*: 11–4.

Page, G., Khidir, F.A.L., Pain, S., Barrier, L., Fauconneau, B., Guillard, O., et al. (2006). Group I metabotropic glutamate receptors activate the p70S6 kinase via both mammalian target of rapamycin (mTOR) and extracellular signal-regulated kinase (ERK 1/2) signaling pathways in rat striatal and hippocampal synaptoneurosomes. Neurochem. Int. *49*: 413–421.

Paoletti, P., Bellone, C., and Zhou, Q. (2013). NMDA receptor subunit diversity: impact on receptor properties, synaptic plasticity and disease. Nat. Rev. Neurosci. *14*: 383–400.

Paolillo, M., Montecucco, A., Zanassi, P., and Schinelli, S. (1998). Potentiation of dopamine-induced cAMP formation by group I metabotropic glutamate receptors via protein kinase C in cultured striatal neurons. Eur. J. Neurosci. *10*: 1937–1945.

Papoutsi, M., Labuschagne, I., Tabrizi, S.J., and Stout, J.C. (2014). The cognitive burden in Huntington's disease: Pathology, phenotype, and mechanisms of compensation. Mov. Disord. *29*: 673–683.

Parsons, M.P., and Raymond, L.A. (2014). Extrasynaptic NMDA receptor involvement in central nervous system disorders. Neuron.

Parsons, M.P., and Raymond, L.A. (2015). Huntington Disease. In Neurobiology of Brain Disorders: Biological Basis of Neurological and Psychiatric Disorders, (Elsevier), pp 303–320.

Paterson, N.E., and Markou, A. (2005). The metabotropic glutamate receptor 5

antagonist MPEP decreased break points for nicotine, cocaine and food in rats. Psychopharmacology (Berl). *179*: 255–261.

Paulsen, J.S. (2011). Cognitive Impairment in Huntington Disease: Diagnosis and Treatment. Curr. Neurol. Neurosci. Rep. *11*: 474–483.

Pavese, N., Gerhard, A., Tai, Y.F., Ho, A.K., Turkheimer, F., Barker, R.A., et al. (2006). Microglial activation correlates with severity in Huntington disease: A clinical and PET study. Neurology *66*: 1638–1643.

Pelkey, K.A., Calvigioni, D., Fang, C., Vargish, G., Ekins, T., Auville, K., et al. (2020). Paradoxical network excitation by glutamate release from VGluT3+ GABAergic interneurons. Elife *9*:.

Perluigi, M., Domenico, F. Di, and Butterfield, D.A. (2015). mTOR signaling in aging and neurodegeneration: At the crossroad between metabolism dysfunction and impairment of autophagy. Neurobiol. Dis. *84*: 39–49.

Perry, T.L., Hansen, S., and Kloster, M. (1973). Huntington's chorea. Deficiency of gamma-aminobutyric acid in brain. N. Engl. J. Med. *288*: 337–42.

Persson, S., Boulland, J.-L., Aspling, M., Larsson, M., Fremeau, R.T., Edwards, R.H., et al. (2006). Distribution of vesicular glutamate transporters 1 and 2 in the rat spinal cord, with a note on the spinocervical tract. J. Comp. Neurol. *497*: 683–701.

Peters, J., and Kalivas, P.W. (2006). The group II metabotropic glutamate receptor agonist, LY379268, inhibits both cocaine- and food-seeking behavior in rats. Psychopharmacology (Berl). *186*: 143–149.

Philpott, A.L., Cummins, T.D.R., Bailey, N.W., Churchyard, A., Fitzgerald, P.B., and Georgiou-Karistianis, N. (2016). Cortical inhibitory deficits in premanifest and early Huntington's disease. Behav. Brain Res. *296*: 311–317.

Piiponniemi, T.O., Parkkari, T., Heikkinen, T., Puoliväli, J., Park, L.C., Cachope, R., et al. (2018). Impaired Performance of the Q175 Mouse Model of Huntington's Disease in the Touch Screen Paired Associates Learning Task. Front. Behav. Neurosci. *12*:.

Pin, J.-P., Galvez, T., Prézeau, L., and Prezeau, L. (2003). Evolution, structure, and activation mechanism of family 3/C G-protein-coupled receptors. Pharmacol. Ther. *98*: 325–354.

Pino, I. del, Brotons-Mas, J.R., Marques-Smith, A., Marighetto, A., Frick, A., Marín, O., et al. (2017). Abnormal wiring of CCK+ basket cells disrupts spatial information coding. Nat. Neurosci. *20*: 784–792.

Pisani, A., Bonsi, P., Catania, M.V., Giuffrida, R., Morari, M., Marti, M., et al. (2002). Metabotropic Glutamate 2 Receptors Modulate Synaptic Inputs and Calcium Signals in Striatal Cholinergic Interneurons. J. Neurosci. *22*: 6176.

Pisani, A., Bonsi, P., Centonze, D., Bernardi, G., and Calabresi, P. (2001). Functional coexpression of excitatory mGluR1 and mGluR5 on striatal cholinergic interneurons. Neuropharmacology *40*: 460–463.

Porta, C., Paglino, C., and Mosca, A. (2014). Targeting PI3K/Akt/mTOR Signaling in Cancer. Front. Oncol. *4*:.

Pottier, C., Bieniek, K.F., Finch, N.C., Vorst, M. van de, Baker, M., Perkersen, R., et al. (2015). Whole-genome sequencing reveals important role for TBK1 and OPTN mutations in frontotemporal lobar degeneration without motor neuron disease. Acta Neuropathol. *130*: 77–92.

Pouladi, M.A., Morton, A.J., and Hayden, M.R. (2013). Choosing an animal model for the study of Huntington's disease. Nat. Rev. Neurosci. *14*: 708–21.

Preobraschenski, J., Zander, J.-F., Suzuki, T., Ahnert-Hilger, G., and Jahn, R. (2014). Vesicular Glutamate Transporters Use Flexible Anion and Cation Binding Sites for Efficient Accumulation of Neurotransmitter. Neuron *84*: 1287–1301.

Puig, M.V., Rose, J., Schmidt, R., and Freund, N. (2014). Dopamine modulation of learning and memory in the prefrontal cortex: insights from studies in primates, rodents, and birds. Front. Neural Circuits *8*:.

Puighermanal, E., Cutando, L., Boubaker-Vitre, J., Honoré, E., Longueville, S., Hervé, D., et al. (2017). Anatomical and molecular characterization of dopamine D1 receptor-expressing neurons of the mouse CA1 dorsal hippocampus. Brain Struct. Funct. *222*: 1897–1911.

Qi, J., Zhang, S., Wang, H.-L., Wang, H., Jesus Aceves Buendia, J. de, Hoffman, A.F., et al. (2014). A glutamatergic reward input from the dorsal raphe to ventral tegmental area dopamine neurons. Nat. Commun. *5*: 5390.

Rahman, M.M., Kedia, S., Fernandes, G., and Chattarji, S. (2017). Activation of the same mGluR5 receptors in the amygdala causes divergent effects on specific versus indiscriminate fear. Elife *6*:.

Rai, S.N., Dilnashin, H., Birla, H., Singh, S. Sen, Zahra, W., Rathore, A.S., et al. (2019). The Role of PI3K/Akt and ERK in Neurodegenerative Disorders. Neurotox. Res. *35*: 775–795.

Ramet, L., Zimmermann, J., Bersot, T., Poirel, O., Gois, S. De, Silm, K., et al. (2017). Characterization of a Human Point Mutation of VGLUT3 (p.A211V) in the Rodent Brain Suggests a Nonuniform Distribution of the Transporter in Synaptic Vesicles. J. Neurosci. *37*: 4181–4199.

Ravalia, A.S., Lau, J., Barron, J.C., Purchase, S.L.M., Southwell, A.L., Hayden, M.R., et al. (2021). Super-resolution imaging reveals extrastriatal synaptic dysfunction in presymptomatic Huntington disease mice. Neurobiol. Dis. *152*: 105293.

Raymond, L.A., André, V.M., Cepeda, C., Gladding, C.M., Milnerwood, A.J., and Levine, M.S. (2011). Pathophysiology of Huntington's disease: time-dependent alterations in synaptic and receptor function. Neuroscience *198*: 252–273.

Rehani, R., Atamna, Y., Tiroshi, L., Chiu, W.-H., Jesús Aceves Buendía, J. de, Martins, G.J., et al. (2019). Activity Patterns in the Neuropil of Striatal Cholinergic Interneurons in Freely Moving Mice Represent Their Collective Spiking Dynamics. Eneuro *6*:

ENEURO.0351-18.2018.

Reiner, A., Lafferty, D.C., Wang, H.B., Mar, N. Del, and Deng, Y.P. (2012). The group 2 metabotropic glutamate receptor agonist LY379268 rescues neuronal, neurochemical and motor abnormalities in R6/2 Huntington's disease mice. Neurobiol. Dis. *47*: 75–91.

Reiner, A., and Levitz, J. (2018). Glutamatergic Signaling in the Central Nervous System: Ionotropic and Metabotropic Receptors in Concert. Neuron *98*: 1080–1098.

Reisine, T.D., Wastek, G.J., Speth, R.C., Bird, E.D., and Yamamura, H.I. (1979). Alterations in the benzodiazepine receptor of Huntington's diseased human brain. Brain Res. *165*: 183–187.

Rezaie, T., Child, A., Hitchings, R., Brice, G., Miller, L., Coca-Prados, M., et al. (2002). Adult-onset primary open-angle glaucoma caused by mutations in optineurin. Science *295*: 1077–1079.

Rezaie, T., and Sarfarazi, M. (2005). Molecular cloning, genomic structure, and protein characterization of mouse optineurin. Genomics *85*: 131–138.

Rezaie, T., Waitzman, D.M., Seeman, J.L., Kaufman, P.L., and Sarfarazi, M. (2005). Molecular Cloning and Expression Profiling of Optineurin in the Rhesus Monkey. Investig. Opthalmology Vis. Sci. *46*: 2404.

Ribeiro, F.M., DeVries, R.A., Hamilton, A., Guimaraes, I.M., Cregan, S.P., Pires, R.G.W., et al. (2014). Metabotropic glutamate receptor 5 knockout promotes motor and biochemical alterations in a mouse model of Huntington's disease. Hum. Mol. Genet. *23*: 2030–2042.

Ribeiro, F.M., Paquet, M., Ferreira, L.T., Cregan, T., Swan, P., Cregan, S.P., et al. (2010). Metabotropic glutamate receptor-mediated cell signaling pathways are altered in a mouse model of Huntington's disease. J. Neurosci. *30*: 316–324.

Ribeiro, F.M., Pires, R.G.W., and Ferguson, S.S.G. (2011). Huntington's disease and group I metabotropic glutamate receptors. Mol. Neurobiol. *43*: 1–11.

Ribeiro, F.M., Vieira, L.B., Pires, R.G.W., Olmo, R.P., and Ferguson, S.S.G. (2017). Metabotropic glutamate receptors and neurodegenerative diseases. Pharmacol. Res. *115*: 179–191.

Richfield, E.K., O'Brien, C.F., Eskin, T., and Shoulson, I. (1991). Heterogeneous dopamine receptor changes in early and late Huntington's disease. Neurosci. Lett. *132*: 121–126.

Richter, B., Sliter, D.A., Herhaus, L., Stolz, A., Wang, C., Beli, P., et al. (2016). Phosphorylation of OPTN by TBK1 enhances its binding to Ub chains and promotes selective autophagy of damaged mitochondria. Proc. Natl. Acad. Sci. *113*: 4039–4044.

Robin Hiley, C., and Bird, E.D. (1974). Decreased muscarinic receptor concentration in post-mortem brain in Huntington's chorea. Brain Res. *80*: 355–358.

Rocha, N.P., Ribeiro, F.M., Furr-Stimming, E., and Teixeira, A.L. (2016).

Neuroimmunology of Huntington's Disease: Revisiting Evidence from Human Studies. Mediators Inflamm. *2016*: 1–10.

Romano, C., Sesma, M.A., McDonald, C.T., O'malley, K., Pol, A.N. van den, and Olney, J.W. (1995). Distribution of metabotropic glutamate receptor mGluR5 immunoreactivity in rat brain. J. Comp. Neurol. *355*: 455–469.

Ronesi, J.A., and Huber, K.M. (2008). Homer Interactions Are Necessary for Metabotropic Glutamate Receptor-Induced Long-Term Depression and Translational Activation. J. Neurosci. *28*: 543–547.

Rong, R., Ahn, J.-Y., Huang, H., Nagata, E., Kalman, D., Kapp, J.A., et al. (2003). PI3 kinase enhancer–Homer complex couples mGluRI to PI3 kinase, preventing neuronal apoptosis. Nat. Neurosci. *6*: 1153–1161.

Rook, J.M., Xiang, Z., Lv, X., Ghoshal, A., Dickerson, J.W., Bridges, T.M., et al. (2015). Biased mGlu5-Positive Allosteric Modulators Provide InVivo Efficacy without Potentiating mGlu5 Modulation of NMDAR Currents. Neuron *86*: 1029–1040.

Rosenblatt, A., Liang, K.Y., Zhou, H., Abbott, M.H., Gourley, L.M., Margolis, R.L., et al. (2006). The association of CAG repeat length with clinical progression in Huntington disease. Neurology *66*: 1016–1020.

Ross, C.A. (1997). Intranuclear neuronal inclusions: A common pathogenic mechanism for glutamine-repeat neurodegenerative diseases? Neuron *19*: 1147–1150.

Ross, C.A., and Tabrizi, S.J. (2011). Huntington's disease: From molecular pathogenesis to clinical treatment. Lancet Neurol. *10*: 83–98.

Rothe, T., Deliano, M., Wójtowicz, A.M., Dvorzhak, A., Harnack, D., Paul, S., et al. (2015). Pathological gamma oscillations, impaired dopamine release, synapse loss and reduced dynamic range of unitary glutamatergic synaptic transmission in the striatum of hypokinetic Q175 Huntington mice. Neuroscience *311*: 519–538.

Ruel, J., Emery, S., Nouvian, R., Bersot, T., Amilhon, B., Rybroek, J.M. Van, et al. (2008). Impairment of SLC17A8 Encoding Vesicular Glutamate Transporter-3, VGLUT3, Underlies Nonsyndromic Deafness DFNA25 and Inner Hair Cell Dysfunction in Null Mice. Am. J. Hum. Genet. *83*: 278–292.

Rui, Y.-N., Xu, Z., Patel, B., Chen, Z., Chen, D., Tito, A., et al. (2015). Huntingtin functions as a scaffold for selective macroautophagy. Nat. Cell Biol. *17*: 262–275.

Russell, R.C., Tian, Y., Yuan, H., Park, H.W., Chang, Y.-Y., Kim, J., et al. (2013). ULK1 induces autophagy by phosphorylating Beclin-1 and activating VPS34 lipid kinase. Nat. Cell Biol. *15*: 741–750.

Ryan, T.A., and Tumbarello, D.A. (2018). Optineurin: A Coordinator of Membrane-Associated Cargo Trafficking and Autophagy. Front. Immunol. *9*:.

Sahl, S.J., Weiss, L.E., Duim, W.C., Frydman, J., and Moerner, W.E. (2012). Cellular inclusion bodies of mutant huntingtin exon 1 obscure small fibrillar aggregate species. Sci. Rep. *2*: 1–7.

Sahlender, D.A., Roberts, R.C., Arden, S.D., Spudich, G., Taylor, M.J., Luzio, J.P., et al. (2005). Optineurin links myosin VI to the Golgi complex and is involved in Golgi organization and exocytosis. J. Cell Biol. *169*: 285–295.

Sakae, D.Y., Marti, F., Lecca, S., Vorspan, F., Martín-García, E., Morel, L.J., et al. (2015). The absence of VGLUT3 predisposes to cocaine abuse by increasing dopamine and glutamate signaling in the nucleus accumbens. Mol. Psychiatry *20*: 1448–1459.

Sakae, D.Y., Ramet, L., Henrion, A., Poirel, O., Jamain, S., Mestikawy, S. El, et al. (2019). Differential expression of VGLUT3 in laboratory mouse strains: Impact on drug-induced hyperlocomotion and anxiety-related behaviors. Genes, Brain Behav. *18*: e12528.

Sassone-Corsi, P. (2012). The Cyclic AMP Pathway. Cold Spring Harb. Perspect. Biol. *4*: a011148–a011148.

Sathasivam, K., Neueder, A., Gipson, T.A., Landles, C., Benjamin, A.C., Bondulich, M.K., et al. (2013). Aberrant splicing of HTT generates the pathogenic exon 1 protein in Huntington disease. Proc. Natl. Acad. Sci. *110*: 2366–2370.

Saudou, F., Finkbeiner, S., Devys, D., and Greenberg, M.E. (1998). Huntingtin acts in the nucleus to induce apoptosis but death does not correlate with the formation of intranuclear inclusions. Cell *95*: 55–66.

Savage, J.C., St-Pierre, M.-K., Carrier, M., Hajj, H. El, Novak, S.W., Sanchez, M.G., et al. (2020). Microglial physiological properties and interactions with synapses are altered at presymptomatic stages in a mouse model of Huntington's disease pathology. J. Neuroinflammation *17*: 98.

Schäfer, M.K.H., Varoqui, H., Defamie, N., Weihe, E., and Erickson, J.D. (2002). Molecular cloning and functional identification of mouse vesicular glutamate transporter 3 and its expression in subsets of novel excitatory neurons. J. Biol. Chem. *277*: 50734–50748.

Scherzinger, E., Sittler, A., Schweiger, K., Heiser, V., Lurz, R., Hasenbank, R., et al. (1999). Self-assembly of polyglutamine-containing huntingtin fragments into amyloid-like fibrils: Implications for Huntington's disease pathology. Proc. Natl. Acad. Sci. U. S. A. *96*: 4604–4609.

Schiefer, J., Sprünken, A., Puls, C., Lüesse, H.-G., Milkereit, A., Milkereit, E., et al. (2004). The metabotropic glutamate receptor 5 antagonist MPEP and the mGluR2 agonist LY379268 modify disease progression in a transgenic mouse model of Huntington's disease. Brain Res. *1019*: 246–254.

Schiöth, H.B., and Fredriksson, R. (2005). The GRAFS classification system of G-protein coupled receptors in comparative perspective. Gen. Comp. Endocrinol. *142*: 94–101.

Schippling, S., Schneider, S.A., Bhatia, K.P., Münchau, A., Rothwell, J.C., Tabrizi, S.J., et al. (2009). Abnormal Motor Cortex Excitability in Preclinical and Very Early Huntington's Disease. Biol. Psychiatry *65*: 959–965.

Schneider, C.A., Rasband, W.S., and Eliceiri, K.W. (2012). NIH Image to ImageJ: 25 years of image analysis. Nat. Methods *9*: 671–675.

Schoepp, D.D. (2001). Unveiling the functions of presynaptic metabotropic glutamate receptors in the central nervous system. J. Pharmacol. Exp. Ther. *299*: 12–20.

Schotanus, S.M., and Chergui, K. (2008). Dopamine D1 receptors and group I metabotropic glutamate receptors contribute to the induction of long-term potentiation in the nucleus accumbens. Neuropharmacology *54*: 837–844.

Schwab, C., Yu, S., McGeer, E.G., and McGeer, P.L. (2012). Optineurin in Huntington's disease intranuclear inclusions. Neurosci. Lett. *506*: 149–154.

Schwamborn, K., Weil, R., Courtois, G., Whiteside, S.T., and Israël, A. (2000). Phorbol esters and cytokines regulate the expression of the NEMO-related protein, a molecule involved in a NF-κB-independent pathway. J. Biol. Chem. *275*: 22780–22789.

Seal, R.P., Akil, O., Yi, E., Weber, C.M., Grant, L., Yoo, J., et al. (2008). Sensorineural Deafness and Seizures in Mice Lacking Vesicular Glutamate Transporter 3. Neuron *57*: 263–275.

Sengupta, A., and Holmes, A. (2019). A Discrete Dorsal Raphe to Basal Amygdala 5-HT Circuit Calibrates Aversive Memory. Neuron *103*: 489-505.e7.

Senter, R.K., Ghoshal, A., Walker, A.G., Xiang, Z., Niswender, C.M., and Conn, P.J. (2016). The Role of mGlu Receptors in Hippocampal Plasticity Deficits in Neurological and Psychiatric Disorders: Implications for Allosteric Modulators as Novel Therapeutic Strategies. Curr. Neuropharmacol. *14*: 455–73.

Sethna, F., Zhang, M., Kaphzan, H., Klann, E., Autio, D., Cox, C.L., et al. (2016). Calmodulin activity regulates group I metabotropic glutamate receptor-mediated signal transduction and synaptic depression. J. Neurosci. Res. *94*: 401–408.

Settembre, C., Malta, C. Di, Polito, V.A., Arencibia, M.G., Vetrini, F., Erdin, S., et al. (2011). TFEB Links Autophagy to Lysosomal Biogenesis. Science *332*: 1429–1433.

Shehata, M., Matsumura, H., Okubo-Suzuki, R., Ohkawa, N., and Inokuchi, K. (2012). Neuronal Stimulation Induces Autophagy in Hippocampal Neurons That Is Involved in AMPA Receptor Degradation after Chemical Long-Term Depression. J. Neurosci. *32*: 10413–10422.

Shen, W.C., Li, H.Y., Chen, G.C., Chern, Y., and Tu, P.H. (2015). Mutations in the ubiquitin-binding domain of OPTN/optineurin interfere with autophagy- mediated degradation of misfolded proteins by a dominant-negative mechanism. Autophagy *11*: 685–700.

Shen, X., Ying, H., Qiu, Y., Park, J.-S., Shyam, R., Chi, Z.-L., et al. (2011). Processing of Optineurin in Neuronal Cells. J. Biol. Chem. *286*: 3618–3629.

Shibata, M., Lu, T., Furuya, T., Degterev, A., Mizushima, N., Yoshimori, T., et al. (2006). Regulation of intracellular accumulation of mutant Huntingtin by Beclin 1. J. Biol. Chem. *281*: 14474–14485.

Shigemoto, R., Nomura, S., Ohishi, H., Sugihara, H., Nakanishi, S., and Mizuno, N. (1993). Immunohistochemical localization of a metabotropic glutamate receptor, mGluR5, in the rat brain. Neurosci. Lett. *163*: 53–57.

Shirasaki, D.I., Greiner, E.R., Al-Ramahi, I., Gray, M., Boontheung, P., Geschwind, D.H., et al. (2012). Network Organization of the Huntingtin Proteomic Interactome in Mammalian Brain. Neuron *75*: 41–57.

Sieradzan, K.A., Mechan, A.O., Jones, L., Wanker, E.E., Nukina, N., and Mann, D.M.A. (1999). Huntington's Disease Intranuclear Inclusions Contain Truncated, Ubiquitinated Huntingtin Protein. Exp. Neurol. *156*: 92–99.

Simmons, D.A., Rex, C.S., Palmer, L., Pandyarajan, V., Fedulov, V., Gall, C.M., et al. (2009). Up-regulating BDNF with an ampakine rescues synaptic plasticity and memory in Huntington's disease knockin mice. Proc. Natl. Acad. Sci. *106*: 4906–4911.

Sitcheran, R., Comb, W.C., Cogswell, P.C., and Baldwin, A.S. (2008). Essential role for epidermal growth factor receptor in glutamate receptor signaling to NF-kappaB. Mol. Cell. Biol. *28*: 5061–70.

Sladeczek, F., Pin, J.-P., Récasens, M., Bockaert, J., and Weiss, S. (1985). Glutamate stimulates inositol phosphate formation in striatal neurones. Nature *317*: 717–719.

Slow, E.J., Raamsdonk, J. van, Rogers, D., Coleman, S.H., Graham, R.K., Deng, Y., et al. (2003). Selective striatal neuronal loss in a YAC128 mouse model of Huntington disease. Hum. Mol. Genet. *12*: 1555–67.

Slowicka, K., Vereecke, L., and Loo, G. van (2016). Cellular Functions of Optineurin in Health and Disease. Trends Immunol. *37*: 621–633.

Smith-Dijak, A.I., Sepers, M.D., and Raymond, L.A. (2019). Alterations in synaptic function and plasticity in Huntington disease. J. Neurochem. *150*: 346–365.

Smith, G.A., Rocha, E.M., McLean, J.R., Hayes, M.A., Izen, S.C., Isacson, O., et al. (2014). Progressive axonal transport and synaptic protein changes correlate with behavioral and neuropathological abnormalities in the heterozygous Q175 KI mouse model of Huntington's disease. Hum. Mol. Genet. *23*: 4510–4527.

Smith, K.M., and Dahodwala, N. (2014). Sex differences in Parkinson's disease and other movement disorders. Exp. Neurol. *259*: 44–56.

Smith, R., Chung, H., Rundquist, S., Maat-Schieman, M.L.C., Colgan, L., Englund, E., et al. (2006). Cholinergic neuronal defect without cell loss in Huntington's disease. Hum. Mol. Genet. *15*: 3119–3131.

Solomon, A.C., Stout, J.C., Johnson, S.A., Langbehn, D.R., Aylward, E.H., Brandt, J., et al. (2007). Verbal episodic memory declines prior to diagnosis in Huntington's disease. Neuropsychologia *45*: 1767–1776.

Somogyi, J., Baude, A., Omori, Y., Shimizu, H., Mestikawy, S. El, Fukaya, M., et al. (2004). GABAergic basket cells expressing cholecystokinin contain vesicular glutamate transporter type 3 (VGLUT3) in their synaptic terminals in hippocampus and isocortex

of the rat. Eur. J. Neurosci. *19*: 552–69.

Soto, C. (2003). Unfolding the role of protein misfolding in neurodegenerative diseases. Nat. Rev. Neurosci. *4*: 49–60.

Southwell, A.L., Smith-Dijak, A., Kay, C., Sepers, M., Villanueva, E.B., Parsons, M.P., et al. (2016). An enhanced Q175 knock-in mouse model of Huntington disease with higher mutant huntingtin levels and accelerated disease phenotypes. Hum. Mol. Genet.

Souza, J.M. de, Abd-Elrahman, K.S., Ribeiro, F.M., and Ferguson, S.S.G. (2020). mGluR5 regulates REST/NRSF signaling through N-cadherin/β-catenin complex in Huntington's disease. Mol. Brain *13*: 118.

Souza, J.M. de, Ferreira-Vieira, T.H., Maciel, E.M.A., Silva, N.C., Lima, I.B.Q., Doria, J.G., et al. (2022). mGluR5 ablation leads to age-related synaptic plasticity impairments and does not improve Huntington's disease phenotype. Sci. Rep. *12*: 8982.

Spargo, E., Everall, I.P., and Lantos, P.L. (1993). Neuronal loss in the hippocampus in Huntington's disease: a comparison with HIV infection. J. Neurol. Neurosurg. Psychiatry *56*: 487–491.

Stambolic, V., and Woodgett, J.R. (1994). Mitogen inactivation of glycogen synthase kinase-3β in intact cells via serine 9 phosphorylation. Biochem. J. *303*: 701–704.

Stoppel, L.J., Auerbach, B.D., Senter, R.K., Preza, A.R., Lefkowitz, R.J., and Bear, M.F. (2017). β-Arrestin2 Couples Metabotropic Glutamate Receptor 5 to Neuronal Protein Synthesis and Is a Potential Target to Treat Fragile X. Cell Rep. *18*: 2807–2814.

Su, L.-D., Wang, N., Han, J., and Shen, Y. (2022). Group 1 Metabotropic Glutamate Receptors in Neurological and Psychiatric Diseases: Mechanisms and Prospective. Neurosci. *28*: 453–468.

Sudhakar, C., Nagabhushana, A., Jain, N., and Swarup, G. (2009). NF-κB Mediates Tumor Necrosis Factor α-Induced Expression of Optineurin, a Negative Regulator of NF-κB. PLoS One *4*: e5114.

Sun, J., and Nan, G. (2017). The extracellular signal-regulated kinase 1/2 pathway in neurological diseases: A potential therapeutic target (Review). Int. J. Mol. Med. *39*: 1338–1346.

Sun, Y., Lipton, J.O., Boyle, L.M., Madsen, J.R., Goldenberg, M.C., Pascual-Leone, A., et al. (2016). Direct current stimulation induces mGluR5-dependent neocortical plasticity. Ann. Neurol. *80*: 233–246.

Sun, Y., Savanenin, A., Reddy, P.H., and Liu, Y.F. (2001). Polyglutamine-expanded Huntingtin Promotes Sensitization of N-Methyl-d-aspartate Receptors via Post-synaptic Density 95. J. Biol. Chem. *276*: 24713–24718.

Sutton, M.A., Schmidt, E.F., Choi, K.-H., Schad, C.A., Whisler, K., Simmons, D., et al. (2003). Extinction-induced upregulation in AMPA receptors reduces cocaine-seeking behaviour. Nature *421*: 70–75.

Suzuki, N., Hajicek, N., and Kozasa, T. (2009). Regulation and Physiological Functions of G12/13-Mediated Signaling Pathways. Neurosignals *17*: 55–70.

Taber, E., Brodal, A., and Walberg, F. (1960). The raphe nuclei of the brain stem in the cat. I. Normal topography and cytoarchitecture and general discussion. J. Comp. Neurol. *114*: 161–187.

Tabrizi, S.J., Estevez-Fraga, C., Roon-Mom, W.M.C. van, Flower, M.D., Scahill, R.I., Wild, E.J., et al. (2022). Potential disease-modifying therapies for Huntington's disease: lessons learned and future opportunities. Lancet Neurol. *21*: 645–658.

Takumi, Y., Matsubara, A., Rinvik, E., and Ottersen, O.P. (1999). The arrangement of glutamate receptors in excitatory synapses. Ann. N. Y. Acad. Sci. *868*: 474–82.

Tallaksen-Greene, S.J., Kaatz, K.W., Romano, C., and Albin, R.L. (1998). Localization of mGluR1a-like immunoreactivity and mGluR5-like immunoreactivity in identified populations of striatal neurons. Brain Res. *780*: 210–217.

Tang, T.S., Slow, E., Lupu, V., Stavrovskaya, I.G., Sugimori, M., Llinás, R., et al. (2005). Disturbed Ca2+ signalling and apoptosis of medium spiny neurons in Huntington's disease. Proc. Natl. Acad. Sci. U. S. A. *102*: 2602–2607.

Tang, T.S., Tu, H., Chan, E.Y.W., Maximov, A., Wang, Z., Wellington, C.L., et al. (2003). Huntingtin and huntingtin-associated protein 1 influence neuronal calcium signaling mediated by inositol-(1,4,5) triphosphate receptor type 1. Neuron *39*: 227–239.

Tatti, R., Bhaukaurally, K., Gschwend, O., Seal, R.P., Edwards, R.H., Rodriguez, I., et al. (2014). A population of glomerular glutamatergic neurons controls sensory information transfer in the mouse olfactory bulb. Nat. Commun. 2014 51 *5*: 1–16.

Thakur, A.K., Jayaraman, M., Mishra, R., Thakur, M., Chellgren, V.M., L Byeon, I.J., et al. (2009). Polyglutamine disruption of the huntingtin exon 1 N terminus triggers a complex aggregation mechanism. Nat. Struct. Mol. Biol. 2009 164 *16*: 380–389.

Toro, D. del, Alberch, J., Lázaro-Diéguez, F., Martín-Ibáñez, R., Xifró, X., Egea, G., et al. (2009). Mutant Huntingtin Impairs Post-Golgi Trafficking to Lysosomes by Delocalizing Optineurin/Rab8 Complex from the Golgi Apparatus. Mol. Biol. Cell *20*: 1478–1492.

Träger, U., Andre, R., Lahiri, N., Magnusson-Lind, A., Weiss, A., Grueninger, S., et al. (2014). HTT-lowering reverses Huntington's disease immune dysfunction caused by NFκB pathway dysregulation. Brain *137*: 819–833.

Traynelis, S.F., Wollmuth, L.P., McBain, C.J., Menniti, F.S., Vance, K.M., Ogden, K.K., et al. (2010). Glutamate receptor ion channels: structure, regulation, and function. Pharmacol. Rev. *62*: 405–96.

Trettel, F. (2000). Dominant phenotypes produced by the HD mutation in STHdhQ111 striatal cells. Hum. Mol. Genet. *9*: 2799–2809.

Trudeau, L.-E., and Mestikawy, S. El (2018). Glutamate Cotransmission in Cholinergic, GABAergic and Monoamine Systems: Contrasts and Commonalities. Front. Neural

Circuits *12*:.

Tu, J.C., Xiao, B., Naisbitt, S., Yuan, J.P., Petralia, R.S., Brakeman, P., et al. (1999). Coupling of mGluR/Homer and PSD-95 Complexes by the Shank Family of Postsynaptic Density Proteins. Neuron *23*: 583–592.

Tu, J.C., Xiao, B., Yuan, J.P., Lanahan, A.A., Leoffert, K., Li, M., et al. (1998). Homer Binds a Novel Proline-Rich Motif and Links Group 1 Metabotropic Glutamate Receptors with IP3 Receptors. Neuron *21*: 717–726.

Tumbarello, D.A., Waxse, B.J., Arden, S.D., Bright, N.A., Kendrick-Jones, J., and Buss, F. (2012). Autophagy receptors link myosin VI to autophagosomes to mediate Tom1-dependent autophagosome maturation and fusion with the lysosome. Nat. Cell Biol. *14*: 1024–1035.

Ueda, T. (1986). Glutamate Transport in the Synaptic Vesicle. In Excitatory Amino Acids, (London: Palgrave Macmillan UK), pp 173–195.

Varga, V., Losonczy, A., Zemelman, B. V., Borhegyi, Z., Nyiri, G., Domonkos, A., et al. (2009). Fast Synaptic Subcortical Control of Hippocampal Circuits. Science *326*: 449–453.

Veldman, M.B., and Yang, X.W. (2018). Molecular insights into cortico-striatal miscommunications in Huntington's disease. Curr. Opin. Neurobiol. *48*: 79–89.

Vicini, S., Wang, J.F., Li, J.H., Zhu, W.J., Wang, Y.H., Luo, J.H., et al. (1998). Functional and Pharmacological Differences Between Recombinant N -Methyl- d -Aspartate Receptors. J. Neurophysiol. *79*: 555–566.

Vigneault, É., Poirel, O., Riad, M., Prud'homme, J., Dumas, S., Turecki, G., et al. (2015). Distribution of vesicular glutamate transporters in the human brain. Front. Neuroanat. *9*: 1–13.

Vögler, O., Barceló, J.M., Ribas, C., and Escribá, P. V. (2008). Membrane interactions of G proteins and other related proteins. Biochim. Biophys. Acta *1778*: 1640–52.

Voulalas, P.J. (2005). Metabotropic Glutamate Receptors and Dopamine Receptors Cooperate to Enhance Extracellular Signal-Regulated Kinase Phosphorylation in Striatal Neurons. J. Neurosci. *25*: 3763–3773.

Vugt, B. van, Kerkoerle, T. van, Vartak, D., and Roelfsema, P.R. (2020). The Contribution of AMPA and NMDA Receptors to Persistent Firing in the Dorsolateral Prefrontal Cortex in Working Memory. J. Neurosci. *40*: 2458–2470.

Walker, F.O. (2007). Huntington's disease. Lancet *369*: 218–228.

Wang, H.-L., Zhang, S., Qi, J., Wang, H., Cachope, R., Mejias-Aponte, C.A., et al. (2019). Dorsal Raphe Dual Serotonin-Glutamate Neurons Drive Reward by Establishing Excitatory Synapses on VTA Mesoaccumbens Dopamine Neurons. Cell Rep. *26*: 1128-1142.e7.

Wang, R., and Reddy, P.H. (2017). Role of Glutamate and NMDA Receptors in

Alzheimer's Disease. J. Alzheimers. Dis. *57*: 1041–1048.

Wellington, C.L., Ellerby, L.M., Gutekunst, C.-A., Rogers, D., Warby, S., Graham, R.K., et al. (2002). Caspase Cleavage of Mutant Huntingtin Precedes Neurodegeneration in Huntington's Disease. J. Neurosci. *22*: 7862–7872.

Wettschureck, N., and Offermanns, S. (2005). Mammalian G Proteins and Their Cell Type Specific Functions. Physiol. Rev. *85*: 1159–1204.

Wheeler, V.C. (2002). Early phenotypes that presage late-onset neurodegenerative disease allow testing of modifiers in Hdh CAG knock-in mice. Hum. Mol. Genet. *11*: 633–640.

Wheeler, V.C., Auerbach, W., White, J.K., Srinidhi, J., Auerbach, A., Ryan, A., et al. (1999). Length-dependent gametic CAG repeat instability in the Huntington's disease knock-in mouse. Hum. Mol. Genet. *8*: 115–22.

White, J.K., Auerbach, W., Duyao, M.P., Vonsattel, J.-P., Gusella, J.F., Joyner, A.L., et al. (1997). Huntingtin is required for neurogenesis and is not impaired by the Huntington's disease CAG expansion. Nat. Genet. *17*: 404–10.

Wiegand, M., Möller, A.A., Lauer, C.J., Stolz, S., Schreiber, W., Dose, M., et al. (1991). Nocturnal sleep in huntington's disease. J. Neurol. *238*: 203–208.

Wild, P., Farhan, H., McEwan, D.G., Wagner, S., Rogov, V. V, Brady, N.R., et al. (2011). Phosphorylation of the Autophagy Receptor Optineurin Restricts Salmonella Growth. Science *333*: 228–233.

Wilson, N.R. (2005). Presynaptic Regulation of Quantal Size by the Vesicular Glutamate Transporter VGLUT1. J. Neurosci. *25*: 6221–6234.

Wilton, D.K., and Stevens, B. (2020). The contribution of glial cells to Huntington's disease pathogenesis. Neurobiol. Dis. *143*: 104963.

Wojcik, S.M., Rhee, J.S., Herzog, E., Sigler, A., Jahn, R., Takamori, S., et al. (2004). An essential role for vesicular glutamate transporter 1 (VGLUT1) in postnatal development and control of quantal size. Proc. Natl. Acad. Sci. *101*: 7158–7163.

Wold, M.S., Lim, J., Lachance, V., Deng, Z., and Yue, Z. (2016). ULK1-mediated phosphorylation of ATG14 promotes autophagy and is impaired in Huntington's disease models. Mol. Neurodegener. *11*: 76.

Wong, S.-W., Huang, B.-W., Hu, X., Ho Kim, E., Kolb, J.P., Padilla, R.J., et al. (2020). Global deletion of Optineurin results in altered type I IFN signaling and abnormal bone remodeling in a model of Paget's disease. Cell Death Differ. *27*: 71–84.

Wong, Y.C., and Holzbaur, E.L.F. (2014a). Optineurin is an autophagy receptor for damaged mitochondria in parkin-mediated mitophagy that is disrupted by an ALS-linked mutation. Proc. Natl. Acad. Sci. U. S. A. *111*: E4439-48.

Wong, Y.C., and Holzbaur, E.L.F. (2014b). The Regulation of Autophagosome Dynamics by Huntingtin and HAP1 Is Disrupted by Expression of Mutant Huntingtin,

Leading to Defective Cargo Degradation. J. Neurosci. *34*: 1293–1305.

Woodman, B., Butler, R., Landles, C., Lupton, M.K., Tse, J., Hockly, E., et al. (2007). The Hdh(Q150/Q150) knock-in mouse model of HD and the R6/2 exon 1 model develop comparable and widespread molecular phenotypes. Brain Res. Bull. *72*: 83–97.

Wroblewska, B., Wegorzewska, I.N., Bzdega, T., Olszewski, R.T., and Neale, J.H. (2006). Differential negative coupling of type 3 metabotropic glutamate receptor to cyclic GMP levels in neurons and astrocytes. J. Neurochem. *96*: 1071–1077.

Xia, J., Lee, D.H., Taylor, J., Vandelft, M., and Truant, R. (2003). Huntingtin contains a highly conserved nuclear export signal. Hum. Mol. Genet. *12*: 1393–403.

Ying, H., and Yue, B.Y.J.T.J.T. (2016). Optineurin: The autophagy connection. Exp. Eye Res. *144*: 73–80.

Zachari, M., and Ganley, I.G. (2017). The mammalian ULK1 complex and autophagy initiation. Essays Biochem. *61*: 585–596.

Zarate, N., Gundry, K., Yu, D., Casby, J., Eberly, L.E., Öz, G., et al. (2021). In vivo MR spectroscopy reflects synapse density in a Huntington's disease mouse model. BioRxiv 2021.10.26.465951.

Zeitlin, S., Liu, J.-P., Chapman, D.L., Papaioannou, V.E., and Efstratiadis, A. (1995). Increased apoptosis and early embryonic lethality in mice nullizygous for the Huntington's disease gene homologue. Nat. Genet. *11*: 155–163.

Zeron, M.M., Hansson, O., Chen, N., Wellington, C.L., Leavitt, B.R., Brundin, P., et al. (2002). Increased sensitivity to N-methyl-D-aspartate receptor-mediated excitotoxicity in a mouse model of Huntington's disease. Neuron *33*: 849–60.

Zhang, T., Dong, K., Liang, W., Xu, D., Xia, H., Geng, J., et al. (2015). G-protein-coupled receptors regulate autophagy by ZBTB16-mediated ubiquitination and proteasomal degradation of Atg14L. Elife *4*:.

Zhang, Y., Rodriguez, A.L., and Conn, P.J. (2005). Allosteric Potentiators of Metabotropic Glutamate Receptor Subtype 5 Have Differential Effects on Different Signaling Pathways in Cortical Astrocytes. J. Pharmacol. Exp. Ther. *315*: 1212–1219.

Zhang, Z.-Y., Bai, H.-H., Guo, Z., Li, H.-L., He, Y.-T., Duan, X.-L., et al. (2019). mGluR5/ERK signaling regulated the phosphorylation and function of glycine receptor α1ins subunit in spinal dorsal horn of mice. PLOS Biol. *17*: e3000371.

Zheng, S., Clabough, E.B.D., Sarkar, S., Futter, M., Rubinsztein, D.C., and Zeitlin, S.O. (2010). Deletion of the Huntingtin Polyglutamine Stretch Enhances Neuronal Autophagy and Longevity in Mice. PLoS Genet. *6*: e1000838.

Zhong, P., Liu, W., Gu, Z., and Yan, Z. (2008). Serotonin facilitates long-term depression induction in prefrontal cortex via p38 MAPK/Rab5-mediated enhancement of AMPA receptor internalization. J. Physiol. *586*: 4465–4479.

Zhu, G., Wu, C.J., Zhao, Y., and Ashwell, J.D. (2007). Optineurin Negatively Regulates

TNFα- Induced NF-κB Activation by Competing with NEMO for Ubiquitinated RIP. Curr. Biol. *17*: 1438–1443.

Zielonka, D., Marinus, J., Roos, R.A.C., Michele, G. De, Donato, S. Di, Putter, H., et al. (2013). The influence of gender on phenotype and disease progression in patients with Huntington's disease. Park. Relat. Disord. *19*: 192–197.

Zimmermann, J., Herman, M.A., and Rosenmund, C. (2015). Co-release of glutamate and GABA from single vesicles in GABAergic neurons exogenously expressing VGLUT3. Front. Synaptic Neurosci. *7*: 1–9.

Zuccato, C., Ciammola, A., Rigamonti, D., Leavitt, B.R., Goffredo, D., Conti, L., et al. (2001). Loss of Huntingtin-Mediated BDNF Gene Transcription in Huntington's Disease. Science *293*: 493–498.

Zuccato, C., Tartari, M., Crotti, A., Goffredo, D., Valenza, M., Conti, L., et al. (2003). Huntingtin interacts with REST/NRSF to modulate the transcription of NRSE-controlled neuronal genes. Nat. Genet. *35*: 76–83.